Title

Investigating genetic and environmental regulation of neurodevelopment and social behavior

Author

Davis, Matt

Publication Date

2023

Peer reviewed|Thesis/dissertation

Investigating genetic and environmental regulation of neurodevelopment and social behavior

By

Matthew Davis

A dissertation submitted in partial satisfaction of the

requirements for the degree of

Doctor of Philosophy

in

Neuroscience

in the

Graduate Division

of the

University of California, Berkeley

Committee in charge:

Professor Kaoru Saijo, Chair
Professor Annaliese Beery
Professor Linda Wilbrecht
Professor Karthik Shekhar
Professor Lucia Jacobs

Fall 2023

Abstract

Investigating genetic and environmental regulation of neurodevelopment and social behavior

by

Matthew Davis

Doctor of Philosophy in Neuroscience

University of California, Berkeley

Professor Kaoru Saijo, Chair

Social behaviors are a fundamental part of mammalian life, and diverse species of mammals have evolved diverse social behaviors. An ongoing challenge in the field of neuroscience is to understand how genetic diversity gives rise to neural circuits that encode species specific social behaviors. Diversity in genetically encoded developmental mechanisms may promote divergence in neural circuits that encode specific social behaviors, but this hypothesis is difficult to test given our lack of understanding of detailed social behaviors, the neural circuits that encode them, and their developmental origins across genetically diverse organisms. Some major limiting factors include an over-reliance on a single inbred strain of mouse and use of social assays that limit the extent of interactions between animals as tools for understanding the neural encoding of social behaviors. Lastly, it is largely unclear how environmental factors determined by the specialized niches of diverse organisms interact with genetically encoded mechanisms to impact the development of circuits that encode social behaviors. In this dissertation, I present three studies that focus on 1) understanding social behavior at different timescales in genetically distinct strains of mice, 2) a genetically encoded neurodevelopmental mechanism that may contribute to social behaviors in mice and, 3) environmental regulation of brain development in meadow voles, a species with seasonally regulated social behaviors. In all, we identify an example of how recording free social behaviors at both sub-second and multi-day timescales is critical for understanding how subtle genetic variation contributes to differences in multiple subtypes of social investigations, including nose-to-nose and nose-to-rear contacts. We also describe the lipid composition of the fetal brain, and identify a molecule, prostaglandin D2, that is highly concentrated in the fetal brain and has strong potential to be released by macrophages to impact neural development and social behaviors. Lastly we report that social housing conditions and daylengths interact to shape the transcriptional profiles of single nuclei in the dorsal hippocampus in meadow voles, with primary impacts of housing on genes important for the function of oligodendrocytes, microglia, and astrocytes.

Acknowledgments

Thanks to Kelley Power, Karsten Gronert, Elainna Ng, and Eileen Wang, who all played vital roles in conducting this research. Kelley Power helped to collect and process samples for single nucleus RNA sequencing for chapter 3. Karsten Gronert, Elainna Ng, and Eileen Wang helped perform LC/MS/MS studies and data analysis for chapter 2. Lastly, thanks to Fabrice de Chaumont, whose support in setting up the live mouse tracker arena was crucial to the success of chapter 3.

Special thanks to all that helped me along my journey to complete this degree. Family, friends, and mentors at all levels.

A special thanks to all of the trainees that mentored and trained me over the years, including Jennfier Merrit, Katie Grogan, Eva Nichols, Greg Timblin, and DJ Araujo. Your impacts on my research and personal development have been invaluable. Sincere thanks to Kaoru Saijo and Annaliese Beery who provided not only financial support to complete these experiments, but also prioritized my well being and success outside of science at critical times during graduate school.

Thank you to all my friends from UC Berkeley grad school, the Ashby house community, and the Bay Area music community. Through times of mental and physical anguish, your stability, silliness, and validation have meant everything.

Thanks to Mom, Dad, and Kelsey, and all extended family for supporting me in all sorts of ways over the years- financially, emotionally, and teaching me how to navigate the world. I wouldn't have made it here without you.

Thanks to guitar, a boulder amongst rocks these days.

Chapter 1

Introduction

1.1 Social behaviors are encoded by specific neural circuits

Social behaviors are a fundamental component of mammalian life and are critical for survival. Basic social functions such as mating and parental care have evolved to be widespread amongst mammalian species, and additional species-specific social functions have evolved to promote survival and success in particular environmental and social niches (Clutton-Brock, 2021; Kappeler et al., 2013; Zeveloff & Boyce, 1980). Amongst rodents, genetic variability within and between species is known to correlate with differences in sociality. For example, some species of rodents, such as California mice and prairie voles, engage in bi-parental care, whereas paternal behaviors are less common in house mice (Saltzman et al., 2017). Different species of rodents also display different reproductive strategies. As an extreme example, naked mole rats limit reproductive activity to a single female and several males within larger colonies of reproductively suppressed individuals (Holmes & Goldman, 2021). In other rodent species such as house mice, many males and females are reproductively active at once, and each male typically tries to gain access to multiple reproductively active females (Holmes & Goldman, 2021). Within single species, genetic variability at specific gene loci or sets of genes impacts the level or quality of specific social behaviors such as parental care, mating, and social recognition (Robinson et al., 2008). Even subtle and semi-random genetic variation produced by inbreeding amongst largely genetically similar strains of inbred mice promote differences in aggression, ultrasonic vocalizations, and motivation to spend time investigating familiar vs novel individuals (Calhoun, 1956; Faure et al., 2017; Miczek et al., 2001; S. Moy et al., 2007; S. S. Moy et al., 2004).

To this point, it is still largely unclear how the brain encodes diverse social behaviors, and how differences in neural circuitry within and between species may promote differences in the types or quality of social behaviors expressed. It is becoming clear that specific subcomponents, or syllables, of social behaviors are encoded by highly specific neural circuits (Y. Li & Dulac, 2018). One of the most complete examples of this comes from work describing neural circuitry encoding specific parental behaviors in mice. While a large variety of neural circuits throughout the brain likely contribute to parental behaviors, it is clear that the medial preoptic area (MPOA) sends specific galanin positive projections to a variety of cortical and subcortical regions, each of which encodes specific syllables of parental care. For example, MPOA projections to the periaqueductal gray are thought to control the motor control of retrieving pups that have left the nest, whereas projections to the VTA controls the motivation to retrieve pups. Blocking each of these and other MPOA projections individually is sufficient to block specific syllables that control the broad umbrella of parental behaviors (Kohl et al., 2018). While less complete profiling of syllable specific circuits exists for most other social behaviors, aggressive behaviors are also composed of syllables such as fighting, investigation, and mounting, which are thought to be controlled by distinct neural circuits (Hashikawa et al., 2016). In mice, specific subregions of the ventromedial hypothalamus promote fighting behaviors, and input from various other cortical and subcortical regions gate fighting. Notably, a hippocampal projection to the lateral septum relays to the ventromedial hypothalamus to disinhibit fighting (Leroy et al., 2018). By the same token, other brain regions are thought to more generally serve as processing nodes for multiple pieces of social information, and could facilitate broader elements of social decision making. The medial prefrontal cortex is a hub for prosocial behaviors and aggression in multiple species, and disrupting activity in this region can impact multiple social behaviors ranging from aggression to prosocial investigation depending on the specific social context (Ko, 2017; Levy et

al., 2019; Takahashi et al., 2014). Some studies have found evidence that specific subpopulations of neurons in the prefrontal cortex may even encode different types of context specific social information, such as sex of a conspecific (Kingsbury et al., 2020). This evidence suggests that even regions that are thought to more broadly encode social behaviors may actually receive specific projections from individual cell populations that control different social functions, but we may just not understand these circuits fully yet (Huang et al., 2020; Phillips et al., 2019). Given this, it is possible that genetic variability between or within species may promote the formation of unique circuits that control specific syllables of behavior, or could cause differentiation of conserved circuits to adjust the quality of specific behavioral syllables.

Though most species-specific social behaviors across diverse species are better understood from a behavioral than neural perspective, it is clear that some species-specific social behaviors are encoded in part by species-specific circuitry. For example, prairie voles possess an oxytocinergic circuit projecting from the periventricular hypothalamus to the nucleus accumbens that is thought to regulate pair bonding and social preferences (Ross et al., 2009). This circuit is not observed in mice, which are thought to be less prosocial, and do not form pair bonds. While it is not known exactly how genetic differences between mice and voles contribute to this specific circuit, it is likely that a developmental process is involved because some mechanism must be promoting the formation of this circuit in voles but not in mice. Ultimately, species-specific neural circuits like this one may be formed via a combination of genetic and environmental influences, however genetic mechanisms that regulate circuit development appear to be promising candidates for promoting specific social behaviors between and within species (Charvet & Striedter, 2011; Toth & Robinson, 2007). Evolutionary developmental theory posits that genetic variability which impacts early life structures can promote major differences in development which lead to large consequences for physiology and behavior later in life (Finlay & Uchiyama, 2015). In a striking example, human specific genes which regulate developmental processes are thought to be major contributors to the cortical expansion observed in humans over other species of primates and mammals (Franchini, 2021). This cortical expansion likely promotes suites of behavioral differences that impact a variety of social and non-social behaviors in a species-specific manner.

Genes that regulate development and are conserved across species may also serve common functions to regulate general classes of behaviors, and may promote growth and development of unique circuits depending on the specific species and developmental context in which they function. For example, a web of genes involved in neurodevelopment in humans, which are highly correlated to the prevalence of differential social cognition observed in individuals with neurodevelopmental disorders, also impact the development of some social behaviors when disrupted in rodents (Ryan et al., 2019; Schubert et al., 2015). Genetic deletion of multiple genes which are all implicated in autism spectrum disorders, all influence basic social behaviors in mice. Given that social behaviors are so strikingly different in humans and rodents, examples like these raise interesting questions about how subtle differences in conserved genetic programs may influence species specific neural circuitry in a context dependent manner.

1.2 Evolutionarily conserved immune signaling pathways are critical for brain development

Immune and endocrine pathways are critical for multiple functions in survival, tend to be highly conserved across species, and many have alternate roles in development (Järving et al., 2004; Purcell et al., 2006; Schepanski et al., 2018; Verburg-van Kemenade et al., 2017). In

particular, immune molecules can act as morphogens to support the growth and division of immune cells in response to pathogens and tend to be equipped with molecular properties that make them highly effective at influencing development in other cell types (Pearce, 2010; Yi et al., 2010). In the developing brain, multiple cytokines are known to take on alternate roles as factors for neural growth and division (Stolp, 2013). These molecules can initiate diverse signaling cascades depending on the cell type and context they are signaling in, which creates potential for them to have multiple roles in neural development.

Brain development in mice occurs in several functional phases that occur on overlapping timelines. In mice, the neural crest, filled with the initial neural progenitors derived from pluripotent cells begins to form around embryonic day 8.5 (e 8.5; Mosser et al., 2017). These cells subsequently divide and form the ganglionic eminences, which contain the neural progenitor cells that divide into region specific subtypes of neurons (Bellion & Métin, 2005). Neural progenitors continue to divide throughout embryonic development, and each individual brain region exhibits a slightly different timeline of neural division. Generally cell division starts to slow down in mid embryonic development as newly divided cells are actively migrating to their target destinations in the brain. Neural migration continues until the end of embryonic development and can occur even after birth, at which point the major developmental focus of neurons becomes forming synaptic connections and wiring (Hatten, 1999). These processes continue throughout life, and several postnatal waves of neural development are critical for forming social behaviors. In particular, perinatal and pubertal influxes in steroid hormones actively shape neuronal wiring and contribute to sex specific social behaviors in rodents(Lenz et al., 2018; Paul et al., 2018; Yoest et al., 2023).

Interestingly, immune cells are present in the developing brain throughout all these developmental processes, and begin to inhabit even the earliest niches of neuronal progenitors around e9.5 in mice (Mosser et al., 2017). Microglia and border associated macrophages (BAMs) arise from separate lineages of yolk-sac derived macrophages, which develop independently from neural progenitor cells (Utz et al., 2020). Both cell types actively survey the neuronal environment to impact development, but microglia localize to the brain parenchyma whereas BAMs localize to the meninges (Utz et al., 2020) . In the prenatal brain, some of the critical developmental functions of embryonic macrophages include phagocytosis of live and dead neural progenitor cells, pruning synapses, and secreting growth factors that influence the migration of neural cells (Brown & Neher, 2014; Mosser et al., 2017). Interestingly, embryonic macrophages appear to take on multiple roles of interacting nonspecifically with surrounding cells or interacting with specific cell types. During mid embryonic development, microglia form specific interactions with striatal interneurons and are thought to promote development of specific populations of dopamine receptor bearing neurons, which are important for later life motor behaviors (Squarzoni et al., 2014). Microglia also form specific cell interactions with interneurons in the cortical plate during mid embryonic development, where they impact the migration of these inhibitory neurons (Hattori et al., 2020). Around and after birth, microglia continue to be critical players in refining circuits by pruning synapses and clearing neuronal debris during postnatal waves of cell death (Ashwell, 1990). Of note, microglia are highly hormone responsive and are known to shape social behaviors in response to sex hormones during several periods in development, including the postnatal and pubertal waves of sex hormones (Lenz et al., 2013). Though it is not entirely clear whether microglia and BAMs perform similar functions across species, the molecular programs of these cells are highly conserved across species in adulthood, and have similar molecular programs even in humans (Geirsdottir et al.,

2019). A few studies have examined embryonic microglial properties in diverse species, and have provided some evidence for potentially genetically determined species specific functions of microglia. Late in embryonic development, microglia interact with specific Tbr2+ neurons in the developing neocortex, and actively contribute to culling this population through phagocytosis of live neurons (Cunningham et al., 2013). This process occurs differently in rats than in rhesus macaques, as microglia of macaques are more actively culling this population of neural progenitors (Cunningham et al., 2013). Macaques and humans also have a greater number of microglia inhabiting early proliferative zones of the developing brain than rats or ferrets, another model of expanded cortical development (Penna et al., 2021). However, limited evidence suggests that animals with expanded cortices or prolonged gestation compared to mice and rats, ferrets and fruit bats, suggest that microglia also take on different spatial distributions in these developmental contexts (Martínez-Cerdeño et al., 2018; Mizuguchi et al., 2018). Together this evidence raises a possibility that evolutionarily conserved immune signaling programs in microglial may generally promote the development of circuits that encode social behaviors, and may take on specific functions depending on the species, developmental timing, location in the brain, and surrounding cell types. However, the specific molecular signaling pathways, and genetic mechanisms that control microglial functions in development, even in mice, are still not very well understood. Therefore basic research of microglial properties in any species is critical for aiding hypotheses about how genetic programs within and between species may impact microglial function and subsequent neuronal development and social behaviors. Here I present a study addressing how a highly evolutionarily conserved hormonal mechanism may give rise to the development of neural circuits in mice.

1.3 Research on neural encoding of social behaviors are largely limited to B6 mice

While understanding elements of brain development and social behavior in mice is important, much more work is needed to profile both developmental functions and social behaviors across a diverse range of species to better understand how species specific behaviors are impacted by developmental function. As of a study published in 2015, over 80% of animal studies in neuroscience utilized a single strain of inbred mouse, C57BL/6J (B6J) (Ellenbroek & Youn, 2016). Though the genetic tools available in B6J have unquestionably facilitated massive advances in our understanding of the brain, this focus on B6J overlooks some fundamental problems with this model. Of note, the genome of inbred mice such as B6J has shrunk dramatically over the course of inbreeding over the past century (Mouse Genome Sequencing Consortium, 2002). While the genome of B6J is stable, it lacks elements of genetic diversity that drive diverse social behaviors in wild organisms and contribute to our understanding of how particular genes impact social behaviors (Salcedo et al., 2007; Zilkha et al., 2016). As an extreme example, white throated sparrows exhibit a chromosomal inversion within species that drives alternative mating strategies as well as differences in aggression and parental care (Maney et al., 2020). Less extreme genetic variation, such as single nucleotide polymorphisms (SNPs), also contribute to divergence in social behaviors within species. In prairie voles, SNPs in the oxytocin receptor gene correspond to regional differences in oxytocin receptor expression and prosocial behaviors (Ahern et al., 2021; King et al., 2016). Though diversity in mice has been largely ignored in the field of neuroscience, the field of immunology has been more privy to using diverse mouse models. Unsurprisingly, wild mice have dramatically different immune properties which impacts the behavior of immune cells (Abolins et al., 2018). This follows with interesting

questions of whether unique immune properties across species may give rise to differential development of social behaviors that are regulated by early life immune function.

B6J is just one of over 40 strains of inbred mice with major genetic differences that have arisen from inbreeding and outbreeding to wild populations dating back to the early 1900s (https://www.criver.com/eureka/history-black-6-mouse). The international mouse phenotyping consortium has quantified behaviors as well as physiological metrics of these strains in detail, and it is clear that there are major differences across a multitude of behaviors (Groza et al., 2023). Of note, studies collected over the past century predating this modern phenotyping panel have identified clear differences in social behaviors across different strains of mice. One study from 2005 noted remarkable differences in locomotor behaviors such as activity in an open field and performance on the rotarod task between 15 strains of inbred and outbred mice (Bothe at al., 2005). B6J and DBA2 strains also differ in performance in the radial maze, a task designed to assess spatial navigation, fear response, and multiple other behaviors (Calhoun, 1956; Faure et al., 2017; S. S. Moy et al., 2004). It is unsurprising that 10 strains of inbred and outbred mice exhibit differences in common assays used to assess social behavior in mice, the three chamber social novelty and three chamber sociability tests (S. Moy et al., 2007). Despite these numerous differences in behavior identified between the strains, it is still largely unclear how genetic variation differentially influences neural development let alone adult neural function in these strains. Limited work has identified neural divergence between these inbred strains, calling into question the use of B6J as a reference point for studies investigating neural function in other species, such as humans. Hippocampal oscillations, dopamine signaling, serotonin signaling in the gut brain axis, gene expression in cortical and limbic regions, and other neural characteristics have all been shown to differ across inbred and outbred strains (Jansen et al., 2009; Neal et al., 2009; Puglisi-Allegra & Cabib, 1997).

Despite clear evidence that inbred strains differ in their expression of multiple social behaviors and components of brain function, there have yet to be impactful links between the two. In part this may be due to the limited resolution of the conventional behavioral assays used to assess social behavior across strains. Given that these assays involve trapping a stimulus animal under a wire cup, they prevent full interactions, and thus have limited power in describing how specific syllables of social behavior controlled by specific brain regions may differ across these strains. This is a necessary step for understanding potential developmental differences that could give rise to adult differences in behavior via specific neural circuits.

Here I present a study that quantifies strain differences in social behavior on subsecond to multi-day timescales using machine vision and learning algorithms that track posture and detailed social behaviors. This study should lay the groundwork for future research to investigate strain differences in neural function regulating specific social syllables, and provide a model for investigating detailed differences in social behavior across a wider variety of strains and species of mice.

1.4 Meadow voles are a natural model of gene - environment interactions in social development

Though various strains of mice allow for a wide array of established methods for profiling developmental processes and behavior, a primary goal of this dissertation work was to bring modern genomic and behavioral techniques used frequently in mice into other genetically diverse species with compelling social behaviors. Given that the genome of inbred mice is largely homogenous within each strain, examining social behavior and its developmental origins

in wild derived animals offer additional opportunities to explore how the roles of naturally occurring combinations of genes impact the circuit and behavioral development. Here I also present results from a study that describes neural differences that correspond to a developmentally and environmentally regulated pattern of prosociality in Meadow Voles. This study used single nucleus RNA sequencing, which is apt for use in non-model organisms and provides a broader unbiased understanding of how many genetic pathways can contribute to neural function in individual cell types.

Multiple species of vole, particularly prairie voles (*Microtus ochrogaster)*, have become common model species for prosocial behaviors. Prairie voles form close prosocial relationships with reproductive partners and peers, whom they prefer to spend time with over unfamiliar individuals (Kenkel et al., 2021). Notably this preference to spend time with familiar peers is opposite the trend observed in Bl6J mice, which typically display a preference for spending time with unfamiliar individuals in similar social choice assays (Beery & Shambaugh, 2021; Moy et al., 2007). While the neural bases of close prosocial bonds are not entirely understood, substantial progress has been made in these animals. Multiple neural systems appear to be involved in pair bonding behaviors, and oxytocin signaling is one of the primary mechanisms that supports this behavior (Inoue et al., 2022). Oxytocin receptor binding is more highly expressed in brain regions involved in social reward in this species than other species of voles that do not display pair bonding behavior and in mice (Freeman et al., 2020; Horie et al., 2020).

Although much work has been done to characterize this behavior in adulthood, it is still fairly unclear how developmental processes give rise to pair bonding behaviors in adulthood. Some evidence in prairie voles suggests that the serotonin system is critical for proper development of circuits regulating pair bonding behaviors. Administration of fluoxetine, selective serotonin reuptake inhibitor during the first postnatal week of life is sufficient to alter oxytocin binding in multiple brain regions as well as pair-bonding (Lawrence et al., 2020). Other work focused on environmental contributors to the development of pair bonding behavior has suggested parental care is critical for normal development of pair bonding behaviors, similar to the development of different social behaviors in other rodent species (Kohl et al., 2018; Prounis & Ophir, 2019; Valera-Marín et al., 2021). Though these neuromodulators such as oxytocin and serotonin are clearly involved in pair bonding behavior and its development, evidence is lacking of how a broader range of potential genetic mechanisms could regulate this species specific behavior.

A closely related species, meadow voles (*Microtus pennsylvanicus)*, undergoes a natural developmental process that impacts prosocial bonding, similar to that seen in prairie voles, and serves as a model to understand how circuits encoding prosociality come online. Meadow voles exhibit a seasonal difference in reproductive activity as well as prosociality (Beery & Zucker, 2010a; Kerbeshian et al., 1994; Lee et al., 2019). In the wintertime they are reproductively quiescent and live in large social groups, whereas in the summertime they are mostly solitary and aggressive (Madison et al., 1984). In the lab, it is possible to recreate prosocial and aggressive phenotypes by shifting the light cycle during post-weaning development for about 40 days. Thus photoperiodic differences in prosociality offer an opportunity to understand how the brain encodes prosocial behaviors in this species. Though other species of voles, like prairie voles, exhibit seasonal shifts in behavior, they generally exhibit similar bonding behaviors across the seasons. This suggests that genetic factors that control the development of circuits encoding prosociality are regulated by environmental factors in meadow voles. Here we provide limited evidence of transcriptional contributors to seasonal differences in brain states in meadow voles,

to lay the groundwork for understanding which genetic components may be important markers for seasonal differences in brain and prosocial behavior in this species.

References

Abolins, S., Lazarou, L., Weldon, L., Hughes, L., King, E. C., Drescher, P., Pocock, M. J. O., Hafalla, J. C. R., Riley, E. M., & Viney, M. (2018). The ecology of immune state in a wild mammal, Mus musculus domesticus. *PLOS Biology*, *16*(4), e2003538. https://doi.org/10.1371/journal.pbio.2003538

Ahern, T. H., Olsen, S., Tudino, R., & Beery, A. K. (2021). Natural variation in the oxytocin receptor gene and rearing interact to influence reproductive and nonreproductive social behavior and receptor binding. *Psychoneuroendocrinology*, *128*, 105209. https://doi.org/10.1016/j.psyneuen.2021.105209

Ashwell, K. (1990). Microglia and cell death in the developing mouse cerebellum. *Developmental Brain Research*, *55*(2), 219–230. https://doi.org/10.1016/0165-3806(90)90203-B

Beery, A. K., & Shambaugh, K. L. (2021). Comparative Assessment of Familiarity/Novelty Preferences in Rodents. *Frontiers in Behavioral Neuroscience*, *15*, 648830. https://doi.org/10.3389/fnbeh.2021.648830

Beery, A. K., & Zucker, I. (2010). Oxytocin and same-sex social behavior in female meadow voles. *Neuroscience*, *169*(2), 665–673. https://doi.org/10.1016/j.neuroscience.2010.05.023

Bellion, A., & Métin, C. (2005). Early regionalisation of the neocortex and the medial ganglionic eminence. *Brain Research Bulletin*, *66*(4–6), 402–409. https://doi.org/10.1016/j.brainresbull.2005.07.010

Brown, G. C., & Neher, J. J. (2014). Microglial phagocytosis of live neurons. *Nature Reviews Neuroscience*, *15*(4), 209–216. https://doi.org/10.1038/nrn3710

Calhoun, J. B. (1956). A Comparative Study of the Social Behavior of Two Inbred Strains of House Mice. *Ecological Monographs*, *26*(1), 81–103. https://doi.org/10.2307/1943578

Charvet, C. J., & Striedter, G. F. (2011). Developmental Modes and Developmental Mechanisms can Channel Brain Evolution. *Frontiers in Neuroanatomy*, *5*. https://doi.org/10.3389/fnana.2011.00004

Clutton-Brock, T. (2021). Social evolution in mammals. *Science*, *373*(6561), eabc9699. https://doi.org/10.1126/science.abc9699

Cunningham, C. L., Martínez-Cerdeño, V., & Noctor, S. C. (2013). Microglia Regulate the Number of Neural Precursor Cells in the Developing Cerebral Cortex. *The Journal of Neuroscience*, *33*(10), 4216–4233. https://doi.org/10.1523/JNEUROSCI.3441-12.2013

Ellenbroek, B., & Youn, J. (2016). Rodent models in neuroscience research: Is it a rat race? *Disease Models & Mechanisms*, *9*(10), 1079–1087. https://doi.org/10.1242/dmm.026120

Faure, A., Pittaras, E., Nosjean, A., Chabout, J., Cressant, A., & Granon, S. (2017). Social behaviors and acoustic vocalizations in different strains of mice. *Behavioural Brain Research*, *320*, 383–390. https://doi.org/10.1016/j.bbr.2016.11.003

Finlay, B. L., & Uchiyama, R. (2015). Developmental mechanisms channeling cortical evolution. *Trends in Neurosciences*, *38*(2), 69–76. https://doi.org/10.1016/j.tins.2014.11.004

Franchini, L. F. (2021). Genetic Mechanisms Underlying Cortical Evolution in Mammals. *Frontiers in Cell and Developmental Biology*, *9*, 591017. https://doi.org/10.3389/fcell.2021.591017

Freeman, A. R., Aulino, E. A., Caldwell, H. K., & Ophir, A. G. (2020). Comparison of the distribution of oxytocin and vasopressin 1a receptors in rodents reveals conserved and

derived patterns of nonapeptide evolution. *Journal of Neuroendocrinology*, *32*(4), e12828. https://doi.org/10.1111/jne.12828

Geirsdottir, L., David, E., Keren-Shaul, H., Weiner, A., Bohlen, S. C., Neuber, J., Balic, A., Giladi, A., Sheban, F., Dutertre, C.-A., Pfeifle, C., Peri, F., Raffo-Romero, A., Vizioli, J., Matiasek, K., Scheiwe, C., Meckel, S., Mätz-Rensing, K., Van Der Meer, F., … Prinz, M. (2019). Cross-Species Single-Cell Analysis Reveals Divergence of the Primate Microglia Program. *Cell*, *179*(7), 1609-1622.e16. https://doi.org/10.1016/j.cell.2019.11.010

Groza, T., Gomez, F. L., Mashhadi, H. H., Muñoz-Fuentes, V., Gunes, O., Wilson, R., Cacheiro, P., Frost, A., Keskivali-Bond, P., Vardal, B., McCoy, A., Cheng, T. K., Santos, L., Wells, S., Smedley, D., Mallon, A.-M., & Parkinson, H. (2023). The International Mouse Phenotyping Consortium: Comprehensive knockout phenotyping underpinning the study of human disease. *Nucleic Acids Research*, *51*(D1), D1038–D1045. https://doi.org/10.1093/nar/gkac972

Hashikawa, K., Hashikawa, Y., Falkner, A., & Lin, D. (2016). The neural circuits of mating and fighting in male mice. *Current Opinion in Neurobiology*, *38*, 27–37. https://doi.org/10.1016/j.conb.2016.01.006

Hatten, M. E. (1999). CENTRAL NERVOUS SYSTEM NEURONAL MIGRATION. *Annual Review of Neuroscience*, *22*(1), 511–539. https://doi.org/10.1146/annurev.neuro.22.1.511

Hattori, Y., Naito, Y., Tsugawa, Y., Nonaka, S., Wake, H., Nagasawa, T., Kawaguchi, A., & Miyata, T. (2020). Transient microglial absence assists postmigratory cortical neurons in proper differentiation. *Nature Communications*, *11*(1), 1631. https://doi.org/10.1038/s41467-020-15409-3

Holmes, M. M., & Goldman, B. D. (2021). Social Behavior in Naked Mole-Rats: Individual Differences in Phenotype and Proximate Mechanisms of Mammalian Eusociality. In R. Buffenstein, T. J. Park, & M. M. Holmes (Eds.), *The Extraordinary Biology of the Naked Mole-Rat* (Vol. 1319, pp. 35–58). Springer International Publishing. https://doi.org/10.1007/978-3-030-65943-1_2

Horie, K., Inoue, K., Nishimori, K., & Young, L. J. (2020). Investigation of Oxtr-expressing Neurons Projecting to Nucleus Accumbens using Oxtr-ires-Cre Knock-in prairie Voles (Microtus ochrogaster). *Neuroscience*, *448*, 312–324. https://doi.org/10.1016/j.neuroscience.2020.08.023

Huang, Y., Iosif, A.-M., Hansen, R. L., & Schmidt, R. J. (2020). Maternal polyunsaturated fatty acids and risk for autism spectrum disorder in the *MARBLES* high-risk study. *Autism*, *24*(5), 1191–1200. https://doi.org/10.1177/1362361319877792

Inoue, K., Ford, C. L., Horie, K., & Young, L. J. (2022). Oxytocin receptors are widely distributed in the prairie vole (*Microtus ochrogaster)* brain: Relation to social behavior, genetic polymorphisms, and the dopamine system. *Journal of Comparative Neurology*, *530*(16), 2881–2900. https://doi.org/10.1002/cne.25382

Jansen, R., Linkenkaer‐Hansen, K., Heistek, T., Timmerman, J., Mansvelder, H. D., Brussaard, A. B., De Gunst, M., & Van Ooyen, A. (2009). Inbred mouse strains differ in multiple hippocampal activity traits. *European Journal of Neuroscience*, *30*(6), 1092–1100. https://doi.org/10.1111/j.1460-9568.2009.06883.x

Järving, R., Järving, I., Kurg, R., Brash, A. R., & Samel, N. (2004). On the Evolutionary Origin of Cyclooxygenase (COX) Isozymes. *Journal of Biological Chemistry*, *279*(14), 13624–13633. https://doi.org/10.1074/jbc.M313258200

Kappeler, P. M., Barrett, L., Blumstein, D. T., & Clutton-Brock, T. H. (2013). Constraints and

flexibility in mammalian social behaviour: Introduction and synthesis. *Philosophical Transactions of the Royal Society B: Biological Sciences*, *368*(1618), 20120337. https://doi.org/10.1098/rstb.2012.0337

Kenkel, W. M., Gustison, M. L., & Beery, A. K. (2021). A Neuroscientist's Guide to the Vole. *Current Protocols*, *1*(6), e175. https://doi.org/10.1002/cpz1.175

Kerbeshian, M. C., Bronson, F. H., & Bellis, E. D. (1994). Variation in Reproductive Photoresponsiveness in a Wild Population of Meadow Voles1. *Biology of Reproduction*, *50*(4), 745–750. https://doi.org/10.1095/biolreprod50.4.745

King, L. B., Walum, H., Inoue, K., Eyrich, N. W., & Young, L. J. (2016). Variation in the Oxytocin Receptor Gene Predicts Brain Region–Specific Expression and Social Attachment. *Biological Psychiatry*, *80*(2), 160–169. https://doi.org/10.1016/j.biopsych.2015.12.008

Kingsbury, L., Huang, S., Raam, T., Ye, L. S., Wei, D., Hu, R. K., Ye, L., & Hong, W. (2020). Cortical Representations of Conspecific Sex Shape Social Behavior. *Neuron*, *107*(5), 941-953.e7. https://doi.org/10.1016/j.neuron.2020.06.020

Ko, J. (2017). Neuroanatomical Substrates of Rodent Social Behavior: The Medial Prefrontal Cortex and Its Projection Patterns. *Frontiers in Neural Circuits*, *11*, 41. https://doi.org/10.3389/fncir.2017.00041

Kohl, J., Babayan, B. M., Rubinstein, N. D., Autry, A. E., Marin-Rodriguez, B., Kapoor, V., Miyamishi, K., Zweifel, L. S., Luo, L., Uchida, N., & Dulac, C. (2018). Functional circuit architecture underlying parental behaviour. *Nature*, *556*(7701), 326–331. https://doi.org/10.1038/s41586-018-0027-0

Lawrence, R. H., Palumbo, M. C., Freeman, S. M., Guoynes, C. D., & Bales, K. L. (2020). Developmental Fluoxetine Exposure Alters Behavior and Neuropeptide Receptors in the Prairie Vole. *Frontiers in Behavioral Neuroscience*, *14*, 584731. https://doi.org/10.3389/fnbeh.2020.584731

Lee, N. S., Goodwin, N. L., Freitas, K. E., & Beery, A. K. (2019). Affiliation, Aggression, and Selectivity of Peer Relationships in Meadow and Prairie Voles. *Frontiers in Behavioral Neuroscience*, *13*, 52. https://doi.org/10.3389/fnbeh.2019.00052

Lenz, K. M., Nugent, B. M., Haliyur, R., & McCarthy, M. M. (2013). Microglia Are Essential to Masculinization of Brain and Behavior. *The Journal of Neuroscience*, *33*(7), 2761–2772. https://doi.org/10.1523/JNEUROSCI.1268-12.2013

Lenz, K. M., Pickett, L. A., Wright, C. L., Davis, K. T., Joshi, A., & McCarthy, M. M. (2018). Mast Cells in the Developing Brain Determine Adult Sexual Behavior. *The Journal of Neuroscience*, *38*(37), 8044–8059. https://doi.org/10.1523/JNEUROSCI.1176-18.2018

Leroy, F., Park, J., Asok, A., Brann, D. H., Meira, T., Boyle, L. M., Buss, E. W., Kandel, E. R., & Siegelbaum, S. A. (2018). A circuit from hippocampal CA2 to lateral septum disinhibits social aggression. *Nature*, *564*(7735), 213–218. https://doi.org/10.1038/s41586-018-0772-0

Levy, D. R., Tamir, T., Kaufman, M., Parabucki, A., Weissbrod, A., Schneidman, E., & Yizhar, O. (2019). Dynamics of social representation in the mouse prefrontal cortex. *Nature Neuroscience*, *22*(12), 2013–2022. https://doi.org/10.1038/s41593-019-0531-z

Li, Y., & Dulac, C. (2018). Neural coding of sex-specific social information in the mouse brain. *Current Opinion in Neurobiology*, *53*, 120–130. https://doi.org/10.1016/j.conb.2018.07.005

Madison, D. M., FitzGerald, R. W., & McShea, W. J. (1984). Dynamics of social nesting in

overwintering meadow voles (Microtus pennsylvanicus): Possible consequences for population cycling. *Behavioral Ecology and Sociobiology*, *15*(1), 9–17. https://doi.org/10.1007/BF00310209

Maney, D. L., Merritt, J. R., Prichard, M. R., Horton, B. M., & Yi, S. V. (2020). Inside the supergene of the bird with four sexes. *Hormones and Behavior*, *126*, 104850. https://doi.org/10.1016/j.yhbeh.2020.104850

Martínez-Cerdeño, V., Camacho, J., Ariza, J., Rogers, H., Horton-Sparks, K., Kreutz, A., Behringer, R., Rasweiler, J. J., & Noctor, S. C. (2018). The Bat as a New Model of Cortical Development. *Cerebral Cortex*, *28*(11), 3880–3893. https://doi.org/10.1093/cercor/bhx251

Miczek, K. A., Maxson, S. C., Fish, E. W., & Faccidomo, S. (2001). Aggressive behavioral phenotypes in mice. *Behavioural Brain Research*, *125*(1–2), 167–181. https://doi.org/10.1016/S0166-4328(01)00298-4

Mizuguchi, K., Horiike, T., Matsumoto, N., Ichikawa, Y., Shinmyo, Y., & Kawasaki, H. (2018). Distribution and Morphological Features of Microglia in the Developing Cerebral Cortex of Gyrencephalic Mammals. *Neurochemical Research*, *43*(5), 1075–1085. https://doi.org/10.1007/s11064-018-2520-0

Mosser, C.-A., Baptista, S., Arnoux, I., & Audinat, E. (2017). Microglia in CNS development: Shaping the brain for the future. *Progress in Neurobiology*, *149–150*, 1–20. https://doi.org/10.1016/j.pneurobio.2017.01.002

Mouse Genome Sequencing Consortium. (2002). Initial sequencing and comparative analysis of the mouse genome. *Nature*, *420*(6915), 520–562. https://doi.org/10.1038/nature01262

Moy, S., Nadler, J., Young, N., Perez, A., Holloway, L., Barbaro, R., Barbaro, J., Wilson, L., Threadgill, D., & Lauder, J. (2007). Mouse behavioral tasks relevant to autism: Phenotypes of 10 inbred strains. *Behavioural Brain Research*, *176*(1), 4–20. https://doi.org/10.1016/j.bbr.2006.07.030

Moy, S. S., Nadler, J. J., Perez, A., Barbaro, R. P., Johns, J. M., Magnuson, T. R., Piven, J., & Crawley, J. N. (2004). Sociability and preference for social novelty in five inbred strains: An approach to assess autistic‐like behavior in mice. *Genes, Brain and Behavior*, *3*(5), 287–302. https://doi.org/10.1111/j.1601-1848.2004.00076.x

Neal, K. B., Parry, L. J., & Bornstein, J. C. (2009). Strain‐specific genetics, anatomy and function of enteric neural serotonergic pathways in inbred mice. *The Journal of Physiology*, *587*(3), 567–586. https://doi.org/10.1113/jphysiol.2008.160416

Paul, M. J., Probst, C. K., Brown, L. M., & De Vries, G. J. (2018). Dissociation of Puberty and Adolescent Social Development in a Seasonally Breeding Species. *Current Biology*, *28*(7), 1116-1123.e2. https://doi.org/10.1016/j.cub.2018.02.030

Pearce, E. L. (2010). Metabolism in T cell activation and differentiation. *Current Opinion in Immunology*, *22*(3), 314–320. https://doi.org/10.1016/j.coi.2010.01.018

Penna, E., Cunningham, C. L., Saylor, S., Kreutz, A., Tarantal, A. F., Martínez-Cerdeño, V., & Noctor, S. C. (2021). Greater Number of Microglia in Telencephalic Proliferative Zones of Human and Nonhuman Primate Compared with Other Vertebrate Species. *Cerebral Cortex Communications*, *2*(4), tgab053. https://doi.org/10.1093/texcom/tgab053

Phillips, M. L., Robinson, H. A., & Pozzo-Miller, L. (2019). Ventral hippocampal projections to the medial prefrontal cortex regulate social memory. *eLife*, *8*, e44182. https://doi.org/10.7554/eLife.44182

Prounis, G. S., & Ophir, A. G. (2019). The Impact of Early Postnatal and Juvenile Social

Environments on the Effects of Chronic Intranasal Oxytocin in the Prairie Vole. *Frontiers in Behavioral Neuroscience*, *13*, 206. https://doi.org/10.3389/fnbeh.2019.00206

Puglisi-Allegra, S., & Cabib, S. (1997). PSYCHOPHARMACOLOGY OF DOPAMINE: THE CONTRIBUTION OF COMPARATIVE STUDIES IN INBRED STRAINS OF MICE. *Progress in Neurobiology*, *51*(6), 637–661. https://doi.org/10.1016/S0301-0082(97)00008-7

Purcell, M. K., Smith, K. D., Aderem, A., Hood, L., Winton, J. R., & Roach, J. C. (2006). Conservation of Toll-like receptor signaling pathways in teleost fish. *Comparative Biochemistry and Physiology Part D: Genomics and Proteomics*, *1*(1), 77–88. https://doi.org/10.1016/j.cbd.2005.07.003

Robinson, G. E., Fernald, R. D., & Clayton, D. F. (2008). Genes and Social Behavior. *Science*, *322*(5903), 896–900. https://doi.org/10.1126/science.1159277

Ross, H. E., Cole, C. D., Smith, Y., Neumann, I. D., Landgraf, R., Murphy, A. Z., & Young, L. J. (2009). Characterization of the oxytocin system regulating affiliative behavior in female prairie voles. *Neuroscience*, *162*(4), 892–903. https://doi.org/10.1016/j.neuroscience.2009.05.055

Ryan, A. M., Berman, R. F., & Bauman, M. D. (2019). Bridging the species gap in translational research for neurodevelopmental disorders. *Neurobiology of Learning and Memory*, *165*, 106950. https://doi.org/10.1016/j.nlm.2018.10.006

Salcedo, T., Geraldes, A., & Nachman, M. W. (2007). Nucleotide Variation in Wild and Inbred Mice. *Genetics*, *177*(4), 2277–2291. https://doi.org/10.1534/genetics.107.079988

Saltzman, W., Harris, B. N., De Jong, T. R., Perea-Rodriguez, J. P., Horrell, N. D., Zhao, M., & Andrew, J. R. (2017). Paternal Care in Biparental Rodents: Intra- and Inter-individual Variation. *Integrative and Comparative Biology*, *57*(3), 589–602. https://doi.org/10.1093/icb/icx047

Schepanski, S., Buss, C., Hanganu-Opatz, I. L., & Arck, P. C. (2018). Prenatal Immune and Endocrine Modulators of Offspring's Brain Development and Cognitive Functions Later in Life. *Frontiers in Immunology*, *9*, 2186. https://doi.org/10.3389/fimmu.2018.02186

Schubert, D., Martens, G. J. M., & Kolk, S. M. (2015). Molecular underpinnings of prefrontal cortex development in rodents provide insights into the etiology of neurodevelopmental disorders. *Molecular Psychiatry*, *20*(7), 795–809. https://doi.org/10.1038/mp.2014.147

Squarzoni, P., Oller, G., Hoeffel, G., Pont-Lezica, L., Rostaing, P., Low, D., Bessis, A., Ginhoux, F., & Garel, S. (2014). Microglia Modulate Wiring of the Embryonic Forebrain. *Cell Reports*, *8*(5), 1271–1279. https://doi.org/10.1016/j.celrep.2014.07.042

Stolp, H. B. (2013). Neuropoietic cytokines in normal brain development and neurodevelopmental disorders. *Molecular and Cellular Neuroscience*, *53*, 63–68. https://doi.org/10.1016/j.mcn.2012.08.009

Takahashi, A., Nagayasu, K., Nishitani, N., Kaneko, S., & Koide, T. (2014). Control of Intermale Aggression by Medial Prefrontal Cortex Activation in the Mouse. *PLoS ONE*, *9*(4), e94657. https://doi.org/10.1371/journal.pone.0094657

Toth, A. L., & Robinson, G. E. (2007). Evo-devo and the evolution of social behavior. *Trends in Genetics*, *23*(7), 334–341. https://doi.org/10.1016/j.tig.2007.05.001

Utz, S. G., See, P., Mildenberger, W., Thion, M. S., Silvin, A., Lutz, M., Ingelfinger, F., Rayan, N. A., Lelios, I., Buttgereit, A., Asano, K., Prabhakar, S., Garel, S., Becher, B., Ginhoux, F., & Greter, M. (2020). Early Fate Defines Microglia and Non-parenchymal Brain Macrophage Development. *Cell*, *181*(3), 557-573.e18.

https://doi.org/10.1016/j.cell.2020.03.021
Valera-Marín, G., Young, L. J., Camacho, F., Paredes, R. G., Rodríguez, V. M., Díaz, N. F., & Portillo, W. (2021). Raised without a father: Monoparental care effects over development, sexual behavior, sexual reward, and pair bonding in prairie voles. *Behavioural Brain Research*, *408*, 113264. https://doi.org/10.1016/j.bbr.2021.113264
Verburg-van Kemenade, B. M. L., Cohen, N., & Chadzinska, M. (2017). Neuroendocrine-immune interaction: Evolutionarily conserved mechanisms that maintain allostasis in an ever-changing environment. *Developmental & Comparative Immunology*, *66*, 2–23. https://doi.org/10.1016/j.dci.2016.05.015
Yi, J. J., Barnes, A. P., Hand, R., Polleux, F., & Ehlers, M. D. (2010). TGF-β Signaling Specifies Axons during Brain Development. *Cell*, *142*(1), 144–157. https://doi.org/10.1016/j.cell.2010.06.010
Yoest, K. E., Henry, M. G., Velisek, H. A., & Veenema, A. H. (2023). Development of social recognition ability in female rats: Effect of pubertal ovarian hormones. *Hormones and Behavior*, *151*, 105347. https://doi.org/10.1016/j.yhbeh.2023.105347
Zeveloff, S. I., & Boyce, M. S. (1980). Parental Investment and Mating Systems in Mammals. *Evolution*, *34*(5), 973. https://doi.org/10.2307/2408002
Zilkha, N., Sofer, Y., Beny, Y., & Kimchi, T. (2016). From classic ethology to modern neuroethology: Overcoming the three biases in social behavior research. *Current Opinion in Neurobiology*, *38*, 96–108. https://doi.org/10.1016/j.conb.2016.04.014

Chapter 2

Investigating the role of Prostaglandin D2 in brain development

Introduction:

Neural development before birth in mice is regulated by a cascade of precisely timed cellular events that arise from genetic programs (Fig1; Chen et al., 2017). These developmental programs often make use of molecular pathways that were first discovered for their functions in adult biology. Well known examples include steroid hormone receptors, bone morphogenic proteins, and transforming growth factor beta, which are now considered as morphogens and transcriptional regulators that are critical for neural development (Krieglstein et al., 2002; McCARTHY, 2008; Mehler et al., 1997; Moses et al., 2016; Sampath & Reddi, 2020; Whitfield et al., 1999). Canonical innate immune pathways often regulate cell division, growth, and migration in adult tissues, making them prime candidates for impacting brain development (Zengeler & Lukens, 2021).

In the prenatal brain, brain resident macrophages (often classified as microglia), contribute to the development of other brain cell types via intercellular signaling of classical immune molecules (Sharma et al., 2021; Zengeler & Lukens, 2021). Given that macrophages are present in the developing brain from the earliest stages of neurogenesis to adulthood (fig 1A), and given that they are dispersed throughout most of the developing brian and meninges, they have expansive potential to shape multiple cell types, developmental processes, brain regions, and behaviors(Thion & Garel, 2017) . Importantly, microglia have been found in multiple instances to impact the development of neural progenitors which are fated to encode social behaviors later in life (Lenz et al., 2013; Missig et al., 2020; Smith et al., 2007; VanRyzin et al., 2016).

One established mechanism by which microglia impact brain development and social behaviors is by secretion of Prostaglandins (PGs) in the early postnatal brain of rats(Lenz et al., 2013). PGs are fatty acid metabolites which canonicaly regulate inflammation in multiple types of immune cells, such as T cells and B cells(Harris et al., 2002). There are tens of subtypes of PGs that are formed by enzymatic digestion of dietary Polyunsaturated fatty acids (PUFAs), including Arachidonic Acid (AA), Docosahexaenoic acid (DHA), Eicosapentaenoic acid (EPA), and Linoleic acid (LA). Series 2 PGs, which are derived from metabolism of AA, are commonly associated with inflammatory processes (Hata & Breyer, 2004; Ricciotti & FitzGerald, 2011). Two rate limiting enzymes, Cyclooxygenase 1 and 2 (Cox-1 and Cox-2), are responsible for metabolizing AA into PG precursors, which are further digested into a family of 5 bioactive prostaglandins by PG-subtype specific synthesizing enzymes(Ricciotti & FitzGerald, 2011). Each subtype of PGs has high affinity for its own class of G-protein coupled receptors, which can have multiple functions depending on the cell type and biological context in which they are expressed and activated (fig 1B)(Hata & Breyer, 2004; Ricciotti & FitzGerald, 2011; Q. Wang et al., 2022).

Historical emphasis has been placed on one subtype of PG, PGE2, in the context of brain development (Amateau & McCarthy, 2004). Of note, COX-1 and COX-2 are the primary targets of non-steroidal anti-inflammatory drugs (NSAIDs, fig 1B), and studies of NSAIDs on brain development have mostly focused on PGE2, while little work has been done on other PG subtypes (Amateau & McCarthy, 2004; Balin et al., 2020; Rai-Bhogal et al., 2018; Wong et al., 2016). This work is built on the landmark finding that PGE2 release by microglia in the POA around the time of birth promotes dendritic outgrowth of neural progenitors in a sex dependent manner, and is critical for the development of normal sexual behaviors in adult males (Lenz et al., 2013). Other work suggests that PGE2 delivered to pregnant mice midway through or at the end of embryonic brain development changes transcriptional patterns in the fetal brain,

modifying expression of molecular pathways involved in cell growth and migration(Rai-Bhogal et al., 2018). COX-2 knockout mice also exhibit behavioral differences from genetically homogenous C57BL/6J (B6J) mice, and this difference has been hypothesized mediated by disruption of PGE2 signaling in the fetal brain (Wong et al., 2019). COX-1 and 2 are rate limiting enzymes for all PG subtypes, but it is unknown to what extent other PGs mediate the effects of COX manipulation during development.

Despite the focus of prior studies on PGE2 in brain development, PGD2 is considered the primary PG in the adult brain, where it regulates activity of hypothalamic neurons that control sleep (Urade & Hayaishi, 2011). A handful of recent studies have suggested that PGD2 is functionally relevant in neurodevelopment. About a week after birth, PGD2 secreted by hypothalamic cells recruits astrocytes by inducing their migration, which results in cell-cell interactions that are critical for the development of sex specific physiology in females (Pellegrino et al., 2021). Before birth, synthesizing enzymes for PGD2 are induced in the fetal brain of mice by maternal exposure to the anesthetic sevoflurane, which alters migration of neural progenitors (Chai et al., 2019). Interestingly PGD2 is an order of magnitude more concentrated than other PGs in the adult brain (Wallace et al., 2022), but it is unclear whether this pattern is conserved during neurodevelopment. Moreover, it is not known which of the many bioactive PGs are present in the brain before birth, and what their relative concentrations are. As a result it is still largely unclear which PGs may be good candidates for impacting brain development before birth.

Here we use Liquid chromatography mass spectrometry to measure concentrations of PGs in the brains of embryonic mice. As multiple studies (Lenz et al., 2013; Pellegrino et al., 2021) have focused on PGs influence on circuit development after birth, we were curious to know just how early in brain development PGs are present. Given that microglia are known producers of PGs in the postnatal and adult brain (Lenz et al., 2013), we hypothesized that PGs are also secreted by microglia prenatally. As a result we expected PGs would be present in the brain from the earliest stages of microglial inhabitance in the brain parenchyma (Thion & Garel, 2017). We further hypothesized that PGD2 would be the predominant PG in the fetal brain given its massive concentration in adult brains..

Although our hypothesis focused on PGs, we recognized that PGs are only one subset of PUFA metabolites with potential to impact brain development. Closely related lipid species in the eicosanoid family include leukotrienes and endocannabinoids, which also impact brain development, but have not been quantified in the fetal brain (Berghuis et al., 2007; Bijlsma et al., 2008). Here we create an open-source database of eicosanoid concentrations in the fetal brain to support new hypotheses of lipid activity in the fetal brain.

Given PGD2's clear role in promoting cell migration in the postnatal brain(Pellegrino et al., 2021), and evidence of high expression of PGD2 synthesizing enzymes in microglia after birth (Mohri et al., 2003), we hypothesize that PGD2 may be secreted from microglia and impact neural migration via signaling with neuronal progenitors. In order to test which cells are capable of receiving and producing PGD2 in the fetal brain, we used fluorescence activated cell sorting of fetal brain macrophages paired with qPCR to quantify cell type specific patterns of expression enzymes and receptors in the PGD2 pathway across the entirety of fetal brain development. Lastly, we tested how loss of function of PGD2 signaling impacts cell type specific functions in the fetal brain. We knocked out the primary PGD2 receptors, DP1 and DP2, and quantified cell type specific transcriptomes in the entire fetal brain with single nucleus RNA seq.

Results

Prostaglandin D2 is the most abundant prostaglandin in the fetal brain

To our knowledge, eicosanoid concentrations have not yet been quantified in the fetal brain. In order to identify candidate eicosanoids that could be relevant for brain development, we used LC/MS/MS on a panel of 41 eicosanoid species. Given that the relevant developmental processes from brain development shift gradually throughout fetal growth (Fig 2.1A) and given that eicosanoids generally affect multiple cellular developmental processes depending on cell type and physiological context, we quantified eicosanoid concentrations at 3 time points spanning fetal brain development in whole fetal brains (Fig 2.2A). We chose embryonic days 12.5, 15,5, and 18.5 (e12.5, e15.5 and e18.5) to sample at even windows across the major period of neurogenesis in the fetal brain (Chen et al., 2017). Of our panel, 20 eicosanoids were consistently detected across samples (Fig 2.2C; $n \geq 5$ per sex within an age group). We did not detect sex differences in concentration of any of these consistently detected eicosanoids within any age group (MANOVA $F(10,21)=1.78$, $p=0.17$) and therefore we combined sexes for all subsequent analyses. We did, however, detect differences in concentration by age group ($F(42,20)=14.47$, $p<.00001$). We measured concentrations of 3 polyunsaturated fatty acids (PUFAs) which serve as major precursors to biologically active eicosanoid mediators of cellular development and inflammation (Fig 2.2B). We found a strikingly high concentration of Arachidonic Acid (AA), which increased with age (Fig 2.2B, Fig2.2D; $F(2)=34.02$, $p=3.19*10^{-8}$). Docosahexaenoic acid (DHA) and Eicosapentaenoic acid (EPA), though less concentrated than Arachidonic acid, were also present throughout development and increased in concentration with age (Fig 2A, C-D; EPA: $F(2)=77.05$, $p=4.12*10^{-12}$, DHA: $F(2)=26.17$, $p=3.91*10^{-7}$). These results suggest that the fetal brain is most rich with PUFAs at embryonic day 18.5.

Of the metabolites of these PUFAs, we focused our attention on the COX products, given their established role in neural development after birth in rodents (Lenz et al., 2013; Pellegrino et al., 2021). Consistent with our hypothesis, we found that PGD2 was the most abundant COX product in the fetal brain at all time points sampled, and its concentration differed by age with a peak in concentration at e18.5 (Fig 2.3A-B; $F(2)=6.70$, $p=.004$). We found that PGE2, which has classically been the focus of discussion about PGs in perinatal brian development (Amateau & McCarthy, 2004), was 10-50 fold less concentrated than PGD2 in the fetal brain. PGE2 concentrations also increased with age (Fig 2.3C ;$F(2)=16.82$, $p=1.5*10^{-5}$), but we did not find a sex difference in PGE2 concentrations at e18.5, despite its known role in sexual differentiation of the postnatal hypothalamus around this age. Thromboxane B2 (TXA2), a COX derivative known to affect neurite outgrowth in vitro (D. Yan et al., 2017), was detected at slightly higher levels in females than males in our sample at e12.5, though this result did not reach statistical significance in our full model. This was followed by a sharp decrease to mostly undetectable levels at e15.5 and e18.5 (Figure 2F; Age: $F(2)=22.88$, $p=1.0*10^{-6}$). Conversely, PGF2 was undetectable in any samples at e12.5 or e15.5, and was detected at low levels in both sexes at e18.5 (Age: $F(2)=38.13$, $p=1.03*10^{-8}$). 13-HODE, which is formed partially by enzymatic activity of COX (Fig 2.3D), is highly concentrated in the e12.5 fetal brain, but we had a low rate of detection at both e15.5 and e18.5, suggesting a greater role for 13-HODE in early brain development (Figure 2G; Age: $F(2)=14.21$, $p=5.4*10^{-5}$). These results suggest that PGD2 is by far the most abundant COX product in the fetal brain; the abundance of PGs generally increases over the course of fetal brain development.

Other eicosanoids with potential relevance for neurodevelopment, including 7 and 14-HDHA (Liu et al., 2022) as well as 5-, 12-, 15 and 20-HETE (Madore et al., 2020) were

present throughout fetal brain development, and had age dependent differences in concentration (Fig 2.2C; 7-HDHA: $F(2)=5.65$, $p=.0086$; 14-HDHA: $F(2)=8.44$, $p=.0013$; 5-HETE: $F(2)=5.53$, $p=.0094$; 12-HETE: $F(2)=11.15$, $p=.00023$; 15-HETE: $F(2)=5.47$, $p=.01$; 20-HETE: $F(2)=12.87$, $p=.0001$). We were generally unable to detect an leukotrienes, lipoxins, maresins, or resolvins across brain development, suggesting that these eicosanoids are either not present in the fetal brain, or have more subtle region-dependent concentrations which are relevant for brain development, but fall below our detection level in the whole brain. To summarize, we found that PUFA concentrations increase with age while eicosanoid concentrations follow different patterns of increase and decrease across ages. We found that PGD2 was the most concentrated eicosanoid throughout fetal brain development and chose to focus on it for further investigation.

Fetal brain macrophages express prostaglandin d2 synthesizing enzymes more highly than non-macrophages in open source scRNAseq datasets.

As PGD2 was expressed highly in the fetal brain, we wanted to learn more about potential cell types involved in PGD2 signaling. PGD2 is produced by a variety of cell types in adult rodents, including macrophages and neurons. Notably, postnatal microglial cells express high quantities of HPGDS, an enzyme that produces PGD2 from prostaglandin precursors (fig 1A) as well as both cyclooxygenase enzymes (Mohri et al., 2003). Therefore, we wanted to understand more about specific patterns of enzymes for PGD2 production in the fetal brain. As a first step, we identified cell type specific expression patterns of four rate limiting enzymes for PGD2 production, COX-1, COX-2, HPGDS, and LPGDS in publicly available databases of gene expression in the fetal neocortex (Fig 2.4A-C; Loo et al., 2019). A single cell RNA seq database from e14.5 fetal mouse brains(Loo et al., 2019) reported expression of rna species, Ptgs1 (COX-1), Hpgds (HPGDS) and Ptgds (L-PGDS). Ptgs2 (COX-2) was not detected in this dataset. All three detected enzymes are expressed more highly in macrophage lineages (clusters labeled as microglial and choroid plexus), than in neural populations. Interestingly the average expression of Ptgs1 (COX-1) was higher in microglial cells than “choroid plexus cells”, suggesting that parenchymal microglia rather than border associated macrophages may be producing COX-1 derived PGD2.

An important technical consideration of this dataset (Loo et al., 2019) is that macrophages make up a small proportion of fetal brain cells. Their study was not designed specifically for high powered analysis of expression in these sparse macrophage populations. Our lab has also collected a detailed database of scRNA expression in ~40,000 Fluorescence activated cell sorting (FACS) sorted e13.5 brain macrophages to allow for more detailed quantification of gene expression in these populations. We re-analyzed our dataset to determine expression levels of the four PGD2 producing enzymes in e13.5 brain macrophages (Fig 2.5A-F). Our dataset largely agreed with that of (Loo et al., 2019). We found high expression of Ptgs1 (COX-1), Ptgds (L-PGDS), and Hpgds (HPGDS) in macrophages but not neural cells. Like Loo et al., Ptgs2 (COX-2) was absent in our dataset. We also found that average expression of Ptgs1 in microglia was significantly higher than that of border associated macrophages, similar to the data collected by Loo et al, 2019. This evidence suggests that both microglia and border associated macrophages possess the enzymatic machinery required to produce PGD2, but microglia may have the capability to produce it at higher levels.

Cell type specific qPCR suggests that non-macrophages express DP1 receptors more highly than macrophages at e15.5 and e18.5.

Because macrophages have been reported to express high levels of PG synthesizing enzymes in adult and fetal brains, but expression of the primary PGD2 receptors, DP1 and DP2, was missing in these databases, we designed a RT-qPCR experiment designed for sensitive quantification of expression of PGD2 synthesizing enzymes in embryonic macrophages and non macrophages across the same 3 time points of brain development studied with LC/MS/MS. We sorted CD45+ CD11b+ cells from embryonic brains with -FACS as a proxy for embryonic macrophages (fig. 2.4). We quantified the expression of *ptgdr* (DP1) and *ptgdr2* (DP2) mRNA in the double positive fraction and also the remaining cells, which we refer to as the non-macrophage population (Fig 2.6A). These cells likely contain a mixture of neural and glial cells. Though our sample size was too small at e18.5 to confidently run stats across all ages (n=3 brains), we quantified differences in expression across e12.5 and e15.5 samples. We did not identify sex differences in any gene measured in the dataset, and grouped data by sex for remaining analyses. Age and cell types as well as their interaction were both significant in the full MANOVA model (Age: $F(6,7)=14.35$,$p=.001$; Cell type: $F(6,7)=47.23$, $p=2.5*10^{-5}$; Age*Cell Type: $F(6,7)=10.25$, $p=.003$, Fig 2.4). Genes included in the full model include both receptor types and four enzymes of interest (described in next section). Overall our power was low to detect differences across ages because we pooled multiple brains from e12.5 litters, resulting in n=3 representing the average of 8 brains per litter. DP1 expression was greater in the neural fraction than in macrophages, but we did not identify an age by cell type interaction (Fig 2.6F; Cell type: $F(2)=4.517$, $p=.055$). Overall the expression for DP2 was variable across samples because its expression neared our threshold for detection in qPCR, and we were unable to detect differences by age or cell type (Fig 2.6G). These results suggest that both DP1 and DP2 are expressed in the fetal brain throughout development, but DP1 receptors may be more consistently expressed at high levels in the fetal brain and preferentially expressed in neural cells.

qPCR confirms higher expression of Ptgs1 and Hpgds in macrophages than non-macrophages across the entirety of fetal brain development.

Given that open source seq databases only describe expression of enzymes for PGD2 production at limited timepoints, and given that some lack detection of key enzymes COX-1 and L-PGDS, we decided to quantify expression of our four PGD2 enzymes of interest alongside DP receptors with FACS and RT-qPCR. We were able to detect *ptgs1* (Cox-1), *ptgs2* (Cox-2), *ptgds* (L-PGDS) and *hpgds* (Hpgds) at all of three time points (Fig2.6B-E). We found higher expression of Hpgds and Cox-1 in macrophages than in neural cells, as well as an age by cell type interaction in Hpgds (Cox-1/cell type: $F(2)=22.79$, $p=.0005$; Hpgds/cell type: $F(2)=107.54$, $p=2.4*10^{-7}$; Hpgds/age*cell type:$F(2)=12.22$, $p=.004$. Lpgds varied highly in level of expression but was expressed more highly in non-macrophages and differed by age and cell type interaction (cell type: $F(2)=16.96$, $p=.0014$; age*cell type: $F(2)=45.43$, $p=2.07*10^{-5}$. This suggests that non-macrophages may be more involved in PGD2 signaling in early fetal development as opposed to later. Together, all of these results suggest that both macrophages and non-macrophages are equipped to receive and produce PGD2, but macrophages may be more likely producers and non-macrophages more likely receivers around mid and late embryonic brain development.

DP1 receptor antagonism during pregnancy had no impact on gene expression in the fetal brain.

After finding differences in expression of both receptors and enzymes in the PGD2 pathway in early vs mid/late development, we sought to validate a method for manipulating the PGD2 system during specific windows of embryonic brain development to test its functional role throughout embryonic brain development. We planned to administer small molecule antagonists for DP1 and DP2 intraperitoneally to pregnant mice at each of our three time points. Here we report the results of a pilot study inhibiting DP1 in utero with a specific antagonist Laripropant. We administered Laripropant at e14.5 and harvested brains of e15.5 embryos 16 hours later for qPCR. We administered two doses of Laripropant: A low dose matched the recommended daily dose in humans (2 mg/kg; n=5 brains from a single litter), and the high dose was four times this low dose (12 mg/kg; n=10 brains from two litters). Each litter was matched with a vehicle control group (DMSO high and low). We quantified the expression of 3 genes (Bcl2, Jun, Erbb4) that are involved in cell differentiation and cell death which are regulated by PGD2 signaling in other tissue types (Moniot et al., 2014). Our initial results from DP1 antagonist treated litters yielded variable results between litters, and lacked strong interpretability (Fig. 2.7A-C). Given our results, we expect that Laripropant may not impact transcription in the fetal brain. Ultimately, experiments involving DP1 and DP2 targeting with antagonists lacked face validity, but more work needs to be done to directly disrupt DP1 and DP2 signaling in utero.

Discussion

Canonical immune signals are critical for brain development (Zengeler & Lukens, 2021), and the diverse mechanisms of immune action on the developing brain are just starting to be understood. In the past several decades, PGs have been recognized as a trophic factors that modulate synaptogenesis and migration of neurons and glia in the postnatal rodent brain (Lenz et al., 2013; Pellegrino et al., 2021). Here we unbiasedly quantified both PGs and other related lipids with LC/MS/MS to test whether PGs or other lipids that may be critical for neurodevelopment are present in the fetal brain. We expected that PGE2, previously identified to have a role in early postnatal development, and PGD2, which is highly concentrated in the adult brain would be present in the fetal brain as well. We show for the first time that PGs are present in the mouse brain well before birth, even during the early days of cortical neurogenesis at e12.5. We found that PGD2 is the most highly concentrated PG in the fetal brain, and that its concentration is stable throughout our time course of prenatal brain development. We further identified that microglial cells and other brain macrophages are predominately equipped with enzymes to synthesize PGD2, while other neural and glial cell types express the DP receptors necessary for integrating PGD2 signals. Together these findings lay the groundwork for a foundational hypothesis of the role of microglial PGD2 signaling in embryonic brain development, which we discuss below. Our findings support the growing pool of evidence that microglia are poised to integrate environmental and genetically encoded signals during brain development (Chuang et al., 2021; Matcovitch-Natan et al., 2016; Nichols et al., 2020). We consider our results in light of evidence that maternal dietary lipids as well as pharmacological inhibitors of lipid synthesis during pregnancy, such as Non-steroidal anti inflammatory drugs (NSAIDs), including Ibuprofen and Acetaminophen, impact brain development and later life social behaviors.

In addition to our main finding of PGD2 concentration in the fetal brain we provide a descriptive analysis of the landscape of fetal brain eicosanoids acoss development. Our data suggests that PGD2 is 2-3 orders of magnitude more highly concentrated in the late embryonic brain than PGE2, even though PGE2 is known to have an impactful effect on hypothalamic spinogenesis with profound functional implications for sexual behaviors later in life (Lenz et al., 2018). It is possible that the smaller concentration of PGE2 is associated with a tighter regional specificity of release than PGD2. This scaling of lipid concentration could provide important clues about the distribution of PGD2 signals in the fetal brain, but more work needs to be done to localize these PGD2 signaling components in the fetal brain. In addition, future work should directly test the effects of PGD2 disruption on fetal brain development and social behavior later in life. DP1 and DP2 knockout mice as well as Hpgds knockouts have been used by multiple research groups and would be an effective tool for disrupting PGD2 signaling in the fetal brain (Hata & Breyer, 2004; Oyesola et al., 2020; Taniguchi et al., 2007; Urade & Hayaishi, 2011). Ideally, embryonic macrophages and neurons could be harvested for single nucleus RNA seq during fetal development in DP1 and DP2 knockouts to assess the role of DP singling on the development of diverse cell types. e15.5 would be an appropriate time point for this experiment, given that brain cells are undergoing multiple major developmental functions, such as division, migration, and wiring at this time. We expect that snRNAseq in these animals would reveal a similar cell type distribution of PG signaling enzymes observed in our bioinformatic and RT-qpcr studies. We expect, given high expression of DP receptors in neurons rather than macrophages, that knocking out DP1 and DP2 would have a greater impact on neuronal development, and may impact expression of genes involved in functional pathways for migration

or other major developmental functions. This study would allow for identification of putative progenitor populations that might be most impacted by fetal deletion of DP receptors, which could be followed into adulthood based on their transcriptional type and location in the fetal brain, providing opportunities to confirm the role of these populations in social behavior by directly manipulating them in adult behaving animals. Given the high conservation of at least some of the genetically encoded enzymes and receptors for PGD2 signaling across mammals (Ahmad et al., 2019), we expect that this sort of experiment could lay the groundwork to investigate whether PGD2 could have similar functions in other species, or contribute to species specific shaping of neural architecture.

Aside from PGD2, several other AA metabolites were highly concentrated in the fetal brain. Of note, 13-HODE was concentrated at similar levels as PGD2 at e12.5, and its concentration decreased with age. 13-HODE has hardly been studied in the context of brain development, but one recent study suggests that it influences axonal outgrowth in neuronal cultures(Hennebelle et al., 2020). Given that neuronal migration out of the proliferative zones into cortical and subcortical regions is occurring throughout e12.5 to e15.5 (Di Bella et al., 2021), and given the large concentrations of 13-HODE that we found in the whole brain, it is possible that it may serve as a migratory factor across multiple regions of the fetal brain during early brain development. We also found high concentrations of 12-HETE at e12.5, which decreased over our sampling of ages. Though less is known about the role of 12-HETE in developing brain cells, one study recently found that maternal dietary restriction of n-3 PUFAs during pregnancy resulted in reduced concentrations of 12-HETE in the the brains of offspring at p21, an effect which mediated enhanced levels of microglial phagocytosis in this group via regulation of complement proteins (Madore et al., 2020). This study primarily investigated the neural impacts of n-3 dietary restriction, and did not address social behavior in these animals. However they did find that their manipulation caused differences in spatial processing in the Y-maze, suggesting at least that n-3 dietary restriction is sufficient to change behavior later in life. Microglia are known to be actively phagocytosing live neural progenitor cells early in development, and are thought to be able to control the fate of neural cells via this process (Brown & Neher, 2014). Given our results that 12-HETE is highly concentrated at e12.5, it is possible that this lipid might be responsible for early developmental phagocytic properties of microglia.

Madore et al. provide just one example in a growing pool of evidence that dietary restrictions or supplementation of n-3 PUFAs during pregnancy can lead to altered neuronal development and behavior later in life. PUFAs are the primary source of membrane phospholipids that form fetal brain cells, and they cannot be generated by the body (Crawford et al., 1976). As a result, all of the necessary PUFAs for cell formation must derive from the maternal diet and transfer through the placenta. On the broadest scale, a doubling of membrane phospholipids is necessary for each neural cell division, and cell size and gray matter density are modulated by dietary DHA (Echeverría et al., 2017; Jackowski, 1996). Our results support prior findings that levels of n-3 PUFAs, such as DHA, peak in the rat and human fetal brain towards the end of pregnancy and continue to rise during early postnatal development (Green & Yavin, 1998; Martínez & Mougan, 1998). A bulk of evidence suggests that DHA may have functional implications for circuit and behavioral development. Dietary supplementation of DHA in the third trimester of pregnancy and the first years of life results in children with denser gray matter and improved performance on cognitive tasks (Mulder et al., 2018; Ogundipe et al., 2018). In rodents, DHA supplementation increases hippocampal synaptic density, suggesting potential effects both on broad cytoarchitectonic features as well as microcircuit function. Though the

behavioral impacts of DHA during development are less examined, one study showed a 40% reduction in presence of autism amongst offspring of human mothers who supplemented with Omega 3s in the second half of pregnancy (Huang et al., 2020). Given that autism spectrum disorders are characterized by differences in social cognition, this suggests that maternal PUFAs could impact social behaviors.

Importantly, it is not totally clear whether these neurological and behavioral changes are due to biological activity of large chain PUFAs themselves or their numerous metabolites. We hypothesize that the metabolites of these PUFAs, measured here, may be important mediators of the impact of maternal PUFAs on circuit development and social behaviors in offspring. We expect that each metabolite could have different roles in brain development depending on the specific cell type in which it signals, and where in the fetal brain those cells are located. It is clear that maternal diet impacts concentration of PUFA metabolites in brains of offspring measured after birth (Madore et al., 2020; Rey et al., 2018), but it is still not clear how maternal diet impacts PUFA metabolites directly in the fetal brain. We expect that our dataset describing the landscape of n-3 PUFA metabolites during fetal brain development will serve as a key resource for future work in this area. Given our findings of PGD2 concentration and function in the fetal brain, we expect that PGD2 levels could be impacted by n-3 PUFA composition in maternal diets, and it will be important for future work to determine whether restriction of supplementation of n-3 PUFAs alters circuit and behavioral development via impacts on the PGD2 system.

Although the relationship between maternal diet and PGD2 remains to be determined, recent evidence suggests that the anesthetic sevoflurane alters neuronal migration in utero by altering expression of HPGDS and subsequently PGD2 synthesis (Chai et al., 2019). Given that PG production is inducible under inflammatory conditions (Yao & Narumiya, 2019), and given the impacts of PGD2 on brain development identified here, it is possible that PGD2 could be a major mechanism by which inflammatory perturbations during pregnancy could be detected and relayed by microglia to alter brain development.

A handful of studies suggest that pharmacological compounds directly targeting n-3 PUFA enzymatic metabolism can alter the course of brain development and later life behaviors. NSAIDs,which inhibit COX enzymes, have been known to be mutagenic for developing embryos for decades, and are highly discouraged for use during pregnancy (Koren et al., 2006). Multiple studies in rats have shown the maternal exposure to Ibuprofen or aspirin, COX1 and 2 dual inhibitors, are sufficient to prevent PGE2 signaling in the MPOA and prevent masculinization of behavior (Amateau & McCarthy, 2004; Balin et al., 2020). Interestingly one prominent impact of COX-1 and 2 inhibitors during pregnancy occurs via regulation of PGD2 synthesis in the testis, where endogenous PGD2 is known to be critical for normal testis development (Ben Maamar et al., 2017; Moniot et al., 2014). Given this work and our findings, we expect that PGD2 could be disrupted by prenatal COX inhibitors in the brain. We see an increase in expression of PGD2 synthesizing enzymes between e12.5 and e15.5, which overlaps with PGD2s known effect on testis development (Moniot et al., 2014). We predict that this time window could generally be important for coordinated waves of PGD2 regulation of developmental events in mouse fetuses.

Given PGD2s clear role in controlling testis development, and evidence of PGE2s sex dependent impacts on MPOA development, one might expect to find sex differences in the expression of the PGD2 signaling system in the fetal brain. We were surprised to observe no sex differences in PGD2 concentrations, or enzyme or receptor expression in the fetal brain. Given

the large concentration of PGD2 we observed in both sexes, it is possible the PGD2 signaling may be non-sexually differentiated in the fetal brain. Alternatively, enzymes and receptors for producing and receiving PGD2 could be differentially localized amongst brain regions across sexes, a hypothesis which should be directly tested by quantifying expression of these signaling components in situ.

Perhaps more importantly, we hope to emphasize the highly complex network of COX products that is present in the fetal brain. Here we detected around five COX mediated AA metabolites in the fetal brain, a handful of which are highly concentrated (Figure 2, Table 1). Though we mainly focus on discussion of AA metabolites here, both DHA and EPA, which we detected high levels of in our dataset, are also metabolized by COX and LOX enzymes. We show that COX derived DHA metabolites, 14- and 12- HDHA are concentrated highly at e12.5. Because COX and LOX enzymes have multiple molecular targets, we advise caution in interpreting results of studies that use COX inhibitors as a tool for disrupting prostaglandins or any other particular lipid concentrations in the fetal brain. For example, animals with COX knockout or inhibition in pregnancy display a range of cognitive differences from animals with non-manipulated COX systems (Balin et al., 2020; Wong et al., 2019). These behaviors range from altered working memory, to increased marble burying, and altered social interaction(Balin et al., 2020). These findings are consistent with our results of a large landscape of COX products in the fetal brain, which may control the development of multiple diverse circuits depending on metabolite subtype. Future research should focus their attention on targeting individual COX products detected here with specific genetic manipulations or small molecule antagonists during pregnancy in order to develop a more specific understanding of how particular COX products contribute to circuit development and individual behaviors.

Interestingly, maternal diet is proposed to be a potential driver of brain expansion in carnivores and hominids (Cunnane & Crawford, 2014). Classic theories of brain evolution suggest that caloric availability for mothers in their environmental niche could either constrain brain size or facilitate brain growth over evolutionary time (Foley and Lee, 1991; Weisbecker et al., 2015). Some evidence suggests that the presence of DHA in ancient hominid diets, mainly in the form of omega-rich seafood, could have been one of the key factors contributing to brain expansion in our evolutionary lineage (Broadhurst et al., 1998; Cunnane & Crawford, 2014). This evidence aligns with the profound impacts of maternal dietary supplementation of omega 3s on neuronal growth and brain size in offspring. Given that brain expansion in hominids is thought to be one of the key drivers of social complexity amongst mammals (Dunbar, 2009), it is interesting to speculate whether PUFAs in maternal diets might have been a key factor in the evolution of sociality as well as a proximate driver of the development of circuits that encode social behaviors. Future work should investigate whether highly social species have different concentrations of PUFAs and their metabolites in the fetal brain. Perhaps PUFA metabolites, such as PGD2, are well poised to take on species specific functions in regulating brain development across lineages with different dietary fat compositions. Though these theories focus on the role of PUFAs in the evolution of neuronal tissue, it is also interesting to speculate whether PUFAs may have additional impacts on the ontology of species specific neural circuits that encode social behaviors. Or, given the known functions of microglia to phagocytose live and dead cortical progenitors to control the size of progenitor populations (Brown & Neher, 2014; Cunningham et al., 2013), perhaps PUFA signaling might impact microglial regulation of progenitor pools and have ultimate consequences for brain size across species.

Methods:

Timed pregnancies

Two female C57BL/6J mice (Jackson Labs- Product #000664) between 6 and 12 weeks of age were paired with a single male. Animals were housed in our breeding colony at UC Berkeley (AUP-2023-01-16019). The presence of a sperm plug in the female vaginal opening was visualized before 10AM the following morning. Plug positive females were separated into a female-only cage with at least one other female until the day of experiment. Plug negative females continued to pair with males on consecutive days until a plug was identified.

Brain harvest for Liquid Chromatography/Mass Spectrometry (LC-MS/MS)

Embryos were extracted from timed pregnant mice on embryonic days 12.5, 15.5, and 18.5. Brains were removed from the skull and frozen immediately in crushed dry ice. Embryonic tails were collected for DNA extraction and sex genotyping (described below). Brains were kept at -80^{o}C for up to 2 months before LC-MS/MS.

Liquid Chromatography/Mass Spectrometry (LC-MS/MS)

LC-MS/MS was performed on a panel of polyunsaturated fatty acids and eicosanoids, including: arachidonic acid (AA), Docosahexaenoic acid (DHA), Eicosapentaenoic acid (EPA), 5-Hydroxyeicosatetraenoic acid (5-HETE), 12-HETE, 15-HETE, 20-HETE, 5-oxo-ETE, 4-hydroxy Docosahexaenoic Acid (4-HDHA), 7-HDHA,14-HDHA, 17-HDHA, 12-Hydroxyeicosapentaenoic acid (12-HEPE), 15-HEPE, 18-HEPE, 13-Hydroxyoctadecadienoic acid (13-HODE), Prostaglandin E2 (PGE2), PGD2, PGF2a, 6-keto-PGF1a, 15-deoxy-PGJ2,Lipoxin A 4 (LXA4), LXB4, Leukotriene B4 (LTB4), 6-trans-LTB4, 20-hydroxy-LTB4, 20-carboxy-LTB4, LTB6, LTC4, LTD4, LTE4, Resolvin D1 (RvD1), RvD2, RvD3, RvD5, RvE1, Thromboxane B2 (TXB2), Neuroprotectin D1 (NPD1), Maresin-1, and Maresin-2 using an established protocol (Livne-Bar et al., 2017). Data was analyzed using a MANOVA model including sex and age as independent variables, and each of the 15 consistently detected lipids as dependent variables. Consistent detection was defined as a lipid being present detected in at least ⅓ of samples. Sex was removed from further analysis after failing to reach significance in the full MANOVA model. Post-hoc ANOVAs were conducted for each lipid using age as an independent variable with alpha=.01.

Sex genotyping

To extract genomic DNA, embryonic tails were placed in 100µL 10M NaOH at 98oC until tails were no longer visible. The reaction was stopped with 25 µL of Tris-HCl, and DNA was stored at 4oC until further processing. PCR was conducted with primers targeting the Sry gene (IDT; F: TTGTCTAGAGAGCATGGAGGGC, R: CCACTCCTCTGTGACACTTTAGC), using the Kappa 2G hot start genotyping kit. Sry DNA was visualized on a 2% agarose gel using Kappa Sybr Safe under UV light.

Cell dissociation for FACS

Embryos aged e12.5, 15.5, and 18.5 for FACS and qPCR were extracted and placed into ice cold 1xPBS. After embryonic tails were collected for sex PCR, whole fetal brains were removed from the skull, minced with a feather blade scalpel, and triturated with a flame-polished Pasteur pipette until pieces were approximately 1 mm in size or less. Samples were kept constantly on ice or at 4^{o}C during centrifugation and sorting. For e12.5 dissections, all brains were pooled from

each litter within sex to increase cell numbers and starting material for downstream qPCR and FACS. All brains from each embryo remained separate for e15.5 and e18.5 litters. Pooled or unpooled brain samples were spun at 1000xg for 5 minutes and re-suspended in digestion buffer (10mL 1xHBSS with Ca 2+ and Mg 2+ containing Liberase and 400 U of DNAse-I). Samples were rotated at 37ºC for 15 minutes, and triturated a final time. Next, the samples were strained on ice once through a 100um cell strainer and washed with 4 mL of cold Wash Buffer 1 (1xHBSS without Ca 2+ and Mg 2+ containing 200 U of DNAseI and 10% FBS) into a 50 mL conical tube. Cells were then strained once through a 70 µm cell strainer into a fresh 50 mL conical tube. 22 mL of ice-cold Wash Buffer 2 (1xHBSS without Ca 2+ and Mg 2+ containing 10% FBS) was spun down at 1200xg for 10 minutes. Before FACS, cells were strained a final time through a 40 µm cell strainer into FACS tubes.

Cell Sorting of embryonic macrophages

After cell dissociation, cells were stained with Fluorophore conjugated antibodies against CD11b and CD45 (Cd45.2-PE - 1:100; Invitrogen ref. no. 12-0454-83 and Cd11b-PE-Cy7 - 1:100; eBioscience cat. no. 25-0112-81). Embryonic macrophages were isolated with fluorescence activated cell sorting (FACS) by selecting CD11b+CD45+ cells. DAPI was added immediately prior to sorting at a concentration of 1:100 to assess viability. The double negative fraction, containing mostly neural progenitor cells and neurons, was also collected. Cells were sorted into Trizol LS reagent (Invitrogen 10296028) for lysis and frozen at -80oC for no more than two weeks before RNA extraction.

Intraperitoneal injection of Laripropant

Laripropant (MK-052; Cayman– CAS #571170-77-9) was dissolved in PBS containing 10% DMSO and administered at two doses (12 mg/kg and 2 mg/kg). Vehicle control contained 10% DMSO in PBS only, and was matched for injection volume with treatment groups based on animal weight. IP injections and cell harvest were balanced between groups such that each experiment always included one treatment litter and one control litter. A single injection of Laripropant or vehicle was given to each pregnant female on the evening of e14.5 at approximately 7:00pm. 14 hours later, embryos were dissected and brains were extracted into ice cold 1xPBS. After embryonic tails were collected for sex PCR, whole fetal brains were extracted into single cell suspensions as described above, lysed in Trizol LS (Invitrogen 10296028), and stored at -80ºC for up to 8 weeks before RNA extraction.

Quantitative reverse transcription PCR (RT-qPCR)

After cell storage in Trizol, total RNA was extracted from sorted or unsorted cells using the Direc-Zol RNA mini-prep kit(Zymo #R2051). RNA was reverse transcribed into cDNA using the Invitrogen superscript III kit (18080093). cDNA was amplified on 96 well plates for qPCR using Kapa Sybr Safe fluorescent probe for 45 cycles. Primers were acquired through Integrative DNA Technologies, with sequences as follows (*cox-1*- F:CCAGAGTCATGAGTCGAAGGA, R: CCTGGTTCTGGCACGGATAG; *cox-2*- F:TGAGTACGCAACGCTTCT, R:CAGCCATTTCCTTCTCTCCTGT ; *ptgds*- F:CTCCTTCTGCCCAGTTTTCCT, R:CGCCCCAGGAACTTGTCTT ; *hpgds*- F:GCACCTCGCCTTCTGAAAGA, R:GTCTGCCCAGGTTACATAATTGC ; *ptgdr*- F:AACACCGTCTCACTGTAGGCTT, R:CTGGTTTCCCAACTCATTTCTC ; *ptgdr2*- F:TCACGACTCAACCCTGTGC, R:AGCCTGCAGCCTCTCTGC ; *jun*- F:TGAAAGCTGTGTCCCCTGTC,

R:ATCACAGCACATGCCACTTC ; *bcl2*- F:GGTGAACTGGGGGAGGATTG,
R:GTTCCACAAAGGCATCCCAG ; *erbb4*- F:CGGGCCATTCCACTTTACCA,
R:GGGCTCTACCAGCTCTGTCT).

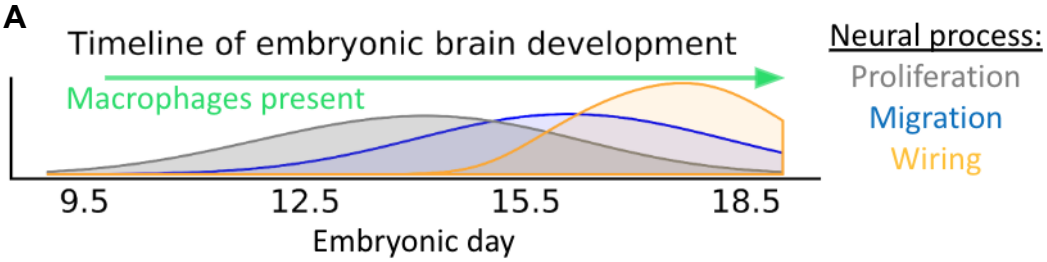
A
Timeline of embryonic brain development
Macrophages present
9.5
12.5
15.5
18.5
Embryonic day
Neural process:
Proliferation
Migration
Wiring

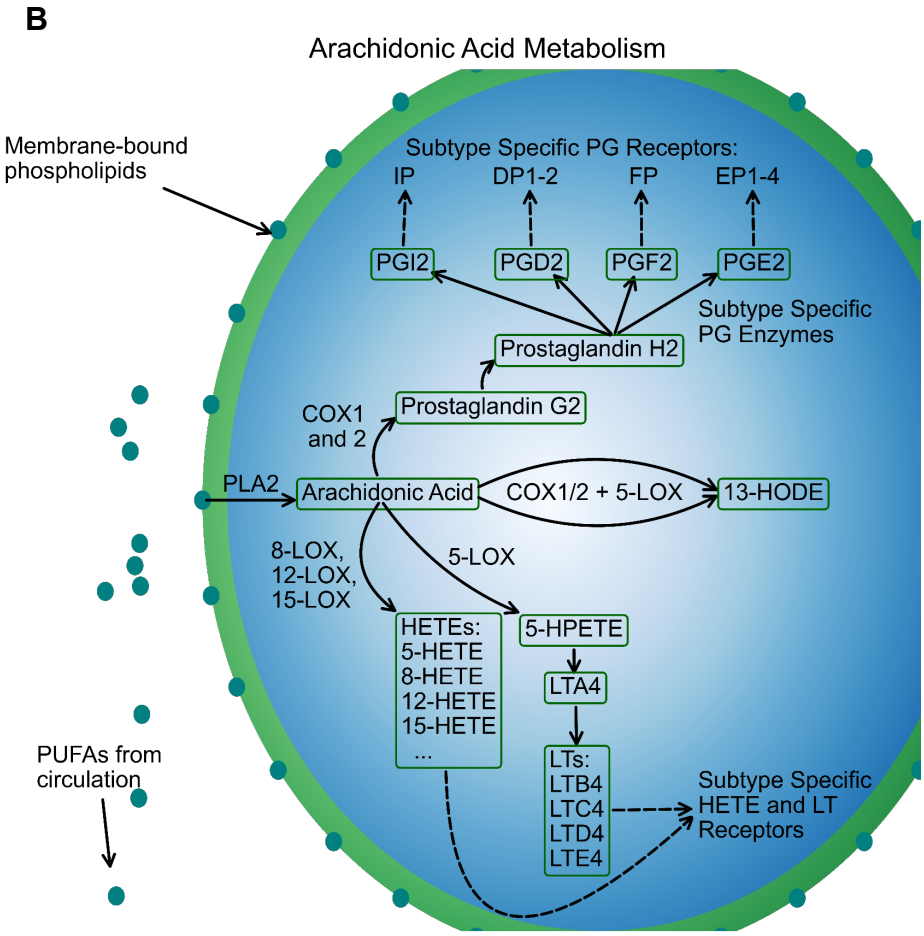
B
Arachidonic Acid Metabolism
Membrane-bound phospholipids
Subtype Specific PG Receptors:
IP
DP1-2
FP
EP1-4
PGI2
PGD2
PGF2
PGE2
Subtype Specific PG Enzymes
Prostaglandin H2
Prostaglandin G2
COX1 and 2
PLA2
Arachidonic Acid
COX1/2 + 5-LOX
13-HODE
8-LOX, 12-LOX, 15-LOX
5-LOX
HETEs: 5-HETE 8-HETE 12-HETE 15-HETE ...
5-HPETE
LTA4
LTs: LTB4 LTC4 LTD4 LTE4
Subtype Specific HETE and LT Receptors
PUFAs from circulation

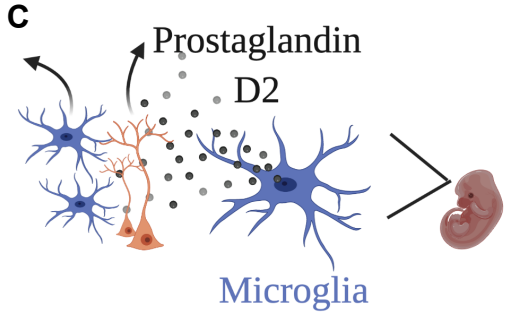
C
Prostaglandin D2
Microglia

Fig 2.1. Microglia may impact developing brain cells via signaling of arachidonic acid metabolites. A) Summary of major biological events in embryonic brain development. Macrophages are present in the fetal brain as early as proliferation begins (e9.5), and may influence proliferation, migration, and wiring of neural progenitor cells via intercellular immune signalling. B) Possible pathways of arachidonic acid metabolism in an embryonic macrophage. Poly-unsaturared fatty acids (PUFAs) from dietary intake are circulated into the brain, where they integrate into the phospholipid bilayer of cells. Phospholipase A2 (PLA2) induces release of Arachidonic Acid from the cell membrane, which is metabolized in two major enzymatic pathways that lead to Prostaglandin (PG) or Leukotriene (LT) production. Lipids are boxed in green. Solid arrows represent enzymatic activity. Dotted arrows indicate ligand secretion and binding to receptors. LTs and PGs are capable of both intracellular and intercellular secretion and signalling. C) Graphical hypothesis of signaling routes of PGD2 in the embryonic brain. Microglia may secrete PGD2, which binds to neural progenitors and other neural cell types to impact the major developmental processes listed in A (represented by arrows). Abbreviations: COX: Cyclooxegenase, LOX: Lipoxegnase, PLA2: Phospholipase A2, HETE: Hydroxyeicosatetraenoic acid, HpETE: Hydroxyperoxyeicosatetraenoic acid, HODE: Hydroxyoctadecadienoic acid, LT: Leukotriene.

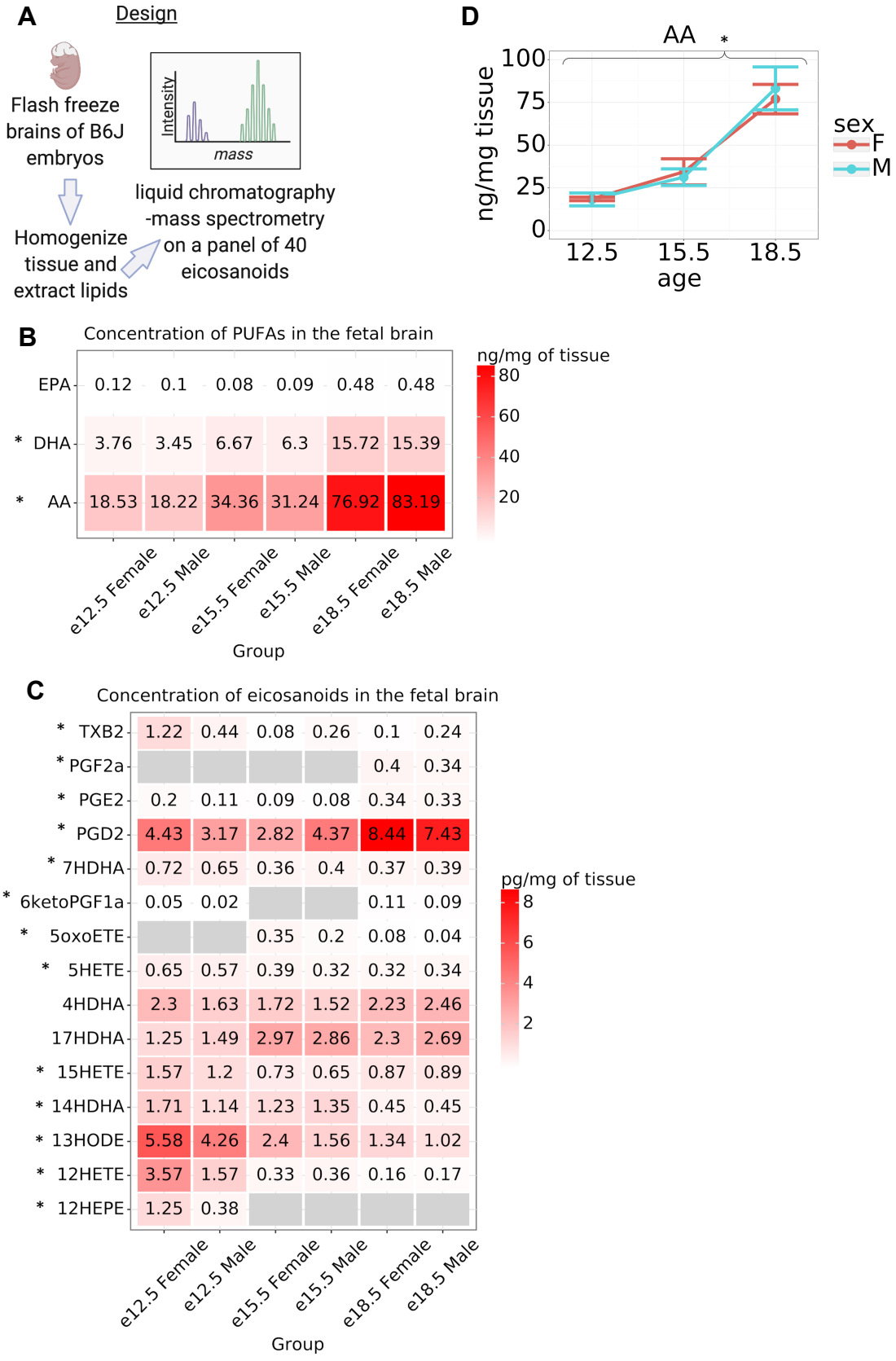
A
Design
Flash freeze brains of B6J embryos
Intensity
mass
liquid chromatography -mass spectrometry on a panel of 40 eicosanoids
Homogenize tissue and extract lipids
D
AA
*
ng/mg tissue
100
75
50
25
0
12.5
15.5
18.5
age
sex
F
M
B
Concentration of PUFAs in the fetal brain
ng/mg of tissue
80
60
40
20
EPA 0.12 0.1 0.08 0.09 0.48 0.48
* DHA 3.76 3.45 6.67 6.3 15.72 15.39
* AA 18.53 18.22 34.36 31.24 76.92 83.19
e12.5 Female
e12.5 Male
e15.5 Female
e15.5 Male
e18.5 Female
e18.5 Male
Group
C
Concentration of eicosanoids in the fetal brain
pg/mg of tissue
8
6
4
2
* TXB2 1.22 0.44 0.08 0.26 0.1 0.24
* PGF2a 0.4 0.34
* PGE2 0.2 0.11 0.09 0.08 0.34 0.33
* PGD2 4.43 3.17 2.82 4.37 8.44 7.43
* 7HDHA 0.72 0.65 0.36 0.4 0.37 0.39
* 6ketoPGF1a 0.05 0.02 0.11 0.09
* 5oxoETE 0.35 0.2 0.08 0.04
* 5HETE 0.65 0.57 0.39 0.32 0.32 0.34
4HDHA 2.3 1.63 1.72 1.52 2.23 2.46
17HDHA 1.25 1.49 2.97 2.86 2.3 2.69
* 15HETE 1.57 1.2 0.73 0.65 0.87 0.89
* 14HDHA 1.71 1.14 1.23 1.35 0.45 0.45
* 13HODE 5.58 4.26 2.4 1.56 1.34 1.02
* 12HETE 3.57 1.57 0.33 0.36 0.16 0.17
* 12HEPE 1.25 0.38
e12.5 Female
e12.5 Male
e15.5 Female
e15.5 Male
e18.5 Female
e18.5 Male
Group

Fig 2.2. Prostaglandin D2 is the most abundant Cyclooxygenase product in the fetal brain. A) Experimental design for liquid chromatography mass spectroscopy of eicosanoids in the fetal brain. Brains were harvested at e12.5, e15.5, and e18.5. B) Summary heatmap of concentrations of n-3 and n-5 polyunsaturated fatty acids (PUFAs) in the fetal brain across embryonic age and sex; Color intensity=concentration. D) Heatmap of all consistently detected lipids (passed threshold for detection in more than ⅓ of samples). C) Timeline of Arachidonic Acid concentrations in male and female embryonic brains. (* = significant by age)

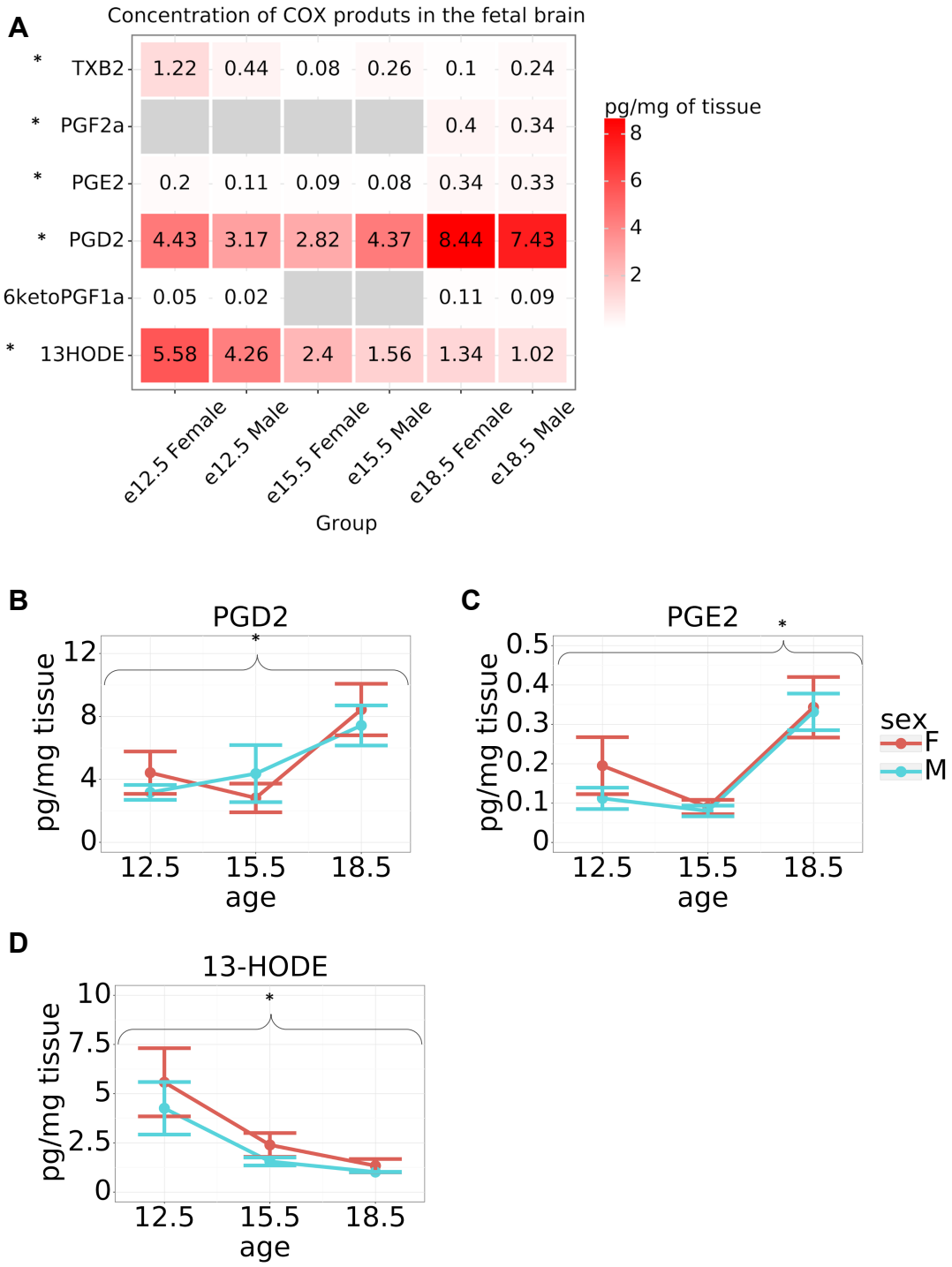
A
Concentration of COX produts in the fetal brain
TXB2
PGF2a
PGE2
PGD2
6ketoPGF1a
13HODE
1.22 0.44 0.08 0.26 0.1 0.24
0.4 0.34
0.2 0.11 0.09 0.08 0.34 0.33
4.43 3.17 2.82 4.37 8.44 7.43
0.05 0.02 0.11 0.09
5.58 4.26 2.4 1.56 1.34 1.02
pg/mg of tissue
8
6
4
2
e12.5 Female
e12.5 Male
e15.5 Female
e15.5 Male
e18.5 Female
e18.5 Male
Group
B
PGD2
pg/mg tissue
12
8
4
0
12.5
15.5
18.5
age
C
PGE2
pg/mg tissue
0.5
0.4
0.3
0.2
0.1
0
sex
F
M
D
13-HODE
pg/mg tissue
10
7.5
5
2.5
0

Fig 2.3. Prostaglandin D2 is the most abundant Cyclooxygenase product in the fetal brain. A) E) Identical data as in Figure 2.2, subsetted to display cyclooxygenase derived eicosanoids. C-E) Timeline of Prostaglandin D2, Prostaglandin E2, and 13-HODE concentrations in male and female embryonic brains across development. (* = significant by age)

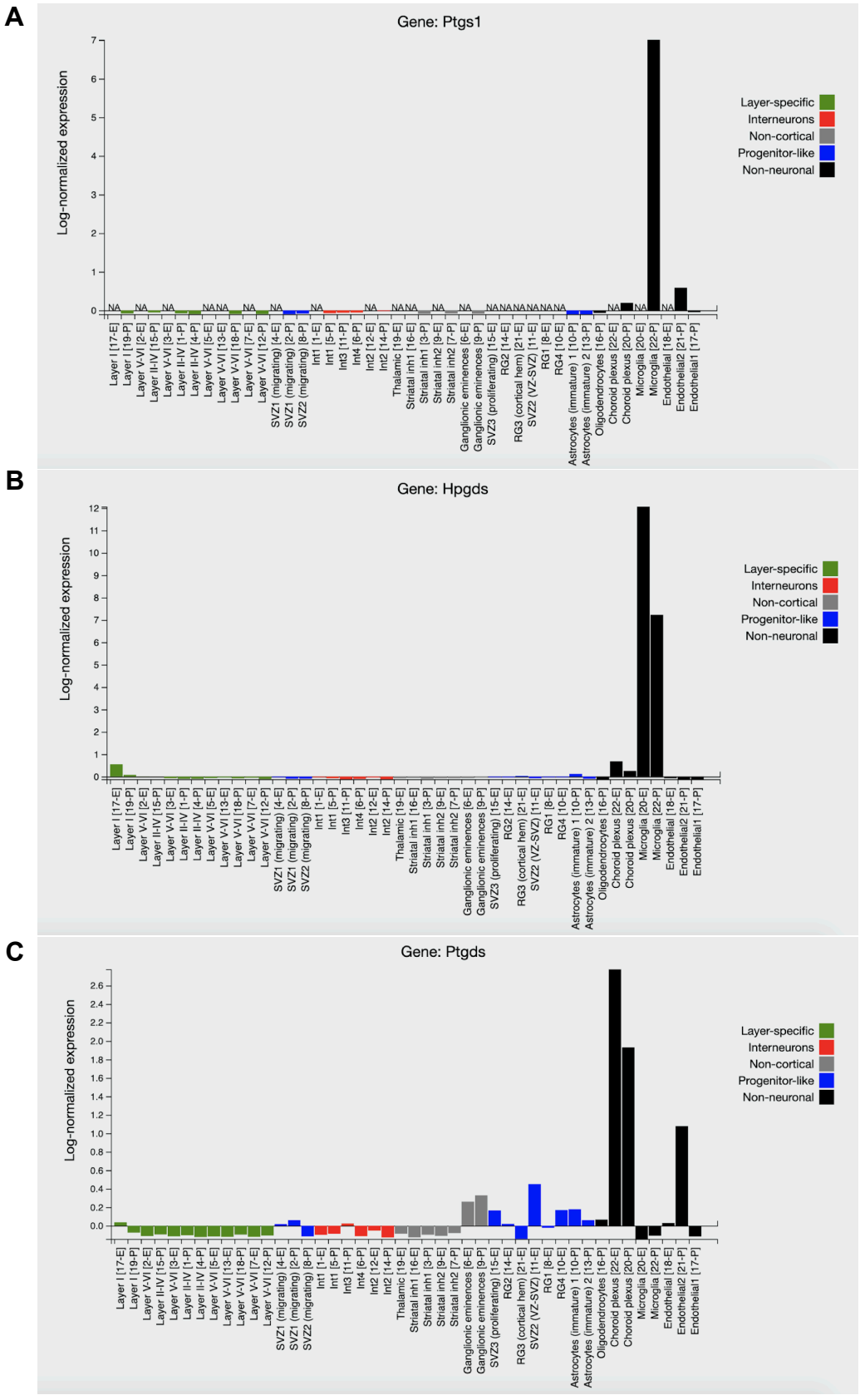
A
Gene: Ptgs1
Log-normalized expression
Layer-specific
Interneurons
Non-cortical
Progenitor-like
Non-neuronal
B
Gene: Hpgds
Log-normalized expression
Layer-specific
Interneurons
Non-cortical
Progenitor-like
Non-neuronal
C
Gene: Ptgds
Log-normalized expression
Layer-specific
Interneurons
Non-cortical
Progenitor-like
Non-neuronal

Fig 2.4. scRNAseq dataset from Loo et al. reveals that enzymes for PGD2 synthesis are abundant in prenatal brain macrophages. A-C) scRNAseq Data from e13.5 embryonic mouse brains(Loo et al., 2019). Cell type levels of expression of enzymes for PGD2 production, **A.** Ptgs1 (COX-1), **B.** Ptgds (L-PGDS), and **C.** Hpgds (HPGDS) in e13.5 embryonic brains. Proportion cells from brain macrophage clusters expressing all three enzymes is greater than that of neural and non-macrophage glial clusters (Kruskal Wallace log2FC>0.5, bonferroni corrected $p<.05$). Average expression of Ptgs1 is higher in microglia than in choroid plexus cells (Border associated macrophages).

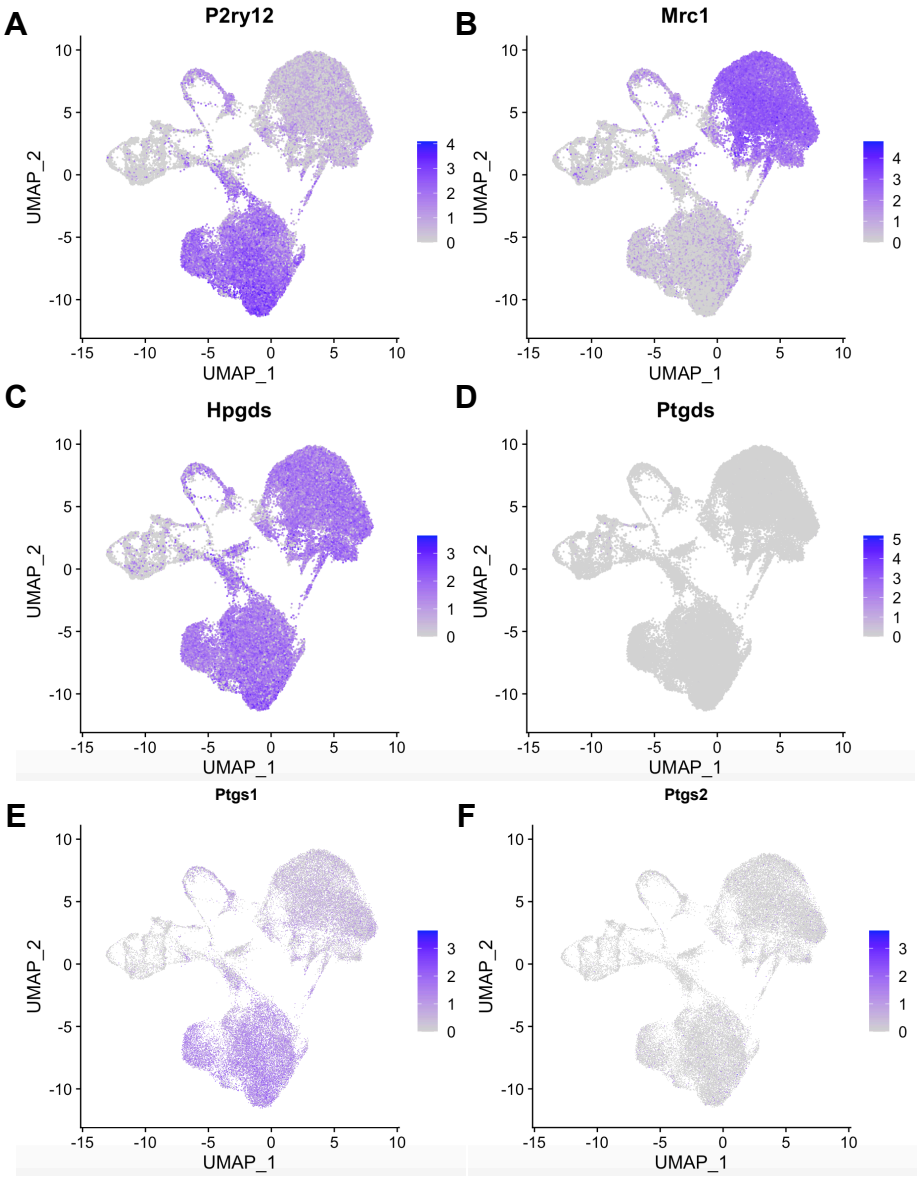
A
P2ry12
B
Mrc1
C
Hpgds
D
Ptgds
E
Ptgs1
F
Ptgs2
UMAP_1
UMAP_2

Fig 2.5. scRNAseq dataset from Nichols and Chuang et al. reveal that PGD2 synthesis are abundant in prenatal brain macrophages (part 2). A-F) ScRNAseq data of FACS isolated macrophages from e12.5 mouse brains (Nichols and Chuang et al., 2021). **A-B**) Cluster defined cell type specific markers for border associated macrophages (Mrc1) and microglia (p2ry12). **C-F)** Hpgds and Ptgs1 are more highly expressed in macrophage clusters than neural clusters (Kruskal Wallace log2FC>0.5, bonferroni corrected p<.05). Proportion of microglial clusters expressing Ptgs1 is greater than macrophage clusters (Kruskal Wallace log2FC>0.5, bonferroni corrected p<.05).

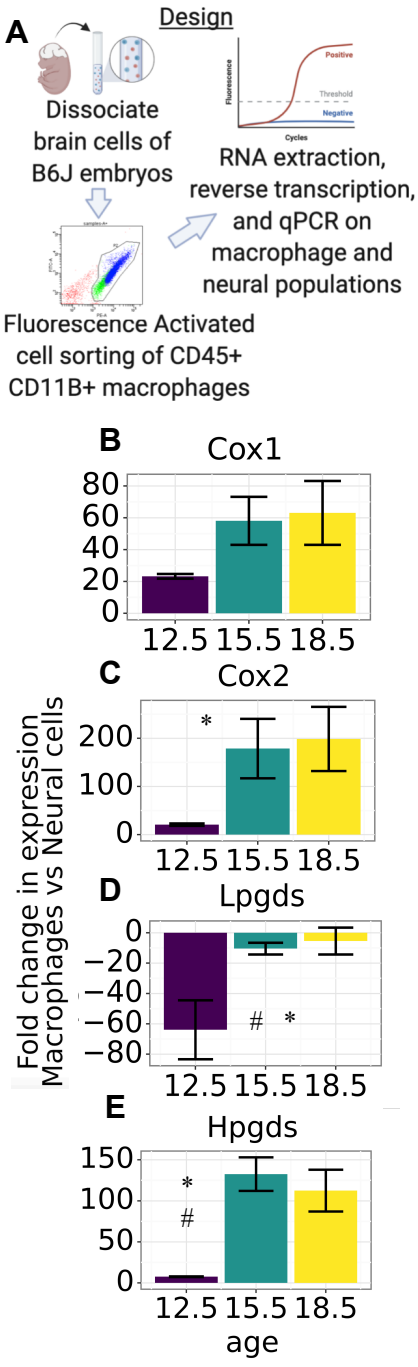
A
Design
Dissociate brain cells of B6J embryos
RNA extraction, reverse transcription, and qPCR on macrophage and neural populations
Fluorescence Activated cell sorting of CD45+ CD11B+ macrophages
B
Cox1
C
Cox2
D
Lpgds
E
Hpgds
Fold change in expression Macrophages vs Neural cells
12.5 15.5 18.5
age

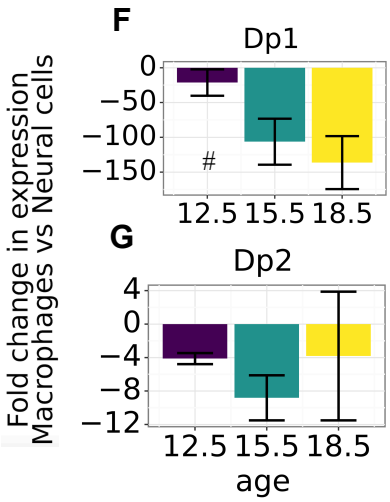
F
Dp1
G
Dp2
Fold change in expression Macrophages vs Neural cells
12.5 15.5 18.5
age

Fig 2.6. Non- macrophages in the mid to late embryonic brain highly express DP1 receptors, whereas macrophages highly express COX-1, COX-2, and HPGDS . A) Experimental design for isolating macrophages from prenatal brains with Fluorescence activated cell sorting (FACS) and quantifying gene expression with QPCR. Dissociated brain cells from 3 embryonic time points were sorted into CD11b+ CD45+ (macrophages) and the remaining fraction (non-macrophages). B-F) mRNA expression of indicated genes plotted as average difference in fold change in expression intensity between macrophages and non macrophage populations. Error bars represent standard error of the mean (e12.5 n= 3 litters, 15.5 n= 8 brains, 18.5 n=3 brains; #=p<.05 cell type; *=p<.05 age*cell type).

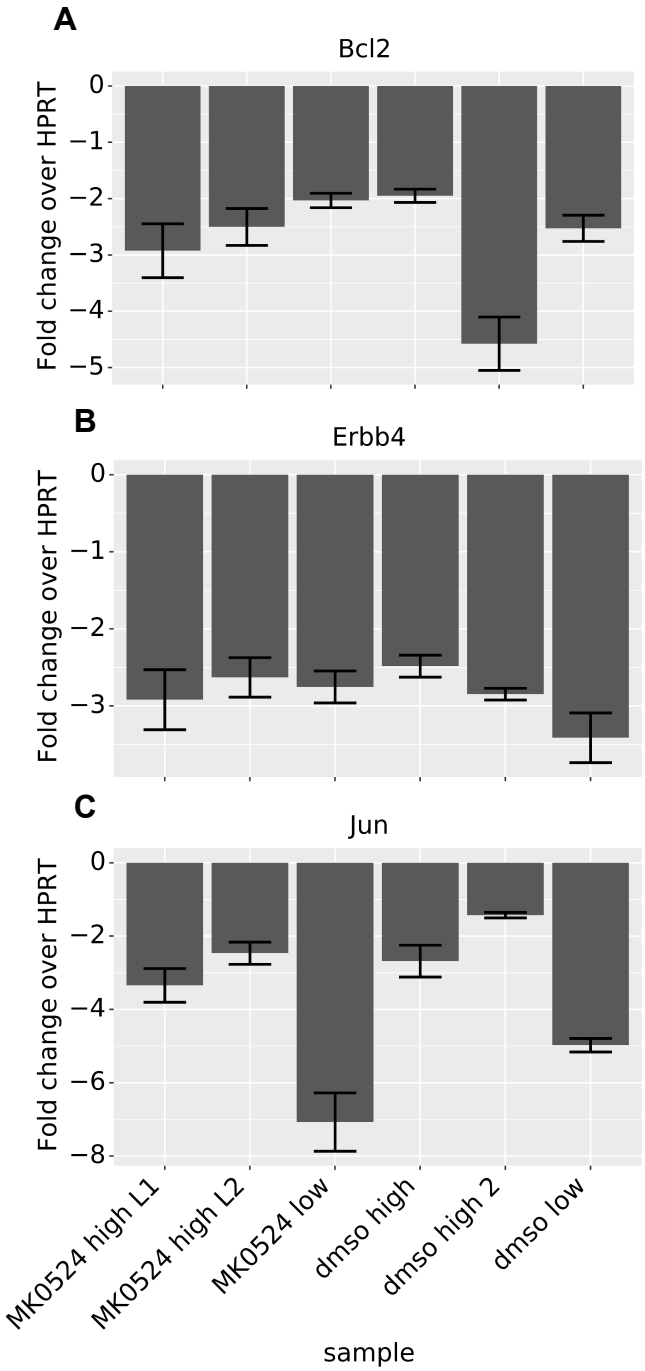
A
Bcl2
Fold change over HPRT
0
−1
−2
−3
−4
−5
B
Erbb4
Fold change over HPRT
0
−1
−2
−3
C
Jun
Fold change over HPRT
0
−2
−4
−6
−8
MK0524 high L1
MK0524 high L2
MK0524 low
dmso high
dmso high 2
dmso low
sample

Fig 2.7. Prenatal DP1 antagonist has no impact on markers of cell death and differentiation in the fetal brain. A-C) Fold change in expression of genes indicated in the above panels vs expression of Hprt. Each bar represents an averaged expression in n=5 brains (mixed sex) from a single litter. No statistical analyses were performed on this data due to failure to meet assumptions with small sample size. Error bars represent standard error from 3 technical replicates in qPCR.

References

Ahmad, A. S., Ottallah, H., Maciel, C. B., Strickland, M., & Doré, S. (2019). Role of the L-PGDS-PGD2-DP1 receptor axis in sleep regulation and neurologic outcomes. *Sleep*, *42*(6), zsz073. https://doi.org/10.1093/sleep/zsz073

Amateau, S. K., & McCarthy, M. M. (2004). Induction of PGE2 by estradiol mediates developmental masculinization of sex behavior. *Nature Neuroscience*, *7*(6), 643–650. https://doi.org/10.1038/nn1254

Balin, P. D. S., Jorge, B. C., Leite, A. R. R., Borges, C. S., Oba, E., Silva, E. J. R., De Barros, A. L., Horta- Júnior, J. D. A. C., & Arena, A. C. (2020). Maternal exposure to ibuprofen can affect the programming of the hypothalamus of the male offspring. *Regulatory Toxicology and Pharmacology*, *111*, 104576. https://doi.org/10.1016/j.yrtph.2020.104576

Ben Maamar, M., Lesné, L., Hennig, K., Desdoits-Lethimonier, C., Kilcoyne, K. R., Coiffec, I., Rolland, A. D., Chevrier, C., Kristensen, D. M., Lavoué, V., Antignac, J.-P., Le Bizec, B., Dejucq-Rainsford, N., Mitchell, R. T., Mazaud-Guittot, S., & Jégou, B. (2017). Ibuprofen results in alterations of human fetal testis development. *Scientific Reports*, *7*(1), 44184. https://doi.org/10.1038/srep44184

Berghuis, P., Rajnicek, A. M., Morozov, Y. M., Ross, R. A., Mulder, J., Urbán, G. M., Monory, K., Marsicano, G., Matteoli, M., Canty, A., Irving, A. J., Katona, I., Yanagawa, Y., Rakic, P., Lutz, B., Mackie, K., & Harkany, T. (2007). Hardwiring the Brain: Endocannabinoids Shape Neuronal Connectivity. *Science*, *316*(5828), 1212–1216. https://doi.org/10.1126/science.1137406

Bijlsma, M. F., Peppelenbosch, M. P., Spek, C. A., & Roelink, H. (2008). Leukotriene Synthesis Is Required for Hedgehog-Dependent Neurite Projection in Neuralized Embryoid Bodies but Not for Motor Neuron Differentiation. *Stem Cells*, *26*(5), 1138–1145. https://doi.org/10.1634/stemcells.2007-0841

Broadhurst, C. L., Cunnane, S. C., & Crawford, M. A. (1998). Rift Valley lake fish and shellfish provided brain-specific nutrition for early Homo. *British Journal of Nutrition*, *79*(1), 3–21. https://doi.org/10.1079/BJN19980004

Brown, G. C., & Neher, J. J. (2014). Microglial phagocytosis of live neurons. *Nature Reviews Neuroscience*, *15*(4), 209–216. https://doi.org/10.1038/nrn3710

Chai, D., Cheng, Y., Sun, Y., Yan, J., Hu, R., Zhang, L., & Jiang, H. (2019). Multiple sevoflurane exposures during pregnancy inhibit neuronal migration by upregulating prostaglandin D2 synthase. *International Journal of Developmental Neuroscience*, *78*(1), 77–82. https://doi.org/10.1016/j.ijdevneu.2019.09.001

Chen, V. S., Morrison, J. P., Southwell, M. F., Foley, J. F., Bolon, B., & Elmore, S. A. (2017). Histology Atlas of the Developing Prenatal and Postnatal Mouse Central Nervous System, with Emphasis on Prenatal Days E7.5 to E18.5. *Toxicologic Pathology*, *45*(6), 705–744. https://doi.org/10.1177/0192623317728134

Chuang, H.-C., Nichols, E. K., Rauch, I., Chang, W.-C., Lin, P. M., Misra, R., Kitaoka, M., Vance, R. E., & Saijo, K. (2021). Lytic Cell Death in Specific Microglial Subsets Is Required for Preventing Atypical Behavior in Mice. *Eneuro*, *8*(1), ENEURO.0342-20.2020. https://doi.org/10.1523/ENEURO.0342-20.2020

Crawford, M. A., Williams, G., Hassam, A. G., & Whitehouse, W. L. (1976). ESSENTIAL FATTY ACIDS AND FETAL BRAIN GROWTH. *The Lancet*, *307*(7957), 452–453. https://doi.org/10.1016/S0140-6736(76)91476-8

Cunnane, S. C., & Crawford, M. A. (2014). Energetic and nutritional constraints on infant brain development: Implications for brain expansion during human evolution. *Journal of Human Evolution*, *77*, 88–98. https://doi.org/10.1016/j.jhevol.2014.05.001

Cunningham, C. L., Martínez-Cerdeño, V., & Noctor, S. C. (2013). Microglia Regulate the Number of Neural Precursor Cells in the Developing Cerebral Cortex. *The Journal of Neuroscience*, *33*(10), 4216–4233. https://doi.org/10.1523/JNEUROSCI.3441-12.2013

Di Bella, D. J., Habibi, E., Stickels, R. R., Scalia, G., Brown, J., Yadollahpour, P., Yang, S. M., Abbate, C., Biancalani, T., Macosko, E. Z., Chen, F., Regev, A., & Arlotta, P. (2021). Molecular logic of cellular diversification in the mouse cerebral cortex. *Nature*, *595*(7868), 554–559. https://doi.org/10.1038/s41586-021-03670-5

Dunbar, R. I. M. (2009). The social brain hypothesis and its implications for social evolution. *Annals of Human Biology*, *36*(5), 562–572. https://doi.org/10.1080/03014460902960289

Echeverría, F., Valenzuela, R., Catalina Hernandez-Rodas, M., & Valenzuela, A. (2017). Docosahexaenoic acid (DHA), a fundamental fatty acid for the brain: New dietary sources. *Prostaglandins, Leukotrienes and Essential Fatty Acids*, *124*, 1–10. https://doi.org/10.1016/j.plefa.2017.08.001

Ecology and energetics of encephalization in hominid evolution. (1991). *Philosophical Transactions of the Royal Society of London. Series B: Biological Sciences*, *334*(1270), 223–232. https://doi.org/10.1098/rstb.1991.0111

Green, P., & Yavin, E. (1998). Mechanisms of docosahexaenoic acid accretion in the fetal brain. *Journal of Neuroscience Research*, *52*(2), 129–136. https://doi.org/10.1002/(SICI)1097-4547(19980415)52:2<129::AID-JNR1>3.0.CO;2-C

Harris, S. G., Padilla, J., Koumas, L., Ray, D., & Phipps, R. P. (2002). Prostaglandins as modulators of immunity. *Trends in Immunology*, *23*(3), 144–150. https://doi.org/10.1016/S1471-4906(01)02154-8

Hata, A. N., & Breyer, R. M. (2004). Pharmacology and signaling of prostaglandin receptors: Multiple roles in inflammation and immune modulation. *Pharmacology & Therapeutics*, *103*(2), 147–166. https://doi.org/10.1016/j.pharmthera.2004.06.003

Hennebelle, M., Morgan, R. K., Sethi, S., Zhang, Z., Chen, H., Grodzki, A. C., Lein, P. J., & Taha, A. Y. (2020). Linoleic acid‐derived metabolites constitute the majority of oxylipins in the rat pup brain and stimulate axonal growth in primary rat cortical neuron‐glia co‐cultures in a sex‐dependent manner. *Journal of Neurochemistry*, *152*(2), 195–207. https://doi.org/10.1111/jnc.14818

Huang, Y., Iosif, A.-M., Hansen, R. L., & Schmidt, R. J. (2020). Maternal polyunsaturated fatty acids and risk for autism spectrum disorder in the *MARBLES* high-risk study. *Autism*, *24*(5), 1191–1200. https://doi.org/10.1177/1362361319877792

Jackowski, S. (1996). Cell Cycle Regulation of Membrane Phospholipid Metabolism. *Journal of Biological Chemistry*, *271*(34), 20219–20222. https://doi.org/10.1074/jbc.271.34.20219

Koren, G., Florescu, A., Costei, A. M., Boskovic, R., & Moretti, M. E. (2006). Nonsteroidal Antiinflammatory Drugs During Third Trimester and the Risk of Premature Closure of the Ductus Arteriosus: A Meta-Analysis. *Annals of Pharmacotherapy*, *40*(5), 824–829. https://doi.org/10.1345/aph.1G428

Krieglstein, K., Strelau, J., Schober, A., Sullivan, A., & Unsicker, K. (2002). TGF-β and the regulation of neuron survival and death. *Journal of Physiology-Paris*, *96*(1–2), 25–30. https://doi.org/10.1016/S0928-4257(01)00077-8

Lenz, K. M., Nugent, B. M., Haliyur, R., & McCarthy, M. M. (2013). Microglia Are Essential to

Masculinization of Brain and Behavior. *The Journal of Neuroscience*, *33*(7), 2761–2772. https://doi.org/10.1523/JNEUROSCI.1268-12.2013

Lenz, K. M., Pickett, L. A., Wright, C. L., Davis, K. T., Joshi, A., & McCarthy, M. M. (2018). Mast Cells in the Developing Brain Determine Adult Sexual Behavior. *The Journal of Neuroscience*, *38*(37), 8044–8059. https://doi.org/10.1523/JNEUROSCI.1176-18.2018

Liu, J., Sahin, C., Ahmad, S., Magomedova, L., Zhang, M., Jia, Z., Metherel, A. H., Orellana, A., Poda, G., Bazinet, R. P., Attisano, L., Cummins, C. L., Peng, H., & Krause, H. M. (2022). The omega-3 hydroxy fatty acid 7(*S*)-HDHA is a high-affinity PPARα ligand that regulates brain neuronal morphology. *Science Signaling*, *15*(741), eabo1857. https://doi.org/10.1126/scisignal.abo1857

Livne-Bar, I., Wei, J., Liu, H.-H., Alqawlaq, S., Won, G.-J., Tuccitto, A., Gronert, K., Flanagan, J. G., & Sivak, J. M. (2017). Astrocyte-derived lipoxins A4 and B4 promote neuroprotection from acute and chronic injury. *Journal of Clinical Investigation*, *127*(12), 4403–4414. https://doi.org/10.1172/JCI77398

Loo, L., Simon, J. M., Xing, L., McCoy, E. S., Niehaus, J. K., Guo, J., Anton, E. S., & Zylka, M. J. (2019). Single-cell transcriptomic analysis of mouse neocortical development. *Nature Communications*, *10*(1), 134. https://doi.org/10.1038/s41467-018-08079-9

Madore, C., Leyrolle, Q., Morel, L., Rossitto, M., Greenhalgh, A. D., Delpech, J. C., Martinat, M., Bosch-Bouju, C., Bourel, J., Rani, B., Lacabanne, C., Thomazeau, A., Hopperton, K. E., Beccari, S., Sere, A., Aubert, A., De Smedt-Peyrusse, V., Lecours, C., Bisht, K., … Layé, S. (2020). Essential omega-3 fatty acids tune microglial phagocytosis of synaptic elements in the mouse developing brain. *Nature Communications*, *11*(1), 6133. https://doi.org/10.1038/s41467-020-19861-z

Martínez, M., & Mougan, I. (1998). Fatty Acid Composition of Human Brain Phospholipids During Normal Development. *Journal of Neurochemistry*, *71*(6), 2528–2533. https://doi.org/10.1046/j.1471-4159.1998.71062528.x

Matcovitch-Natan, O., Winter, D. R., Giladi, A., Vargas Aguilar, S., Spinrad, A., Sarrazin, S., Ben-Yehuda, H., David, E., Zelada González, F., Perrin, P., Keren-Shaul, H., Gury, M., Lara-Astaiso, D., Thaiss, C. A., Cohen, M., Bahar Halpern, K., Baruch, K., Deczkowska, A., Lorenzo-Vivas, E., … Amit, I. (2016). Microglia development follows a stepwise program to regulate brain homeostasis. *Science*, *353*(6301), aad8670. https://doi.org/10.1126/science.aad8670

McCARTHY, M. M. (2008). Estradiol and the Developing Brain. *Physiological Reviews*, *88*(1), 91–134. https://doi.org/10.1152/physrev.00010.2007

Mehler, M. F., Mabie, P. C., Zhang, D., & Kessler, J. A. (1997). Bone morphogenetic proteins in the nervous system. *Trends in Neurosciences*, *20*(7), 309–317. https://doi.org/10.1016/S0166-2236(96)01046-6

Missig, G., Robbins, J. O., Mokler, E. L., McCullough, K. M., Bilbo, S. D., McDougle, C. J., & Carlezon, W. A. (2020). Sex-dependent neurobiological features of prenatal immune activation via TLR7. *Molecular Psychiatry*, *25*(10), 2330–2341. https://doi.org/10.1038/s41380-018-0346-4

Mohri, I., Eguchi, N., Suzuki, K., Urade, Y., & Taniike, M. (2003). Hematopoietic prostaglandin D synthase is expressed in microglia in the developing postnatal mouse brain. *Glia*, *42*(3), 263–274. https://doi.org/10.1002/glia.10183

Moniot, B., Ujjan, S., Champagne, J., Hirai, H., Aritake, K., Nagata, K., Dubois, E., Nidelet, S., Nakamura, M., Urade, Y., Poulat, F., & Boizet-Bonhoure, B. (2014). Prostaglandin D2

acts through the Dp2 receptor to influence male germ cell differentiation in the foetal mouse testis. *Development*, *141*(18), 3561–3571. https://doi.org/10.1242/dev.103408

Moses, H. L., Roberts, A. B., & Derynck, R. (2016). The Discovery and Early Days of TGF-β: A Historical Perspective. *Cold Spring Harbor Perspectives in Biology*, *8*(7), a021865. https://doi.org/10.1101/cshperspect.a021865

Mulder, K. A., Elango, R., & Innis, S. M. (2018). Fetal DHA inadequacy and the impact on child neurodevelopment: A follow-up of a randomised trial of maternal DHA supplementation in pregnancy. *British Journal of Nutrition*, *119*(3), 271–279. https://doi.org/10.1017/S0007114517003531

Nichols, E. K., Chuang, H.-C., Davis, M. T., Geiger, K. M., Li, R. Z., Arnold, M. L., Lin, P. M., Misra, R., Coscoy, L., & Saijo, K. (2020). *Fetal innate immunity contributes to the induction of atypical behaviors in a mouse model of maternal immune activation* [Preprint]. Neuroscience. https://doi.org/10.1101/2020.10.09.333815

Ogundipe, E., Tusor, N., Wang, Y., Johnson, M. R., Edwards, A. D., & Crawford, M. A. (2018). Randomized controlled trial of brain specific fatty acid supplementation in pregnant women increases brain volumes on MRI scans of their newborn infants. *Prostaglandins, Leukotrienes and Essential Fatty Acids*, *138*, 6–13. https://doi.org/10.1016/j.plefa.2018.09.001

Oyesola, O. O., Duque, C., Huang, L. C., Larson, E. M., Früh, S. P., Webb, L. M., Peng, S. A., & Tait Wojno, E. D. (2020). The Prostaglandin D2 Receptor CRTH2 Promotes IL-33–Induced ILC2 Accumulation in the Lung. *The Journal of Immunology*, *204*(4), 1001–1011. https://doi.org/10.4049/jimmunol.1900745

Pellegrino, G., Martin, M., Allet, C., Lhomme, T., Geller, S., Franssen, D., Mansuy, V., Manfredi-Lozano, M., Coutteau-Robles, A., Delli, V., Rasika, S., Mazur, D., Loyens, A., Tena-Sempere, M., Siepmann, J., Pralong, F. P., Ciofi, P., Corfas, G., Parent, A.-S., … Prevot, V. (2021). GnRH neurons recruit astrocytes in infancy to facilitate network integration and sexual maturation. *Nature Neuroscience*, *24*(12), 1660–1672. https://doi.org/10.1038/s41593-021-00960-z

Rai-Bhogal, R., Wong, C., Kissoondoyal, A., Davidson, J., Li, H., & Crawford, D. A. (2018). Maternal exposure to prostaglandin E2 modifies expression of Wnt genes in mouse brain – An autism connection. *Biochemistry and Biophysics Reports*, *14*, 43–53. https://doi.org/10.1016/j.bbrep.2018.03.012

Rey, C., Nadjar, A., Joffre, F., Amadieu, C., Aubert, A., Vaysse, C., Pallet, V., Layé, S., & Joffre, C. (2018). Maternal n-3 polyunsaturated fatty acid dietary supply modulates microglia lipid content in the offspring. *Prostaglandins, Leukotrienes and Essential Fatty Acids*, *133*, 1–7. https://doi.org/10.1016/j.plefa.2018.04.003

Ricciotti, E., & FitzGerald, G. A. (2011). Prostaglandins and Inflammation. *Arteriosclerosis, Thrombosis, and Vascular Biology*, *31*(5), 986–1000. https://doi.org/10.1161/ATVBAHA.110.207449

Sampath, T. K., & Reddi, A. H. (2020). Discovery of bone morphogenetic proteins – A historical perspective. *Bone*, *140*, 115548. https://doi.org/10.1016/j.bone.2020.115548

Sharma, K., Bisht, K., & Eyo, U. B. (2021). A Comparative Biology of Microglia Across Species. *Frontiers in Cell and Developmental Biology*, *9*, 652748. https://doi.org/10.3389/fcell.2021.652748

Smith, S. E. P., Li, J., Garbett, K., Mirnics, K., & Patterson, P. H. (2007). Maternal Immune Activation Alters Fetal Brain Development through Interleukin-6. *The Journal of*

Neuroscience, *27*(40), 10695–10702. https://doi.org/10.1523/JNEUROSCI.2178-07.2007
Taniguchi, H., Mohri, I., Okabe-Arahori, H., Aritake, K., Wada, K., Kanekiyo, T., Narumiya, S., Nakayama, M., Ozono, K., Urade, Y., & Taniike, M. (2007). Prostaglandin D $_2$ Protects Neonatal Mouse Brain from Hypoxic Ischemic Injury. *The Journal of Neuroscience*, *27*(16), 4303–4312. https://doi.org/10.1523/JNEUROSCI.0321-07.2007
Thion, M. S., & Garel, S. (2017). On place and time: Microglia in embryonic and perinatal brain development. *Current Opinion in Neurobiology*, *47*, 121–130. https://doi.org/10.1016/j.conb.2017.10.004
Urade, Y., & Hayaishi, O. (2011). Prostaglandin D2 and sleep/wake regulation. *Sleep Medicine Reviews*, *15*(6), 411–418. https://doi.org/10.1016/j.smrv.2011.08.003
VanRyzin, J. W., Yu, S. J., Perez-Pouchoulen, M., & McCarthy, M. M. (2016). Temporary Depletion of Microglia during the Early Postnatal Period Induces Lasting Sex-Dependent and Sex-Independent Effects on Behavior in Rats. *Eneuro*, *3*(6), ENEURO.0297-16.2016. https://doi.org/10.1523/ENEURO.0297-16.2016
Wallace, C. H., Oliveros, G., Serrano, P. A., Rockwell, P., Xie, L., & Figueiredo-Pereira, M. (2022). *Prostaglandin D2 pathway in a transgenic rat model of Alzheimer's disease: Therapeutic potential of timapiprant a DP2 antagonist* [Preprint]. Neuroscience. https://doi.org/10.1101/2022.03.30.486444
Wang, Q., Morris, R. J., Bode, A. M., & Zhang, T. (2022). Prostaglandin Pathways: Opportunities for Cancer Prevention and Therapy. *Cancer Research*, *82*(6), 949–965. https://doi.org/10.1158/0008-5472.CAN-21-2297
Weisbecker, V., Blomberg, S., Goldizen, A. W., Brown, M., & Fisher, D. (2015). The Evolution of Relative Brain Size in Marsupials Is Energetically Constrained but Not Driven by Behavioral Complexity. *Brain, Behavior and Evolution*, *85*(2), 125–135. https://doi.org/10.1159/000377666
Whitfield, G. K., Jurutka, P. W., Haussler, C. A., & Haussler, M. R. (1999). Steroid hormone receptors: Evolution, ligands, and molecular basis of biologic function. *Journal of Cellular Biochemistry*, *75*(S32), 110–122. https://doi.org/10.1002/(SICI)1097-4644(1999)75:32+<110::AID-JCB14>3.0.CO;2-T
Wong, C. T., Bestard-Lorigados, I., & Crawford, D. A. (2019). Autism-related behaviors in the cyclooxygenase-2-deficient mouse model. *Genes, Brain and Behavior*, *18*(1), e12506. https://doi.org/10.1111/gbb.12506
Wong, C. T., Ussyshkin, N., Ahmad, E., Rai-Bhogal, R., Li, H., & Crawford, D. A. (2016). Prostaglandin E $_2$ promotes neural proliferation and differentiation and regulates Wnt target gene expression: PGE $_2$ Affects Neural Proliferation and Differentiation. *Journal of Neuroscience Research*, *94*(8), 759–775. https://doi.org/10.1002/jnr.23759
Yan, D., Liu, X., & Guo, S.-W. (2017). Endometriosis-Derived Thromboxane A2 Induces Neurite Outgrowth. *Reproductive Sciences*, *24*(6), 829–835. https://doi.org/10.1177/1933719116670037
Yao, C., & Narumiya, S. (2019). Prostaglandin‐cytokine crosstalk in chronic inflammation. *British Journal of Pharmacology*, *176*(3), 337–354. https://doi.org/10.1111/bph.14530
Zengeler, K. E., & Lukens, J. R. (2021). Innate immunity at the crossroads of healthy brain maturation and neurodevelopmental disorders. *Nature Reviews Immunology*, *21*(7), 454–468. https://doi.org/10.1038/s41577-020-00487-7

Chapter 3

Investigating differences in social behaviors of inbred mice from sub-second to multi-day timescales

Introduction:

Collecting interpretable animal behavior data in a lab setting historically requires a tradeoff between the amount of time spent scoring and interpreting behaviors and the richness of behavioral repertoires that can be documented. In the field of systems neuroscience, which faces the challenge of reconciling behavioral data with complex and under-sampled neural signals, behavioral assays which are highly controlled, have simple scoring metrics, and allow for easy repetition are generally favored over complex behavioral assays that encourage animals to elicit behaviors within their natural repertoires (Chari et al., 2023; Kong et al., 2023; Krakauer et al., 2017). This trend is particularly common in the field of social neuroscience because highly dynamic interactions between multiple individuals add a layer of complexity that can influence experimental results and interpretations (Zilkha et al., 2016). In rodents, some common ways of limiting variability caused by dynamic interactions between individuals include restraining one or more of the animals in a social interaction, presenting social sensory cues, such as odors, instead of another individual, or allowing animals to interact only for a very short amount of time (Buseck et al., 2021; Crawley, 2007; Ferguson et al., 2000; Koolhaas et al., 2013). Over time, the definitions of multiple social behaviors in rodents, such as sociability, social memory, and aggression, have become operationalized as particular patterns of performance in specific assays that inherently compromise natural patterns of behavior for the sake of reproducibility and easy correlations to brain states (Krakauer et al., 2017; Sullivan, 2009).

One of the most common social assays used in mice is the three chamber sociability assay, which involves trapping one or more animals under wire cups and measuring how much time a free roaming focal animal chooses to spend near trapped mice or empty cups (Crawley, 2007). While this style of assay somewhat effectively prevents stimulus animals from influencing the behaviors of the focal animals, it ultimately prevents animals from engaging in critical features of natural social interactions that are necessary for proper interpretation of the emotional valence and intentions driving social investigations. When observed in their entirety, social behaviors occur in sequences of stereotyped syllables which include at least four phases. These include detecting another animal, approaching, investigating, and engaging in a consummatory action appropriate for the particular context determined in the previous phases (Hashikawa et al., 2016; Wei et al., 2021). Some examples of consummatory behaviors include fighting, mating, or fleeing. Even within the class of investigatory behaviors, there are multiple sub-syllables, including anogenital sniffing and nose to nose sniffing. While both actions allow for detection of pheromonal cues, different pheromones may be present in the nose and rear that drive context specific use of either syllable (Liberles, 2014). In rodents, some common contextual variables that impact both phases of social behaviors include the sex, age, number of animals involved, environmental context, and specific genetic backgrounds of inbred strains or wild species involved (Adams, 1985; Åhlgren & Voikar, 2019; Brenes et al., 2016; Calhoun, 1956; Kingsbury et al., 2020; Y. Li & Dulac, 2018; Panksepp & Lahvis, 2007). As a most striking example, male mice paired with either a male or a female will engage in similar approach behaviors but follow with vastly different consummatory behaviors such as fighting or mating depending on the context. Even within a pair of same-sex individuals, social investigation could be followed by aggressive or neutral interactions depending on other features of the environmental context such as the length of the interaction. These behavioral nuances are not only important for the interpretation of the behavior itself, but also drive vastly different patterns of neural activation and should inform which brain regions are targeted for hypothesis driven neural investigation to begin with.

Historically, many of these contextual variables have been overlooked by neuroscientists even within controlled assays, such as the 3 chamber sociability assay mice, where the most common format involves aged matched adult males of the C57Bl/6J (B6J) strain (Zilkha et al., 2016). The insularity of these studies has led to a common presumption that the behavior of B6J animals in this assay represents the norm for mice, despite a landmark study from 2007 showing that male mice of different inbred and outbred strains exhibit marked differences in three chamber assays (S. Moy et al., 2007). While B6J typically show a preference to investigate a novel mouse over a familiar cagemate, even some strains with the most conserved genotypes, such as DBA/2, show the opposite preference (S. Moy et al., 2007). This work supports studies dating as early as the 1940's, following the invention of these strains of mice in the pet trade, show that strains such as DBA/2 and B6J exhibit differences in aggressive behaviors (Calhoun, 1956; Scott, 1942).

A common assay used to measure both investigatory and consummatory behaviors is the reciprocal social interaction test, which involves a brief, free interaction between two individuals. Variants of this assay which include different sexes, ages, and environments, are able to capture a broader range of ethologically relevant behaviors such as fighting, mating, and playing(Koolhaas et al., 2013; Panksepp & Lahvis, 2007; Ricceri et al., 2016). But these assays still require a tradeoff between time required to score behaviors and the richness of behaviors quantified. Typically the duration of these assays are limited to 10 to 30 minutes in order to focus on a reproducible segment of behavior during the first introduction of two animals and to limit the length of behavioral videos that must be scored. Though rich behavioral repertoires can be scored in this brief period, relevant behavioral interactions across longer timescales are lost. For example, dominance hierarchies in groups of male mice are typically established between two days and multiple weeks (W. Lee et al., 2019; Williamson et al., 2016). Such studies that quantify social behavior over multiple days are rare, often require sample scoring of short periods of time spread out over multiple days, and even in the best cases require focus on a small number of behaviors (W. Lee et al., 2019). Moreover, such long time-course behavioral studies are not often paired with neural or physiological data, even amongst studies using the most advanced techniques to date to record from the brains of multiple freely interacting animals while automating behavioral scoring (Fustiñana et al., 2021).

The onset of machine vision and machine learning driven behavioral recording and analysis in recent years has opened opportunities for vastly greater ease in scoring semi-natural behaviors over long timescales. These systems typically combine machine learning driven positional tracking, which identifies the movement of body parts of an animal over time, coupled with computational modeling of behaviors(Pereira et al., 2020). In the past several years, some of these positional tracking systems, including Deep Lab Cut and SLEAP have released capabilities to track multiple animals at once (Lauer et al., 2022; Pereira et al., 2022). These algorithms require many additional considerations to effectively track social positions relevant for full repertoires of behavior, but they currently work well to track multiple individuals in dynamic environments where both animals are moving with minimal obstructions. One major issue with machine learning algorithms used to track multiple animals is that they have difficulty keeping the identity of the two animals separate when they come together in close contact. As a result identities are frequently swapped and create difficulties for successfully quantifying individual behaviors in multi-animal contexts.

A recent technological advance that has helped to overcome some of these issues is the Live Mouse Tracker system, which uses a combination of Radio frequency identification (RFID)

and camera tracking to help limit identity swaps, and allow for the tracking of more than two animals simultaneously (De Chaumont et al., 2019). The Live Mouse Tracker software also uses a supervised behavioral classification system that allows for quantifying about 30 commonly observed solo and social behaviors in groups of mice. Like other supervised classification systems, behavioral instances of interest are hand chosen for an algorithm to parameterize for future identification of unlabeled events at high volume (Nilsson et al., 2020). This allows for longer durations of behavioral interactions or more experimental conditions to be used. While the eventual goal of these sorts of systems is to record brain states during extended interactions, they provide exciting opportunities to gain a more complete understanding of behaviors themselves because they can detect sub-second behaviors that unfold over days of continual social interactions. Though initial work conducted with the live mouse tracker showed that the system is effective for quantifying differences in social behaviors between genetically modified and wild type inbred mice over the course of hours, it is still barely understood how specific social behaviors unfold over the course of days at a high level of tracking resolution (De Chaumont et al., 2019).

Here I used the Live Mouse tracker system to record from groups of male B6J and DBA2 mice to determine whether strain differences in investigatory behavior in the three chamber assay previously observed in these strains can be replicated using advanced tracking technology, and to test whether specific syllables of investigatory behavior drive strain differences in behavior (S. Moy et al., 2007). I recorded groups of two same-strain animals over a 90 minute period and groups of three same strain animals over a 48 hour period to begin to understand how behavioral complexity scales with group size and multiple timescales in these strains for the first time. While my analysis focuses mainly on investigatory behaviors identified by the supervised learning software included with the live mouse tracker, I also quantify additional social and non-social behaviors between these strains.

Lastly, while supervised methods for behavioral classification are a major advance from manual scoring, additional benefits may be gained from unsupervised approaches that have the power to reveal behaviors that are relevant for the animals, but the observer does not have prior knowledge or hypotheses about. While unsupervised classification has been successfully implemented for a single freely moving animal, it has not gained traction for classification of social behaviors (Wiltschko et al., 2015). Here I developed a novel unsupervised approach to classifying social behaviors, and present null preliminary results applying this computational pipeline to recordings from the live mouse tracker.

Results

The Live Mouse Tracker successfully labels active social behaviors of B6J and DBA/2

Sexually mature, Unfamiliar B6J and DBA/2 males were recorded in trios for 48 hours periods and later paired in dyads with a novel animal for two hours. All animals were exposed to the arena in trios for the first time, followed by a second measure in dyads (Fig 3.1A). Both trios and dyads had access to a transparent red plastic nest box, food, and water dishes, but the dishes were filled with bedding only for the shorter duration experiments with dyads (Fig 3.1B-C). The live mouse tracker scored active social behaviors occurring outside of the nestbox with high accuracy, and both quality of tracking and as well as accuracy of behavioral scoring visibly decreased in the nest box or when animals were positioned in the same location with minimal movement for several minutes at a time (Fig 3.S1H). I subsetted data to focus on active social contacts outside of the nest box for most behavioral events. Though animals spent most of their time in the nestbox and this subsetting strategy was substantial, I was able to quantify tens of thousands of social contacts per animal over the course of the 48 hour experiment and hundreds of social contacts per animal over the two hour experiment (Fig 3.2B, Fig 3.6A). Animals were generally active most during the initial hours of the experiment, which occurred 2-3 hours before the beginning of the first dark phase, and during the dark phases of their light cycle (Fig 3.1F). Behavioral events accurately scored by the live mouse tracker system ranged from 0.1 seconds to 15 seconds in duration (Fig 3.S1A-G).

DBA2 Trios spend more time in social contact than B6J trios

Given that DBA2 mice are known to be more aggressive than B6J animals, and given that unfamiliar and sexually mature males tend to be aggressive towards one another we expected that DBA2 animals may exhibit more social contacts. Across the entirety of 48 hour trio experiments, DBA2 trios spent significantly more time in social contact ($t(11)=4.09$, $p=.002$), defined by moments when the detected bodies of multiple animals were physically touching (Fig 3.2A-3.2C). Interestingly, the number of social contacts did not differ significantly between the strains. As a first pass analysis, we further quantified subtypes of social and non-social behaviors including nose to nose, nose to rear, and side by side contacts as well as group size, and time spent moving or stationary when alone across the entire experiment. We subsetted these behaviors into two groups: solo behaviors and directional social behaviors where each animal counted as a single sample, and non-directional social behaviors where joint interactions between two animals counted as a single sample. Solo/Directional behaviors included moving while alone, stopped while alone, and nose to rear contacts. Non-directional behaviors included side by side contacts, nose to nose contacts and general contact in groups of two. Both models included numbers and duration of events as dependent variables. We found an overall effect of genotype on behavior for both Solo/Directional events ($F(6,32) = 9.30$, $p = 3.42*10^{-6}$) and Non-Directional events ($F(6,32) = 9.80$, $p = 3.86*10^{-6}$) and post-hoc tests identified that DBA2 animals spent significantly more time in groups of 2 over the course of the experiment ($t(37) = -4.83$, $p = 2.43*10^{-5}$), which likely is driving the effect of higher duration of social contact seen in this strain (Fig 3.2C-D). No other social behaviors differed between strains across the entire experiment, but B6J animals spent more time moving alone ($t(37) = 5.89$, $p = 9.05*10^{-7}$), and had higher numbers of events moving alone ($t(37) = 6.52$, $p = 1.25*10^{-7}$) or stopped alone ($t(37) = 5.52$, $p = 2.74*10^{-6}$).

DBA2 Trios spend more time in nose to rear investigations in the second dark phase
Given the long time course of our study, we wanted to better understand if specific behaviors occurred in a time-dependent manner. As expected given our subsetting strategy, most of the behaviors we quantified occurred during active periods at night, and we focus on these times for our analysis. Given previous work showing that DBA2 animals engage in more social investigation of novel animals in the three chamber sociability assay (S. Moy et al., 2007), we expected that DBA2 animals would be more social during the start of the assay. For statistical analysis we used repeated measures MANOVA with experiment hour and genotype as independent variables. At the broadest level, we found significant interactions between genotype and experimental hour for both solo/directional behaviors ($F(48,1813)=3.13$, $p<.001$) and undirected social behaviors ($F(48,1813)=2.75$, $p<.001$). Though we present the hourly trends for duration and number of events for all syllables measured (Fig 3.3 ,Fig 3.4, Fig 3.5, Fig 3.S2, Fig 3.S3, Fig 3.S4), we focused post-hoc analyses on the durations of nose to nose, nose to rear, and side-by-side contacts to increase our power to detect effects over so many time points. Interestingly, DBA2 animals began to express these specific syllables for longer durations than B6J in the second dark phase of the experiment, but not at the beginning of the experiment (Fig 3.3). During the second dark phase DBA2 animals spent more time making nose to rear contacts at 10PM, 11PM, and 12AM (10PM: $t(37)= -3.84$, $p=.032$; 11PM: $t(37)= -3.80$, $p=.036$; 12AM: $t(37)= -4.33$, $p=.008$; Bonferroni corrected p values), nose to nose contacts at 12AM ($t(37)= -3.79$, $p=.036$), and side to side contacts at 11PM and 1AM (11PM: $t(37)= -3.74$, $p=.042$; 1AM: $t(37)= -3.69$, $p=.049$. Notably these significant values represent the peak times where DBA2 animals spend longer making these social contacts, but differences between the genotypes gradually ramp up and down over the course of the second dark period. To our surprise, we did not find any differences in nose to nose or nose to rear investigations during the first hour of the experiment, or during the first dark phase (Fig 3.3A). We note that for each of these syllables, the number of events generally follows similar patterns over time . As expected, this is true also for duration spent in contact in groups of two, which should consist of multiple of the specific social syllables we describe here and others (Fig 3.4). We also note that time spent moving alone generally follows the same pattern as social contacts, and B6J animals exhibit a trend for more solo activity during the second dark phase than DBA2, although we did not quantify this directly with post-hoc statistical tests (Fig 3.5).

DBA2 dyads engage in longer durations of social contact than B6J dyads
Similar to experiments in trios, DBA2 dyads display longer durations in social contact but similar numbers of social contacts than B6J animals across the entire duration of the two hour experiment ($t(13)=2.78$; Fig 3.6A-D). We found an overall effect of genotype on Solo/Unidirectional behaviors ($F(4,294)= 71.8$, $p< 2.2*10^{-16}$), and post hoc tests revealed that B6J animals also displayed more solo behaviors. This included more time spent moving alone ($t(3.46)=28$ $p= .002$), a higher number of events classified as moving alone ($t(3.06)=28$ $p= .005$), and a higher number of events characterized as being stopped alone ($t(3.0)=28$, $p=.005$) (Fig 6C-D). Non-directional social behaviors did not differ by genotype suggesting that no single social syllable drove the effect of difference in social contact time across genotypes.

DBA2 and B6J dyads show similar trends in social behavior over time

Similar to experiments in trios, we chunked this experiment up into 10 minute blocks to assess whether specific syllables differed during specific times in the experiment (Fig 3.7 and Fig 3.8). Repeated measures MANOVA revealed a significant gene by experiment time interaction on solo/undirected social behaviors ($F(11,336)=2.55$, $p=.004$), but not directed social behaviors ($F(11,156)=1.18$, $p=0.309$; Fig 7). Post hoc tests to identify differences in social behavior across genotypes over different times in the experiment revealed a significant interaction between experiment minute and genotype on the number of nose to rear contacts from 30-40 minutes and from 50-60 minutes as well as the total duration of these events from 50-60 minutes (Fig 3.8A-D; 30m number: $t(28)=3.49$, $p=.002$; 50m number: $t(28)=2.82$, $p=.009$; 50m duration: $t(28)=2.85$ $p=.008$). In all cases, B6J animals express higher numbers and durations of nose-rear contacts. Ultimately the social behavior of DBA2 and B6J dyads was largely similar across the time course of the experiment with few remarkable differences in social syllables.

Unsupervised clustering did not produce reliable behavioral syllables

While the supervised analysis from the live mouse tracker package was able to identify multiple subtypes of social contact and investigation, I attempted to classify dyadic social behaviors in more detail using unsupervised clustering. Given previous work showing that social behaviors occur in sequences of syllables, I chose to model small units of behavioral syllables over sub-second to second long timescales that could potentially give rise to larger social sequences. When manually scoring supervised events, it was clear that these events often took place within sequences, which were composed of multiple types of investigation, chase, fleeing, and fighting. We found that frequency and duration of different social behaviors scored by the live mouse tracker within pairs of animals were generally more correlated to one another than to non social behaviors, raising a possibility that multiple social syllables could be happening around the same instances of social contact (Fig 3.S6A-H).

Given that functionally similar social behaviors can occur in different areas of the arena and at different timescales, I chose to model space and time independent features of behavioral syllables such as relative speeds, accelerations, distance and direction of the nose centroid and rear of each animal in a pair. To allow for functionally similar syllables of different lengths, I adapted a changepoint detection approach used as a preprocessing step for clustering motor behaviors in mice. I used distance between two animals as input for changepoint detection to attempt to segment for syllables that could be characterized by closeness in a pair (Fig 3.9A). After collapsing these variables into a set of time series statistics, including autocorrelation coefficients, means, and variation in the time series over different time windows in each syllable, I dimensionally reduced the data with PCA and clustered using K-means. This approach yielded several clusters that had little relevance for specific behavioral syllables (Fig 3.9B-G). No identifiable pattern was observed during manual scoring. To identify whether specific clusters may have unique signatures of motor features that were used as input to the model, I visualized timewarped representations of each initial feature used for time series modeling over all syllables within a cluster. Time warping revealed no consistent patterns in specific features that may be relevant for defining clusters, suggesting that this modeling approach was inadequate to cluster behavioral syllables.

Discussion

Here we used postural tracking and machine learning based analysis software to classify basic syllables of social behaviors in B6J and DBA2 mice. In our data we see behavioral signatures that closely resemble previously observed differences in social investigation and aggression between these strains(Calhoun, 1956; S. Moy et al., 2007), while describing the behavior in more depth. We believe that this is one of the first examples of a study that describes social behaviors at multiple timescales ranging from the sub seconds to days, and lays the groundwork for more complex time series modeling to describe the relationship between social behaviors at these timescales in more detail.

Our main finding is that DBA2 animals spend more time making nose to nose and nose to rear investigations in the second dark phase during a period of 48 hours of continuous recording in groups of three. Given previous findings that suggest that DBA2 animals spend more time in social investigation than B6J in the three chamber sociability assay (S. Moy et al., 2007), which lasts only 10s of minutes, we were surprised that we did not see more social investigations by DBA2 early on in our recordings of trios or dyads. Given that our animals were most active during the first hour of the experiment and given that our behavioral arena was over twice as large and enriched as compared to a conventional three chamber assay, we suspect that animals spent a lot of time investigating the environment during this time. This pattern of activity and exploration is typical of mice who are introduced into a novel enriched environment (Kazlauckas et al., 2011). We suspect that three highly active animals exploring the environment in similar ways are likely to run into one another, which could explain the high rates of social contact across both groups during this period of time. We noticed that a substantial portion of nose to nose contacts in both genotypes came from joint exploration of the environment, where one animal cued another animal to investigate a specific area in the arena. We have yet to quantify the proportion of joint explorations in our data, but it is possible that a high rate of these events in both genotypes occurs at the onset of the experiment when animals are generally exploring their environment. To our knowledge, joint explorations have not been documented in other studies, even ones that place freely moving animals into a new environment. It is however known that specific hippocampal populations encode the trajectory of other animals(Omer et al., 2018), raising a possibility that related populations of neurons may be involved in the joint exploratory behaviors we observed. It will be interesting to quantify these events in detail and perform follow up studies aimed at understanding if these events function to provide information about the environment, another animal, or both, and whether specific neural populations encode joint explorations vs other types of nose to nose contacts.

We did quantify that DBA2 trios spent more time in contact in groups of 2 in the first dark period. We suggest that animals in our experimental context exhibit more behavioral subtlety than in a traditional short duration social interactions between freely moving or trapped animals, both in the content of their behavioral syllables but also the time course over which they express particular syllables. Overall this finding highlights some potential complexity in attempting to quantify social phenotypes over a short timespan, which may be more the result of stress of changing environments and environmental exploration than intentional social interactions. While the first moments of social interaction can undoubtedly be important, it is possible that a broader array of hard-wired social syllables of natural behaviors unfold over a longer timescale(Williamson et al., 2016). Notably, there has been an increasing trend in recent years to measure behavior directly in the homecage, which could mitigate stress of environmental relocation and help promote natural behaviors. Although similar systems as live

mouse tracker exist for video tracking of a single animal, they are low-throughput and not yet developed for tracking social behaviors of multiple animals (Grieco et al., 2021).

Male mice are frequently aggressive towards one another, and we expect that the social investigations we observe are a function of aggression. The most advanced model of these behaviors in aggressive contexts suggests that sequences of investigations occur at distinct times from aggressive sequences that include tail rattling, fighting, and lunging(W. Lee et al., 2019). Although we have not quantified it directly, we observe these behaviors directly adjacent to aggressive consummatory behaviors such as fighting and mounting in our dataset. This dataset could serve as an interesting tool to test this current model of aggressive sequences with more consistent sampling of behaviors. Given that social hierarchies can take weeks to fully form in mice, we are not surprised to see notable differences in these investigatory behaviors even 24 hours after the mice were introduced to one another (W. Lee et al., 2021). It is possible that the increased social investigation we observed in DBA2 animals during the second dark phase may be a sign that the animals are beginning to display more aggressive behaviors and begin to form a hierarchy. This explanation could fit with prior evidence that DBA2 mice exhibit higher levels of aggression than B6J mice(Calhoun, 1956). Future work should test this hypothesis directly by quantifying natural aggressive behaviors in this specific data set and others.

Although I hoped to identify and quantify a broad range of aggressive behaviors with my unsupervised classification strategy, this strategy did not yield the intended results. Despite the inadequacy of my model, I frequently observed that social contacts quantified by the LMT were surrounded by chases, fights, mounts, circling, biting, and other aggressive behaviors during scoring and manual validation of LMT classified events. This suggests that the lack of classification in my model was due to computational shortcomings rather than lack of these behaviors in the data. One potential cause of the lack of specificity of my clustered syllables was not subsetting enough of the data to focus on only social behaviors. My strategy subsetted the data to moments where animals came within two body lengths of one another, in an attempt to include moments of approach and fleeing as well as close social interactions which occur over a range of distances between animals. However during manual scoring of the LMT events, it was clear that the animals often pass by one another in minimally social events; possibly because the dimensions of the enclosure are relatively small and they all frequently spend time near the food, water, and along the edges of the arena (Fig 3.1D). Some of the missed tracking moments for simple contacts, even from the supervised LMT analysis, occur when two animals are near one another but not directly interacting. This suggests that an unsupervised model with no training data may have equal or more difficulty in filtering through the noise of these events.

Though I have not yet manually quantified the aggressive behaviors that are present in the data, I developed a behavioral scoring tool that allows me to watch the video of hundreds of classified events every hour, and an important next step will be to manually note the proportion of investigatory behaviors surrounded by specific aggressive behaviors using this powerful tool. It is clear through extended observation of the behavioral videos that velocity and acceleration information could be critical for defining changepoints for a range of aggressive behaviors. In particular, fast approaches, fleeing, circling, and fighting, all of which precede or follow nose to nose and nose to rear investigations, appear to involve momentary and rapid fluctuations in velocity and acceleration. I hypothesize that neutral social investigations without these consummatory aggressive events might be characterized by lower rates of velocity and acceleration in the surrounding time series data. I am currently testing this hypothesis directly by analyzing the time-course of velocity and acceleration around nose to nose and nose to rear

investigations labeled by the live mouse tracker software, and subsetting high and low velocity events to score for the proportion of aggressive behaviors in each case. If simple metrics of velocity and acceleration, such as average values preceding and following social investigation, are predictive of some aggressive events, I plan to use these high and low velocity behavioral sequences as a tool for developing an unsupervised pipeline that is more effective at classifying specific aggressive syllables given more refined data. I expect that subsetting the data around moments of live mouse tracker- classified investigations may help filter additional noise. Potentially a combination of distance and velocity is needed to adequately determine boundaries between social behavioral syllables with changepoint detection, and using this approach during windows around LMT identified events could allow for more effective input into an unsupervised model. Generally speaking, this sort of semi-supervised approach may be the most appropriate for classifying social behaviors at this point. Even relatively advanced neural networks, such as variational autoencoders are not able to characterize social behaviors in rodents based on positional tracking data to the level of detail that a human observer can (Bordes et al., 2023; Yi et al., 2022). Either way, finding which unsupervised models have explanatory power to generate parameters that adequately describe general features of social behaviors in rodents and other species is an important next step in automating quantification of social behaviors and identifying relevant behavioral features that human observers have not considered.

One of the most advanced unsupervised algorithms is MoSeq, which is able to classify both motor syllables of a single mouse that occur over multiple durations, as well as the assembly of these syllables into longer sequences of motor behaviors (Wiltschko et al., 2015). MoSeq accomplishes this through a mixture of supervised and unsupervised model layers, which ultimately classify a complex repertoire repertoire of over 70 possible motor behaviors with minimal a priori labeling. Similar to MoSeq, I utilize changepoint detection in order to include behavioral syllables of multiple lengths within a single classified type of syllable, which is an obvious feature of animal behaviors. This approach also creates a challenge for most machine learning models, which are not designed to handle time-series data of multiple lengths. It is possible that my model fell short because I reduced the time dimension into parameters of time series models to prevent this issue. Ultimately creating a more faithful replica of MoSeq, which incorporates multi length sequences into multiple layers of their model, could be a more impactful way of modeling social behaviors.

It is important to note some additional shortcomings of the supervised analysis with the LMT software. Because tracking and scoring of behaviors was minimally effective in the nest box and when animals were stationary for long periods of time, we were forced to subset tracking instances to those in the open field during active periods. This potentially limited our ability to detect interesting and relevant social interactions. For example, social grooming, or barbering, can be a signature of aggression in established dominance hierarchies which occurs during mostly stationary interactions (Long, 1972). A critical next step to accurately classifying social behaviors in diverse situations will be to advance tracking technologies so that they can maintain identities of multiple animals during times of close interaction and minimal movement over long stretches. This innovation will be critical not only for tracking mice, but other species of rodents such as voles, which huddle together for long periods as a primary mode of social interaction.

After subsetting moments of poor tracking, the LMT scoring system has fairly good accuracy, ranging from 80%-95% for the specific behaviors we presented here. However there are still notable moments of tracking loss that make up a smaller portion of tracking errors that

should be easily correctable. For example, reflections off the water bowl account for several percent of the tracking errors for social events. I plan to continue to filter the events in this dataset based on smaller criteria such as the location of the water bowl, in order to refine the tracking efficiency and improve confidence in the results presented here. Despite some of these errors, many missed tracking events frequently confused different types of social contact rather than social and non-social events. This suggests overall that many of the missed tracked events have some relevance for broad social behaviors.

Interestingly, though B6J and DBA2 are highly genetically related, they still exhibit sizable differences in behavior. Though the genetic basis for differences in behaviors has not been identified in these strains, a logical follow-up to this work will be to connect genes to physiology and behavior. Generally, we hope this research provides a point of pause for research groups working with the predominantly used B6J. The operationalization of mouse social or other behaviors as typical behaviors of B6J on standardized tasks should be concerning given that behavior is strikingly different in animals with minute and arbitrary genetic variation. Comparative work classifying genetic variation across mouse strains suggests that B6J and DBA2 may differ by about 5000 SNPs and hundreds of InDels, found in this study between B6J and closely related DBA/1J (Doran et al., 2016). By contrast the genomes of an average set of humans is thought to vary by over 3 million SNPs and thousands of InDels, and the genomes of wild mice are thought to be even more variable (Phifer-Rixey & Nachman, 2015; The 1000 Genomes Project Consortium et al., 2015). Although we didn't use wild mice in this study, it is possible that wild species would escalate to lethal aggression in an experimental design like this one. In the field of neuroscience, had our choice of model genetic mouse been different, would we consider a different set of baseline social behaviors to be the norm for mice? What can we hope to claim about the function of neural circuits that encode specific behaviors, if the specific behaviors we are studying are artifacts of a century of genetic modification from inbreeding and circular experimental designs?

Methods

Animals and Housing

All animals for this study were produced by our breeding colony at the University of California Berkeley (AUP-2023-01-16019), and founder animals were acquired from Jackson Labs (C57/Bl6J: #000664; DBA2/J:#000671). All animals were males between the ages of 8 and 12 weeks old. A total of 21 B6J animals and 18 DBA2 animals were used. Mice were housed in groups of 3 to 4 after weaning until shifting their housing for the experiment. Two weeks before the start of the experiment, each animal was given a suprascapular injection of a unique RFID chip (Biomark APT12/ FDX-B), and immediately placed into housing with a female to initiate full neural maturation associated with exposure to a female (Li & Dulac, 2018). 2-3 weeks after this housing change, animals were introduced to the behavioral arena with non-sibling novel animals for the experiment.

Behavioral recordings

Behavioral recordings were acquired using the live mouse tracker rig and software (De Chaumont et al., 2019). The rig was set up to the exact specifications noted in their set-up instructions (livemousetracker.org), except the arena walls measured 50cm in height. The dimensions of the arena are 50cm by 50cm and all video recordings were taken using an Xbox Kinect sensor V3 (Microsoft) with depth sensing capabilities. The arena was filled with standard wood chip bedding, and did not include nestlet or other bedding materials because they interfere with video tracking. Three novel animals were placed into the arena between 5 and 6 pm, at least two hours before the beginning of the dark cycle at 8pm. The light cycle in the behavioral recording room matched the animal housing room, which was 13L 11D. Trios were left in the apparatus for 50-52 hours, during which time they were provided a bowl of food and water. Before the experiment started I tested that food and water consistently lasted the animals 50-52 hours, and during the experiment, animals were recorded uninterrupted for food and water refills. After the end of the 50 hour experiment, animals were removed from the live mouse tracker rig to a standard mouse cage in their original housing room with the same group as used for the experiment. All animals were kept in this new housing arrangement for one week before re-entering the arena with one other novel animal.

Data cleaning for supervised classification and manual event scoring

All data processing and analysis was done in python. All data used from the live mouse tracker system was subsetted at times when the instantaneous velocity of each animal was no more than 80 cm/s, as moments above this threshold were frequently characterized as tracking swaps and inaccurate jumps. Behavioral events classified by LMT were generated using their default parameters, scored manually for accuracy, and the parameters were adjusted to capture the most true positive events. Nose-Nose, side-by-side contacts, move isolated and stop isolated were subsetted to a minimum of 4 frames (recordings are 30 frames/sec) and a maximum of 210 frames. Nose to rear contacts were subsetted to a minimum of 7 frames and a maximum of 210 frames. Group2 and Group3 events were subsetted to a minimum of 4 frames and a maximum of 450 frames. Events that started in frames where the focal animal was located in the nest box were removed due to frequent tracking errors in that area. Events where animals were classified as being in groups of two for more than 15 seconds before the start of the event were also removed, as animals in the same location in any portion of the arena for long periods would be frequently

interpreted as a single animal. After adjusting parameters, one percent of total frames from each event were randomly selected for manual scoring. Events were balanced across genotypes such that an equal number was scored for both groups.

Data cleaning and feature generation for unsupervised classification

All data processing and analysis was done in python. Raw x, y, and z tracking of each of the front, center, and rear nodes on each animal were extracted across the first 15 minutes of all experiments at moments of less than 80cm/s instantaneous velocity. Missed tracking points removed from velocity thresholding and missed events in the initial tracking were imputed as the value from the last detected frame before the tracking loss. Next the tracking was subsetted to moments where dyads of animals were detected within two body lengths of one another. These time series were considered putative social behavioral sequences. Following subsetting, outliers were removed from each coordinate time series using a hampel filter (package: hampel 1.0.2) and the previous non-outlying data point was imputed in its place. The data was then smoothed with a rolling window mean smoothing over a 5 frame window (detections recorded at 30 frames per second). Following smoothing, features of behavioral interaction were computed for time series analysis. The full set of features used included instantaneous velocity and acceleration of each x, y, and z coordinate for each animal in a pair at each frame, relative velocities and accelerations between each point of the animal, relative direction, instantaneous change in relative direction at each frame distance of between each of the front center and rear body parts of each animal, and rate of change of distance of these points at each frame. Relative direction was defined as the absolute value of subtracted cardinal direction of each animal, where a value of 0 represents that two animals are facing in the same direction, a value of 180 represents that the animals are facing in opposite directions, and a value of 90 represents that the animals are facing perpendicular directions on either the negative or positive axes.

Unsupervised classification

Smoothed traces of distance of center of mass for each segmented close interaction was inputted into Pelt's changepoint detection algorithm with a loss penalty of 3 and minumum size of 15 frames (package: ruptures). Segmented interactions represented putative behavioral syllables for further time series analysis. Each syllable was parameterized using a series of basic time series functions (package: TSfeatures). Computed time series features from TSfeatures included autocorrelation coefficients (acf_features), partial autocorrelation coefficients (pacf_features), holt parameters (holt_params), number of crossing points, entropy, number of flat spots, frequency, heterogeneity, hurst parameter, stability, spikiness, number of peaks, and number of troughs (https://pypi.org/project/tsfeatures/). Time series parameters were then dimensionally reduced using PCA and clustered using K-means (Package sklearn), with 6 PCs used as input to the model. The number of clusters was set by visually inspecting inertia for each cluster. Clustered behavioral syllables were projected onto a 2D space using UMAP for visualization only (package: umap-learn).

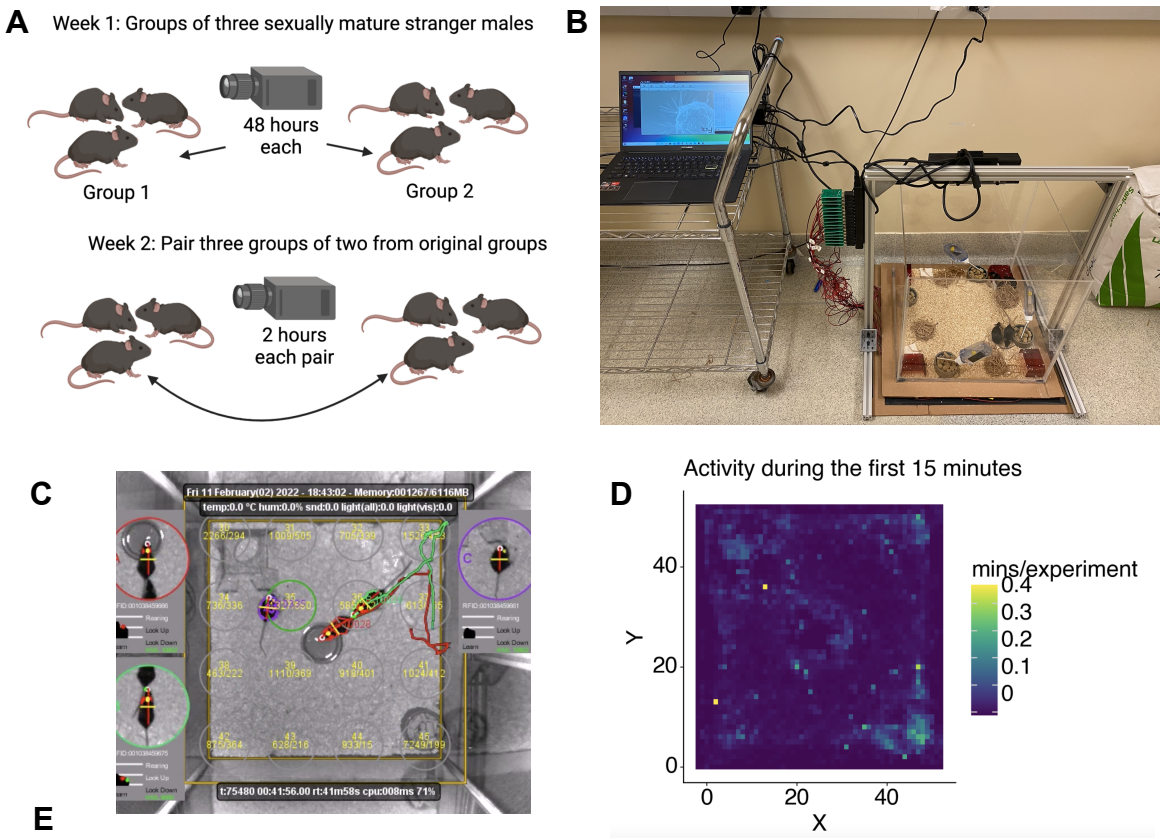
A
Week 1: Groups of three sexually mature stranger males
48 hours each
Group 1
Group 2
Week 2: Pair three groups of two from original groups
2 hours each pair
B
C
D
Activity during the first 15 minutes
mins/experiment
0.4
0.3
0.2
0.1
0
Y
X
E
F
Time line of activity: example B6J trio
dark phase
dark phase
RFID: 8459661 (distance: 5603 m)
RFID: 8459675 (distance: 5917 m)
RFID: 8459666 (distance: 6701 m)
Meters per 15 minutes
D1 - 12:00
D2 - 00:00
D2 - 12:00
D3 - 00:00

Fig 3.1. Experimental design and general patterns of activity of trios. A) Experimental Design. Sexually mature unfamiliar males were recorded in same-genotype trios for 48 hours followed by at least one week of inter experiment time in their normal home cage, and a 2 hour behavioral recording with a new unfamiliar individual from a separate trio. B) Side view of the live mouse tracker rig C) Screenshot of a frame of behavioral video including animal masks. Note that each experiment contained the identical setup with a red plastic nest box in the top left corner, a water cup in the center, and a food cup at the opposite corner D) Heatmap of average activity of B6J and DBA2 trios the first hour of the experiment. E) Representative activity traces of activity for three animals overlaid and each individual animal over the first 15 minutes of a single experiment. F) Overlaid activity traces of the center of mass of three individuals from a single 48 hour experiment, binned at 15 minute intervals. Activity of all animals is closely related.

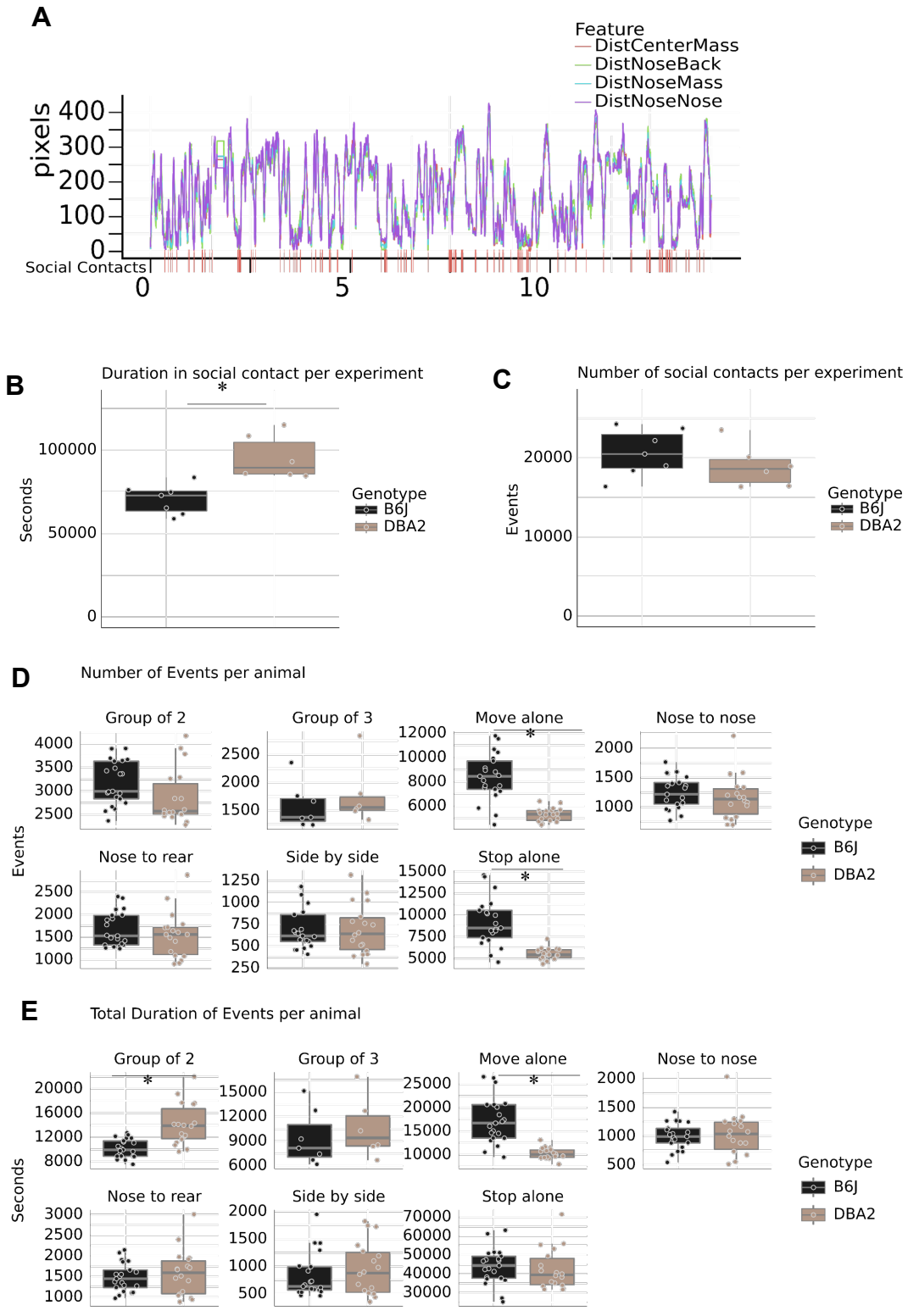
A
Feature
DistCenterMass
DistNoseBack
DistNoseMass
DistNoseNose
pixels
400
300
200
100
0
Social Contacts
0
5
10
B
Duration in social contact per experiment
*
100000
50000
0
Seconds
Genotype
B6J
DBA2
C
Number of social contacts per experiment
20000
10000
0
Events
Genotype
B6J
DBA2
D
Number of Events per animal
Group of 2
Group of 3
Move alone
Nose to nose
Nose to rear
Side by side
Stop alone
Events
Genotype
B6J
DBA2
E
Total Duration of Events per animal
Group of 2
Group of 3
Move alone
Nose to nose
Nose to rear
Side by side
Stop alone
Seconds
Genotype
B6J
DBA2

Fig 3.2. DBA2 trios spend more time in social contact than B6J trios. A) Activity trace of the distance between noses, centers of mass, and rears of two animals from a representative experiment of trios (DistNoseMass=distance between nose of animal A and center of mass of animal B, DistMassMass=distance between center of mass of animal A and center of mass of animal B, DistNoseRear=distance between nose of animal A and rear of animal B). Underneath displays a rug plot of social contacts quantified by the live mouse tracker supervised analysis software time locked to the distance traces. B) Average duration of time spent in social contact amongst trios per experimental group (B6J n=7 trios, DBA2 n=6 trios). C) Number of social contacts per experimental group. D) Duration of individual syllables quantified by the live mouse tracker software over the entire 48 hour experiment (for dyadic and solo events- B6J n=21, DBA2 n=18; triadic events- B6J n=7, DBA2 n=6) E) Number of syllables expressed over the 48 hour experiment.

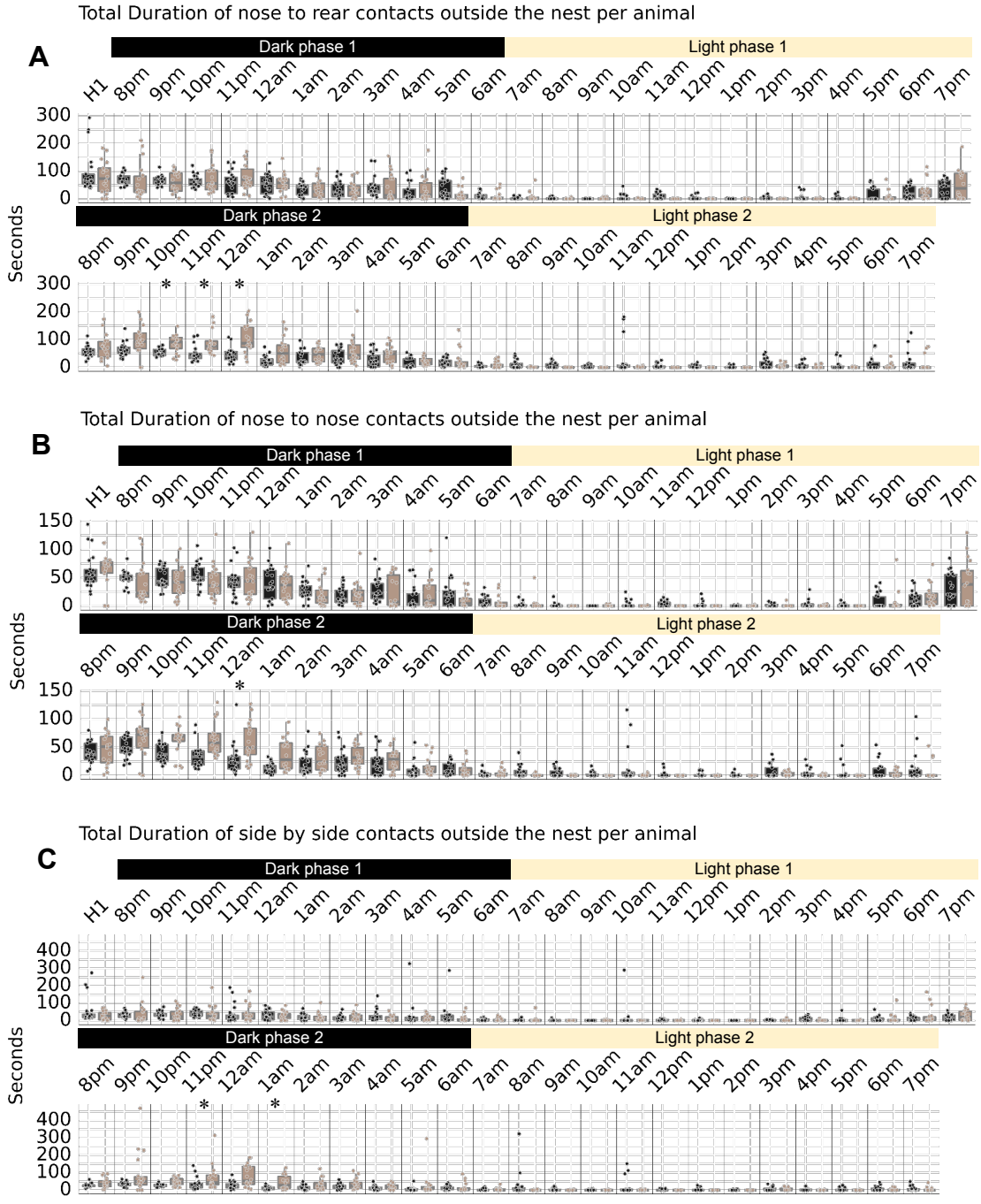
Total Duration of nose to rear contacts outside the nest per animal
A
Dark phase 1
Light phase 1
Dark phase 2
Light phase 2
Seconds
H1 8pm 9pm 10pm 11pm 12am 1am 2am 3am 4am 5am 6am 7am 8am 9am 10am 11am 12pm 1pm 2pm 3pm 4pm 5pm 6pm 7pm
0 100 200 300
Total Duration of nose to nose contacts outside the nest per animal
B
0 50 100 150
Total Duration of side by side contacts outside the nest per animal
C
0 100 200 300 400

Fig 3.3. DBA2 trios spend more time making nose to nose and nose to rear contacts in the second dark phase. A-C) Duration of time spent making nose to nose rear (A), nose to nose (B) and side by side contacts (C) amongst trios during each hour of the experiment. (B6J n=21, DBA2 n=18)

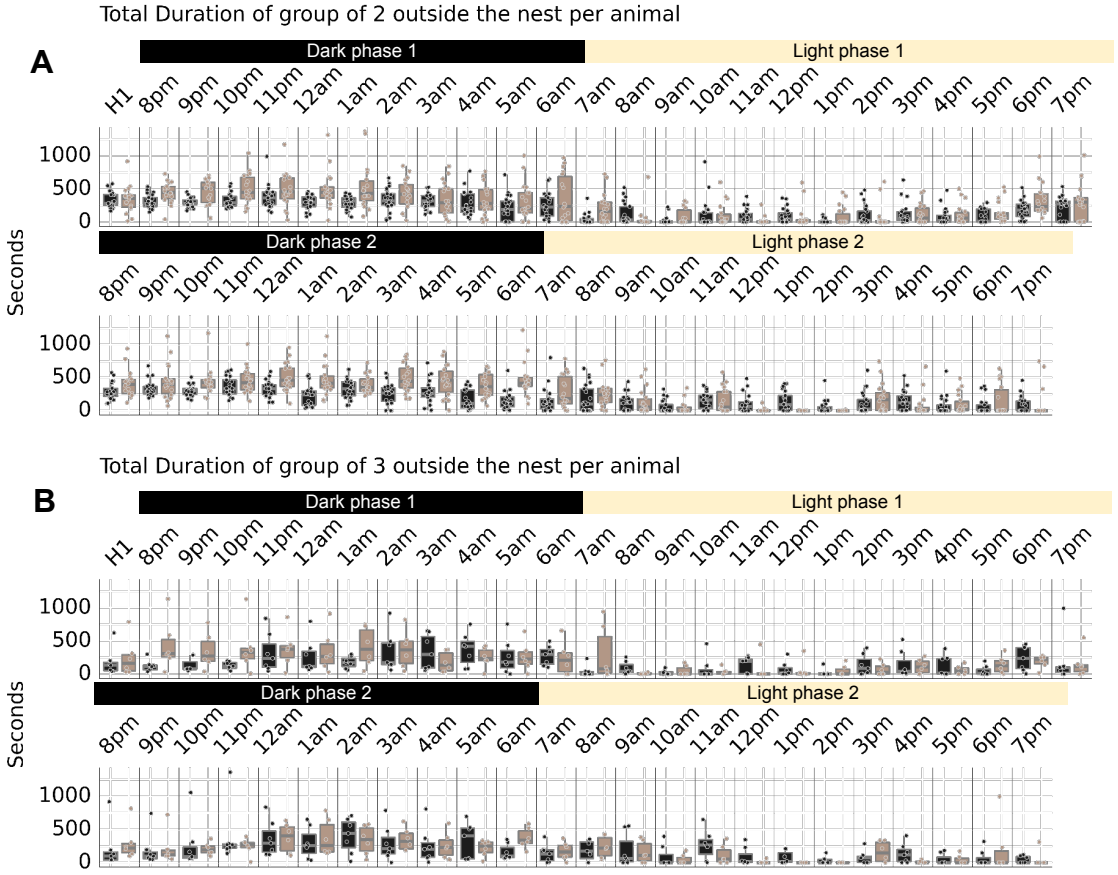
Total Duration of group of 2 outside the nest per animal
A
Dark phase 1
Light phase 1
H1 8pm 9pm 10pm 11pm 12am 1am 2am 3am 4am 5am 6am 7am 8am 9am 10am 11am 12pm 1pm 2pm 3pm 4pm 5pm 6pm 7pm
1000
500
0
Seconds
Dark phase 2
Light phase 2
8pm 9pm 10pm 11pm 12am 1am 2am 3am 4am 5am 6am 7am 8am 9am 10am 11am 12pm 1pm 2pm 3pm 4pm 5pm 6pm 7pm
1000
500
0
Total Duration of group of 3 outside the nest per animal
B
Dark phase 1
Light phase 1
H1 8pm 9pm 10pm 11pm 12am 1am 2am 3am 4am 5am 6am 7am 8am 9am 10am 11am 12pm 1pm 2pm 3pm 4pm 5pm 6pm 7pm
1000
500
0
Seconds
Dark phase 2
Light phase 2
8pm 9pm 10pm 11pm 12am 1am 2am 3am 4am 5am 6am 7am 8am 9am 10am 11am 12pm 1pm 2pm 3pm 4pm 5pm 6pm 7pm
1000
500
0

Fig 3.4. Time spent in groups of two and three amongst trios over each hour of the recording. A-B) Total Duration of time spent in groups of two (A; B6J n=21, DBA2 n=18) and groups of 3 (B; B6J n=7, DBA2 n=6) over each hour of the experiment.

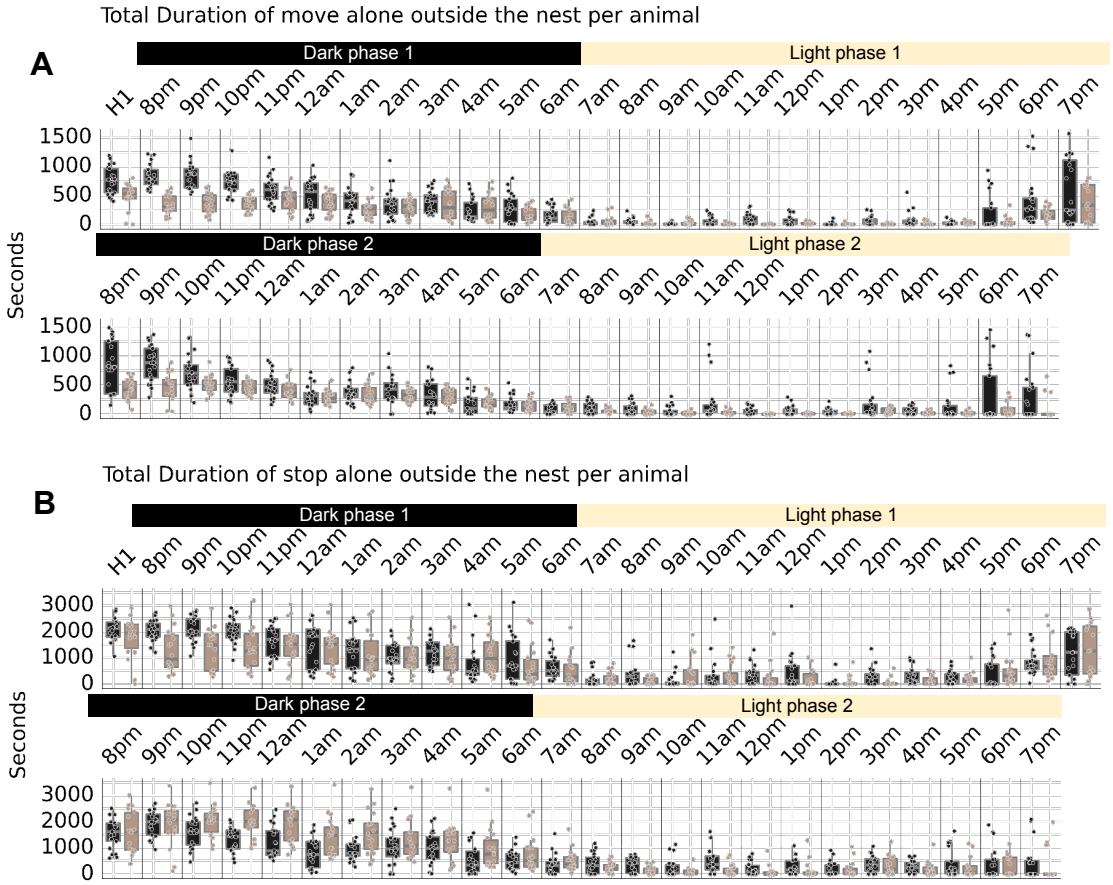
Total Duration of move alone outside the nest per animal
A
Dark phase 1
Light phase 1
H1 8pm 9pm 10pm 11pm 12am 1am 2am 3am 4am 5am 6am 7am 8am 9am 10am 11am 12pm 1pm 2pm 3pm 4pm 5pm 6pm 7pm
1500
1000
500
0
Seconds
Dark phase 2
Light phase 2
8pm 9pm 10pm 11pm 12am 1am 2am 3am 4am 5am 6am 7am 8am 9am 10am 11am 12pm 1pm 2pm 3pm 4pm 5pm 6pm 7pm
1500
1000
500
0
Total Duration of stop alone outside the nest per animal
B
Dark phase 1
Light phase 1
H1 8pm 9pm 10pm 11pm 12am 1am 2am 3am 4am 5am 6am 7am 8am 9am 10am 11am 12pm 1pm 2pm 3pm 4pm 5pm 6pm 7pm
3000
2000
1000
0
Seconds
Dark phase 2
Light phase 2
8pm 9pm 10pm 11pm 12am 1am 2am 3am 4am 5am 6am 7am 8am 9am 10am 11am 12pm 1pm 2pm 3pm 4pm 5pm 6pm 7pm
3000
2000
1000
0

Fig 3.5. Time spent moving and stopped while alone amongst trios over each hour of the recording A-B) Total Duration of time spent moving alone (A) and stopped alone (B) outside of the nest per hour over the course of the experiment (B6J n=21, DBA2 n=18).

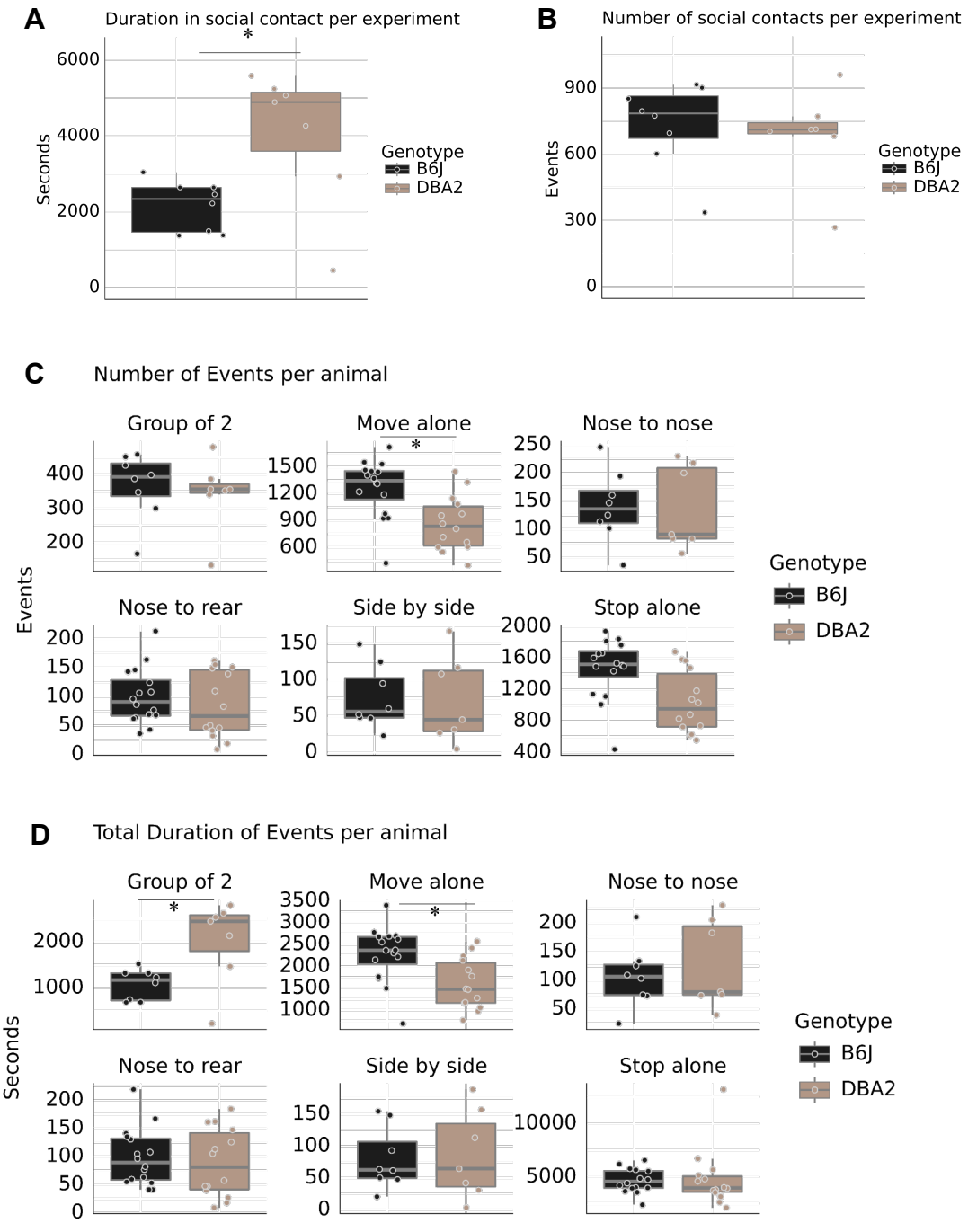
A
Duration in social contact per experiment
Seconds
6000
4000
2000
0
*
Genotype
B6J
DBA2
B
Number of social contacts per experiment
Events
900
600
300
0
Genotype
B6J
DBA2
C
Number of Events per animal
Group of 2
Move alone
Nose to nose
Nose to rear
Side by side
Stop alone
Events
Genotype
B6J
DBA2
D
Total Duration of Events per animal
Group of 2
Move alone
Nose to nose
Nose to rear
Side by side
Stop alone
Seconds
Genotype
B6J
DBA2

Fig 3.6. DBA2 dyads spend more time in social contact than B6J dyads. A) Average duration of time spent in social contact amongst dyads per experimental group over the course of the entire 2 hour experiment (B6J n=8 dyads, DBA2 n=7 dyads). C) Number of social contacts per experimental group. D) Total Duration of individual syllables quantified by the live mouse tracker software over the entire 2 hour experiment E) Total number of syllables expressed over the 2 hour experiment .

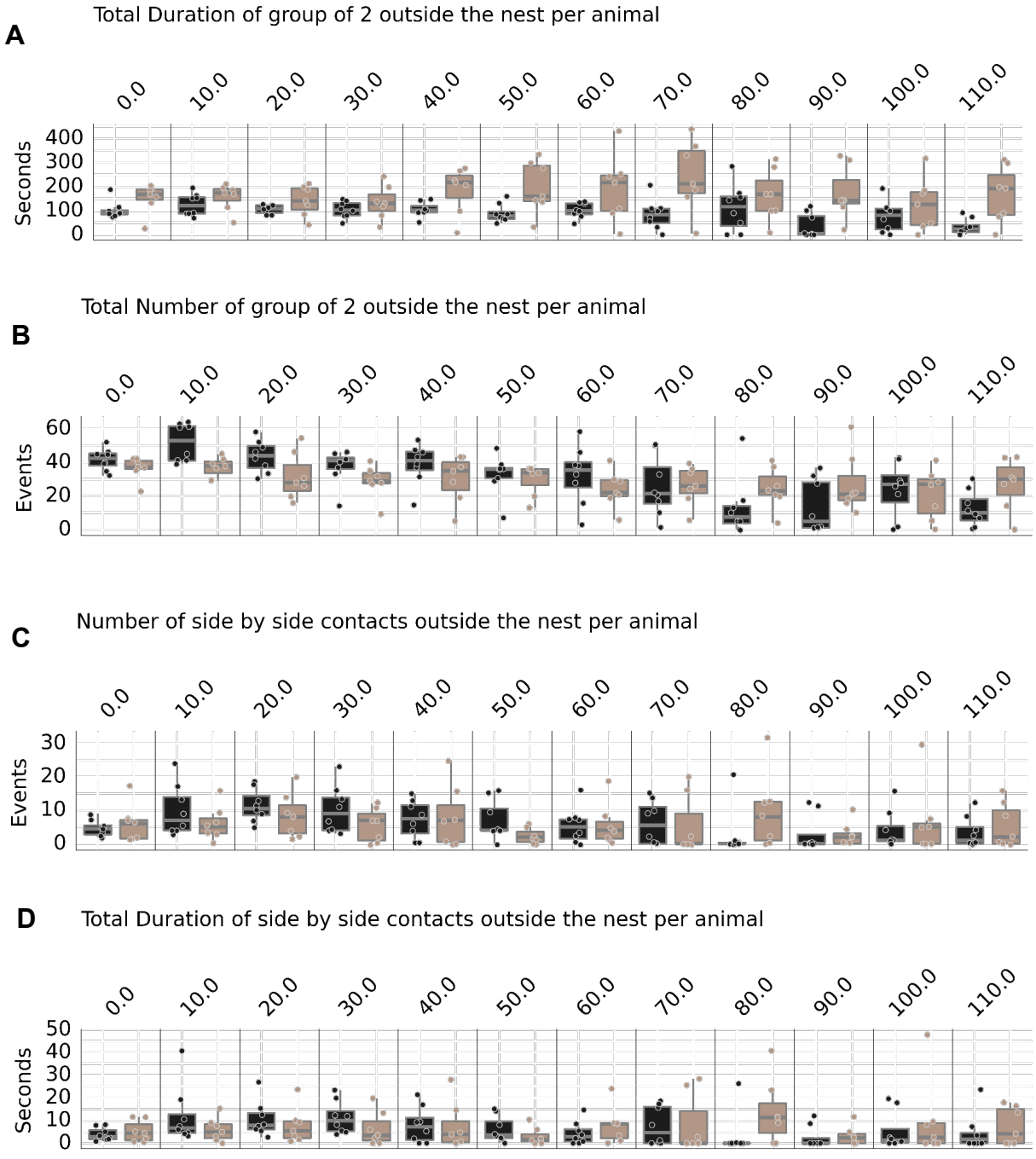
A
Total Duration of group of 2 outside the nest per animal
0.0
10.0
20.0
30.0
40.0
50.0
60.0
70.0
80.0
90.0
100.0
110.0
Seconds
400
300
200
100
0
B
Total Number of group of 2 outside the nest per animal
Events
60
40
20
0
C
Number of side by side contacts outside the nest per animal
Events
30
20
10
0
D
Total Duration of side by side contacts outside the nest per animal
Seconds
50
40
30
20
10
0

Fig 3.7. Social contacts of DBA2 and B6J dyads do not differ within hours. A-B) Total Number and duration of events in groups of two outside the nest per dyad per ten minute bin over the course of the two hour experiment (B6J n=8, DBA2 n=7). C-D) Total number and duration of side by side contacts outside the nest per ten minute bin per dyad.

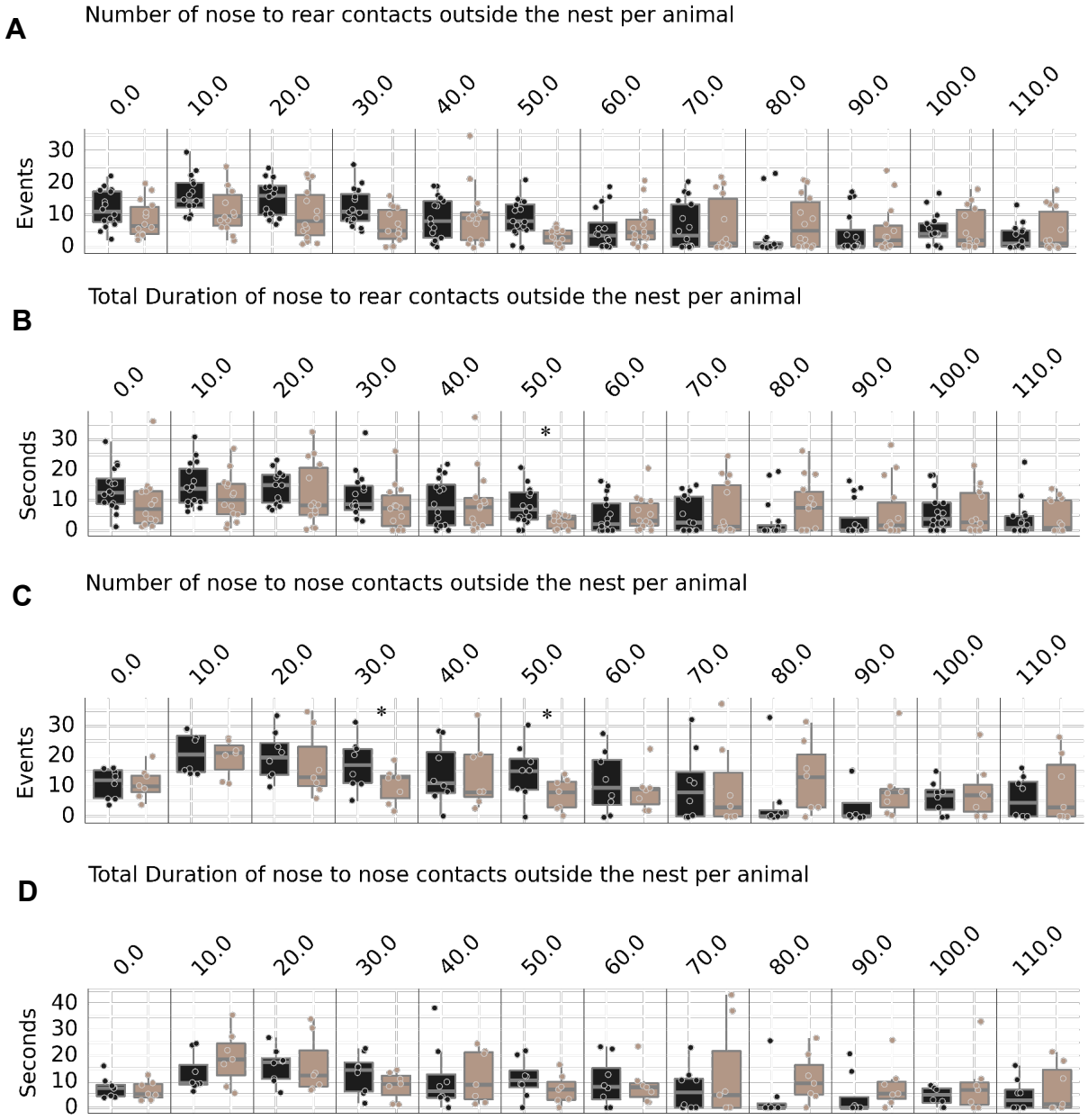
A
Number of nose to rear contacts outside the nest per animal
0.0
10.0
20.0
30.0
40.0
50.0
60.0
70.0
80.0
90.0
100.0
110.0
Events
30
20
10
0
B
Total Duration of nose to rear contacts outside the nest per animal
Seconds
*
C
Number of nose to nose contacts outside the nest per animal
*
*
D
Total Duration of nose to nose contacts outside the nest per animal
40

Fig 3.8. Social investigations of DBA2 and B6J dyads do not differ within hours. A-B) Total Number and duration of nose to nose contacts outside the nest per dyad per ten minute bin over the course of the two hour experiment (B6J n=8, DBA2 n=7). C-D) Total number and duration of nose to rear contacts outside the nest per ten minute bin per dyad.

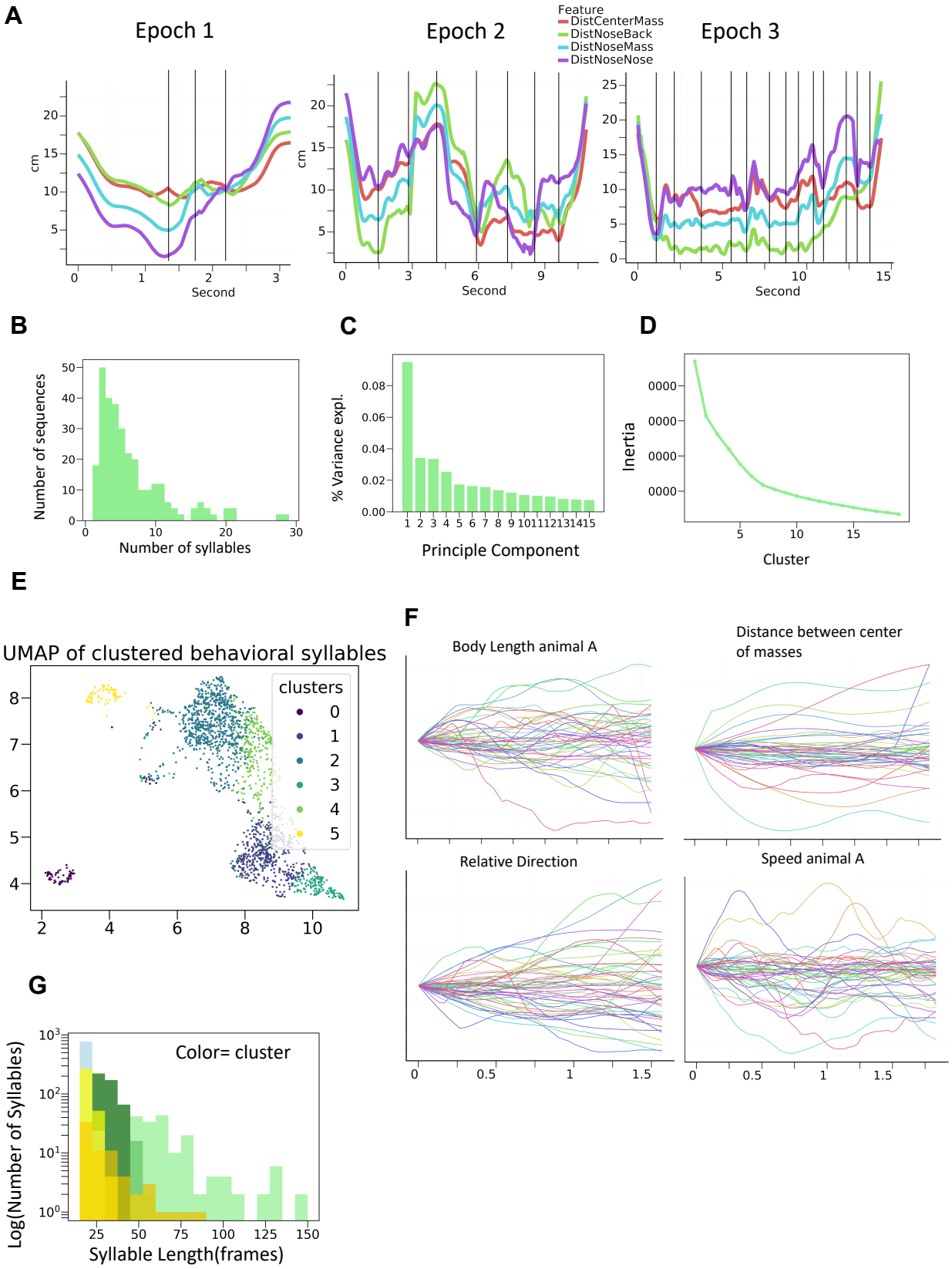
A
Epoch 1
Epoch 2
Epoch 3
Feature
DistCenterMass
DistNoseBack
DistNoseMass
DistNoseNose
cm
Second
B
Number of sequences
Number of syllables
C
% Variance expl.
Principle Component
D
Inertia
Cluster
E
UMAP of clustered behavioral syllables
clusters
0
1
2
3
4
5
F
Body Length animal A
Distance between center of masses
Relative Direction
Speed animal A
G
Color= cluster
Log(Number of Syllables)
Syllable Length(frames)

Fig 3.9 Unsupervised Clustering does not reveal recognizable behavioral syllables A) Example traces of three segmented epochs of close interactions. Plots display the distance between each body part of two animals over several seconds of interaction (DistNoseMass=distance between nose of animal A and center of mass of animal B, DistMassMass=distance between center of mass of animal A and center of mass of animal B, DistNoseRear=distance between nose of animal A and rear of animal b). Vertical lines represent algorithmically determined changepoints in the timeseries of distances between the centers of mass of each pair of animals B) Total number of putative syllables per putative sequence, or the total number of chunks determined by changepoint analysis from longer segmented time series of close social interactions. C) Variance explained by each principal component from PCA. D) Inertia of each cluster returned from K-means clustering. E) UMAP reduction of clustered behavioral syllables. F) Data from 100 random behavioral syllables from cluster 0 of basic features of social interactions. Data is time warped along the x axis and centered by starting magnitude on the y axis. The c axis represents arbitrary time and the y axis represents arbitrary magnitude. Overlaid traces should have similar shapes if these behavioral syllables have similar patterns that influence clustering. G) Distribution of syllable lengths within each cluster.

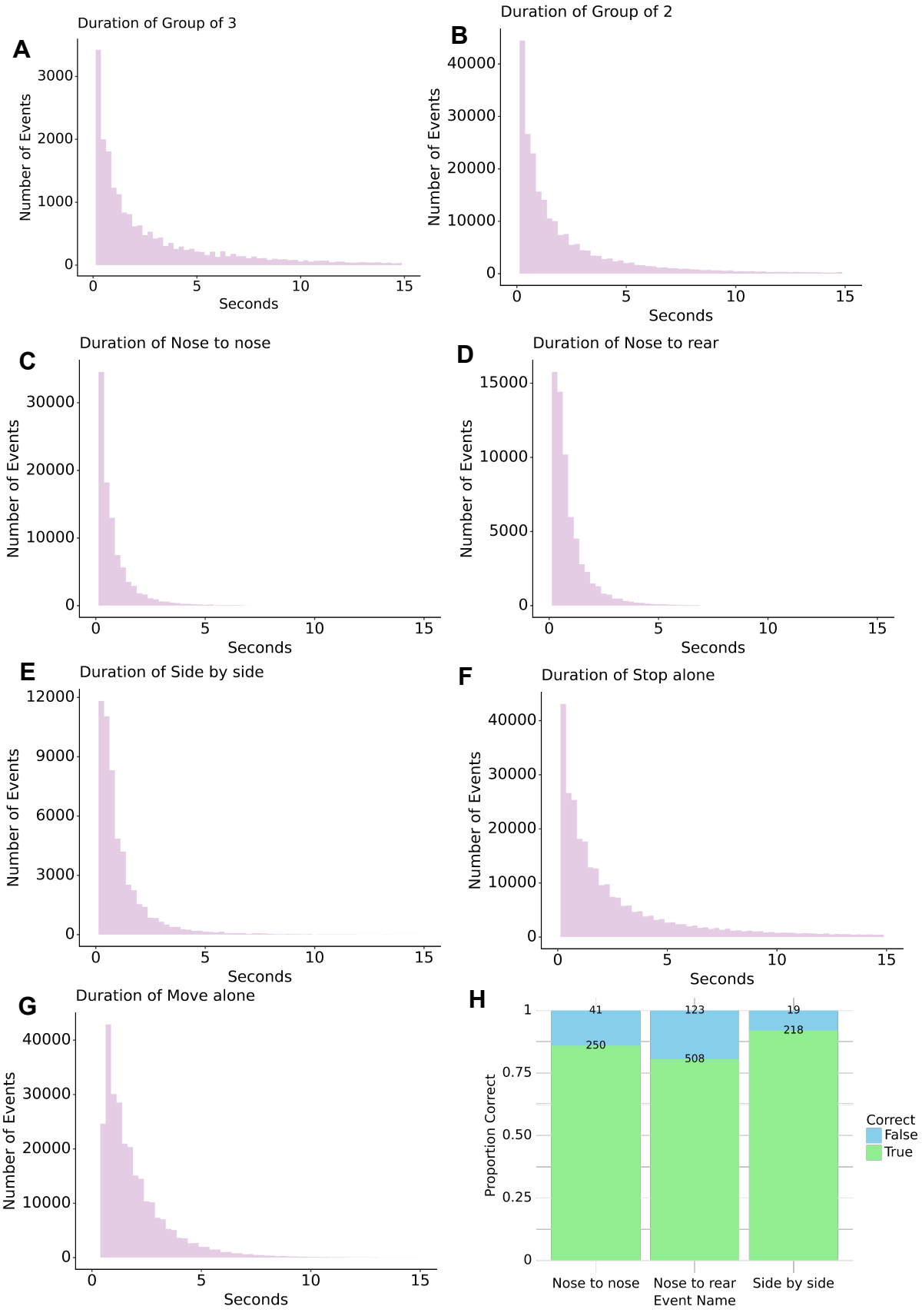
A
Duration of Group of 3
Number of Events
Seconds
B
Duration of Group of 2
Number of Events
Seconds
C
Duration of Nose to nose
Number of Events
Seconds
D
Duration of Nose to rear
Number of Events
Seconds
E
Duration of Side by side
Number of Events
Seconds
F
Duration of Stop alone
Number of Events
Seconds
G
Duration of Move alone
Number of Events
Seconds
H
Proportion Correct
41
250
123
508
19
218
Nose to nose
Nose to rear
Side by side
Event Name
Correct
False
True

Fig 3.S1. Manual validation of behavioral events. A-G) Histogram of durations of each individual labeled behavioral event. H) Proportion of correct machine labeled events in trios as validated by an observer. Numbers in bars represent the number of correct and incorrect events scored.

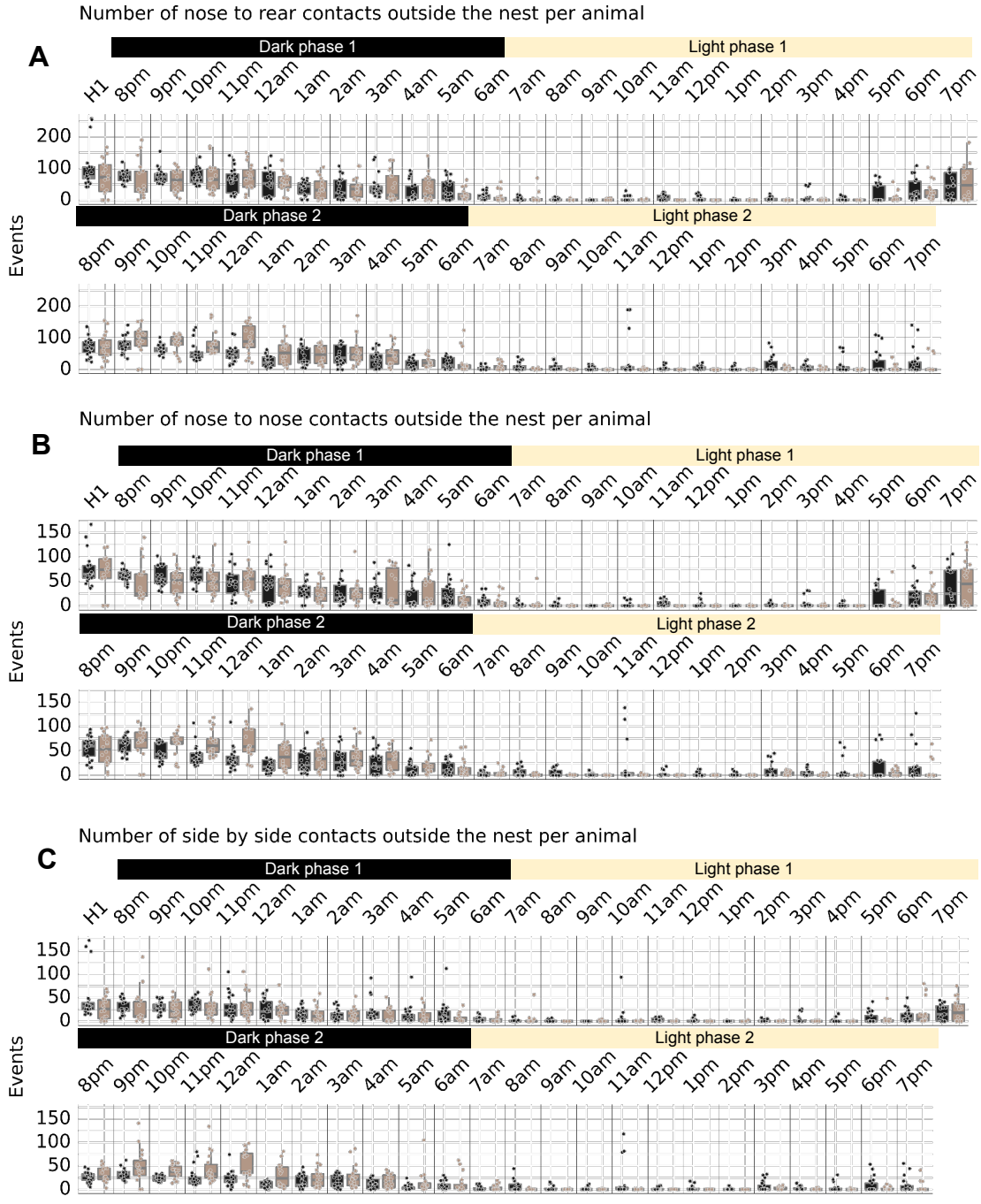
A
Number of nose to rear contacts outside the nest per animal
Dark phase 1
Light phase 1
Dark phase 2
Light phase 2
Events
B
Number of nose to nose contacts outside the nest per animal
C
Number of side by side contacts outside the nest per animal

Fig 3.S2. DBA2 make a greater number of nose to nose and nose to rear contacts in the second dark phase. A-C) Number of time nose to rear (A), nose to nose (B) and side by side contacts (C) amongst trios during each hour of the experiment. (B6J n=21, DBA2 n=18)

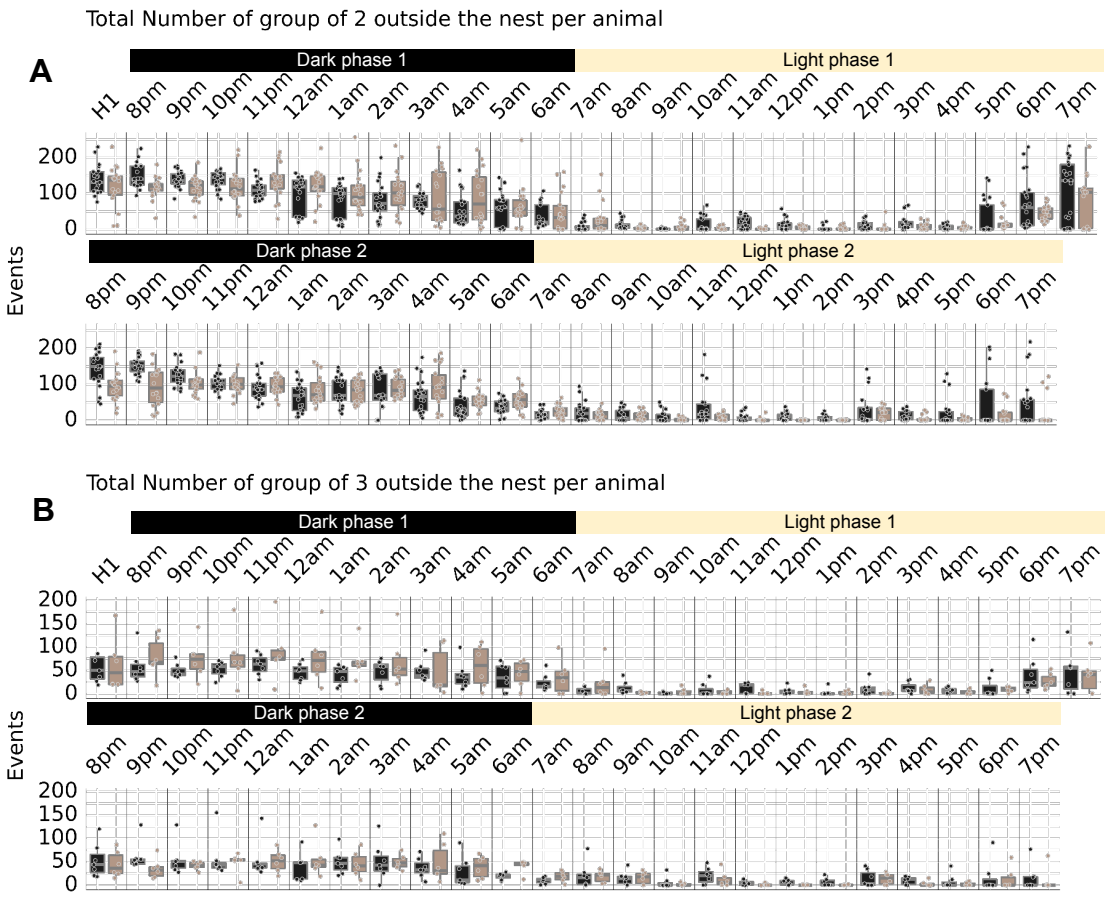
Total Number of group of 2 outside the nest per animal
A
Dark phase 1
Light phase 1
H1 8pm 9pm 10pm 11pm 12am 1am 2am 3am 4am 5am 6am 7am 8am 9am 10am 11am 12pm 1pm 2pm 3pm 4pm 5pm 6pm 7pm
200
100
0
Dark phase 2
Light phase 2
8pm 9pm 10pm 11pm 12am 1am 2am 3am 4am 5am 6am 7am 8am 9am 10am 11am 12pm 1pm 2pm 3pm 4pm 5pm 6pm 7pm
200
100
0
Events
Total Number of group of 3 outside the nest per animal
B
Dark phase 1
Light phase 1
H1 8pm 9pm 10pm 11pm 12am 1am 2am 3am 4am 5am 6am 7am 8am 9am 10am 11am 12pm 1pm 2pm 3pm 4pm 5pm 6pm 7pm
200
150
100
50
0
Dark phase 2
Light phase 2
8pm 9pm 10pm 11pm 12am 1am 2am 3am 4am 5am 6am 7am 8am 9am 10am 11am 12pm 1pm 2pm 3pm 4pm 5pm 6pm 7pm
200
150
100
50
0
Events

Fig 3.S3. Time spent in groups of two and three amongst trios over each hour of the recording. A-B) Total duration of time spent in groups of two (A; B6J n=21, DBA2 n=18) and groups of 3 (B; B6J n=7, DBA2 n=6) over each hour of the experiment.

Fig 3.S4. Time spent moving and stopped while alone amongst trios over each hour of the recording A-B) Total Number of events spent moving alone (A) and stopped alone (B) outside of the nest per hour over the course of the experiment (B6J n=21, DBA2 n=18).

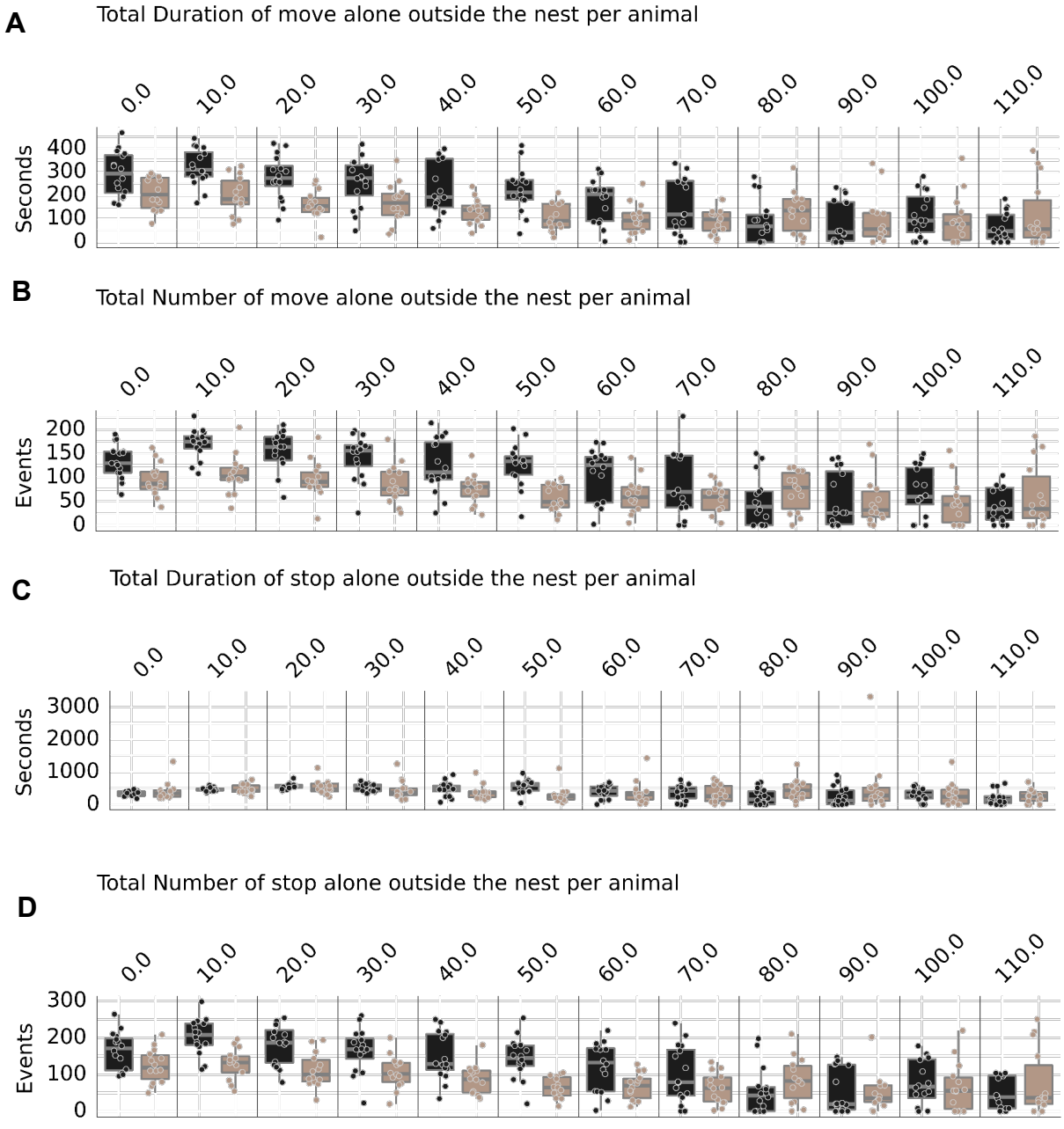
A
Total Duration of move alone outside the nest per animal
0.0
10.0
20.0
30.0
40.0
50.0
60.0
70.0
80.0
90.0
100.0
110.0
Seconds
400
300
200
100
0
B
Total Number of move alone outside the nest per animal
Events
200
150
100
50
0
C
Total Duration of stop alone outside the nest per animal
Seconds
3000
2000
1000
0
D
Total Number of stop alone outside the nest per animal
Events
300
200
100
0

Fig 3.S5. Solo locomotor behaviors of dyads. A-B) Total Number and duration of events moving while isolated outside the nest per dyad per hour. C-D) Total Number and duration of events stopped while isolated outside the nest per dyad per hour. (B6J n=14, DBA2 n=12)

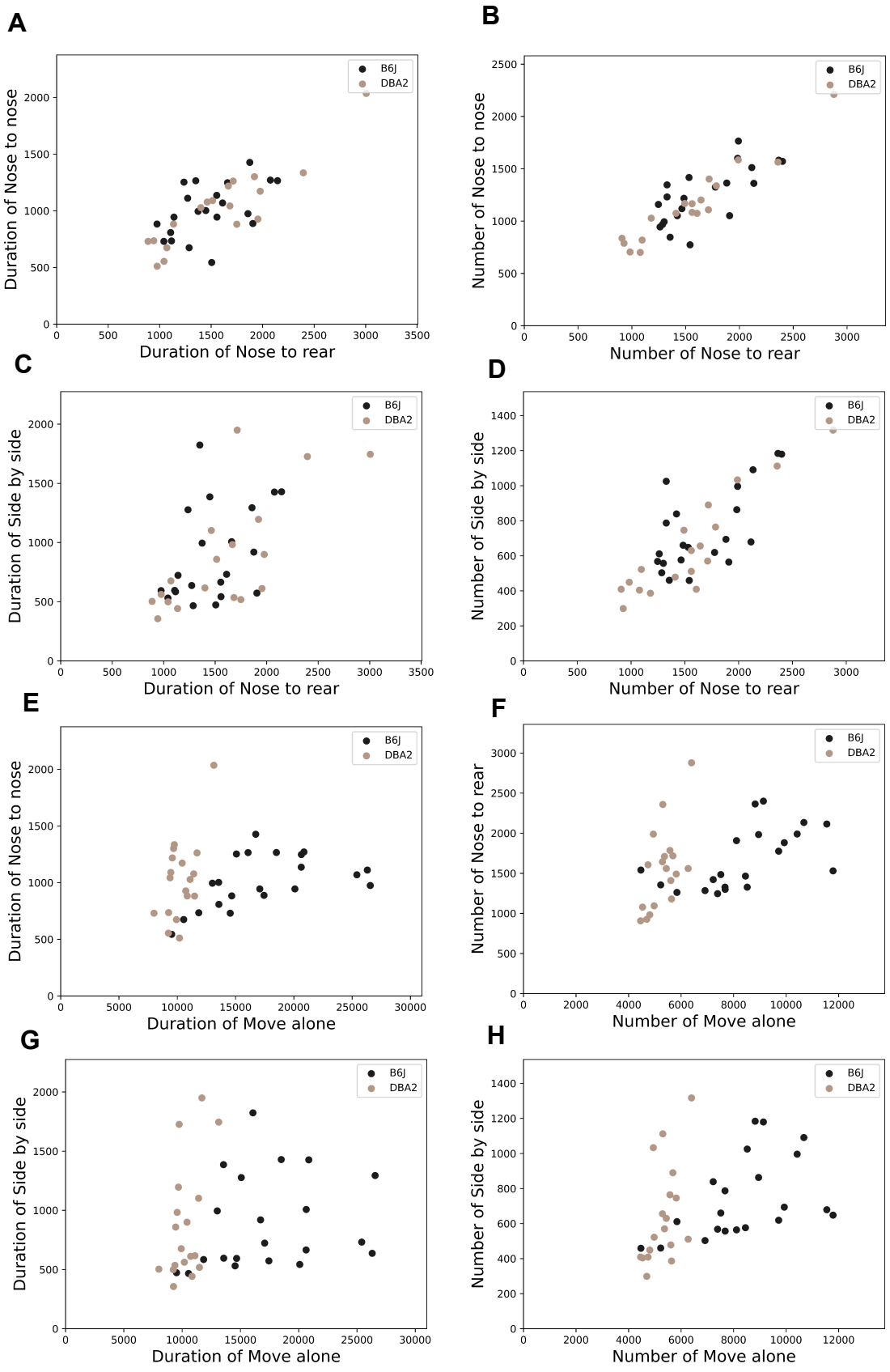
A
Duration of Nose to nose
Duration of Nose to rear
B
Number of Nose to nose
Number of Nose to rear
C
Duration of Side by side
Duration of Nose to rear
D
Number of Side by side
Number of Nose to rear
E
Duration of Nose to nose
Duration of Move alone
F
Number of Nose to rear
Number of Move alone
G
Duration of Side by side
Duration of Move alone
H
Number of Side by side
Number of Move alone
B6J
DBA2

Fig 3.S6. Correlation of number and duration of social and non social events. A-H) Correlations of duration and number of social and non social events scored by the live mouse tracker system. Nose to nose and nose to rear contacts are highly correlated, whereas social behaviors are less correlated to events of moving or stopped isolated.

References

Adams, N. (1985). Establishment of dominance in domestic Norway rats: Effects of the degree of captivity and social experience. *Animal Learning & Behavior*, *13*(1), 93–97. https://doi.org/10.3758/BF03213371

Åhlgren, J., & Voikar, V. (2019). Experiments done in Black-6 mice: What does it mean? *Lab Animal*, *48*(6), 171–180. https://doi.org/10.1038/s41684-019-0288-8

Bordes, J., Miranda, L., Reinhardt, M., Narayan, S., Hartmann, J., Newman, E. L., Brix, L. M., Van Doeselaar, L., Engelhardt, C., Dillmann, L., Mitra, S., Ressler, K. J., Pütz, B., Agakov, F., Müller-Myhsok, B., & Schmidt, M. V. (2023). Automatically annotated motion tracking identifies a distinct social behavioral profile following chronic social defeat stress. *Nature Communications*, *14*(1), 4319. https://doi.org/10.1038/s41467-023-40040-3

Brenes, J. C., Lackinger, M., Höglinger, G. U., Schratt, G., Schwarting, R. K. W., & Wöhr, M. (2016). Differential effects of social and physical environmental enrichment on brain plasticity, cognition, and ultrasonic communication in rats. *Journal of Comparative Neurology*, *524*(8), 1586–1607. https://doi.org/10.1002/cne.23842

Buseck, A., McPherson, K., & Linster, C. (2021). Olfactory recognition memory in mice depends on task parameters. *Behavioral Neuroscience*, *135*(3), 347–353. https://doi.org/10.1037/bne0000421

Calhoun, J. B. (1956). A Comparative Study of the Social Behavior of Two Inbred Strains of House Mice. *Ecological Monographs*, *26*(1), 81–103. https://doi.org/10.2307/1943578

Chari, T., Hernandez, A., & Portera-Cailliau, C. (2023). *A novel head-fixed assay for social touch in mice uncovers aversive responses in two autism models* [Preprint]. Neuroscience. https://doi.org/10.1101/2023.01.11.523491

Crawley, J. N. (2007). Mouse Behavioral Assays Relevant to the Symptoms of Autism*. *Brain Pathology*, *17*(4), 448–459. https://doi.org/10.1111/j.1750-3639.2007.00096.x

De Chaumont, F., Ey, E., Torquet, N., Lagache, T., Dallongeville, S., Imbert, A., Legou, T., Le Sourd, A.-M., Faure, P., Bourgeron, T., & Olivo-Marin, J.-C. (2019). Real-time analysis of the behaviour of groups of mice via a depth-sensing camera and machine learning. *Nature Biomedical Engineering*, *3*(11), 930–942. https://doi.org/10.1038/s41551-019-0396-1

Doran, A. G., Wong, K., Flint, J., Adams, D. J., Hunter, K. W., & Keane, T. M. (2016). Deep genome sequencing and variation analysis of 13 inbred mouse strains defines candidate phenotypic alleles, private variation and homozygous truncating mutations. *Genome Biology*, *17*(1), 167. https://doi.org/10.1186/s13059-016-1024-y

Ferguson, J. N., Young, L. J., Hearn, E. F., Matzuk, M. M., Insel, T. R., & Winslow, J. T. (2000). Social amnesia in mice lacking the oxytocin gene. *Nature Genetics*, *25*(3), 284–288. https://doi.org/10.1038/77040

Fustiñana, M. S., Eichlisberger, T., Bouwmeester, T., Bitterman, Y., & Lüthi, A. (2021). State-dependent encoding of exploratory behaviour in the amygdala. *Nature*, *592*(7853), 267–271. https://doi.org/10.1038/s41586-021-03301-z

Grieco, F., Bernstein, B. J., Biemans, B., Bikovski, L., Burnett, C. J., Cushman, J. D., Van Dam, E. A., Fry, S. A., Richmond-Hacham, B., Homberg, J. R., Kas, M. J. H., Kessels, H. W., Koopmans, B., Krashes, M. J., Krishnan, V., Logan, S., Loos, M., McCann, K. E.,

Parduzi, Q., … Noldus, L. P. J. J. (2021). Measuring Behavior in the Home Cage: Study Design, Applications, Challenges, and Perspectives. *Frontiers in Behavioral Neuroscience*, *15*, 735387. https://doi.org/10.3389/fnbeh.2021.735387

Hashikawa, K., Hashikawa, Y., Falkner, A., & Lin, D. (2016). The neural circuits of mating and fighting in male mice. *Current Opinion in Neurobiology*, *38*, 27–37. https://doi.org/10.1016/j.conb.2016.01.006

Kazlauckas, V., Pagnussat, N., Mioranzza, S., Kalinine, E., Nunes, F., Pettenuzzo, L., O.Souza, D., Portela, L. V., Porciúncula, L. O., & Lara, D. R. (2011). Enriched environment effects on behavior, memory and BDNF in low and high exploratory mice. *Physiology & Behavior*, *102*(5), 475–480. https://doi.org/10.1016/j.physbeh.2010.12.025

Kingsbury, L., Huang, S., Raam, T., Ye, L. S., Wei, D., Hu, R. K., Ye, L., & Hong, W. (2020). Cortical Representations of Conspecific Sex Shape Social Behavior. *Neuron*, *107*(5), 941-953.e7. https://doi.org/10.1016/j.neuron.2020.06.020

Kong, E., Lee, K.-H., Do, J., Kim, P., & Lee, D. (2023). Dynamic and stable hippocampal representations of social identity and reward expectation support associative social memory in male mice. *Nature Communications*, *14*(1), 2597. https://doi.org/10.1038/s41467-023-38338-3

Koolhaas, J. M., Coppens, C. M., De Boer, S. F., Buwalda, B., Meerlo, P., & Timmermans, P. J. A. (2013). The Resident-intruder Paradigm: A Standardized Test for Aggression, Violence and Social Stress. *Journal of Visualized Experiments*, *77*, 4367. https://doi.org/10.3791/4367

Krakauer, J. W., Ghazanfar, A. A., Gomez-Marin, A., MacIver, M. A., & Poeppel, D. (2017). Neuroscience Needs Behavior: Correcting a Reductionist Bias. *Neuron*, *93*(3), 480–490. https://doi.org/10.1016/j.neuron.2016.12.041

Lauer, J., Zhou, M., Ye, S., Menegas, W., Schneider, S., Nath, T., Rahman, M. M., Di Santo, V., Soberanes, D., Feng, G., Murthy, V. N., Lauder, G., Dulac, C., Mathis, M. W., & Mathis, A. (2022). Multi-animal pose estimation, identification and tracking with DeepLabCut. *Nature Methods*, *19*(4), 496–504. https://doi.org/10.1038/s41592-022-01443-0

Lee, W., Dowd, H. N., Nikain, C., Dwortz, M. F., Yang, E. D., & Curley, J. P. (2021). Effect of relative social rank within a social hierarchy on neural activation in response to familiar or unfamiliar social signals. *Scientific Reports*, *11*(1), 2864. https://doi.org/10.1038/s41598-021-82255-8

Lee, W., Fu, J., Bouwman, N., Farago, P., & Curley, J. P. (2019). Temporal microstructure of dyadic social behavior during relationship formation in mice. *PLOS ONE*, *14*(12), e0220596. https://doi.org/10.1371/journal.pone.0220596

Li, Y., & Dulac, C. (2018). Neural coding of sex-specific social information in the mouse brain. *Current Opinion in Neurobiology*, *53*, 120–130. https://doi.org/10.1016/j.conb.2018.07.005

Liberles, S. D. (2014). Mammalian Pheromones. *Annual Review of Physiology*, *76*(1), 151–175. https://doi.org/10.1146/annurev-physiol-021113-170334

Long, S. Y. (1972). Hair-nibbling and whisker-trimming as indicators of social hierarchy in mice. *Animal Behaviour*, *20*(1), 10–12. https://doi.org/10.1016/S0003-3472(72)80167-2

Moy, S., Nadler, J., Young, N., Perez, A., Holloway, L., Barbaro, R., Barbaro, J., Wilson, L., Threadgill, D., & Lauder, J. (2007). Mouse behavioral tasks relevant to autism: Phenotypes of 10 inbred strains. *Behavioural Brain Research*, *176*(1), 4–20. https://doi.org/10.1016/j.bbr.2006.07.030

Nilsson, S. R., Goodwin, N. L., Choong, J. J., Hwang, S., Wright, H. R., Norville, Z. C., Tong, X., Lin, D., Bentzley, B. S., Eshel, N., McLaughlin, R. J., & Golden, S. A. (2020). *Simple Behavioral Analysis (SimBA) – an open source toolkit for computer classification of complex social behaviors in experimental animals* [Preprint]. Animal Behavior and Cognition. https://doi.org/10.1101/2020.04.19.049452

Omer, D. B., Maimon, S. R., Las, L., & Ulanovsky, N. (2018). Social place-cells in the bat hippocampus. *Science*, *359*(6372), 218–224. https://doi.org/10.1126/science.aao3474

Panksepp, J. B., & Lahvis, G. P. (2007). Social reward among juvenile mice. *Genes, Brain and Behavior*, *6*(7), 661–671. https://doi.org/10.1111/j.1601-183X.2006.00295.x

Pereira, T. D., Shaevitz, J. W., & Murthy, M. (2020). Quantifying behavior to understand the brain. *Nature Neuroscience*, *23*(12), 1537–1549. https://doi.org/10.1038/s41593-020-00734-z

Pereira, T. D., Tabris, N., Matsliah, A., Turner, D. M., Li, J., Ravindranath, S., Papadoyannis, E. S., Normand, E., Deutsch, D. S., Wang, Z. Y., McKenzie-Smith, G. C., Mitelut, C. C., Castro, M. D., D'Uva, J., Kislin, M., Sanes, D. H., Kocher, S. D., Wang, S. S.-H., Falkner, A. L., … Murthy, M. (2022). SLEAP: A deep learning system for multi-animal pose tracking. *Nature Methods*, *19*(4), 486–495. https://doi.org/10.1038/s41592-022-01426-1

Phifer-Rixey, M., & Nachman, M. W. (2015). Insights into mammalian biology from the wild house mouse Mus musculus. *eLife*, *4*, e05959. https://doi.org/10.7554/eLife.05959

Ricceri, L., Michetti, C., & Scattoni, M. L. (2016). Mouse Behavior and Models for Autism Spectrum Disorders. In *Neuronal and Synaptic Dysfunction in Autism Spectrum Disorder and Intellectual Disability* (pp. 269–293). Elsevier. https://doi.org/10.1016/B978-0-12-800109-7.00017-0

Scott, J. P. (1942). GENETIC DIFFERENCES IN THE SOCIAL BEHAVIOR OF INBRED STRAINS OF MICE. *Journal of Heredity*, *33*(1), 11–15. https://doi.org/10.1093/oxfordjournals.jhered.a105080

Sullivan, J. A. (2009). The multiplicity of experimental protocols: A challenge to reductionist and non-reductionist models of the unity of neuroscience. *Synthese*, *167*(3), 511–539. https://doi.org/10.1007/s11229-008-9389-4

The 1000 Genomes Project Consortium, Corresponding authors, Auton, A., Abecasis, G. R., Steering committee, Altshuler, D. M., Durbin, R. M., Abecasis, G. R., Bentley, D. R., Chakravarti, A., Clark, A. G., Donnelly, P., Eichler, E. E., Flicek, P., Gabriel, S. B., Gibbs, R. A., Green, E. D., Hurles, M. E., Knoppers, B. M., … Abecasis, G. R. (2015). A global reference for human genetic variation. *Nature*, *526*(7571), 68–74. https://doi.org/10.1038/nature15393

Wei, D., Talwar, V., & Lin, D. (2021). Neural circuits of social behaviors: Innate yet flexible. *Neuron*, *109*(10), 1600–1620. https://doi.org/10.1016/j.neuron.2021.02.012

Williamson, C. M., Lee, W., & Curley, J. P. (2016). Temporal dynamics of social hierarchy formation and maintenance in male mice. *Animal Behaviour*, *115*, 259–272. https://doi.org/10.1016/j.anbehav.2016.03.004

Wiltschko, A. B., Johnson, M. J., Iurilli, G., Peterson, R. E., Katon, J. M., Pashkovski, S. L., Abraira, V. E., Adams, R. P., & Datta, S. R. (2015). Mapping Sub-Second Structure in Mouse Behavior. *Neuron*, *88*(6), 1121–1135. https://doi.org/10.1016/j.neuron.2015.11.031

Yi, D., Musall, S., Churchland, A., Padilla-Coreano, N., & Saxena, S. (2022). *Disentangled*

multi-subject and social behavioral representations through a constrained subspace variational autoencoder (CS-VAE) [Preprint]. Neuroscience. https://doi.org/10.1101/2022.09.01.506091

Zilkha, N., Sofer, Y., Beny, Y., & Kimchi, T. (2016). From classic ethology to modern neuroethology: Overcoming the three biases in social behavior research. *Current Opinion in Neurobiology*, *38*, 96–108. https://doi.org/10.1016/j.conb.2016.04.014

Chapter 4

Investigating hippocampal single nucleus transcriptomes of a seasonally prosocial vole

Introduction

Genetically encoded social behaviors are often regulated by environmental stimuli. Some species have evolved to develop specific behavioral repertoires during different seasons to promote survival in different weather conditions. Seasonally breeding species are reproductively active during particular times of the year in order to maximize reproductive success in times of food availability. Such seasonal changes can be associated with dramatic differences in social behaviors such as mating and aggression. Studying corresponding changes in neural circuitry across seasons can help us understand both how specific social behaviors are encoded and how the environment can impact the development of these circuits. Here we apply this framework to the study of prosocial behaviors by quantifying seasonal differences in gene expression in the brains of a seasonally prosocial rodent.

Meadow voles (*Microtus pennsylvanicus*) undergo seasonal changes in social behavior, reproductive physiology, and features of neural circuitry. In the summer, female meadow voles are reproductively active, territorial, and aggressive (Beery et al., 2008; Spritzer et al., 2017). In the winter, their gonads regress and reproductive activity wanes, while their tolerance for group living dramatically increases (Kerbeshian et al., 1994). During this time they transition from living alone to living in groups of 8 to 10 in burrows (Getz, 1961; Madison et al., 1984). Social tolerance is a foundational component of prosocial behaviors, but the neural bases for tolerance are hardly known. Thus, this naturally occurring seasonal difference in social tolerance of meadow voles offers a compelling opportunity to understand both the behavior and the neural circuits that encode it.

Day length and social housing promote behavioral differences in the lab

A few studies have examined seasonal differences in social tolerance and other behaviors of meadow voles in a lab setting. Seasonal phenotypes in social behavior can be recreated in the lab by housing meadow voles in short and long day lengths (N. S. Lee et al., 2019). Meadow voles raised in winter-like short days (SDs) exhibit higher social selectivity voles raised in summer-like long days (LDs). Selective preference in voles is assayed with a 3 chamber social preference assay, called the partner preference test (PPT), which measures time spent in chambers consisting of a familiar cagemate or unfamiliar stranger. Mice and rats do not exhibit a selective preference for familiar animals, whereas voles typically do (Beery & Shambaugh, 2021). In the PPT, SD female meadows exhibit a much stronger selective preference for cagemates than LD females, which spend most of their time alone in the empty chamber. Though the selective preference for familiarity in SD animals is robust, the effect is not as extreme as seen between mated pairs of prairie voles, which are known to form tight selective bonds with a single individual (Beery et al., 2009; Beery & Shambaugh, 2021). Interestingly SD meadow voles engage in some prosocial contacts with unfamiliar individuals in this assay, which is not seen often in prairie voles. This evidence suggests that SD meadow voles form close selective bonds with their home social group, but have the flexibility to tolerate and spend time with new individuals as well. In contrast, LD meadow voles are mostly uninterested in engaging with conspecifics prosocially.

Along with seasonal differences in social behavior, there are some clues that meadow voles also exhibit seasonal differences in stress responsivity. This species exhibits a seasonal difference in circulating stress hormones as well as as neuropeptide receptors that impact stress signaling in the brain (Anacker et al., 2016; Beery et al., 2014). Meadow voles also exhibit more anxiety-like behavior in the open field test than prairie voles, suggesting that physiological

systems regulating anxiety could be upregulated in this species (N. S. Lee et al., 2019). Importantly, these seasonal differences have been identified in females but not males. We therefore focus on females for this study.

An outstanding question remains whether seasonal or daylength differences in social behaviors of meadow voles are driven by environmental impacts of the social atmosphere during development, which are tightly correlated with daylength. Housing SD animals alone reduces prosocial contacts in a social interaction test with a stranger, and results in a similar behavioral profile to that observed in LD animals (N. S. Lee et al., 2019). This suggests that both season and social housing conditions interact to impact development, but rigorous studies comparing neural and behavioral differences across both social and lighting environments have not been completed.

Seasonal differences in brain states associated with behavior in meadow voles

A few studies have started to unravel neuroanatomical and functional neuronal phenotypes underlying differences in social behaviors across daylengths. Interestingly, differences in behavioral phenotypes seen across daylengths in the lab persist even when temperature in housing rooms is held constant at 70 degrees F (Beery et al., 2008; N. S. Lee et al., 2019). This suggests that while a physiological drive for warmth is an ultimate driver of close social interactions in the winter, it is not the proximate one. It is likely that brain circuitry has evolved to activate gregarious behavior with a seasonal change in daylight separate from those controlling thermoregulation. In addition, gonadectomy of LD female meadows, which should diminish differences in circulating estrogens across daylengths, is not sufficient to increase selective preferences and gregariousness of LD voles (Beery et al., 2008). A consequence must be that circuits not immediately impacted by circulating estrogens differ between long and short day animals.

Little is known about meadow vole brains in general, let alone what neural circuits regulate their selective bonding and gregarious behaviors. However, meadow voles do exhibit a seasonal difference in white matter thickness of a sub region of the hippocampus, the hilus, as well as a difference in the number of proliferating cells in the hippocampal dentate gyrus (Galea & McEwen, 1999; Spritzer et al., 2017). Interestingly, volumetric and cellular differences in the hippocampus and whole brain are common across seasonally breeding rodents, birds, and Eulipotyphlans (Jacobs, 1996; Lázaro et al., 2017). Given that a primary role of the hippocampus is spatial memory and navigation, these differences have been contextualized primarily in terms of differences in use of space in the environment across seasons (Jacobs, 1996; Jacobs et al., 1990; Zemla & Basu, 2017). Notably, hippocampal volume and space use are thought to be associated with reproductive schemes in voles. Hippocampal volume does not differ by sex in monogamous pine voles, for which both males and females have small and similar home ranges (Jacobs et al., 1990; Sherry et al., 1992). Some work suggests that hippocampal volume may differ by sex and is associated with home range size in polygynous meadow voles (Sherry et al., 1992). Males have larger home ranges and may have larger hippocampal volume. Another study did not find sex differences in hippocampal volume in this species, but did find a clear difference in volume associated with circulating hormone levels within sex (Galea et al., 1999). Therefore, differences in homerange size across seasons in both sexes could be an important factor that promotes differences in hippocampal volume in meadow voles.

While the hippocampus is primarily associated with spatial cognition and working memory, recent work suggests that there may be distinct and overlapping neural populations that

are relevant for social behaviors. A projection from dorsal CA1 to ventral CA2 of the hippocampus that is regulated by Oxytocin encodes social memory in mice (Meira et al., 2018; Raam et al., 2017). In addition, Pharmacological manipulation of histamine, dopamine, or B-adrenergic receptors in dorsal CA1 all impact social recognition memory in rats (Garrido Zinn et al., 2016). Given that social memory may be a core component of neural function controlling social tolerance and selectivity, the dorsal hippocampus is a compelling region to understand in more depth in meadow voles. Other work has identified hippocampal place cells that track the location of another individual but not the location of oneself in the local environment (Omer et al., 2018). While this finding is more difficult to directly connect to social tolerance and selectivity, it could be that tracking others in the environment takes different importance in different social contexts across seasons, characterized by either aggression or tolerance. The hippocampus has also been shown to directly encode a variety of social information and emotionally driven not directly relating to memory or space (Chang & Gean, 2019; Leroy et al., 2018; Menon et al., 2022), including social touch and sex of conspecifics (Rao et al., 2019). This evidence further suggests that this region may have broad functions relevant for social tolerance and selectivity.

Other evidence of neural differences between LD and SD meadow voles come from autoradiography studies of neuropeptides that regulate social behavior and stress (Beery et al., 2014; Beery & Zucker, 2010). Oxytocin receptors (OTRs), which are known facilitators of social reward, social memory, and close social bonds in a variety of mammalian and avian species, including closely related prairie voles, differ in intensity and localization of expression across daylengths. Peripherally administered Oxytocin (OT) enhances SD voles' preference to engage in prosocial contact with a familiar cagemate over a stranger in the PPT, but an OTR antagonist alone has no effect on behavior suggesting that OT is only partially responsible for selective social bonding in this species (Beery & Zucker, 2010b). Corticotropin releasing factor receptors (CRFRs), which are known to regulate anxiety related behaviors, social stress, social bonding, and social memory also differ in neural patterns of expression across day lengths in meadow voles (Beery et al., 2014a), but causal evidence for their role in stress or social bonding in meadow voles has not been established. Notably, the dorsal hippocampus is one region with differences in both CRFR and OTR expression across daylengths.

A possible role for 5-HT in seasonal regulation of prosocial behaviors

These pieces of evidence are valuable in understanding potential brain mechanisms contributing to seasonal differences in behavior, but ultimately represent a small minority of potential mechanisms. While the list of possible candidates is long, serotonin (5-HT) is a strong candidate to modulate social tolerance and stress across daylengths because other species exhibit photoperiod induced changes in expression of components of the 5HT system, and it is known to modulate social and anxiety-like behaviors (Mc Mahon et al., 2018; Molnar et al., 2010; Tyrer et al., 2016). While it is unclear whether serotonin levels differ with day length in meadow voles, seasonally breeding chipmunks and quail as well as non-seasonal C57/Bl6J mice have higher levels of serotonin in the dorsal raphe nucleus when housed in long photoperiods (Goda et al., 2015; Tiwari et al., 2006). Serotonin is a precursor to melatonin, which has a well known role in facilitating photoperiod associated changes in behavior of multiple species, and is known to modulate serotonin production (Bueno et al., 2023; Kirsz & Zieba, 2012; Míguez et al., 1995; Munley et al., 2022). 5HT impacts a wide variety of receptors across many brain regions, but multiple pieces of evidence suggest that the hippocampus may be a hub for 5HTs action on social

behavior and anxiety, particularly via the 5HT1a receptor (Andrews et al., 1994; Mineur et al., 2015). In Mandarin voles, chronic social defeat stress causes differences in expression of 5HT and 5HT1a receptors in CA3 of the intermediate hippocampus as well as reduced social recognition (L. Wang et al., 2019). Interestingly a 5HT1a antagonist administered to this region impaired social recognition, and chemogenetic activation of 5HT1a bearing neurons in CA3 was sufficient to reverse the effects of chronic social defeat stress on social recognition. BTBR mice show enhanced social investigation with infusion of a Serotonin receptor 1A agonist or an antagonist of the serotonin reuptake transporter to the hippocampus (Gould et al., 2011). Hippocampal 5-HT also regulates positive social experience in B6J mice. Optogenetic activation of serotonergic terminals projecting from the dorsal raphe to the dorsal hippocampus are sufficient to reinforce positive social interactions, but the exact 5HT receptors involved in this circuit are unknown (Nagai et al., 2023). In humans, 5HT is thought to be involved in seasonally regulated anxiety behaviors, as well as social and emotional behaviors. It has been proposed to be a key factor regulating seasonal affective disorder, a change in anxiety and depressive states corresponding to seasonal changes in light (Mc Mahon et al., 2018; Molnar et al., 2010; Tyrer et al., 2016).

Assessing environmental regulators of hippocampal transcription with snRNAseq

Here we used single nucleus RNA sequencing on dorsal hippocampi from meadow vole brains to gain a broader understanding of differences in cell type specific gene expression across daylengths and social housing conditions that might be contributing to differences in social behavior. We believe this is the first single nucleus or single cell RNA seq study conducted in vole brain tissue. We used a targeted approach to assess the landscape of hippocampal serotonin receptors in meadow voles, while also using unbiased unsupervised analyses to detect differences in a broad range of brain cell types and transcriptional pathways. Our analyses revealed unexpected differences in transcription in glial cell clusters between solo housed and pair housed SD meadow voles.

Results

snRNAseq resulted in 44,000 good quality nuclei for downstream analyses

We sequenced 62,000 single nuclei from the dorsal hippocampus of 18 female meadow voles housed in one of four conditions: long day length and solo housed, long day length and pair housed, short day length and solo housed, short day length and pair housed (LD solo, LD pair, SD solo, SD pair). ¾ of each group underwent the forced swim immediately before nuclei collection in an attempt to quantify stress response in the form of immediate early genes (Fig 4.1B; forced swim not discussed in this work). RNAseq reads were mapped to the prairie vole genome with STAR, because there is currently no publicly available annotation for the meadow vole genome (Fig 3.1C;Dobin & Gingeras, 2015). We achieved a mapping efficiency of approximately 51% for all samples, and returned a median 2,091 genes per cell, which are similar to industry standards for snRNAseq in mice (https://kb.10xgenomics.com/hc/en-us/articles/360015646532). All samples exhibited similar cell numbers, mitochondrial content and median transcripts per cell, suggesting similar quality across samples (Fig 4.S6 and Fig 4.S7). After filtering out unlysed cells by thresholding percent mitochondrial transcripts, and doublets based on transcript counts, we were left with 44,000 usable single nuclei for analysis.

Clustering and feature detection revealed 35 distinct cell types in the dorsal hippocampus

We clustered cells using the standard Seurat pipeline, using the single cell transform function for normalization and feature detection. We projected K- means clusters onto a UMAP space for visualization revealing an initial 39 clusters (Fig 4.2A; Hao et al., 2021). Differential expression analyses revealed top markers for each bioinformatically determined cell class. Many of these markers, though highly differentially expressed from cluster to cluster, were not informative markers for determining cell type. We further sorted differentially expressed genes to identify specific markers that were expressed in a high percentage of each cluster of interest but not in other clusters. This approach yielded sets of cell type specific markers which we were able to associate back to major brain cell types for most of our clusters (Fig 4.3A-E). Some of the major markers we used included *Snap25* for neurons, *Slc17a7* for excitatory neurons, *Gad2* for inhibitory neurons, and *Slc1a3* for astrocytes, Mbp for oligodendrocytes, *Pdgfra* for oligodendrocyte precursors (OPCs), and *Csf1r* for Microglia. (Batiuk et al., 2020; Masuda et al., 2020; Nagy et al., 2020). Interestingly, some markers that are highly expressed in mouse hippocampus were not present at high levels in our dataset, including inhibitory marker *Gad2*, microglial marker *Aif1*, and oligodendrocyte markers Olig1 and Olig2 (Cembrowski et al., 2016, https://shorturl.at/jGWXY).

We next attempted to map our cell populations onto known markers for regional subtypes of hippocampal neurons in mice (Figs 4.3F, Fig 4.S1; (Cembrowski et al., 2016; Rattner et al., 2020, https://shorturl.at/jGWXY). Clusters containing Granule cells of the dentate gyrus were classified as those with high Prox1 expression. CA1,CA2, CA3, and subicular areas of the hippocampus all contain overlapping sets of markers, and we found it necessary to use multiple markers for each. CA1 clusters were characterized by high expression of *Man1a* and *Kcnh7*, and low expression of CA3 markers, including *Grik4* and *Cpne4* (Fig 3.3G-H). CA3 clusters were characterized by the opposite pattern of expression. Interestingly we could not identify any specific cluster pertaining to CA2 cells in our dataset despite this region being a major contributor to excitatory neurons in the hippocampus. However we expect that these cells are

mixed in with other clusters given the high overlap of markers between all CA regions identified in mice. We identified multiple clusters of potential subicular cells, however we did not find that specific markers of subicular sub regions such as the pre- and post-subiculum separated into unique clusters (Ding et al., 2020). Therefore we classify all of these regions as putative subicular cells for the following analyses (Fig4.3I-K).

Serotonin receptor expression does not differ by daylength

We found multiple 5HT receptors expressed in the dorsal hippocampus, including *Htr2a, Htr2c, Htr3a, Htr4, and Htr7*. Of these, *Htr4* was expressed most highly in the data set and its expression was mostly located in clusters containing cells from CA1, CA3, Dentate gyrus, and Oligodendrocytes. *Htr7* was moderately expressed in cells from CA1, CA3, the subiculum, and in interneurons. Other 5HT receptors were barely expressed in our dataset (Fig 4.S2). To test whether SD and LD animals had differential expression of 5HT signaling molecules, we ran pairwise differential expression analyses for all clusters across day lengths for all variable genes in our data set. Contrary to our hypothesis, we did not find that any 5HT receptors differed significantly in expression across day lengths within any cluster after correcting for multiple comparisons (Fig 4.S3).

Housing has a greater impact on cell type specific transcription than daylength

After directly testing our hypothesis concerning 5HT receptors, we broadened our search to explore additional differences between DL and housing conditions with an unsupervised lens. To understand whether cells from any of our housing and DL groups were enriched within any cluster, we compared the number of cells per cluster across housing and daylength. We found that proportions of cells from LD and SD animals were significantly different only in cluster Sub/Ctx-2, as determined by a proportion test permuted 10,000 times, Fig 4.4A). Of note, cluster UID-2 contained cells from only one sample, so we omitted significant results pertaining to this cluster. Proportions of cells from solo and pair housed animals differed in several clusters including Sub/Ctx-1 and Sub/Ctx-2. Pairwise comparisons of proportions of cells across housing conditions within daylength revealed that both LD and SD paired animals had larger proportions of cells in cluster Sub/Ctx-1 than LD and SD solo animals respectively. LD paired animals had the greatest proportion of cells within this cluster (Fig 4.4A).

To investigate overall differences in transcription across all groups and clusters, we ran a first pass of differential expression analyses for every pairwise comparison of housing and daylength conditions across all of clusters. Surprisingly, we found that most differentially expressed genes corresponded to comparisons across housing conditions (Fig 4.4B). Sparse sets of genes were differentially expressed across daylengths.

The housing comparison within SD animals contained the highest proportion of differentially expressed genes at log2FC cutoffs of 0.5 and 0.25 (Fig 4.4C-D). Genes with high log2FC in differential expression were spread across many clusters, limiting our ability to perform analyses requiring large numbers of significantly DE genes within a cluster. Therefore we choose to focus on genes with log2FC>0.5 for discussion of individual genes that may impact the function of cells in each cluster, but include genes with log2FC>0.25 for analyses of larger networks of lowly expressed genes that could combinatorially impact cellular function within clusters.

The most prominent set of differentially expressed genes belonging to a single comparison and cluster at log2FC>0.5 corresponded to cluster Sub/Ctx-1 (Fig 4.4C). This fits

with our finding that housing impacts the number of cells in this group as differential expression is computed both on the number of cells expressing a given gene and its log fold change in expression across groups.

We found large proportions of genes differentially expressed between solo and paired housed SD animals in clusters containing microglia, oligodendrocytes, astrocytes, with smaller sets of differential expression in clusters containing excitatory neurons (Fig 4.4C-D). At log2FC>0.5, DE in this group was distributed across many clusters, with relatively few differences within each cluster. Therefore we chose to focus first on the prominent set of highly differentially expressed genes between LD animals in cluster Sub/Ctx-1, followed by analyses of more subtle differences in expression between solo and pair housed SD animals from glial cells .

LD Paired animals have an enriched subicular cell type with reduced expression of markers of glutamatergic function and process formation

Given the large difference in proportion of cells across housing groups in cluster Sub/Ctx-1, we wanted to further investigate the identity of this cluster. And given that differential expression analyses of single cell RNA seq data take into account both the percentage of cells per condition expressing a gene and the log fold change in expression, and given the large difference in number of cells across conditions, we set a stringent threshold for DE analysis. 40% of cells in each condition needed to express a gene with an average log2FC>0.5 for it to be considered for DE. This approach left 13 differentially expressed genes between solo and paired LD animals. This list consisted of genes primarily involved in cell adhesion and morphogenesis, including *Astn2, Fat3, Lsamp, Unc5d, and Brinp3* (Fig 4.5A-B; Avilés et al., 2022; Behesti et al., 2018; Berkowicz et al., 2017; Jackson et al., 2016; Philips et al., 2015). There were not enough DE genes on this list to successfully run gene ontology analysis.

As an additional approach to understanding the function of this cluster, we compared its gene expression with a neighboring, closely related subicular cluster that contained equal proportions of cells across conditions. This analysis revealed significant upregulation of some genes associated with process formation and synaptic function and neuronal wiring, including Schamonnin interacting protein one (*Schip1*), which is upregulated in cluster Sub/Ctx-1 vs Sub-2 (Fig 4.5C-D; Klingler et al., 2015). Genes involved in synaptic function and NMDA receptor signalling, such as *Gpc6*, and in glutamate trafficking and AMPA receptor function, such as *Sorcs1*, were upregulated in cluster Sub-2 as compared to cluster Sub/Ctx-1 (Fig 4.5C; (Allen et al., 2012; K. Sato et al., 2016; Savas et al., 2015)). These results generally suggest differential mechanisms for synaptic function and glutamatergic signaling between cluster Sub/Ctx-1 and Sub-2.

We then used gene ontology to summarize how differential genes correspond to biological function across these two clusters. Nine significant go terms with at least 2 genes were returned (Fig 4.5D). The most prominent term was “nitrogen compound metabolic process”. Although this term is broad, this process is commonly associated with glutamate synthesis in the brain, further supporting that clusters Sub/Ctx-1 and Sub-2 may have functional differences in glutamatergic signaling. Other significant GO terms included regulation of neuronal migration and focal adhesion assembly, both of which could be associated with axon dendritic spine and synapse formation in the adult brain.

We next identified cluster specific features with differential expression across solo and paired LD animals by cross referencing DE genes across conditions within cluster 9 and DE

genes between clusters Sub/Ctx-1 and Sub-2. We found that 4 of the 13 genes in our conditional DE overlapped with DE genes between cluster Sub/Ctx-1 and Sub-2 (Fig 4.6A-B). Though the overlapping gene set was too limited to run ontology, several of these genes are associated with adhesion and dendrite growth, including *Unc5d, Brinp3, and Fmn1* (Berkowicz et al., 2017; Jackson et al., 2016; Kawabata Galbraith & Kengaku, 2019). All of these genes were upregulated in LD solo animals vs paired animals. Together these findings suggest that cell adhesion and morphogenesis are important features of Sub/Ctx-1 cells, and that cells of solo LD animals have a more connective, morphogenic phenotype than those of paired LD animals.

Daylength impacts expression of genes contributing to myelination in oligodendrocytes

Although the majority of group differences corresponded to social housing type, we also found that daylength impacted transcription in some clusters. Short day animals expressed Tmem132d, a marker for differentiated and myelinating oligodendrocytes, more highly than long day animals in the major oligodendrocyte cluster, Olig-1 (Fig 4.7A-B; Nomoto, 2003). Short day animals also express higher levels of *Rassf4 and Nav3*, genes involved in cell growth and process formation, a function known to be involved in oligodendroglial growth and myelination (Fig 4.7C; Bauer et al., 2009; Stringham & Schmidt, 2009). Long day animals express higher levels of *Ppfia2*, a negative regulator of cell adhesion, and *DHCR7*, an enzyme involved in cholesterol biosynthesis and maintaining myelin after loss (Berghoff et al., 2021; Szklarczyk et al., 2019). A targeted search for differences in expression of genes directly involved in myelin production also revealed moderate upregulation of *Mog* and *Mag*, but not *Mbp* in paired SD animals, supporting potential enhancement of white matter in paired vs solo animals (P. R. Lee, 2009). Gene ontology was not appropriate for genes differentially expressed between daylengths in cluster Olig-1 because few genes in this comparison overall met our p value and logfc thresholds for differential expression.

Given that many significant genes within the Olig-1 cluster were expressed in a smaller subset of cells, and that previous single cell work with oligodendrocytes has successfully clustered into a variety of subtypes, we wondered whether initial clustering including all variably expressed genes within the dataset limited our ability to resolve smaller groups of cells within this cluster. To investigate this, we subsetted the Olig-1 cluster and re-clustered these cells based on a new set of variable features specific to this group of cells (Fig 4.8A). We attempted to identify subtypes of oligodendrocytes including newly formed and immature myelin forming oligodendrocytes by mapping known markers for these subtypes onto the four clusters identified in our dataset. We found that subclustering did not clearly separate this cluster into previously identified functionally distinct subtypes. Markers for mature and myelin forming oligodendrocytes (*Mal, Mog, Mbp, Ptgds, and Apod*) were intermixed throughout the sub clusters identified in Olig1 (Fig 4.8B-C), and there was no visible expression of identified markers for committed oligodendrocytes or newly formed oligodendrocytes (*Tcf7l2, Casr, Vcan, Bcas1, Gpr17, Nkx2-2, Sox6, Bmp4, Gpr17, Neu4, Sox10, Olig2*) (Marques et al., 2016). This suggests that Olig-1 is homogeneously composed of mature and myelinating oligodendrocytes with no clearly defined subtypes by specific marker expression. In further analyses with Olig-1, we analyzed the cluster as a whole.

Social Housing in SD animals impacts transcription in glial clusters

We found that a large proportion of the differentially expressed genes across all conditions pertained to differences in expression within glial clusters of SD animals across social

housing conditions (Fig 4.4D). Of note, *Tmem132d*, which was highly differentially expressed in Olig-1 across daylengths, was expressed even more highly in SD paired animals than SD solo animals (Fig 3.6B). Other top differentially expressed genes in Olig-1 between social housing conditions in SD animals included *Dthd1* and *Zbtb16* (Fig 4.9B), both involved in cell division in other cell types but whose function is unknown in oligodendrocytes (Szklarczyk et al., 2019; Usui et al., 2021; Xiong et al., 2023). Of note, we found that the 5HT receptor *Htr4* was mildly but significantly upregulated in Solo vs paired SD animals (Fig 4.S9). Gene ontology analysis for differentially expressed genes at a threshold of LogFC>0.25 revealed broad categories of enriched biological processes, including developmental growth, calcium transport, and glutamatergic signaling (Fig 4.9C). All of these ontologies may be relevant for regulating myelination in SD animals.

Social housing in SD animals also influenced expression of a large number of genes in primary astrocyte cluster Astro-1. Top differentially expressed genes upregulated in paired animals include the estrogen responsive gene *Ugt1a1* (Davenport, 2012). Epha5, known to contribute to glia-neuron interactions at synapses, and Csmd3, involved in astrocyte development, were upregulated in SD solo animals (Fig 4.10B; Murai & Pasquale, 2011; Song et al., 2022). Gene ontology analysis revealed significantly enriched biological processes in SD solo animals compared to SD pair, including regulation of ion transport, membrane potential, and postsynaptic transmission (Fig 4.10C), suggesting that astrocytes of solo SD animals may be more excitable and uptake ions at different rates.

In the microglial cluster MG-1, SD paired animals expressed a potential anti-inflammatory marker, *Ptprm* (Kim et al., 2018). While solo animals expressed higher levels of *Nav1*, involved in microglial migration, generally regarded as a proinflammatory function (Fig 4.11B; Black et al., 2009). Ontology revealed enrichment for morphogenic, growth, and homeostatic functions in SD solo animals, which further supports a potential pro-inflammatory, M2-like phenotype in this group (Fig 4.11D). Interestingly, the 5HT receptor Htr4 was significantly upregulated in Solo vs paired SD animals within MG-1 as well (Fig S7). Lastly, it is worth noting that SD animals overall expressed moderately more Rora than LD solo vs paired animals in MG-1 (Fig 4.11C). This gene is linked to melatonin signaling and controls clock pathways in other brain regions (Ma et al., 2021; T. K. Sato et al., 2004).

Social Housing in SD animals impacts plasticity related genes in CA3 cells

Although the DE genes associated with social housing in SD animals were spread diffusely across clusters, some interesting genes were DE in our primary cluster of CA3 cells, CA3-1. Of note, *Kirrel3*, a gene involved in synapse formation, and *Agap1*, involved in endosomal trafficking were upregulated in paired animals compared to solo (Fig 4.10A-B; Arnold et al., 2016; Taylor et al., 2020). *Piezo2*, a mechanosensitive ion channel, and *Kcnh7*, a potassium channel were both upregulated in solo animals over paired animals (Fig 4.10A-B (Shin et al., 2019)). As mentioned in the previous section, too few genes met our significance threshold to effectively run gene ontology on this cluster and comparison. However it is possible that these genes are involved in differential neurotransmission and synapse formation across housing conditions.

Notably, a smaller cluster of CA3 cells, CA3-2 also exhibited a large set of differentially expressed genes across housing conditions amongst SD animals. *Kirrel3* was upregulated in SD animals in this cluster as well, suggesting that it is a common feature of SD paired animals across CA3 subtypes (Fig 4.10A-B). Other upregulated transcripts included another adhesion molecule

Negr1, and a gene involved calcium vesicle transport, *Cadsp2* (Shinoda et al., 2018; Singh et al., 2019).

Discussion

Here we present the first single cell nucleus RNA seq data set in any species of vole. We found primary impacts of social housing on transcription of genes involved in glial function in SD animals. The overall impact of housing in SD animals may fit with previous evidence that SD animals housed alone express dramatic changes in prosocial behavior, with phenotypes similar to LD animals (Lee et al., 2019). Multiple studies from a variety of prosocial species suggest that social isolation during development can dramatically impact hippocampal function. Post weaning social isolation in rats is associated with reduced dendritic spine length in CA1 pyramidal cells (Ferdman et al., 2007). A week of social isolation in swiss mice is sufficient to reduce glutamatergic transmission in dorsal CA1 (Almeida-Santos et al., 2019). Moreover, striking changes in glial biology arise due to social isolation. In mice, chronic social isolation reduces expression of myelin basic protein (*Mbp*), in the prefrontal cortex (Liu et al., 2017). While we did not find a difference in *Mbp* expression between oligodendrocytes of solo and pair housed animals, we did find that expression of two other critical genes for myelin production, *Mag* and *Mog*, were reduced in SD solo vs paired animals. Liu et al., also found an associated decrease in the number of myelinated axons in isolated animals. By extension, this suggests a potential for difference in myelination between solo and paired SD animals. Aside from *Mag* and *Mog*, we found that multiple genes involved in process formation, ion transmission, and cell adhesion were differentially expressed between oligodendrocytes of solo and paired SD animals. Though ion transmission is classically considered as a primary function of neurons, it is also critical for myelin production (Butt, 2006). In vitro, primary oligodendrocyte cultures grown without neurons emit spontaneous calcium transients. In vivo calcium imaging also suggests that calcium transients in oligodendrocytes are associated with retraction of myelin sheaths during myelination (Baraban et al., 2018). These findings further support that differences we have observed between oligodendrocytes of solo and paired SD animals may be associated with functional differences in myelination.

By extension, we observed a smaller set of differentially expressed genes between oligodendrocytes of SD and LD animals, including *Tmem132d*. This marker for mature myelinating oligodendrocytes is a cell adhesion molecule whose precise function in oligodendrocytes is not known (Nomoto, 2003). However other transmembrane proteins, such as *Tmem108*, are known to control myelin production and proliferation in oligodendrocytes (Wu et al., 2022). Given that *Tmem132d* is enriched in SD paired animals over SD solo animals, it is possible that SD paired animals exhibit the most pro-myelinating phenotype, and may have the most typical phenotypes of myelin production for their daylength (Galea & McEwen, 1999; Spritzer et al., 2017). Given that SD animals are gregarious, it is possible that housing them against their natural social preference could reduce myelin to levels similar to LD animals. This hypothesis should be tested directly in future work comparing myelin thickness in animals reared socially and in isolation across day lengths. In the long run, manipulating myelin across day lengths and social housing conditions after seasonal development could eventually reveal a more direct connection between myelin and social tolerance. Myelin restoring compounds are an active area of research for therapeutic applications, and could serve as valuable tools to enhance levels of hippocampal myelin in LD animals to that of SD animals (Manousi et al., 2021).

We also found that social housing impacted expression of genes related to critical membrane potential properties of astrocytes as well as inflammatory functions in microglia. Astrocytes are the most abundant cell type in the brain, and exert powerful influences on synaptic function. Each astrocyte can contact around 100,000 synapses, for which they tune the intensity of synaptic potentials via exchange of ions and other molecules that drive expression of molecules relevant for neurotransmission such as postsynaptic receptors (Chung et al., 2015). In addition, astrocytes actively contribute to neuronal wiring by refining synapses via phagocytosis of inactive synapses or prompting synapse formation (Chung et al., 2015). One of the top upregulated molecules we identified in SD paired animals was *Epha5*. Though the function of *Epha5* in astrocytes is not known, disrupting signaling of related *Epha3* or *Epha4*, both involved in Epherin signaling, induces growth of abnormal dendritic spines (Murai & Pasquale, 2011). This suggests that astrocytes of SD paired animals may be better equipped with molecular machinery to adequately prune hippocampal synapses and aid their proper development. Like neurons, astrocytes exhibit a resting potential that is driven by flow of ions across their membranes, so it is not surprising that many differentially expressed genes between SD solo and pair housed animals were related to membrane function and ion transmission. Recent work has shown that changes to resting potentials of astrocytes can induce release of neurotransmitters that reach postsynaptic receptors located on neurons to alter synaptic function (Deemyad et al., 2018). Additionally, astrocytes are thought to serve as a cellular sink for ions and neurotransmitters by absorbing excess molecules from synapses, which can further modify their resting potential (Furness et al., 2008; S. Song et al., 2020). In light of our own findings, it is possible that astrocytes of SD solo and pair housed animals exhibit differences in their ability to regulate their resting membrane potential which could have implications for synaptic function. Neurophysiological studies directly measuring membrane potentials in astrocytes or measuring synaptic activity as a function of fluctuation in membrane potential associated with synaptic activity in neurons could be valuable future directions in assessing the functional impacts of the transcriptional differences we observe in astrocytes across housing conditions here.

Microglial cells also contact many neurons and contribute to synaptic function via phagocytosis (Galloway et al., 2019). Interestingly we observed differences in expression of Rora, a putative melatonin receptor that is known to be associated with inflammatory function in microglia, between LD solo and paired animals (J. Li et al., 2022; T. K. Sato et al., 2004). Generally inflammatory pathways in microglia promote a more ramified, active state whereby these cells are more closely interacting with neurons and phagocytosing synaptic materials (Tang & Le, 2016). Given that melatonin is secreted during periods of low light, it is thought that photoperiodic species release more melatonin during winter months or in SD (Baekelandt et al., 2020; Xu et al., 2018). We observed higher levels of expression of *RORa* in LD solo animals than pair animals, and no difference in *RORa* across day lengths. This could suggest that the brains of animals held in constant photoperiods may have fully adapted to differences in melatonin production. Given that stress can modulate melatonin levels, it is possible that constant stress from social housing could be an active modulator of melatonin and impact neural signatures of melatonin signaling (Barriga et al., 2001). Though we found few overall differences in gene expression between LD and SD microglia, we observed expression of an antiinflammatory marker *Ptprm1* in SD paired animals and potential proinflammatory marker *Nav1* in SD solo animals (Black et al., 2009; Kim et al., 2018). Though further testing is needed, this finding could suggest that paired animals have less inflammatory microglial cells than SD solo animals. This would be consistent with other findings that social isolation stress increases

inflammatory processes in microglia. In addition to validating differentially expressed genes we observe here across housing conditions with in situ hybridization, it would be interesting to test whether microglia are involved in earlier development of day length specific behaviors, as microglia are known to respond to sex hormones to modulate various elements of neuronal development and physiology (Nelson et al., 2019; Saijo et al., 2013). Immunohistochemical profiling of microglial ramification, which is known to differ in response to sex hormones, at multiple time points during the 40 day transition from LD housing to SD housing in these animals could be an appropriate starting point to test this hypothesis.

Despite a logical connection between serotonin and seasonally regulated behaviors, we did not detect differences in expression of serotonin signaling components across the day lengths in the dorsal hippocampus. One reason for this could be that we found overall low levels of expression of serotonin receptors in our dataset. This is not uncommon for g-protein coupled receptors in RNA seq data, as they are generally expressed at low rates and RNA seq is only capable of detecting the most highly expressed genes in a given tissue (Sriram et al., 2019). We did find a small difference in expression of our most abundantly expressed serotonin receptor, *Htr4*, between solo and paired SD animals in oligodendrocytes and microglia. While the function of *Htr4* in these cell types is not well understood, it is clear that serotonin impacts glial function. Administration of excess exogenous serotonin to oligodendrocytes impacts both their development and myelination (Fan et al., 2015). Serotonin also initiates signaling cascades that regulate inflammatory processes in microglia, and serotonin signaling in these cells is thought to actively contribute microglial involvement in adult neurogenesis of dentate gyrus cells(Turkin et al., 2021).

Of note, we observed far fewer differences in expression in glial clusters between solo and paired LD animals than SD animals in these glial clusters. And overall we find more differences in expression between solo animals across day lengths than paired animals across day lengths in these clusters. These findings suggest that solo housing in SD animals creates more extreme phenotypic change than pair housing LD animals, both of which go against the animals natural housing preferences. This may suggest that social isolation stress in the typically gregarious SD animals causes drastic changes in hippocampal circuitry, whereas social environment matters less for LD animals.

Though the majority of our findings come from differential expression in glial cells we did report several findings in neuronal clusters. In particular we found that a cluster of subicular cells with reduced markers of glutamate transmission and process formation as compared to a closely related subicular cluster was more populated amongst LD solo animals than LD pair animals. The subiculum serves as an output region of the hippocampus that forms an intermediate node of circuits projecting to cortex, hypothalamus and other regions of the brain (O'Mara, 2006; J.-J. Yan et al., 2022). Interestingly, the dorsal subiculum has become known for its control of head direction in the context of spatial navigation, but this region is poised to regulate social and emotional behaviors as well (Petrulis et al., 2005; Robertson et al., 1999; J.-J. Yan et al., 2022). Most work investigating the role of the subiculum in social behaviors in mice has focused on the ventral subiculum, which we were unlikely to capture with our dissection strategy. The ventral subiculum is thought to be involved in social recognition and discrimination between social odors in mice, and post weaning social isolation in rats impacts LTP in a CA1 projection to the ventral subiculum (Petrulis et al., 2005; Roberts & Greene, 2003). It is possible that dorsal CA1 to subiculum projections may take on species specific social functions in meadow voles because dorsal CA1 is a hotspot for oxytocin receptor expression in meadows,

whereas in mice, oxytocin receptor is expressed in dorsal CA2 and CA3 but not CA1 (Beery & Zucker, 2010; Young & Song, 2020). Within cluster Sub/Ctx-1, LD solo animals also expressed higher levels of *Brinp3*, a schizophrenia risk gene that has been implicated in social behavior(Berkowicz et al., 2016). Together these results suggest that LD paired animals might have reduced subicular glutamatergic transmission which may be relevant for social behavior. Given that LD animals are highly territorial and aggressive, It is possible that paired housing conditions in LD animals might act as a stressor similar to solo housing in SD animals. Interestingly, deficits in social recognition induced by ventral subicular lesions in rats are restored by housing rats in short photoperiods (Subhadeep et al., 2020), adding further evidence that photoperiod may play a role in subicular control of social behaviors. Here we report primary impacts of housing on subicular transcription in LD but not SD animals, which might be a result of photoperiod driven differences in the response of subicular cells to environmental stimuli, such as stress. Our findings provide clues of altered plasticity in subicular cells in LD paired animals in response to a potentially stressful social environment, but this should be validated by assessing differences in protein expression related to synaptic function in LD animals reared in different social housing conditions.

Lastly we observed traces of differential neurotransmission and synaptic function in CA3 cells of SD solo and pair housed animals. SD paired animals express *Kirrel3* significantly higher than SD solo animals. Interestingly, this gene causes hyperactive CA3 neurons when knocked out in mice, suggesting that SD solo animals could have aberrant activity in CA3 cells(Martin et al., 2015). This gene is also necessary for the development of olfactory circuits regulating aggression in male mice, but it is unclear how *Kirrel3* in CA3 cells might be important for social behaviors (Prince et al., 2013). Though multiple other differentially expressed genes in this cluster suggest potential functional differences in dendritic morphology and endosomal function, there were too few differentially expressed genes to successfully run ontology. It is possible that enriching for CA3 cells with cell sorting could provide a larger sample size with which to assess differential expression within this region.

Beyond differential expression, we believe this dataset will serve as a valuable resource for understanding the basic biology of hippocampal cell types in meadow voles vs other species of rodents with single cell RNA seq datasets of hippocampal cells, such as mice. Interestingly we did not find any CA2 cells in our dataset, as defined by region specific markers identified in mice. This finding was surprising given that cells from most other hippocampal regions successfully mapped onto markers that have been identified in mice. Given the functional similarity and high overlap of transcriptional markers between CA1, CA2, and CA3 and given that CA2 is the smallest subregion of CA pyramidal cells, we suspect that CA2 cells are present in our dataset but mixed into other clusters of CA pyramidal cells. However it is possible that CA2 could be molecularly unique in meadow voles as compared to mice, and this hypothesis should be tested directly in future work by comparing cell type specific transcriptomic profiles of cells in our dataset to those found in mice with a more unbiased lens. This indeed is a compelling direction for all the cell types in our dataset, as it would be interesting to know whether meadow voles possess species specific cell types or molecular profiles that could be relevant for species specific behavior.

While we hope that we have supported an established finding of seasonal differences in hippocampal myelination in meadow voles (Galea & McEwen, 1999), we failed to replicate some other established findings in our data. In addition to seasonal differences in volume in the hilus, some studies have identified seasonal differences in the number of proliferating cells in the

dentate gyrus, as identified by proliferative markers *Ki67* and *DCX* (Spritzer et al., 2017). In our dataset, we did not see high expression of general markers for cell proliferation or adult neurogenesis including *Ki67* and *DCX*. This could be due to a lack of well described transcriptional markers for proliferation in the adult brain, as most common studies localize proteins of markers for hippocampal neurogenesis. We also did not replicate previous findings of differences in Crfr1, Crfr2, and Oxtr expression across daylengths (Beery et al., 2014; Beery & Zucker, 2010). We did detect low levels of all three genes in our dataset, but we suspect that G-protein coupled receptors such as these are expressed at too low of levels to detect differences in expression with our sequencing strategy. A similar story emerged with serotonin receptors, which were generally too lowly expressed in our dataset to detect differential expression. Potentially sequencing more cells at a higher sequencing depth could begin to confirm these differences, but ultimately other more sensitive assays, such as in- situ hybridization or spatial transcriptomics with curated probe sets should be used to confirm these findings. Of note, studies that have identified differences in neuropeptide expression across day lengths in meadow voles have used autoradiography, as working antibodies are not often available in non-model organisms (Beery et al., 2014b; Beery & Zucker, 2010a). Because autoradiography is agnostic to cell type specific expression, we cannot say which cell types these behaviorally relevant neuropeptide receptors are expressed in. Here we have generated a toolbox of species specific markers for nearly all major subtypes of hippocampal cells that can be colocalized with mRNA from genes of interest to identify in detail how lowly expressed genes are distributed amongst different cell types in the hippocampus of this species. Not only this but we lay the experimental groundwork for using single nucleus RNA seq as a tool for identifying differences in expression of these genes across daylengths and housing conditions. In general all findings of differential expression observed here should be validated using similar approaches of in situ hybridization, spatial transcriptomics, and protein localization with immunohistochemistry. Overall we believe this dataset to be an impressive resource for future work to characterize neural function in genetically diverse non-model organisms with unique social behaviors.

Methods

Animals

All meadow voles were housed in a breeding colony at the University of California berkeley (AUP-2022-02-15085). All animals were born in a room with a LD light cycle consisting of 14 hours of light and 10 hours of dark (14L:10D). On postnatal day 21 animals were group weaned into a cage containing littermates for up to five days, and then moved to their final housing. "Solo" animals were housed alone, and "Paired" animals were housed with a single same sex littermate. Animals in the SD group were moved to a separate housing room with a 10L:14D cycle. For at least 40 days, an established window of time to promote daylength induced changes in reproductive physiology, prior to the experiment start. All animals were between 69 and 87 days old at the start of the experiment. In total the experiment included 18 animals (LD solo n=5, SD solo n=4, LD pair n=4, SD pair n=5).

Forced Swim Stressor

Three of four animals from each of the day length/housing groups were subjected to a forced swim stressor immediately before harvesting nuclei. One animal from each group was randomly selected to be a no-swim control. In each experiment, two animals were processed in parallel. Animals in the swim group were moved to a separate experimental room on a wheel cart approximately five minutes before the experiment started. Each of the two animals were placed in their own buckets of water for three minutes, with the first animal beginning their swim two minutes before the second to facilitate timing in later brain dissection steps. Anecdotally, voles can swim downwards seeking escape routes and inadvertently drown. We monitored our voles and scooped them out of the water and replaced them at the surface if they began to swim down for more than 10 seconds. Immediately after the swim, animals were scooped out of the water with a strainer, dried in a bath towel, and placed in an isoflurane chamber to begin euthanasia within one minute of the end of the swim. Control/ no-swim animals were removed from their housing room immediately before euthanasia. Animals were carried by hand to the experimental room in order to mitigate potentially stressful impacts of travel on carts. The first animal was carried about two minutes ahead of the second and began euthanasia while the second animal was in transit to facilitate later timing in dissection steps.

Euthanasia and brain dissection

After the forced swim test, euthanasia and brain dissection was precisely timed to maximize the chance of detecting nuclear immediate early gene transcripts, which can leave the nucleus within 12 minutes (Guzowski et al., 1999). Isoflurane dose was controlled so that animals died within two minutes of exposure. Animals were placed in a drop jar containing 9mL of isoflurane on a paper towel within an empty pipette tip box to prevent contact with the isoflurane. 9mL was the minimum amount of isoflurane needed in order for the voles to consistently die within 2 minutes. 17/18 voles died within 2 minutes of exposure. All animals were kept in the iso chamber for exactly two minutes, regardless of their time of death. The animal that did not die while under isoflurane was removed at two minutes and euthanized by rapid decapitation. Brains were removed from the skull within approximately two minutes of euthanasia, and placed on ice cold PBS for the remainder of the hippocampal dissection. To remove the dorsal hippocampi, the brain was first bisected with a cold razor blade. A feather blade scalpel was used to make an incision through the anterior portion of the fornix on the medial surface of the brain, below the

anterior-most portion of the dorsal horn of the hippocampus. The hippocampus and cortex were lifted from the midbrain as a single unit and a second incision was made on the wall of the intermediate hippocampus just below the ventral surface of the dorsal hippocampus. This dissection strategy achieved tissue samples primarily composed of dorsal hippocampus, with some intermediate hippocampus, but omitting the ventral horn. Both dorsal hippocampi were placed in a 1.5 mL tube containing ice cold PBS before further dissection.

Nuclear Dissociation

We began nuclear dissociation approximately 10 minutes after the end of the dissection. All steps for the remainder of the dissociation protocol were performed on ice. Hippocampi were chopped with a feather blade into pieces smaller than $1mm^2$ and resuspended into an ice cold dounce containing 1 mL of nuclear homogenization buffer containing 5 mM rnase inhibitor (Thermo Fisher AM2696), 10mM 10% triton X100 and 25mM DTT. Cell homogenate was dounced with a loose pestle 6 times followed by a tight pestle 15 times, as optimized for nuclei release from our tissue. After douncing, nuclei were filtered through a 40 µm cell strainer and diluted to approximately 1:4 concentration in fresh nuclei homogenization buffer. Nuclei were spun at 50g for 10 minutes in a swinging bucket centrifuge and resuspended in cold nuclei buffer from the Parse Biosciences fixation kit.

Nuclear Fixation, library prep, and Sequencing

The remainder of fixation steps were carried out according to the parse nuclear fixation protocol, beginning at step 4. Samples were frozen for up to four weeks before being sent to collaborators at UC Davis for library prep. Reverse transcription, split-pool barcoding, and library prep followed the exact specifications of the Parse library prep protocol, resulting in 8 sub libraries of pooled cells from all samples. Libraries were analyzed via bioanalyzer (agilent 2100) to ensure that cDNA fragment sizes were within the optimal range for snRNAseq. Paired end sequencing was performed on two lanes of the Element AVITI according to the Parse's sequencing specification. Read one, containing barcode sequences, was sequenced at 86 cycles and read 2, containing transcript information was sequenced at 64 cycles.

Demultiplexing and read mapping

Demultiplexing of sublibrary composition in sequencing reads was performed with Bases2Fastq, with standard parameters except for length of read two set to 86pb. Afterwards, cell and sample barcodes were demultiplexed using the Parse split-pipe package. Reads were mapped with STAR to the prairie vole genome (*Microtus ochrogaster*), a closely related species of vole, due to the lack of quality annotation of the meadow vole genome at the time of this analysis.

Bioinformatic Analysis

Downstream analysis steps were performed with the standard Seurat pipeline in R. Nuclei with less than 5% mitochondrial content and rna counts within 2 x IQR of the median gene expression were determined to be viable single nuclei. Of 63,000 nuclei total, 44,000 met these criteria. The top 5,000 variable genes were included for principal components analysis and clustering. K-means clustering was performed with 30 principle components with a resolution parameter of 0.6. UMAP visualizations were performed with all standard parameters from the Seurat UMAP function. Differential expression analyses were performed for all pairwise comparisons across daylength and housing conditions using a Kruskall Wallace test with Bonferroni corrected p

values. Proportions of cells between conditions within clusters were analyzed using a permuted proportions test with 10,000 permutations (R package: scProportionTest) and Bonferonni corrected p-values. Gene ontology analysis was performed using the biological processes database from TopGo after identifying orthologous gene names in mice with OrthoGene. Eliminated genes after orthologue identification included only the unannotated genes in the prairie vole genome.

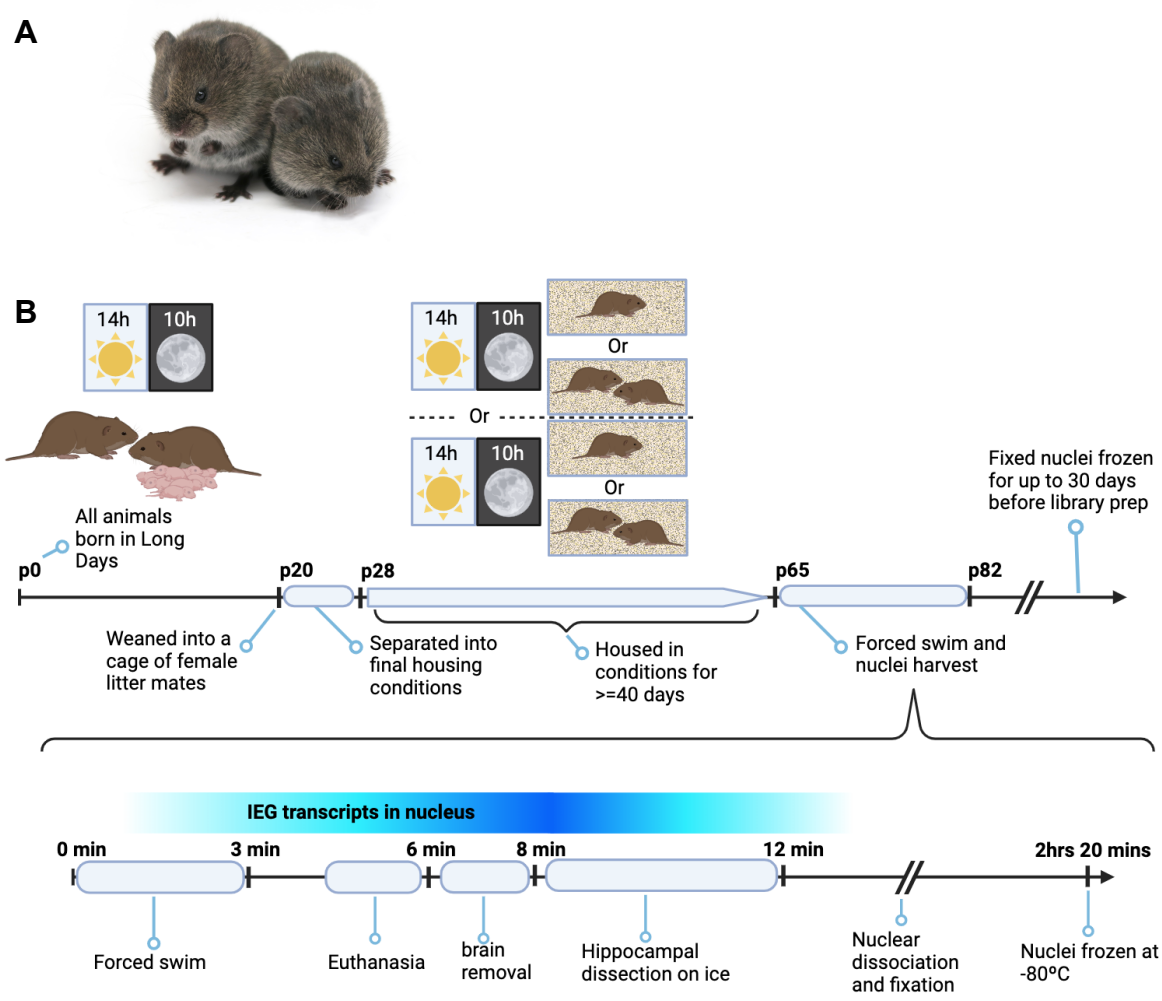
A
B
14h
10h
Or
All animals born in Long Days
p0
p20
p28
p65
p82
Fixed nuclei frozen for up to 30 days before library prep
Weaned into a cage of female litter mates
Separated into final housing conditions
Housed in conditions for >=40 days
Forced swim and nuclei harvest
IEG transcripts in nucleus
0 min
3 min
6 min
8 min
12 min
2hrs 20 mins
Forced swim
Euthanasia
brain removal
Hippocampal dissection on ice
Nuclear dissociation and fixation
Nuclei frozen at -80°C
C
Split-Seq style library prep with Parse Biosciences
Short read paired end sequencing on AVITI Elements
Reads mapped to prairie vole genome with STAR
Bioinformatics with Seurat
Exon
Intron
Exon
m. orchogaster
UMAP1
UMAP2

Fig 4.1. Design of nuclear harvest and sequencing experiments. A) Image of meadow voles engaging in huddling behavior. **B)** Timeline of nuclear harvest. Animals were born into LD and transferred to pair or solo housing conditions in long and short days at weaning. ¾ animals in each experimental group underwent forced swim immediately before nuclei harvest. Hippocampi were rapidly dissected and placed on ice within the timeline of immediate early gene expression in nuclei after forced swim. **C)** After library prep and paired end sequencing, reads were mapped the the prairie vole genome before bioinformatic analysis.

A

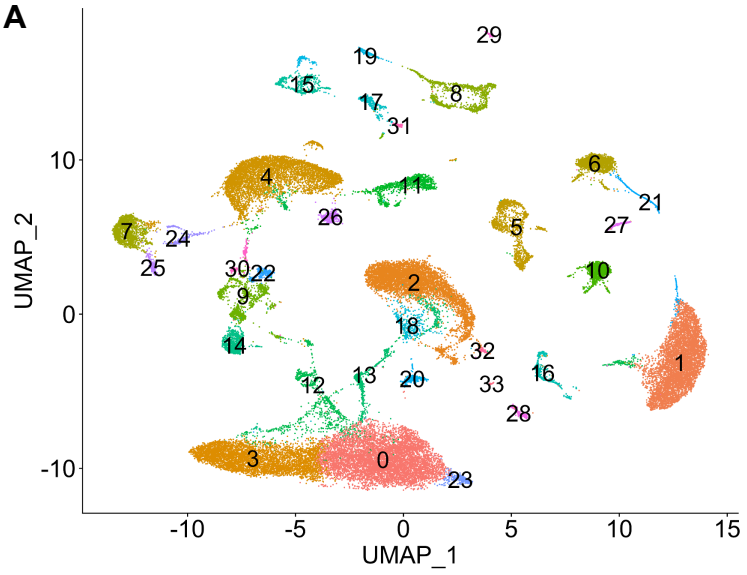

B

Condition	Cell Count
LD_PAIR	9374
LD_SOLO	12593
SD_PAIR	11935
SD_SOLO	10771

Fig 4.2. Initial clustering revealed 38 distinct cell types in the dorsal hippocampus. A) UMAP dimensional reduction of k-means clustered cells. A total of 44,000 quality nuclei remained after quality control. **B)** Table of nuclei numbers across sample types.

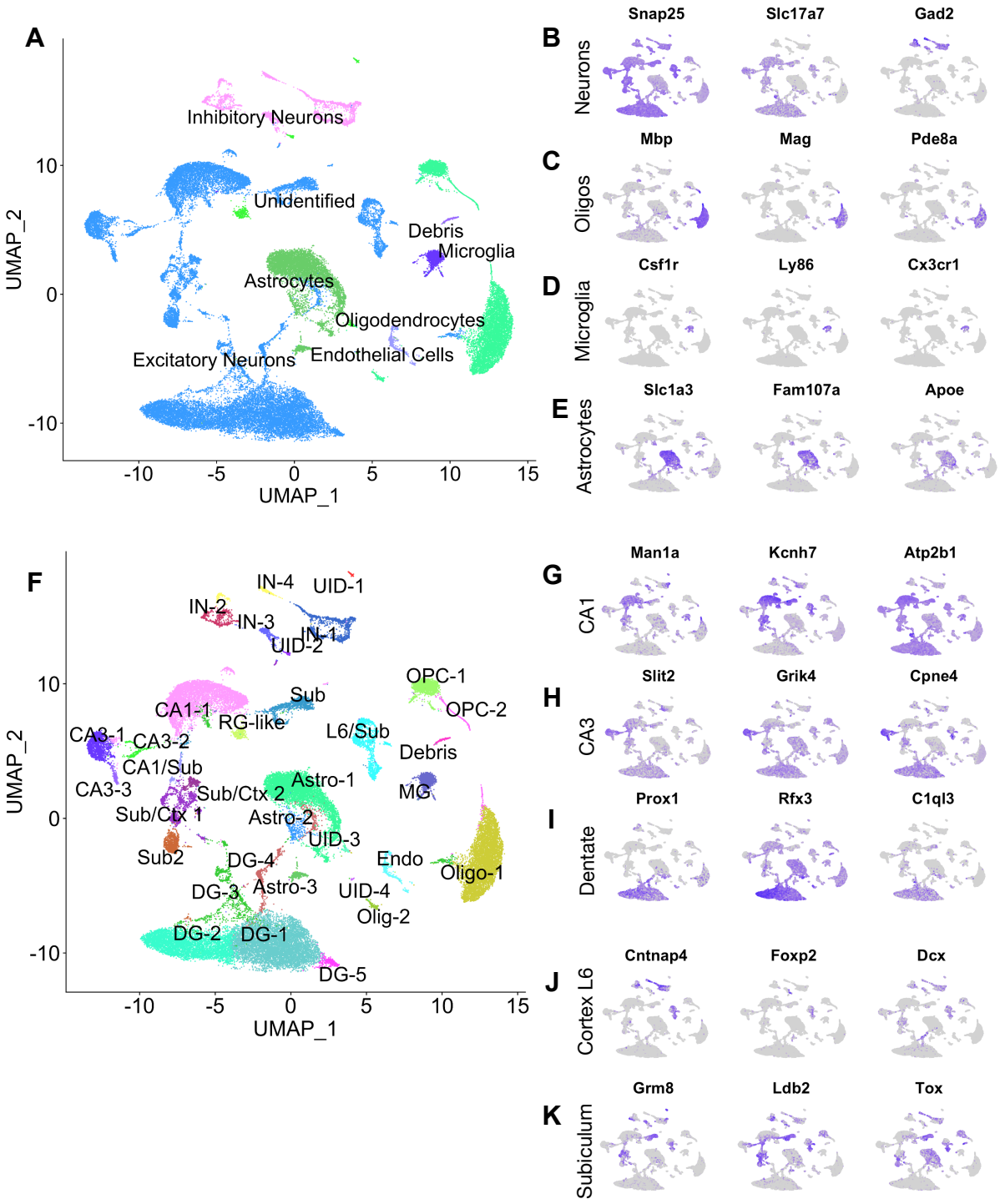
A
Inhibitory Neurons
Unidentified
Debris
Microglia
Astrocytes
Oligodendrocytes
Excitatory Neurons
Endothelial Cells
UMAP_2
UMAP_1
B
Neurons
Snap25
Slc17a7
Gad2
C
Oligos
Mbp
Mag
Pde8a
D
Microglia
Csf1r
Ly86
Cx3cr1
E
Astrocytes
Slc1a3
Fam107a
Apoe
F
IN-4
UID-1
IN-2
IN-3
IN-1
UID-2
OPC-1
Sub
OPC-2
CA1-1
RG-like
L6/Sub
CA3-1
CA3-2
Debris
CA1/Sub
CA3-3
Astro-1
MG
Sub/Ctx 2
Sub/Ctx 1
Astro-2
UID-3
Sub2
DG-4
Endo
Oligo-1
DG-3
Astro-3
UID-4
Olig-2
DG-2
DG-1
DG-5
UMAP_2
UMAP_1
G
CA1
Man1a
Kcnh7
Atp2b1
H
CA3
Slit2
Grik4
Cpne4
I
Dentate
Prox1
Rfx3
C1ql3
J
Cortex L6
Cntnap4
Foxp2
Dcx
K
Subiculum
Grm8
Ldb2
Tox

Fig 4.3. Cell type specific markers identify molecular and regionally defined populations. **A)** UMAP dimensional reduction of clustered cells, highlighted by major neuronal and glial cell classes. **B-E)** Representative UMAPs containing heatmaps of expression of features used to define major cell type identity. Blue= high expression, Gray= low expression. **F)** UMAP of all cells labeled by cluster specific sub populations of neurons and glia. **G-K)** Representative UMAPs containing heatmaps of expression of features used to define subpopulation identity. Abbreviations: **Astro**= Astrocyte, **DG**=Dentate Gyrus, **Endo**=Endothelial, **IN**=Interneuron, **MG**=Microglia, **Oligo**=Oligodendrocyte, **OPC**=Oligodendrocyte precursor, **RG-like=** Radial glia-like, **Sub**=Subiculum, **UID**=Unidentified.

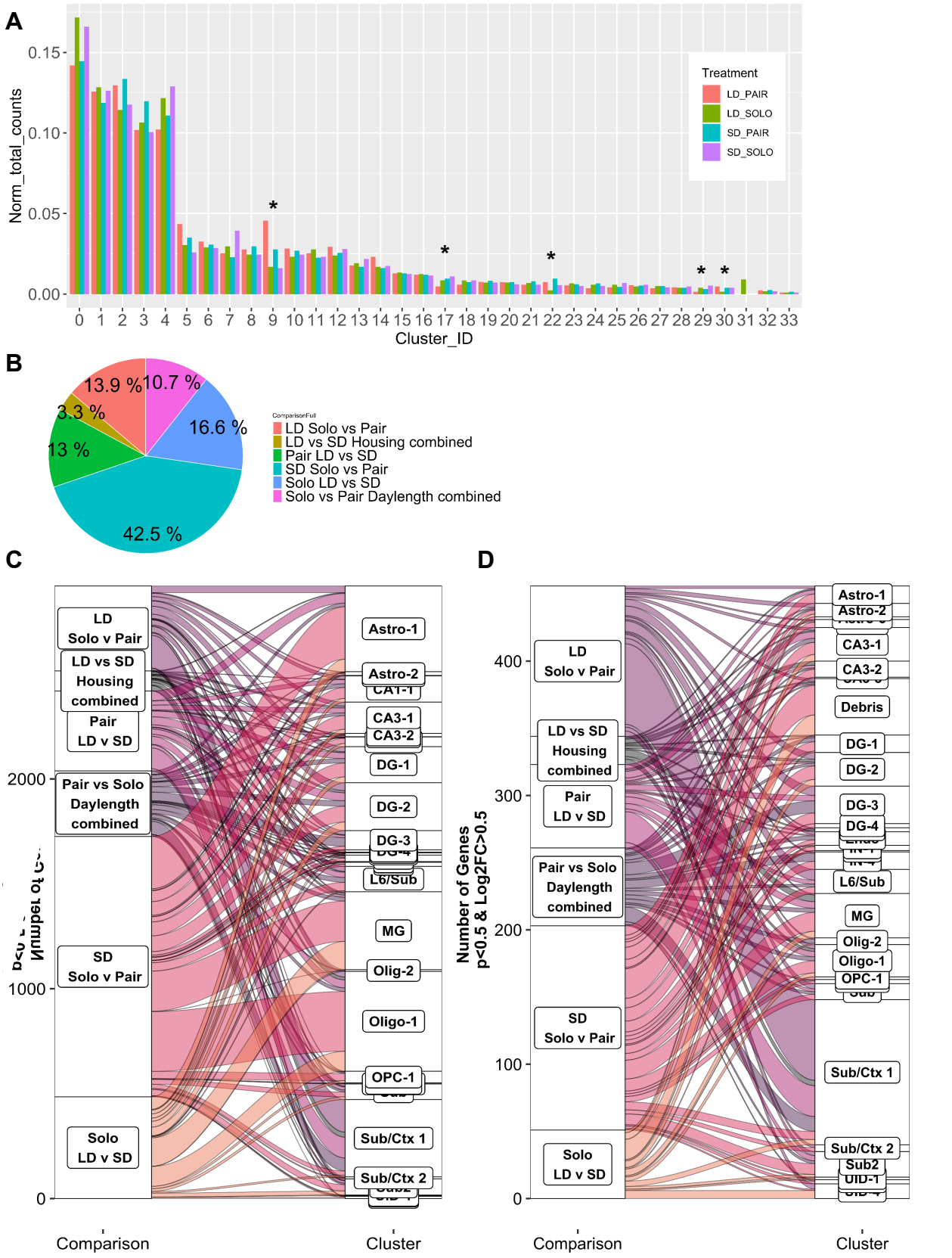
A
Norm_total_counts
0.15
0.10
0.05
0.00
0 1 2 3 4 5 6 7 8 9 10 11 12 13 14 15 16 17 18 19 20 21 22 23 24 25 26 27 28 29 30 31 32 33
Cluster_ID
Treatment
LD_PAIR
LD_SOLO
SD_PAIR
SD_SOLO
B
13.9 %
10.7 %
3.3 %
16.6 %
13 %
42.5 %
ComparisonFull
LD Solo vs Pair
LD vs SD Housing combined
Pair LD vs SD
SD Solo vs Pair
Solo LD vs SD
Solo vs Pair Daylength combined
C
LD Solo v Pair
LD vs SD Housing combined
Pair LD v SD
Pair vs Solo Daylength combined
SD Solo v Pair
Solo LD v SD
2000
1000
0
Astro-1
Astro-2
CA3-1
CA3-2
DG-1
DG-2
DG-3
L6/Sub
MG
Olig-2
Oligo-1
OPC-1
Sub/Ctx 1
Sub/Ctx 2
Comparison
Cluster
D
Number of Genes p<0.5 & Log2FC>0.5
400
300
200
100
0
LD Solo v Pair
LD vs SD Housing combined
Pair LD v SD
Pair vs Solo Daylength combined
SD Solo v Pair
Solo LD v SD
Astro-1
Astro-2
CA3-1
CA3-2
Debris
DG-1
DG-2
DG-3
DG-4
L6/Sub
MG
Olig-2
Oligo-1
OPC-1
Sub/Ctx 1
Sub/Ctx 2
Sub2
Comparison
Cluster

Fig 4.4. Housing has a greater impact on cell type specific transcription than daylength. **A)** Bar plot of cells per experimental condition per cluster. Cell counts within each cluster and condition are normalized by total cell counts in the entire dataset for each condition (* - proportion of cells differ between LD solo and pair animals, $p<.05$) **B)** Percent of first 1000 DE genes represented in each pairwise comparison. **C-D)** Alluvial diagram of all DE genes. Connector thickness is weighted by the number of DE genes that correspond to a specific comparison and cluster. Significance thresholds for DE calculation- C) Bonferonni corrected Kruskall Wallace test; $p<.05$ and $Log2FC>0.25$; D) Bonferonni corrected Kruskall Wallace test $p<.05$ and $Log2FC>0.5$.

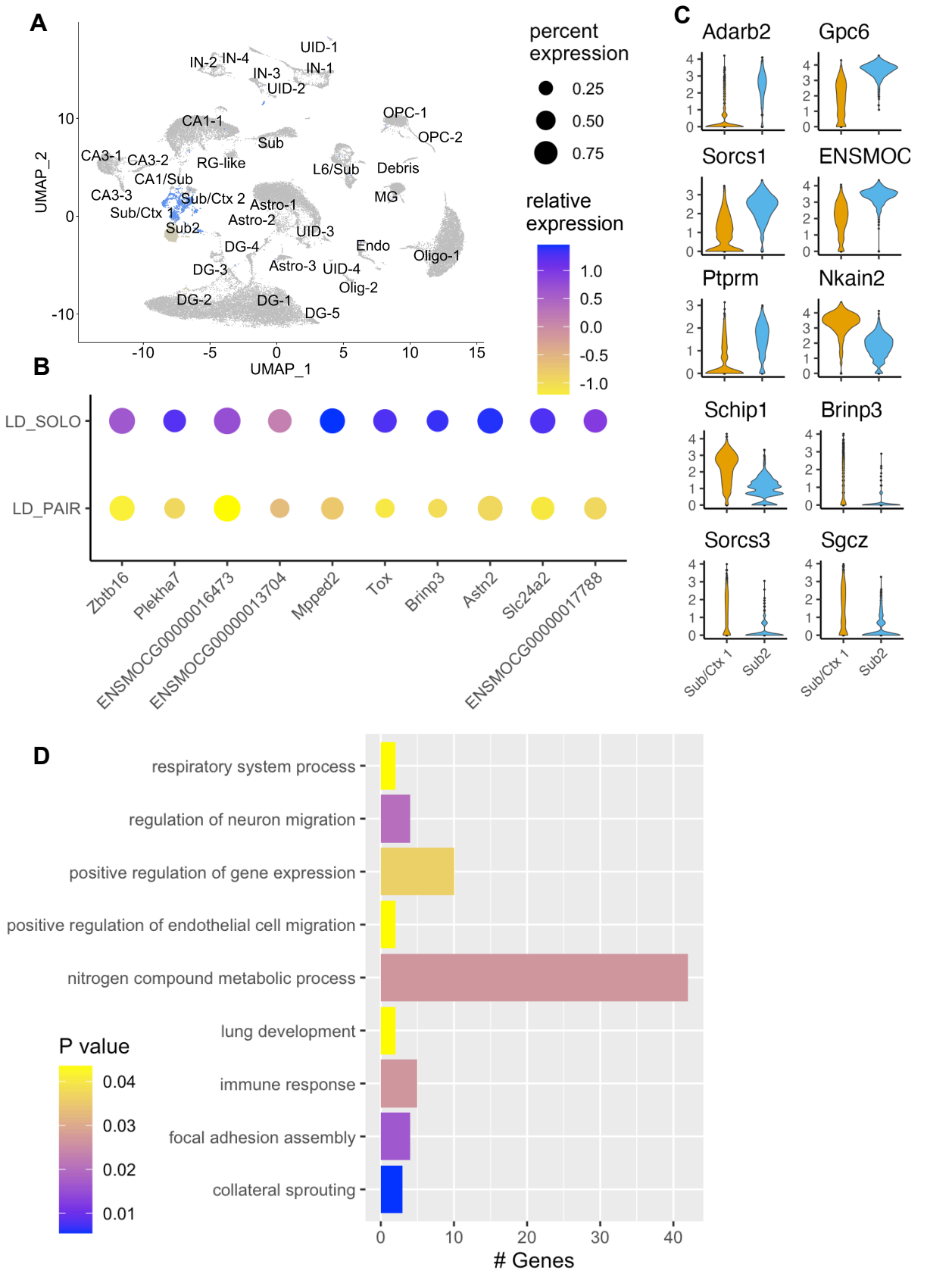
A
UMAP_2
UMAP_1
IN-2
IN-4
UID-1
IN-3
IN-1
UID-2
CA1-1
OPC-1
OPC-2
Sub
CA3-1
CA3-2
RG-like
L6/Sub
Debris
CA1/Sub
CA3-3
Sub/Ctx 2
Astro-1
MG
Sub/Ctx 1
Astro-2
Sub2
UID-3
DG-4
Endo
Oligo-1
DG-3
Astro-3
UID-4
Olig-2
DG-2
DG-1
DG-5
percent expression
0.25
0.50
0.75
relative expression
1.0
0.5
0.0
-0.5
-1.0
B
LD_SOLO
LD_PAIR
Zbtb16
Plekha7
ENSMOCG00000016473
ENSMOCG00000013704
Mpped2
Tox
Brinp3
Astn2
Slc24a2
ENSMOCG00000017788
C
Adarb2
Gpc6
Sorcs1
ENSMOC
Ptprm
Nkain2
Schip1
Brinp3
Sorcs3
Sgcz
Sub/Ctx 1
Sub2
D
respiratory system process
regulation of neuron migration
positive regulation of gene expression
positive regulation of endothelial cell migration
nitrogen compound metabolic process
lung development
immune response
focal adhesion assembly
collateral sprouting
P value
0.04
0.03
0.02
0.01
Genes

Fig 4.5. LD Paired animals have an enriched subicular cell type with reduced expression of markers of glutamatergic function and process formation. A) UMAP highlighting Sub/Ctx-1 and Sub2, closely related clusters of interest used for DE analysis. **B)** Dot plot of top differentially expressed genes between LD solo and paired animals in cluster Sub/Ctx-1. Dot size represents percent of cells within the cluster expressing those cells. Expression is scaled based on relative expression of to the median expression level amongst all genes in the entire dataset. All genes differentially expressed at $p<0.5$ and $Log2FC>0.5$. **C)** Violin plots of differentially expressed genes between clusters of interest. Width represents number of cells expressing the gene at each level of expression. All genes differentially expressed with Bonferonni corrected Kruskall Wallace test; $p<.05$ and $Log2FC>0.25$. **D)** Gene ontology for differentially expressed genes between clusters of interest, Kolmolgorov Smirnov test; $p<.05$. Bar length represents number of genes associated with a given ontology term that are differentially expressed between clusters of interest Bonferonni corrected Kruskall Wallace test; $p<.05$ and $Log2FC>0.25$.

A

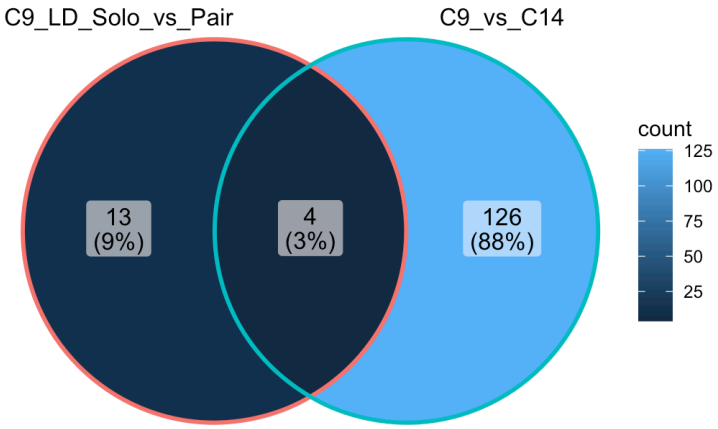
C9_LD_Solo_vs_Pair
C9_vs_C14
13
(9%)
4
(3%)
126
(88%)
count
125
100
75
50
25

B

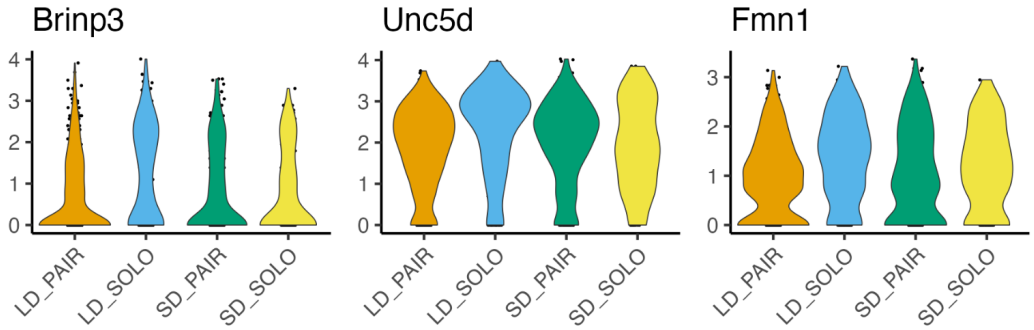
Brinp3
Unc5d
Fmn1
4
3
2
1
0
LD_PAIR
LD_SOLO
SD_PAIR
SD_SOLO

Fig 4.6. Differentially expressed markers between Sub/Ctx-1 and Sub-2 overlap with genes differentially expressed by housing in LD animals. A) Venn diagram of overlapping genes between DE comparisons across LD solo and paired animals within Sub/Ctx-1 and across Sub/Ctx-1 and Sub-2. The overlapping portion represents cluster specific genes that are upregulated in LD solo animals. **B)** Violin plots of DE genes from the overlap of panel E.

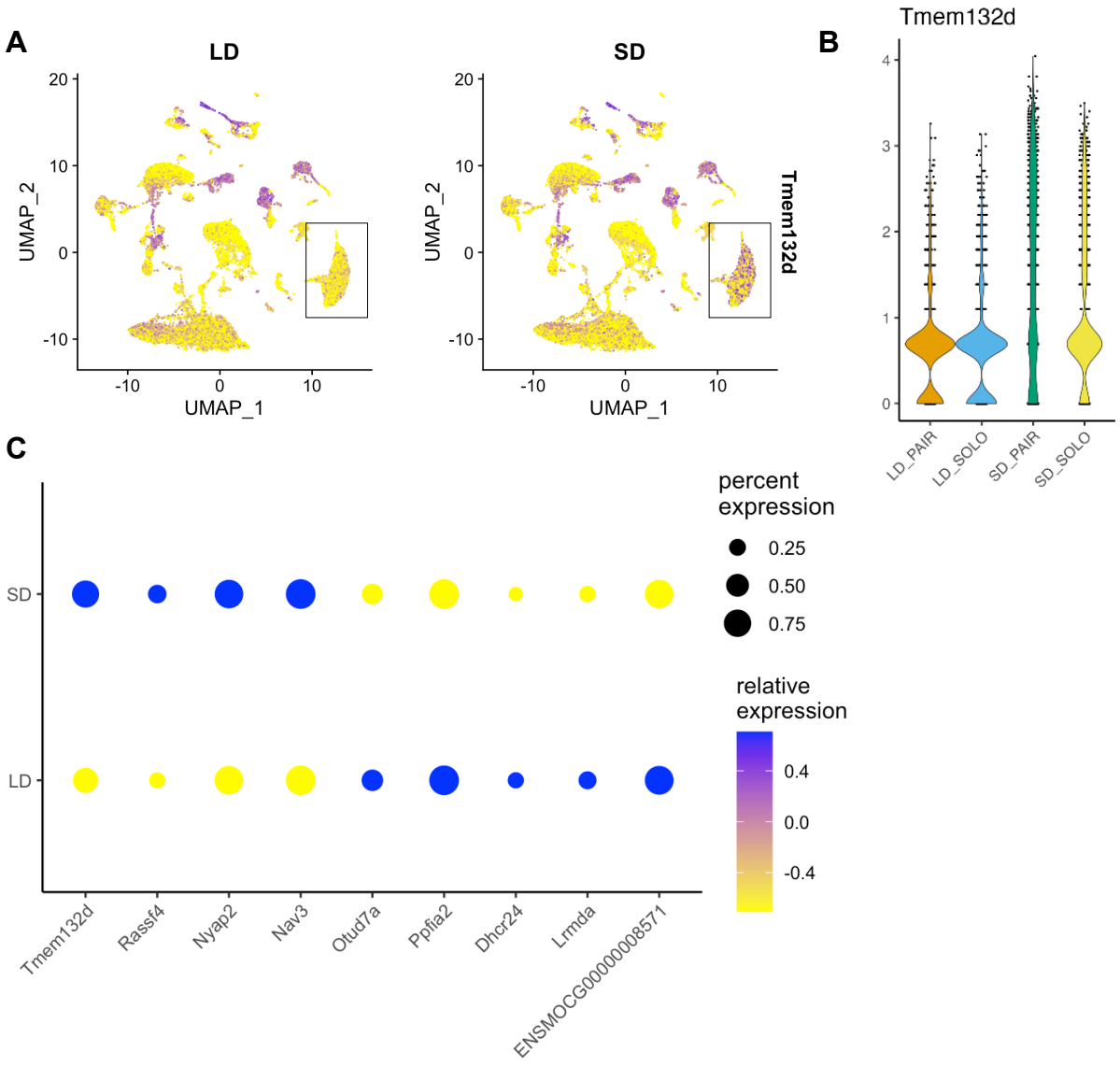
A
LD
SD
UMAP_2
UMAP_1
Tmem132d
B
Tmem132d
LD_PAIR
LD_SOLO
SD_PAIR
SD_SOLO
C
percent expression
0.25
0.50
0.75
relative expression
0.4
0.0
-0.4
SD
LD
Tmem132d
Rassf4
Nyap2
Nav3
Otud7a
Ppfia2
Dhcr24
Lrmda
ENSMOCG00000008571

Fig 4.7. Daylength impacts expression of genes contributing to myelination in oligodendrocytes. A) Feature plot containing a heatmap of expression of Tmem132d. Yellow represents low expression, green represents high expression. **B)** Violin plot of expression of Tmem132d. Comparison between daylengths, Bonferonni corrected Kruskal wallace test; $p=3.0x10^{-135}$, Log2FC=1.39. **C)** Dot plot of highly differentially expressed genes between LD and SD animals in cluster Olig-1.

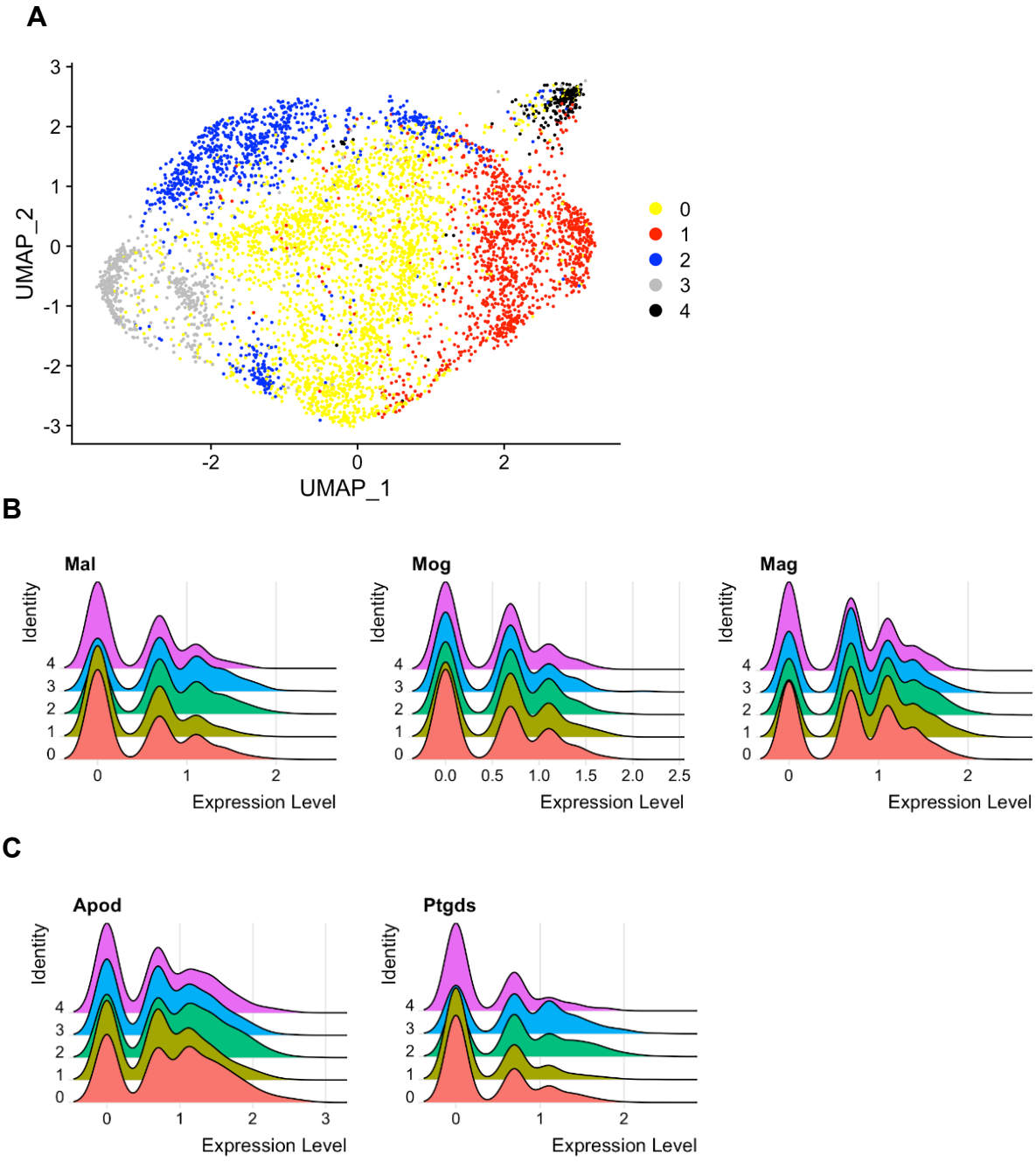
A
UMAP_2
UMAP_1
0
1
2
3
4
B
Mal
Mog
Mag
Identity
Expression Level
C
Apod
Ptgds

Fig 4.8. Sub clustering olig-1 does not identify distinct oligodendrocyte populations. A) Umap dimensional reduction of k-means clustering of Olig-1 in a new feature space of variable genes within the cluster. **B-C)** Ridgeplot of expression of mature (B) and developing (C) oligodendrocyte markers amongst subclusters of Olig1. Ridge height corresponds to the number of cells expressing a gene at a given expression level. Mature oligodendoctye markers are expressed in all sub-clusters.

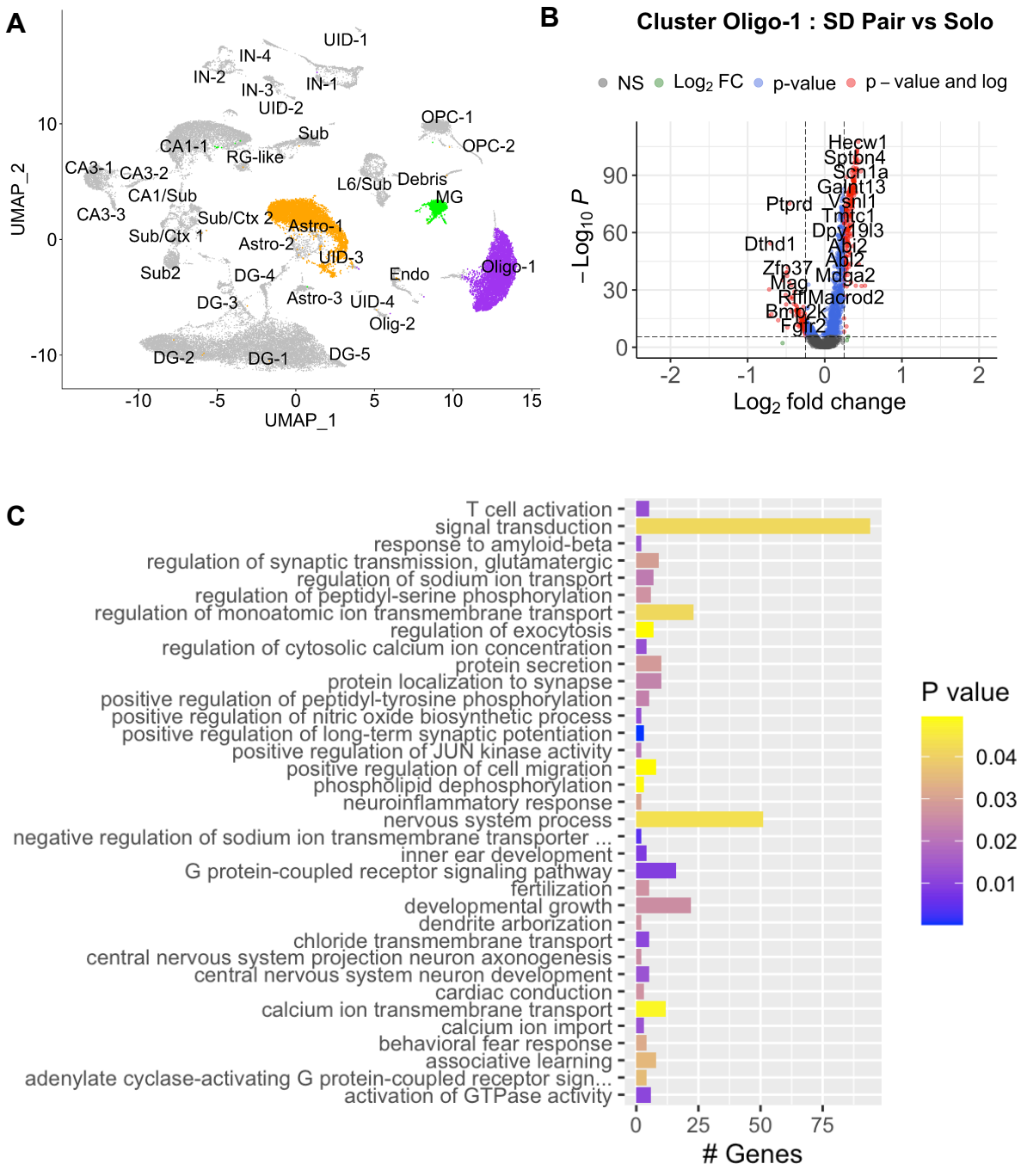
A
UID-1
IN-4
IN-2
IN-3
IN-1
UID-2
OPC-1
Sub
OPC-2
CA1-1
RG-like
CA3-1
CA3-2
L6/Sub
Debris
CA1/Sub
MG
CA3-3
Sub/Ctx 2
Astro-1
Sub/Ctx 1
Astro-2
UID-3
Sub2
DG-4
Endo
Oligo-1
DG-3
Astro-3
UID-4
Olig-2
DG-2
DG-1
DG-5
UMAP_2
UMAP_1
B
Cluster Oligo-1 : SD Pair vs Solo
NS
Log2 FC
p-value
p – value and log
Hecw1
Sptbn4
Scn1a
Galnt13
Ptprd
Vsnl1
Tmtc1
Dpy19l3
Dthd1
Abi2
Abi2
Zfp37
Mdga2
Mag
Rffl
Macrod2
Bmp2k
Fgfr2
−Log10 P
Log2 fold change
C
T cell activation
signal transduction
response to amyloid-beta
regulation of synaptic transmission, glutamatergic
regulation of sodium ion transport
regulation of peptidyl-serine phosphorylation
regulation of monoatomic ion transmembrane transport
regulation of exocytosis
regulation of cytosolic calcium ion concentration
protein secretion
protein localization to synapse
positive regulation of peptidyl-tyrosine phosphorylation
positive regulation of nitric oxide biosynthetic process
positive regulation of long-term synaptic potentiation
positive regulation of JUN kinase activity
positive regulation of cell migration
phospholipid dephosphorylation
neuroinflammatory response
nervous system process
negative regulation of sodium ion transmembrane transporter ...
inner ear development
G protein-coupled receptor signaling pathway
fertilization
developmental growth
dendrite arborization
chloride transmembrane transport
central nervous system projection neuron axonogenesis
central nervous system neuron development
cardiac conduction
calcium ion transmembrane transport
calcium ion import
behavioral fear response
associative learning
adenylate cyclase-activating G protein-coupled receptor sign...
activation of GTPase activity
Genes
P value

Fig 4.9. Social Housing in SD animals impacts transcription in oligodendrocytes. A) UMAP plot highlighting major glial cell clusters. **B)** Volcano plot of DE genes between SD solo and paired animals in cluster Oligo-1. **C)** Significant gene ontology terms for DE genes between SD solo and paired animals in cluster Olig-1.

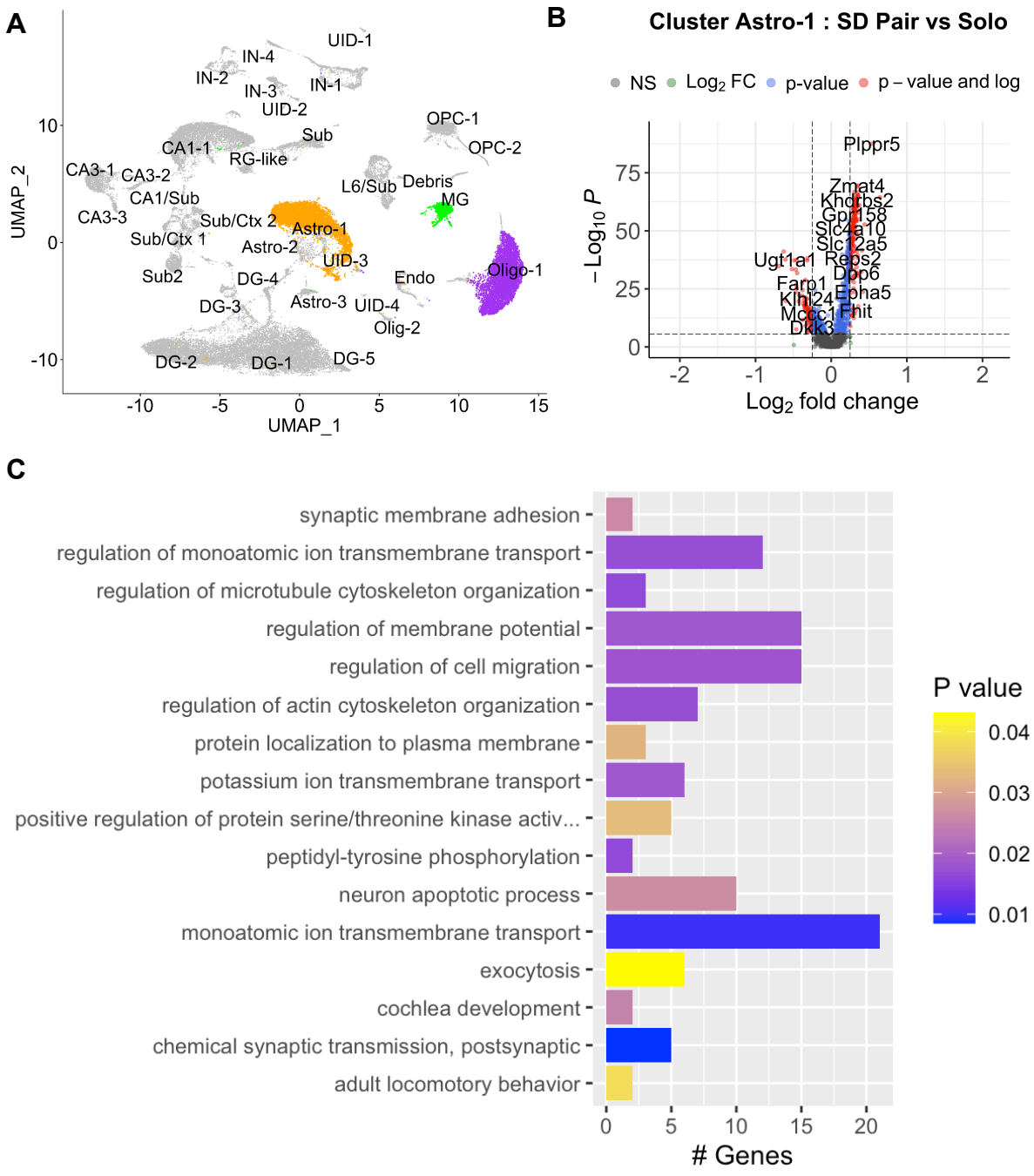
A
UID-1
IN-4
IN-2
IN-3
IN-1
UID-2
OPC-1
Sub
OPC-2
CA1-1
RG-like
CA3-1
CA3-2
L6/Sub
Debris
CA1/Sub
MG
CA3-3
Sub/Ctx 2
Astro-1
Sub/Ctx 1
Astro-2
UID-3
Sub2
DG-4
Endo
Oligo-1
DG-3
Astro-3
UID-4
Olig-2
DG-2
DG-1
DG-5
UMAP_2
UMAP_1
B
Cluster Astro-1 : SD Pair vs Solo
NS
Log2 FC
p-value
p – value and log
Plppr5
Zmat4
Khdrbs2
Gpr158
Slc4a10
Slc12a5
Ugt1a1
Reps2
Dpp6
Farp1
Epha5
Khl24
Mccc1
Fhit
Dkk3
– Log10 P
Log2 fold change
C
synaptic membrane adhesion
regulation of monoatomic ion transmembrane transport
regulation of microtubule cytoskeleton organization
regulation of membrane potential
regulation of cell migration
regulation of actin cytoskeleton organization
protein localization to plasma membrane
potassium ion transmembrane transport
positive regulation of protein serine/threonine kinase activ...
peptidyl-tyrosine phosphorylation
neuron apoptotic process
monoatomic ion transmembrane transport
exocytosis
cochlea development
chemical synaptic transmission, postsynaptic
adult locomotory behavior
Genes
P value
0.04
0.03
0.02
0.01

Fig 4.10. Social Housing in SD animals impacts transcription in astrocytes. A) UMAP plot highlighting major glial cell clusters. **B)** Volcano plot of DE genes between SD solo and paired animals in cluster Astro-1. **C)** Significant gene ontology terms for DE genes between SD solo and paired animals in cluster Astro-1.

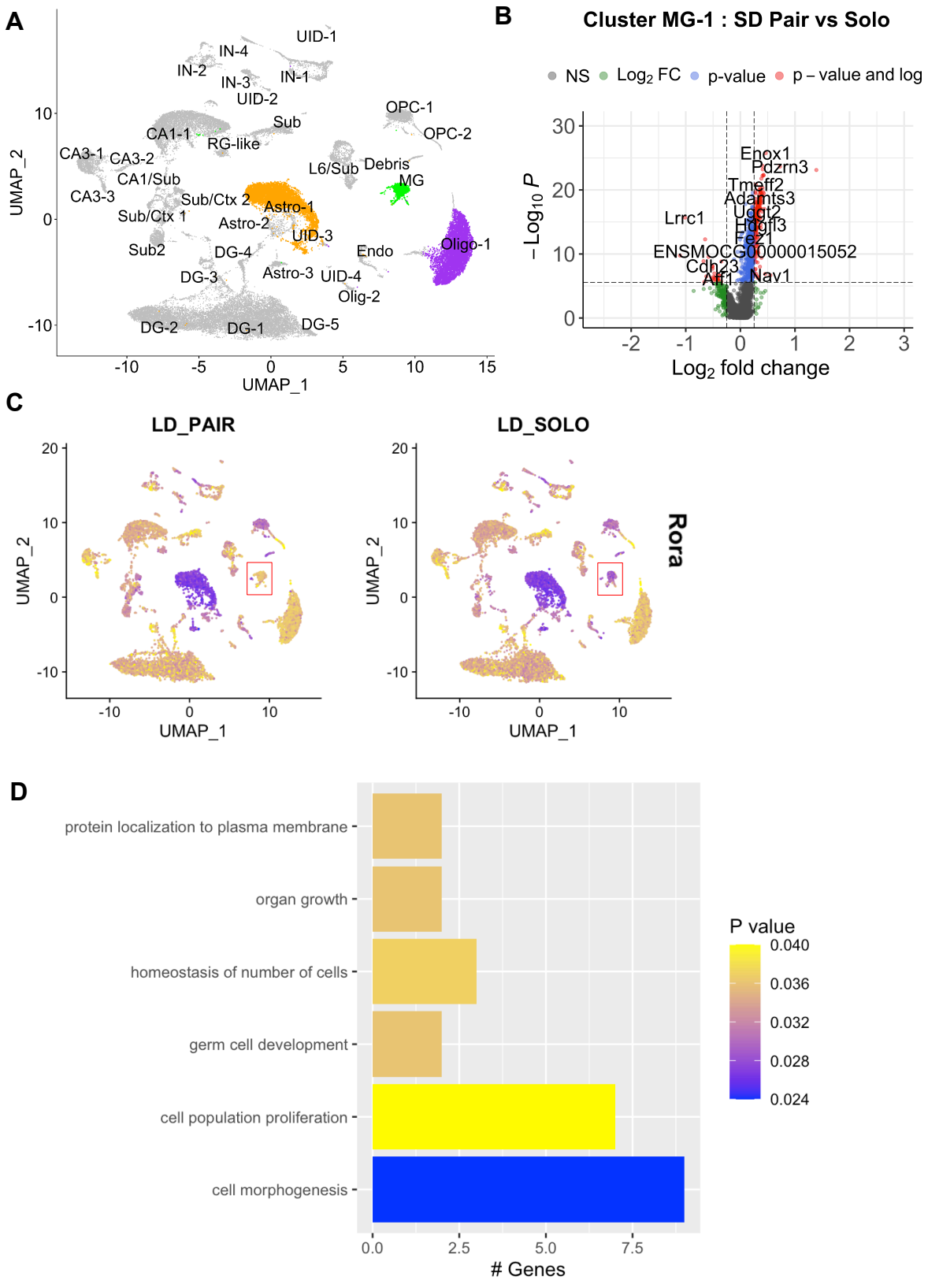
A
UID-1
IN-4
IN-2
IN-3
IN-1
UID-2
OPC-1
Sub
OPC-2
CA1-1
RG-like
CA3-1
CA3-2
L6/Sub
Debris
CA1/Sub
MG
CA3-3
Sub/Ctx 2
Astro-1
Sub/Ctx 1
Astro-2
UID-3
Sub2
DG-4
Endo
Oligo-1
DG-3
Astro-3
UID-4
Olig-2
DG-2
DG-1
DG-5
UMAP_2
UMAP_1
B
Cluster MG-1 : SD Pair vs Solo
NS
Log2 FC
p-value
p – value and log
Enox1
Pdzrn3
Tmeff2
Adamts3
Lrrc1
Ugt2
Hdgfl3
Fez1
ENSMOCG00000015052
Cdh23
Aff1
Nav1
−Log10 P
Log2 fold change
C
LD_PAIR
LD_SOLO
Rora
UMAP_2
UMAP_1
D
protein localization to plasma membrane
organ growth
homeostasis of number of cells
germ cell development
cell population proliferation
cell morphogenesis
P value
0.040
0.036
0.032
0.028
0.024
Genes

Fig 4.11. Social Housing in SD animals impacts transcription in microglia. A) UMAP plot highlighting major glial cell clusters. **B)** Volcano plot of DE genes between SD solo and paired animals in cluster MG-1. **C)** UMAP plot of difference in expression of RORa in cluster MG-1 across comparisons. LD solo vs pair, bonferonni corrected kruskall wallace test; p=1.5x10^-67, Log2FC=2.73. **D)** Significant gene ontology terms for DE genes between SD solo and paired animals in cluster MG-1.

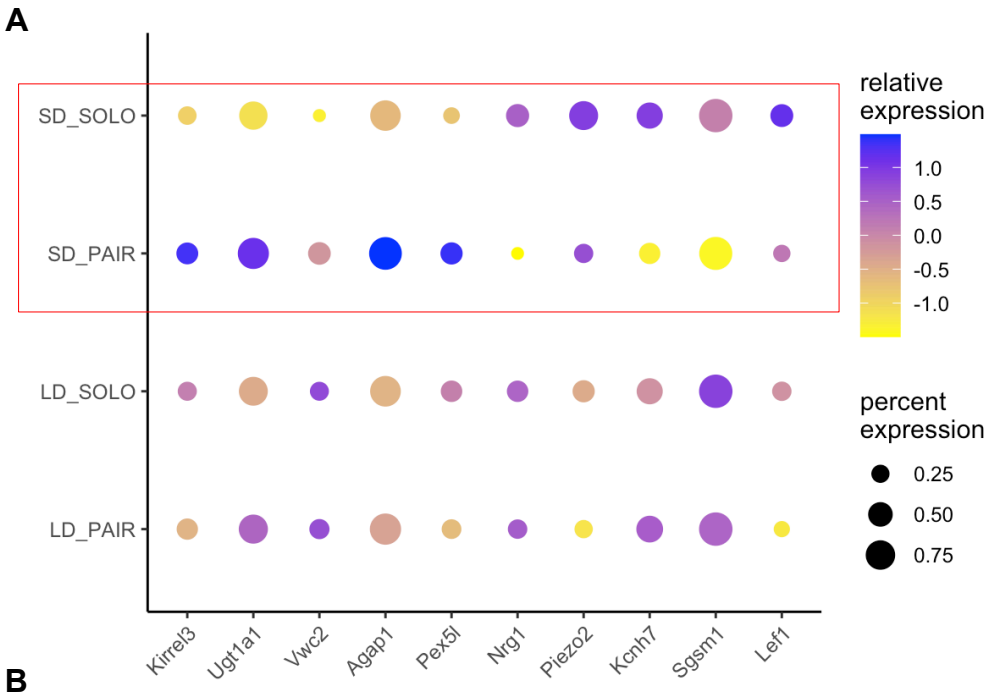
A
SD_SOLO
SD_PAIR
LD_SOLO
LD_PAIR
Kirrel3
Ugt1a1
Vwc2
Agap1
Pex5l
Nrg1
Piezo2
Kcnh7
Sgsm1
Lef1
relative expression
1.0
0.5
0.0
-0.5
-1.0
percent expression
0.25
0.50
0.75

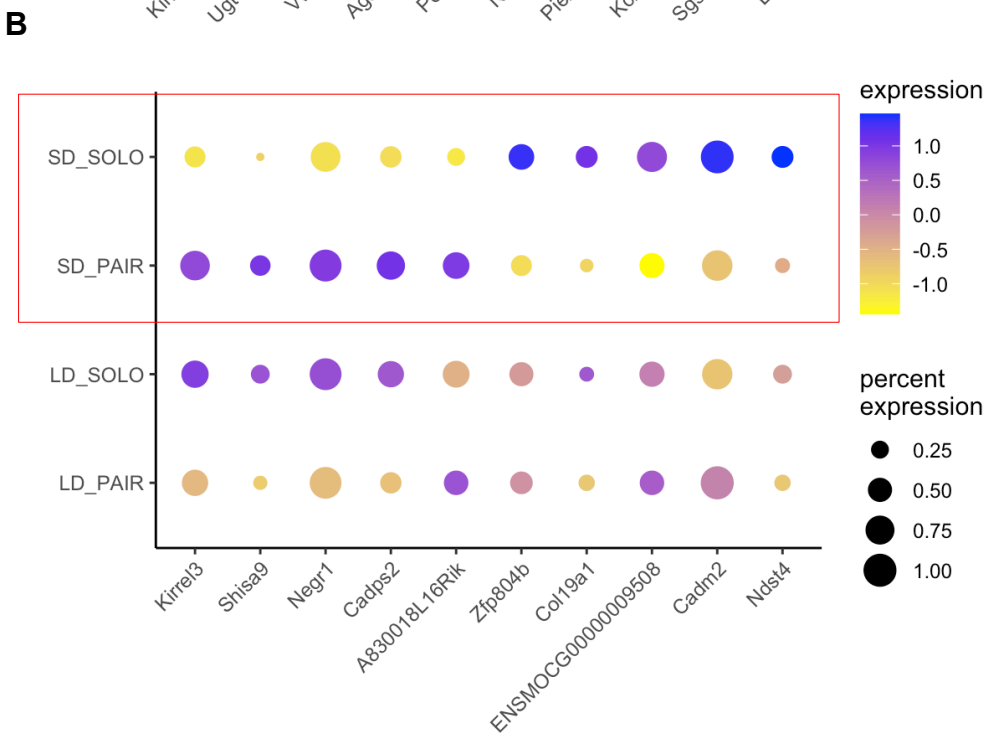
B
SD_SOLO
SD_PAIR
LD_SOLO
LD_PAIR
Kirrel3
Shisa9
Negr1
Cadps2
A830018L16Rik
Zfp804b
Col19a1
ENSMOCG00000009508
Cadm2
Ndst4
expression
1.0
0.5
0.0
-0.5
-1.0
percent expression
0.25
0.50
0.75
1.00

Fig 4.12. Social Housing in SD animals impacts expression of plasticity related genes in CA3 cells. A-B) Differentially expressed genes between SD paired and solo animals and cluster CA3-1. All genes differentially expressed with Bonferonni corrected Kruskall Wallace test, $p<.05$, $Log2FC>0.5$

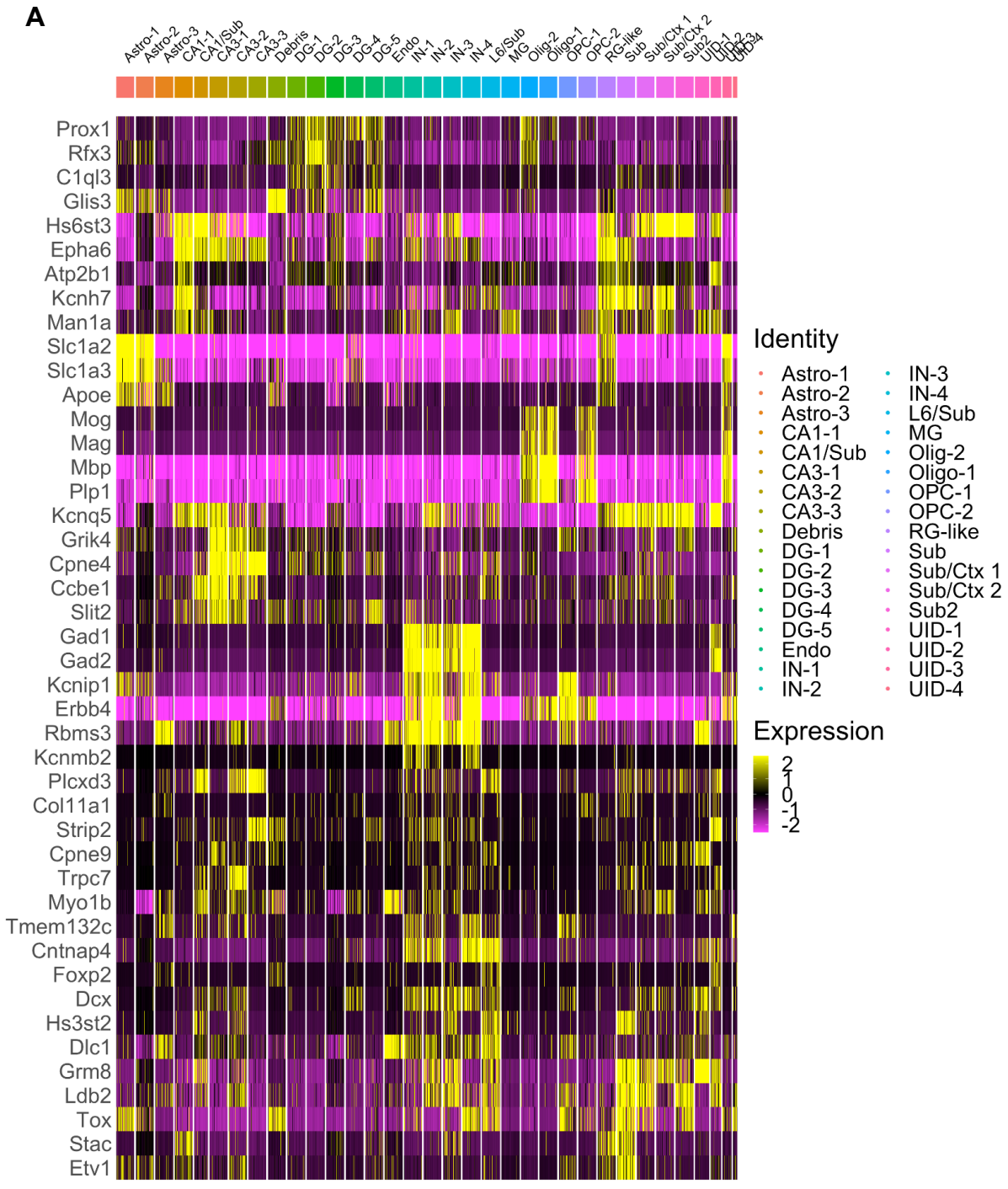
A
Astro-1
Astro-2
Astro-3
CA1-1
CA1/Sub
CA3-1
CA3-2
CA3-3
Debris
DG-1
DG-2
DG-3
DG-4
DG-5
Endo
IN-1
IN-2
IN-3
IN-4
L6/Sub
MG
Olig-2
Oligo-1
OPC-1
OPC-2
RG-like
Sub
Sub/Ctx 1
Sub/Ctx 2
Sub2
UID-1
UID-2
UID-3
UID-4
Prox1
Rfx3
C1ql3
Glis3
Hs6st3
Epha6
Atp2b1
Kcnh7
Man1a
Slc1a2
Slc1a3
Apoe
Mog
Mag
Mbp
Plp1
Kcnq5
Grik4
Cpne4
Ccbe1
Slit2
Gad1
Gad2
Kcnip1
Erbb4
Rbms3
Kcnmb2
Plcxd3
Col11a1
Strip2
Cpne9
Trpc7
Myo1b
Tmem132c
Cntnap4
Foxp2
Dcx
Hs3st2
Dlc1
Grm8
Ldb2
Tox
Stac
Etv1
Identity
Astro-1
Astro-2
Astro-3
CA1-1
CA1/Sub
CA3-1
CA3-2
CA3-3
Debris
DG-1
DG-2
DG-3
DG-4
DG-5
Endo
IN-1
IN-2
IN-3
IN-4
L6/Sub
MG
Olig-2
Oligo-1
OPC-1
OPC-2
RG-like
Sub
Sub/Ctx 1
Sub/Ctx 2
Sub2
UID-1
UID-2
UID-3
UID-4
Expression
2
1
0
-1
-2

Fig 4.S1. Cluster specific expression of hippocampal subtype markers A) Heatmap of specific markers used to determine hippocampal subtype specific identity. Figure adapted from (Rattner et al., 2020)**.**

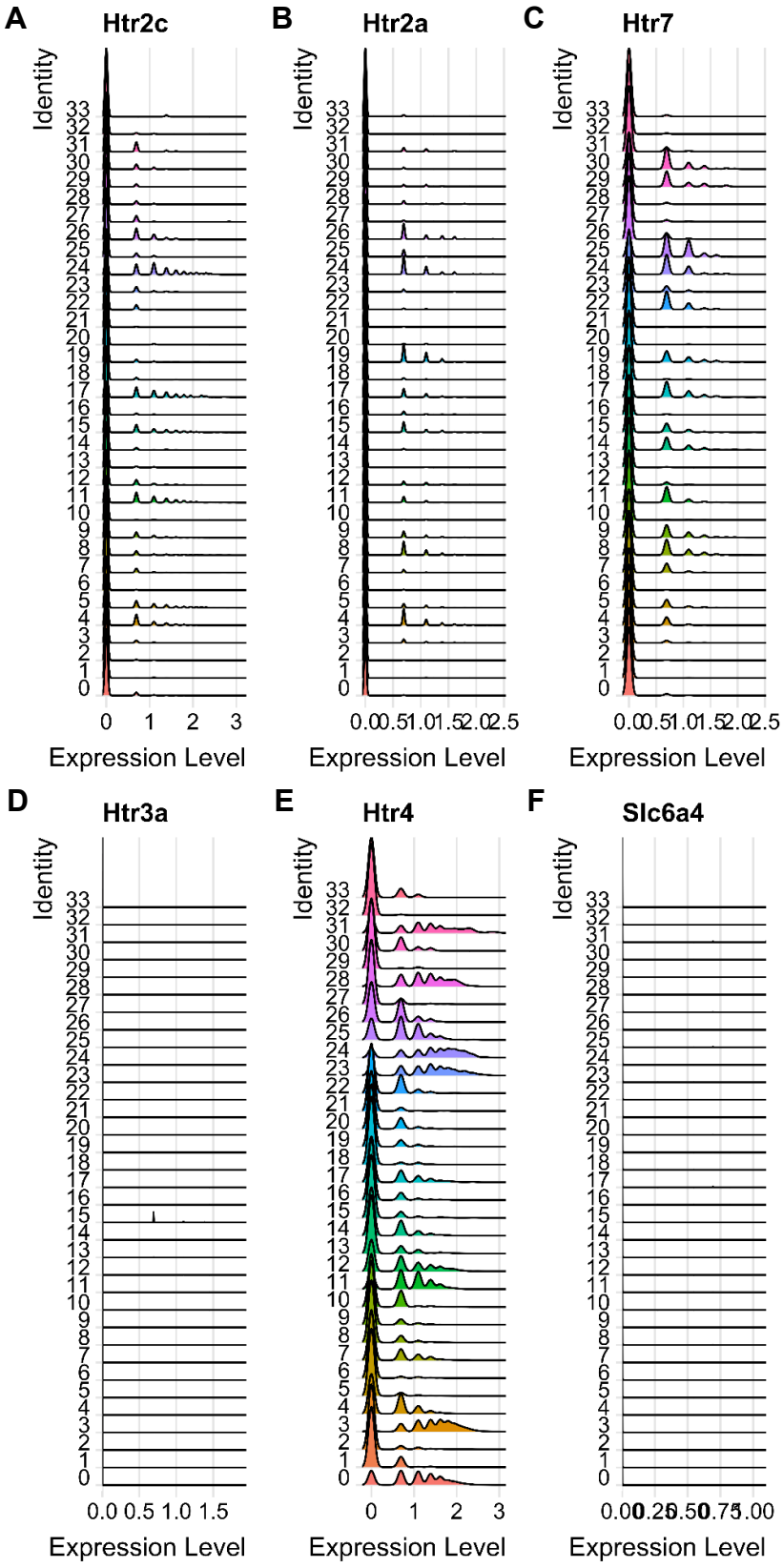
A
Htr2c
B
Htr2a
C
Htr7
D
Htr3a
E
Htr4
F
Slc6a4
Identity
Expression Level

Fig 4.S2. Cluster specific expression of serotonin receptors. A-F) Ridgeplots of expression of all 5HT receptors expressed in our dataset across all clusters. Height of each ridge corresponds to the number of cells expressing a gene at a given expression level.

A

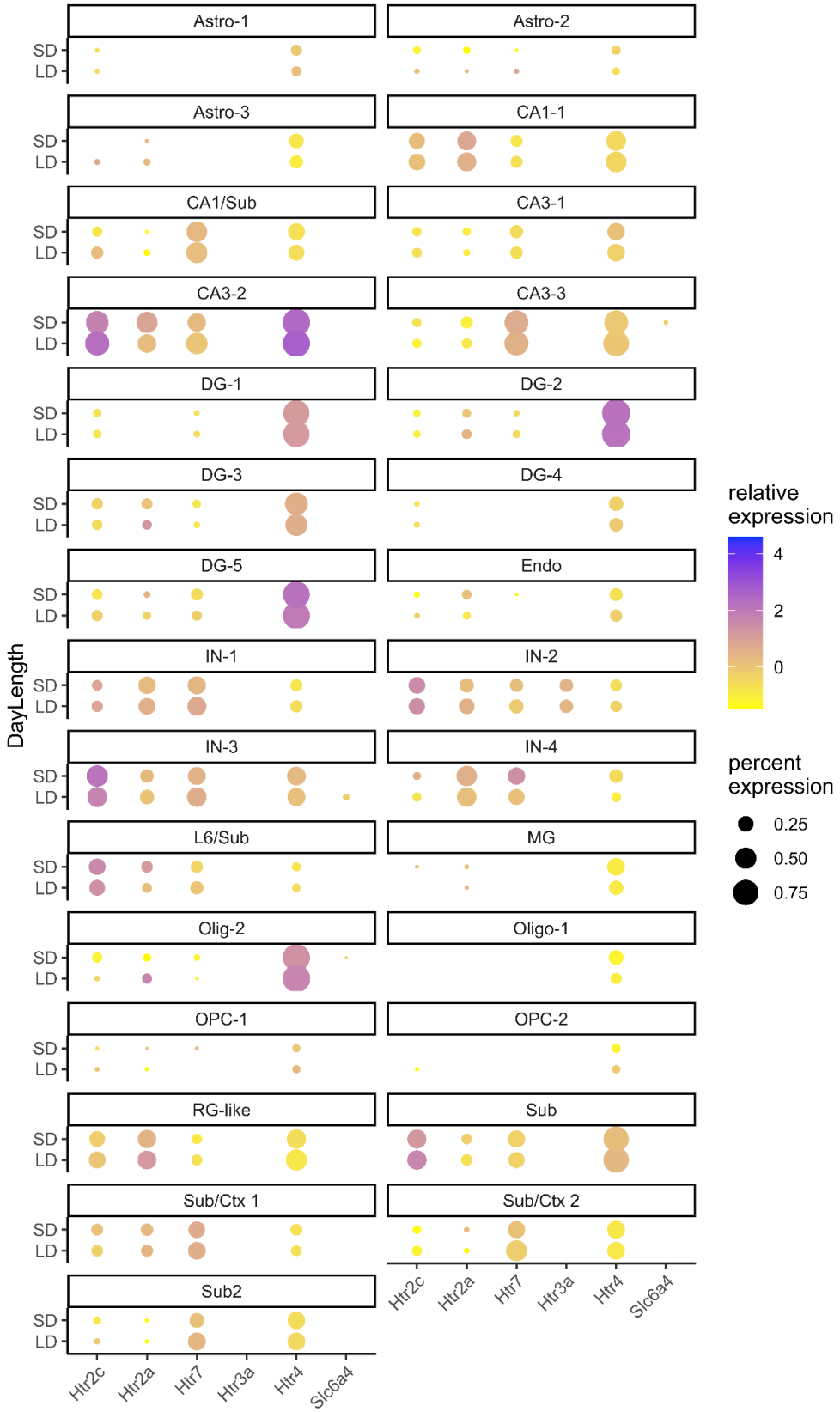
Astro-1
Astro-2
Astro-3
CA1-1
CA1/Sub
CA3-1
CA3-2
CA3-3
DG-1
DG-2
DG-3
DG-4
DG-5
Endo
IN-1
IN-2
IN-3
IN-4
L6/Sub
MG
Olig-2
Oligo-1
OPC-1
OPC-2
RG-like
Sub
Sub/Ctx 1
Sub/Ctx 2
Sub2
SD
LD
DayLength
Htr2c
Htr2a
Htr7
Htr3a
Htr4
Slc6a4
relative expression
4
2
0
percent expression
0.25
0.50
0.75

Fig 4.S3. Serotonin receptor expression does not differ across daylengths. A) Dotplots of expression for all 5HT receptors expressed in our dataset, plotted by expression in each daylength.

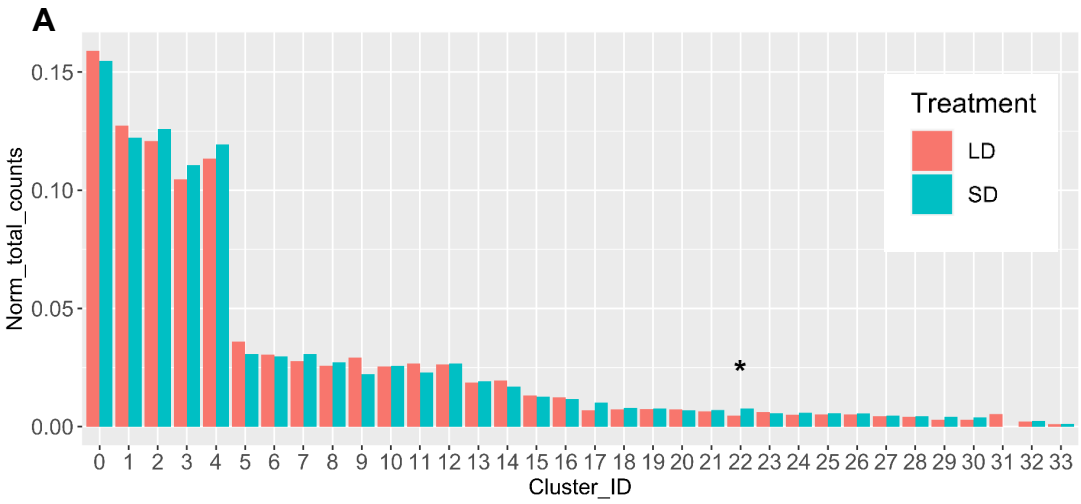
A
Norm_total_counts
0.15
0.10
0.05
0.00
Treatment
LD
SD
*
0 1 2 3 4 5 6 7 8 9 10 11 12 13 14 15 16 17 18 19 20 21 22 23 24 25 26 27 28 29 30 31 32 33
Cluster_ID

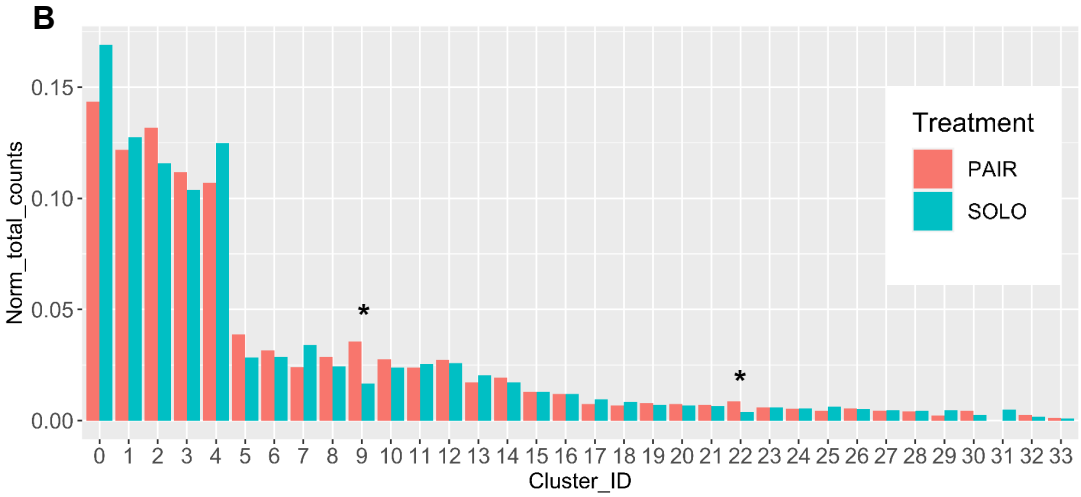
B
Norm_total_counts
0.15
0.10
0.05
0.00
Treatment
PAIR
SOLO
*
*
0 1 2 3 4 5 6 7 8 9 10 11 12 13 14 15 16 17 18 19 20 21 22 23 24 25 26 27 28 29 30 31 32 33
Cluster_ID

Fig 4.S4. Number of cells per cluster in LD, SD, Solo, and Paired animals. A-B) Bar plot of cells per experimental condition per cluster. Cell counts within each cluster and condition are normalized by total cell counts in the entire dataset for each condition (* - proportion of cells differ between conditions animals, $p<.05$)

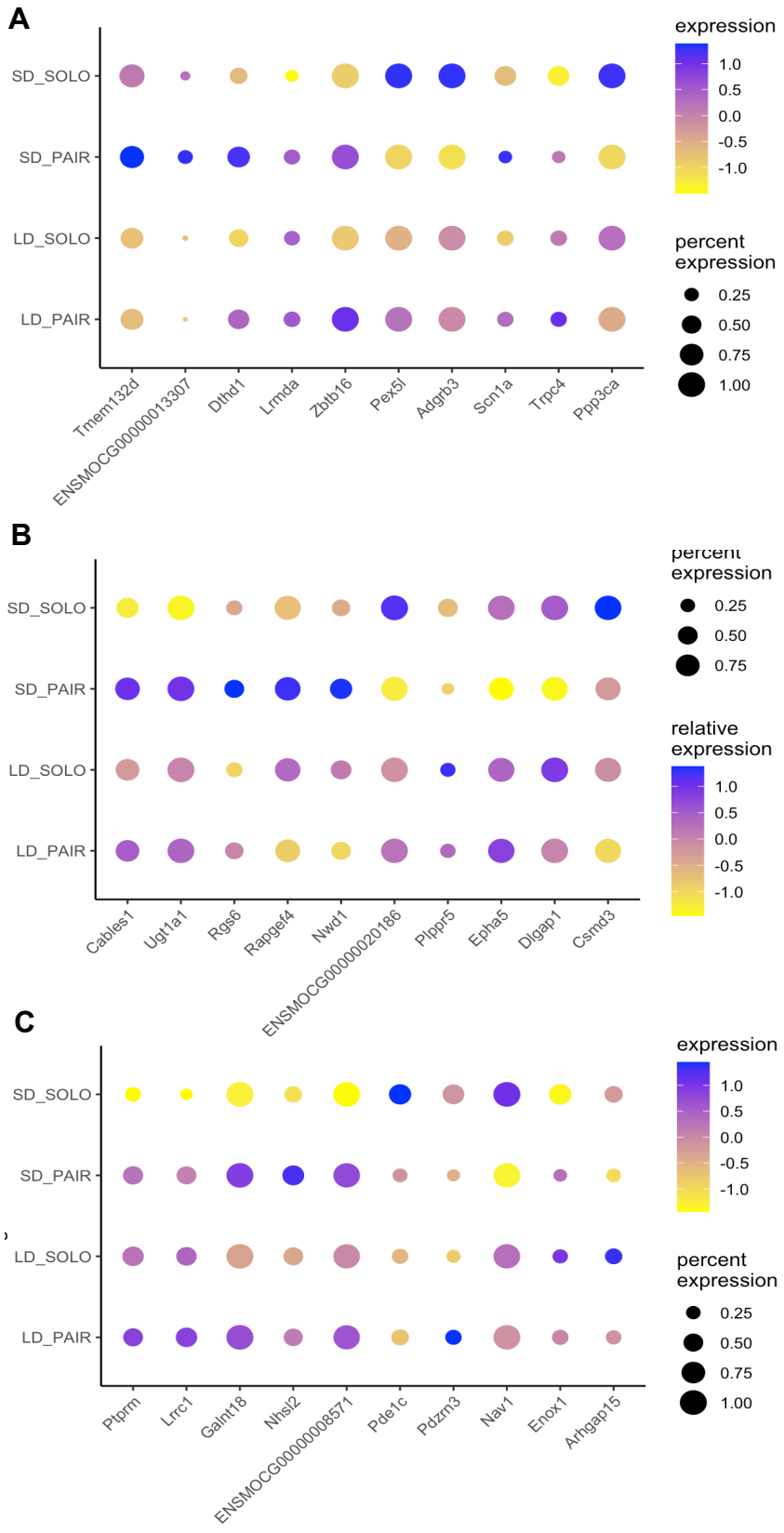
A
SD_SOLO
SD_PAIR
LD_SOLO
LD_PAIR
Tmem132d
ENSMOCG00000013307
Dlhd1
Lrmda
Zbtb16
Pex5l
Adgrb3
Scn1a
Trpc4
Ppp3ca
expression
1.0
0.5
0.0
-0.5
-1.0
percent expression
0.25
0.50
0.75
1.00
B
SD_SOLO
SD_PAIR
LD_SOLO
LD_PAIR
Cables1
Ugt1a1
Rgs6
Rapgef4
Nwd1
ENSMOCG00000020186
Plppr5
Epha5
Dlgap1
Csmd3
percent expression
0.25
0.50
0.75
relative expression
1.0
0.5
0.0
-0.5
-1.0
C
SD_SOLO
SD_PAIR
LD_SOLO
LD_PAIR
Ptprm
Lrrc1
Galnt18
Nhsl2
ENSMOCG00000008571
Pde1c
Pdzrn3
Nav1
Enox1
Arhgap15
expression
1.0
0.5
0.0
-0.5
-1.0
percent expression
0.25
0.50
0.75
1.00

Fig 4.S5. Top differentially expressed genes between SD solo and Paired animals in glial clusters. Dot plots of top differentially expressed genes between SD solo and paired animals in **A)** cluster Olig-1, **B)** cluster Astro-1, and **C)** cluster MG-1. All genes differentially expressed with Bonferoni corrected Kruskall Wallace test, $p<.05$, $Log2FC>0.5$

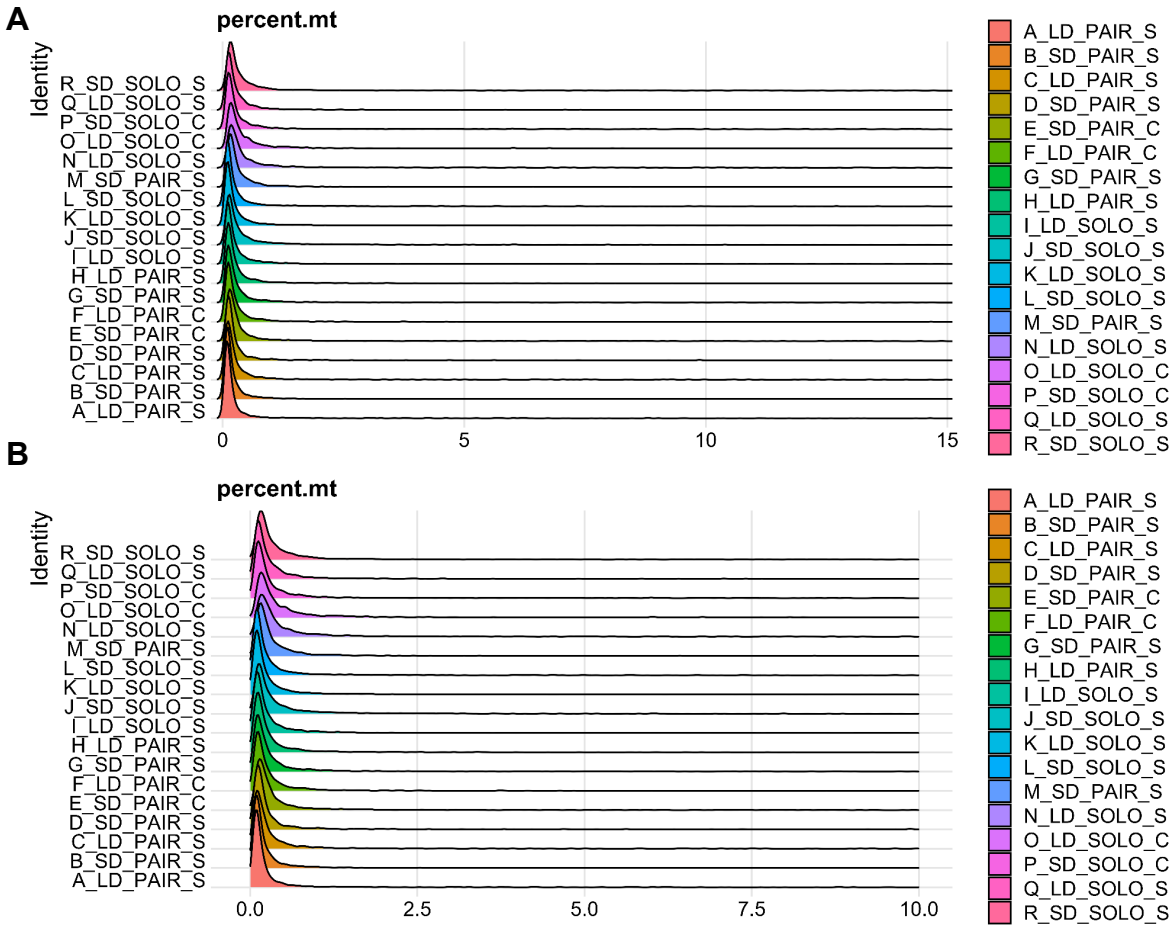
A
percent.mt
Identity
R_SD_SOLO_S
Q_LD_SOLO_S
P_SD_SOLO_C
O_LD_SOLO_C
N_LD_SOLO_S
M_SD_PAIR_S
L_SD_SOLO_S
K_LD_SOLO_S
J_SD_SOLO_S
I_LD_SOLO_S
H_LD_PAIR_S
G_SD_PAIR_S
F_LD_PAIR_C
E_SD_PAIR_C
D_SD_PAIR_S
C_LD_PAIR_S
B_SD_PAIR_S
A_LD_PAIR_S
0
5
10
15
A_LD_PAIR_S
B_SD_PAIR_S
C_LD_PAIR_S
D_SD_PAIR_S
E_SD_PAIR_C
F_LD_PAIR_C
G_SD_PAIR_S
H_LD_PAIR_S
I_LD_SOLO_S
J_SD_SOLO_S
K_LD_SOLO_S
L_SD_SOLO_S
M_SD_PAIR_S
N_LD_SOLO_S
O_LD_SOLO_C
P_SD_SOLO_C
Q_LD_SOLO_S
R_SD_SOLO_S
B
percent.mt
Identity
R_SD_SOLO_S
Q_LD_SOLO_S
P_SD_SOLO_C
O_LD_SOLO_C
N_LD_SOLO_S
M_SD_PAIR_S
L_SD_SOLO_S
K_LD_SOLO_S
J_SD_SOLO_S
I_LD_SOLO_S
H_LD_PAIR_S
G_SD_PAIR_S
F_LD_PAIR_C
E_SD_PAIR_C
D_SD_PAIR_S
C_LD_PAIR_S
B_SD_PAIR_S
A_LD_PAIR_S
0.0
2.5
5.0
7.5
10.0
A_LD_PAIR_S
B_SD_PAIR_S
C_LD_PAIR_S
D_SD_PAIR_S
E_SD_PAIR_C
F_LD_PAIR_C
G_SD_PAIR_S
H_LD_PAIR_S
I_LD_SOLO_S
J_SD_SOLO_S
K_LD_SOLO_S
L_SD_SOLO_S
M_SD_PAIR_S
N_LD_SOLO_S
O_LD_SOLO_C
P_SD_SOLO_C
Q_LD_SOLO_S
R_SD_SOLO_S

Fig 4.S6. Quality control metrics-mitochondrial content per sample. A-B) Ridgeplots representing average percent of gene expression per sample driven by mitochondrial genes. A and B show identical data with different limits on the x-axis.

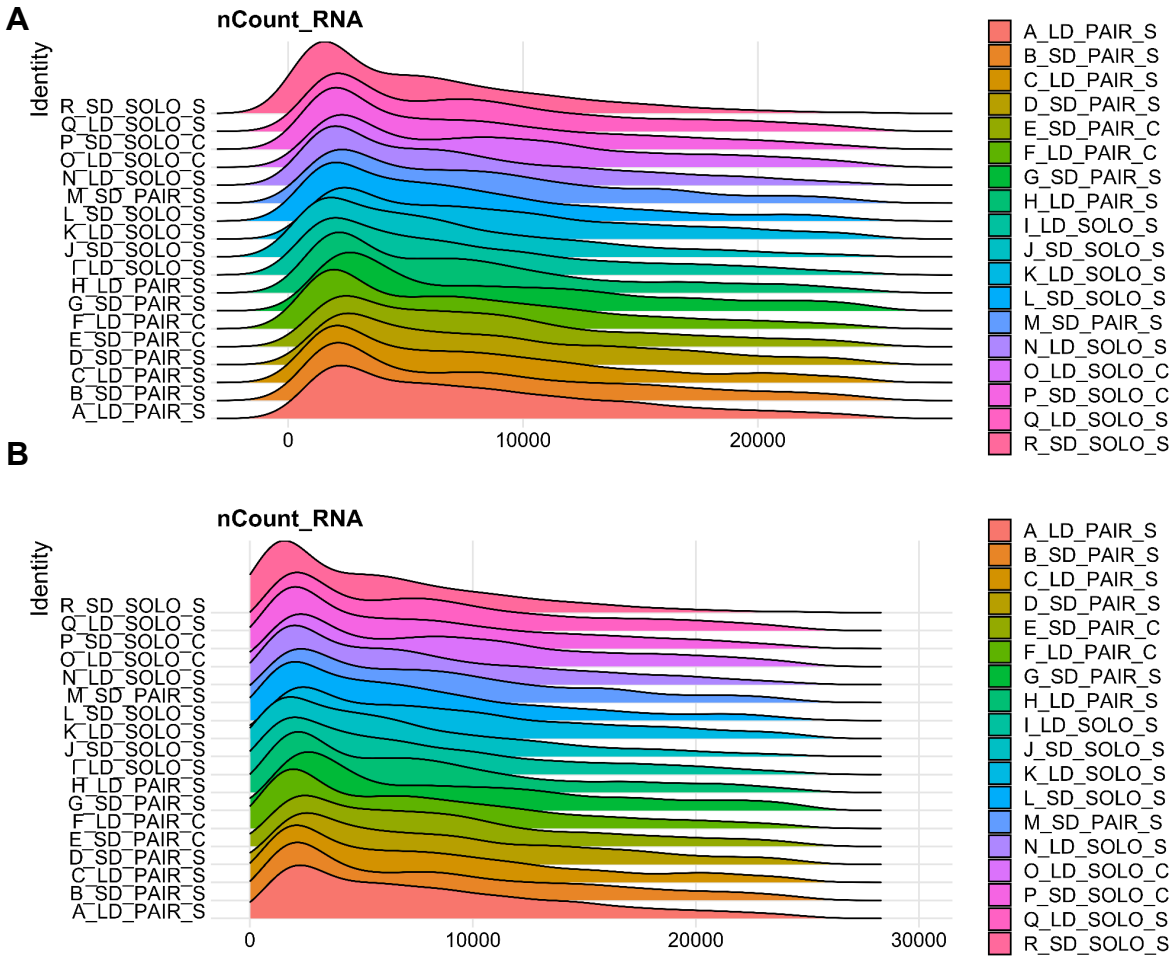
A
nCount_RNA
Identity
R_SD_SOLO_S
Q_LD_SOLO_S
P_SD_SOLO_C
O_LD_SOLO_C
N_LD_SOLO_S
M_SD_PAIR_S
L_SD_SOLO_S
K_LD_SOLO_S
J_SD_SOLO_S
I_LD_SOLO_S
H_LD_PAIR_S
G_SD_PAIR_S
F_LD_PAIR_C
E_SD_PAIR_C
D_SD_PAIR_S
C_LD_PAIR_S
B_SD_PAIR_S
A_LD_PAIR_S
0
10000
20000
A_LD_PAIR_S
B_SD_PAIR_S
C_LD_PAIR_S
D_SD_PAIR_S
E_SD_PAIR_C
F_LD_PAIR_C
G_SD_PAIR_S
H_LD_PAIR_S
I_LD_SOLO_S
J_SD_SOLO_S
K_LD_SOLO_S
L_SD_SOLO_S
M_SD_PAIR_S
N_LD_SOLO_S
O_LD_SOLO_C
P_SD_SOLO_C
Q_LD_SOLO_S
R_SD_SOLO_S
B
nCount_RNA
Identity
R_SD_SOLO_S
Q_LD_SOLO_S
P_SD_SOLO_C
O_LD_SOLO_C
N_LD_SOLO_S
M_SD_PAIR_S
L_SD_SOLO_S
K_LD_SOLO_S
J_SD_SOLO_S
I_LD_SOLO_S
H_LD_PAIR_S
G_SD_PAIR_S
F_LD_PAIR_C
E_SD_PAIR_C
D_SD_PAIR_S
C_LD_PAIR_S
B_SD_PAIR_S
A_LD_PAIR_S
0
10000
20000
30000
A_LD_PAIR_S
B_SD_PAIR_S
C_LD_PAIR_S
D_SD_PAIR_S
E_SD_PAIR_C
F_LD_PAIR_C
G_SD_PAIR_S
H_LD_PAIR_S
I_LD_SOLO_S
J_SD_SOLO_S
K_LD_SOLO_S
L_SD_SOLO_S
M_SD_PAIR_S
N_LD_SOLO_S
O_LD_SOLO_C
P_SD_SOLO_C
Q_LD_SOLO_S
R_SD_SOLO_S

Fig 4.S7. Quality control metrics- RNA count per sample. A-B) Ridgeplots representing the average number of RNA molecules mapping to genes per sample. A and B show identical data with different limits on the x-axis.

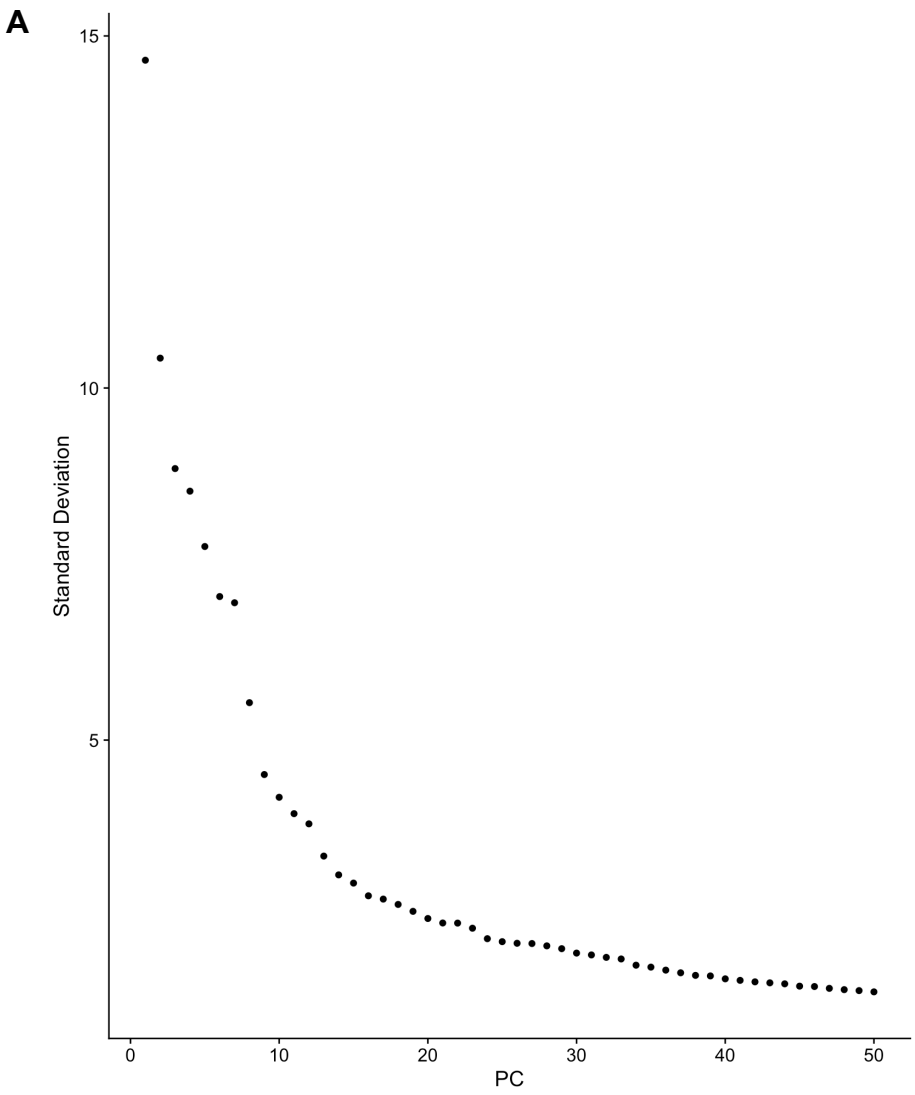
A
15
10
5
Standard Deviation
0
10
20
30
40
50
PC

Fig 4.S8. Quality control metrics - principal component analysis A Elbow plot of explained variance from principal components.

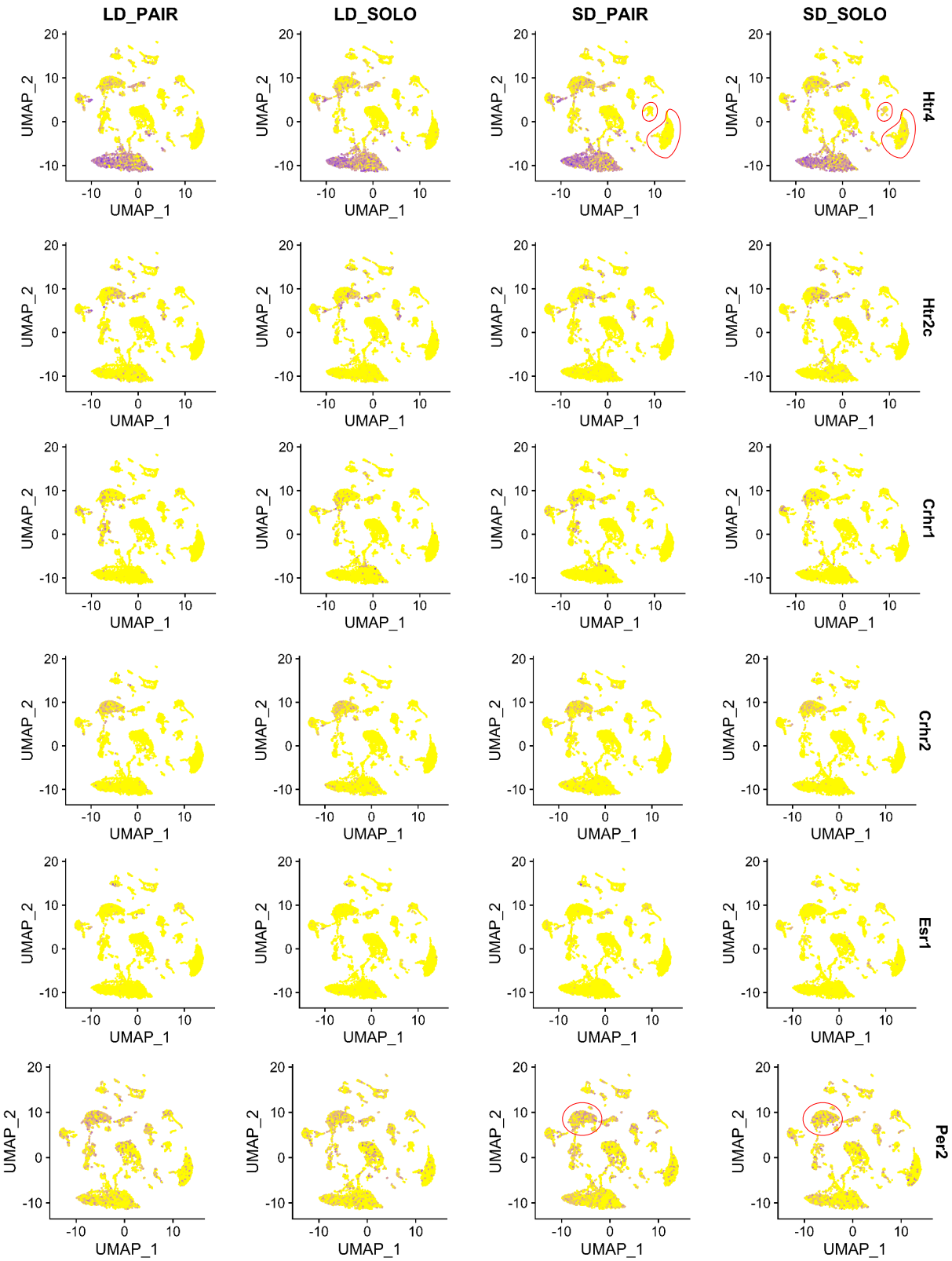
LD_PAIR
LD_SOLO
SD_PAIR
SD_SOLO
Htr4
Htr2c
Crhr1
Crhr2
Esr1
Per2
UMAP_1
UMAP_2

Fig 4.S9. Expression of a priori hypothesized genes across conditions. Representative UMAP plots containing heat maps of gene expression within single cells. Genes were selected based on a priori hypotheses of potential differences across day lengths. Red circles represent significant differential expression across housing conditions with Bonferonni-corrected Kruskall Wallace test, $p<.05$, $Log2FC>0.25$

References

Allen, N. J., Bennett, M. L., Foo, L. C., Wang, G. X., Chakraborty, C., Smith, S. J., & Barres, B. A. (2012). Astrocyte glypicans 4 and 6 promote formation of excitatory synapses via GluA1 AMPA receptors. *Nature*, *486*(7403), 410–414. https://doi.org/10.1038/nature11059

Almeida-Santos, A. F., Carvalho, V. R., Jaimes, L. F., De Castro, C. M., Pinto, H. P., Oliveira, T. P. D., Vieira, L. B., Moraes, M. F. D., & Pereira, G. S. (2019). Social isolation impairs the persistence of social recognition memory by disturbing the glutamatergic tonus and the olfactory bulb-dorsal hippocampus coupling. *Scientific Reports*, *9*(1), 473. https://doi.org/10.1038/s41598-018-36871-6

Anacker, A. M. J., Reitz, K. M., Goodwin, N. L., & Beery, A. K. (2016). Stress impairs new but not established relationships in seasonally social voles. *Hormones and Behavior*, *79*, 52–57. https://doi.org/10.1016/j.yhbeh.2016.01.004

Andrews, N., Hogg, S., Gonzalez, L. E., & File, S. E. (1994). 5-HT1A receptors in the median raphe nucleus and dorsal hippocampus may mediate anxiolytic and anxiogenic behaviours respectively. *European Journal of Pharmacology*, *264*(3), 259–264. https://doi.org/10.1016/0014-2999(94)00473-0

Arnold, M., Cross, R., Singleton, K. S., Zlatic, S., Chapleau, C., Mullin, A. P., Rolle, I., Moore, C. C., Theibert, A., Pozzo-Miller, L., Faundez, V., & Larimore, J. (2016). The Endosome Localized Arf-GAP AGAP1 Modulates Dendritic Spine Morphology Downstream of the Neurodevelopmental Disorder Factor Dysbindin. *Frontiers in Cellular Neuroscience*, *10*. https://doi.org/10.3389/fncel.2016.00218

Avilés, E. C., Krol, A., Henle, S. J., Burroughs-Garcia, J., Deans, M. R., & Goodrich, L. V. (2022). Fat3 acts through independent cytoskeletal effectors to coordinate asymmetric cell behaviors during polarized circuit assembly. *Cell Reports*, *38*(5), 110307. https://doi.org/10.1016/j.celrep.2022.110307

Baekelandt, S., Milla, S., Cornet, V., Flamion, E., Ledoré, Y., Redivo, B., Antipine, S., Mandiki, S. N. M., Houndji, A., El Kertaoui, N., & Kestemont, P. (2020). Seasonal simulated photoperiods influence melatonin release and immune markers of pike perch Sander lucioperca. *Scientific Reports*, *10*(1), 2650. https://doi.org/10.1038/s41598-020-59568-1

Baraban, M., Koudelka, S., & Lyons, D. A. (2018). Ca2+ activity signatures of myelin sheath formation and growth in vivo. *Nature Neuroscience*, *21*(1), 19–23. https://doi.org/10.1038/s41593-017-0040-x

Barriga, C., Martín, M. I., Tabla, R., Ortega, E., & Rodríguez, A. B. (2001). Circadian rhythm of melatonin, corticosterone and phagocytosis: Effect of stress: Melatonin phagocytosis and stress. *Journal of Pineal Research*, *30*(3), 180–187. https://doi.org/10.1034/j.1600-079X.2001.300307.x

Batiuk, M. Y., Martirosyan, A., Wahis, J., De Vin, F., Marneffe, C., Kusserow, C., Koeppen, J., Viana, J. F., Oliveira, J. F., Voet, T., Ponting, C. P., Belgard, T. G., & Holt, M. G. (2020). Identification of region-specific astrocyte subtypes at single cell resolution. *Nature Communications*, *11*(1), 1220. https://doi.org/10.1038/s41467-019-14198-8

Bauer, N. G., Richter‐Landsberg, C., & Ffrench‐Constant, C. (2009). Role of the oligodendroglial cytoskeleton in differentiation and myelination. *Glia*, *57*(16), 1691–1705. https://doi.org/10.1002/glia.20885

Beery, A. K., Loo, T. J., & Zucker, I. (2008). Day length and estradiol affect same-sex affiliative

behavior in the female meadow vole. *Hormones and Behavior*, *54*(1), 153–159. https://doi.org/10.1016/j.yhbeh.2008.02.007
Beery, A. K., Routman, D. M., & Zucker, I. (2009). Same-sex social behavior in meadow voles: Multiple and rapid formation of attachments. *Physiology & Behavior*, *97*(1), 52–57. https://doi.org/10.1016/j.physbeh.2009.01.020
Beery, A. K., & Shambaugh, K. L. (2021). Comparative Assessment of Familiarity/Novelty Preferences in Rodents. *Frontiers in Behavioral Neuroscience*, *15*, 648830. https://doi.org/10.3389/fnbeh.2021.648830
Beery, A. K., Vahaba, D. M., & Grunberg, D. M. (2014). Corticotropin-releasing factor receptor densities vary with photoperiod and sociality. *Hormones and Behavior*, *66*(5), 779–786. https://doi.org/10.1016/j.yhbeh.2014.08.014
Beery, A. K., & Zucker, I. (2010). Oxytocin and same-sex social behavior in female meadow voles. *Neuroscience*, *169*(2), 665–673. https://doi.org/10.1016/j.neuroscience.2010.05.023
Behesti, H., Fore, T. R., Wu, P., Horn, Z., Leppert, M., Hull, C., & Hatten, M. E. (2018). ASTN2 modulates synaptic strength by trafficking and degradation of surface proteins. *Proceedings of the National Academy of Sciences*, *115*(41). https://doi.org/10.1073/pnas.1809382115
Berghoff, S. A., Spieth, L., Sun, T., Hosang, L., Depp, C., Sasmita, A. O., Vasileva, M. H., Scholz, P., Zhao, Y., Krueger-Burg, D., Wichert, S., Brown, E. R., Michail, K., Nave, K.-A., Bonn, S., Odoardi, F., Rossner, M., Ischebeck, T., Edgar, J. M., & Saher, G. (2021). Neuronal cholesterol synthesis is essential for repair of chronically demyelinated lesions in mice. *Cell Reports*, *37*(4), 109889. https://doi.org/10.1016/j.celrep.2021.109889
Berkowicz, S. R., Featherby, T. J., Whisstock, J. C., & Bird, P. I. (2016). Mice Lacking Brinp2 or Brinp3, or Both, Exhibit Behaviors Consistent with Neurodevelopmental Disorders. *Frontiers in Behavioral Neuroscience*, *10*. https://doi.org/10.3389/fnbeh.2016.00196
Berkowicz, S. R., Giousoh, A., & Bird, P. I. (2017). Neurodevelopmental MACPFs: The vertebrate astrotactins and BRINPs. *Seminars in Cell & Developmental Biology*, *72*, 171–181. https://doi.org/10.1016/j.semcdb.2017.05.005
Black, J. A., Liu, S., & Waxman, S. G. (2009). Sodium channel activity modulates multiple functions in microglia. *Glia*, *57*(10), 1072–1081. https://doi.org/10.1002/glia.20830
Bueno, C., Amaral, F. G. D., & Spruyt, K. (2023). Editorial: Melatonin and biological rhythms: from bench to bedside. *Frontiers in Neuroscience*, *17*, 1208878. https://doi.org/10.3389/fnins.2023.1208878
Butt, A. M. (2006). Neurotransmitter‐mediated calcium signalling in oligodendrocyte physiology and pathology. *Glia*, *54*(7), 666–675. https://doi.org/10.1002/glia.20424
Cembrowski, M. S., Wang, L., Sugino, K., Shields, B. C., & Spruston, N. (2016). Hipposeq: A comprehensive RNA-seq database of gene expression in hippocampal principal neurons. *eLife*, *5*, e14997. https://doi.org/10.7554/eLife.14997
Chang, C.-H., & Gean, P.-W. (2019). The Ventral Hippocampus Controls Stress-Provoked Impulsive Aggression through the Ventromedial Hypothalamus in Post-Weaning Social Isolation Mice. *Cell Reports*, *28*(5), 1195-1205.e3. https://doi.org/10.1016/j.celrep.2019.07.005
Chung, W.-S., Allen, N. J., & Eroglu, C. (2015). Astrocytes Control Synapse Formation, Function, and Elimination. *Cold Spring Harbor Perspectives in Biology*, *7*(9), a020370.

https://doi.org/10.1101/cshperspect.a020370
Davenport, A. S. (2012). Characterization of UDP-glucuronosyltransferase (UGT1A1) Promoter Polymorphisms and Gene Expression on Ethnicity, Stage of Disease, and Menopausal Status in Breast Cancer. *Journal of Drug Metabolism & Toxicology*, *s4*. https://doi.org/10.4172/2157-7609.S4-001
Deemyad, T., Lüthi, J., & Spruston, N. (2018). Astrocytes integrate and drive action potential firing in inhibitory subnetworks. *Nature Communications*, *9*(1), 4336. https://doi.org/10.1038/s41467-018-06338-3
Ding, S.-L., Yao, Z., Hirokawa, K. E., Nguyen, T. N., Graybuck, L. T., Fong, O., Bohn, P., Ngo, K., Smith, K. A., Koch, C., Phillips, J. W., Lein, E. S., Harris, J. A., Tasic, B., & Zeng, H. (2020). Distinct Transcriptomic Cell Types and Neural Circuits of the Subiculum and Prosubiculum along the Dorsal-Ventral Axis. *Cell Reports*, *31*(7), 107648. https://doi.org/10.1016/j.celrep.2020.107648
Dobin, A., & Gingeras, T. R. (2015). Mapping RNA‐seq Reads with STAR. *Current Protocols in Bioinformatics*, *51*(1). https://doi.org/10.1002/0471250953.bi1114s51
Fan, L., Bhatt, A., Tien, L., Zheng, B., Simpson, K. L., Lin, R. C. S., Cai, Z., Kumar, P., & Pang, Y. (2015). Exposure to serotonin adversely affects oligodendrocyte development and myelination *in vitro*. *Journal of Neurochemistry*, *133*(4), 532–543. https://doi.org/10.1111/jnc.12988
Ferdman, N., Murmu, R., Bock, J., Braun, K., & Leshem, M. (2007). Weaning age, social isolation, and gender, interact to determine adult explorative and social behavior, and dendritic and spine morphology in prefrontal cortex of rats. *Behavioural Brain Research*, *180*(2), 174–182. https://doi.org/10.1016/j.bbr.2007.03.011
Furness, D. N., Dehnes, Y., Akhtar, A. Q., Rossi, D. J., Hamann, M., Grutle, N. J., Gundersen, V., Holmseth, S., Lehre, K. P., Ullensvang, K., Wojewodzic, M., Zhou, Y., Attwell, D., & Danbolt, N. C. (2008). A quantitative assessment of glutamate uptake into hippocampal synaptic terminals and astrocytes: New insights into a neuronal role for excitatory amino acid transporter 2 (EAAT2). *Neuroscience*, *157*(1), 80–94. https://doi.org/10.1016/j.neuroscience.2008.08.043
Galea, L. A. M., & McEwen, B. S. (1999). Sex and seasonal changes in the rate of cell proliferation in the dentate gyrus of adult wild meadow voles. *Neuroscience*, *89*(3), 955–964. https://doi.org/10.1016/S0306-4522(98)00345-5
Galea, L. A. M., Perrot-Sinal, T. S., Kavaliers, M., & Ossenkopp, K.-P. (1999). Relations of hippocampal volume and dentate gyrus width to gonadal hormone levels in male and female meadow voles. *Brain Research*, *821*(2), 383–391. https://doi.org/10.1016/S0006-8993(99)01100-2
Galloway, D. A., Phillips, A. E. M., Owen, D. R. J., & Moore, C. S. (2019). Phagocytosis in the Brain: Homeostasis and Disease. *Frontiers in Immunology*, *10*, 790. https://doi.org/10.3389/fimmu.2019.00790
Garrido Zinn, C., Clairis, N., Silva Cavalcante, L. E., Furini, C. R. G., De Carvalho Myskiw, J., & Izquierdo, I. (2016). Major neurotransmitter systems in dorsal hippocampus and basolateral amygdala control social recognition memory. *Proceedings of the National Academy of Sciences*, *113*(33). https://doi.org/10.1073/pnas.1609883113
Getz, L. L. (1961). Home Ranges, Territoriality, and Movement of the Meadow Vole. *Journal of Mammalogy*, *42*(1), 24. https://doi.org/10.2307/1377237
Goda, R., Otsuka, T., Iwamoto, A., Kawai, M., Shibata, S., Furuse, M., & Yasuo, S. (2015).

Serotonin levels in the dorsal raphe nuclei of both chipmunks and mice are enhanced by long photoperiod, but brain dopamine level response to photoperiod is species-specific. *Neuroscience Letters*, *593*, 95–100. https://doi.org/10.1016/j.neulet.2015.03.035

Gould, G. G., Hensler, J. G., Burke, T. F., Benno, R. H., Onaivi, E. S., & Daws, L. C. (2011). Density and function of central serotonin (5-HT) transporters, 5-HT1A and 5-HT2A receptors, and effects of their targeting on BTBR T+tf/J mouse social behavior: Central 5-HT regulation and social behavior in BTBR mice. *Journal of Neurochemistry*, *116*(2), 291–303. https://doi.org/10.1111/j.1471-4159.2010.07104.x

Guzowski, J. F., McNaughton, B. L., Barnes, C. A., & Worley, P. F. (1999). Environment-specific expression of the immediate-early gene Arc in hippocampal neuronal ensembles. *Nature Neuroscience*, *2*(12), 1120–1124. https://doi.org/10.1038/16046

Hao, Y., Hao, S., Andersen-Nissen, E., Mauck, W. M., Zheng, S., Butler, A., Lee, M. J., Wilk, A. J., Darby, C., Zager, M., Hoffman, P., Stoeckius, M., Papalexi, E., Mimitou, E. P., Jain, J., Srivastava, A., Stuart, T., Fleming, L. M., Yeung, B., … Satija, R. (2021). Integrated analysis of multimodal single-cell data. *Cell*, *184*(13), 3573-3587.e29. https://doi.org/10.1016/j.cell.2021.04.048

Jackson, V. A., Mehmood, S., Chavent, M., Roversi, P., Carrasquero, M., Del Toro, D., Seyit-Bremer, G., Ranaivoson, F. M., Comoletti, D., Sansom, M. S. P., Robinson, C. V., Klein, R., & Seiradake, E. (2016). Super-complexes of adhesion GPCRs and neural guidance receptors. *Nature Communications*, *7*(1), 11184. https://doi.org/10.1038/ncomms11184

Jacobs, L. F. (1996). The Economy of Winter: Phenotypic Plasticity in Behavior and Brain Structure. *The Biological Bulletin*, *191*(1), 92–100. https://doi.org/10.2307/1543068

Jacobs, L. F., Gaulin, S. J., Sherry, D. F., & Hoffman, G. E. (1990). Evolution of spatial cognition: Sex-specific patterns of spatial behavior predict hippocampal size. *Proceedings of the National Academy of Sciences*, *87*(16), 6349–6352. https://doi.org/10.1073/pnas.87.16.6349

Kawabata Galbraith, K., & Kengaku, M. (2019). Multiple roles of the actin and microtubule-regulating formins in the developing brain. *Neuroscience Research*, *138*, 59–69. https://doi.org/10.1016/j.neures.2018.09.008

Kerbeshian, M. C., Bronson, F. H., & Bellis, E. D. (1994). Variation in Reproductive Photoresponsiveness in a Wild Population of Meadow Voles1. *Biology of Reproduction*, *50*(4), 745–750. https://doi.org/10.1095/biolreprod50.4.745

Kim, M., Morales, L., Jang, I.-S., Cho, Y.-Y., & Kim, D. (2018). Protein Tyrosine Phosphatases as Potential Regulators of STAT3 Signaling. *International Journal of Molecular Sciences*, *19*(9), 2708. https://doi.org/10.3390/ijms19092708

Kirsz, K., & Zieba, D. A. (2012). A review on the effect of the photoperiod and melatonin on interactions between ghrelin and serotonin. *General and Comparative Endocrinology*, *179*(2), 248–253. https://doi.org/10.1016/j.ygcen.2012.08.025

Klingler, E., Martin, P.-M., Garcia, M., Moreau-Fauvarque, C., Falk, J., Chareyre, F., Giovannini, M., Chédotal, A., Girault, J.-A., & Goutebroze, L. (2015). The cytoskeleton-associated protein SCHIP1 is involved in axon guidance, and is required for piriform cortex and anterior commissure development. *Development*, *142*(11), 2026–2036. https://doi.org/10.1242/dev.119248

Lázaro, J., Hertel, M., LaPoint, S., Wikelski, M., Stiehler, M., & Dechmann, D. K. N. (2017).

Cognitive skills of common shrews (*Sorex araneus*) vary with seasonal changes in skull size and brain mass. *Journal of Experimental Biology*, jeb.166595. https://doi.org/10.1242/jeb.166595

Lee, N. S., Goodwin, N. L., Freitas, K. E., & Beery, A. K. (2019). Affiliation, Aggression, and Selectivity of Peer Relationships in Meadow and Prairie Voles. *Frontiers in Behavioral Neuroscience*, *13*, 52. https://doi.org/10.3389/fnbeh.2019.00052

Lee, P. R. (2009). Regulation of myelin genes implicated in psychiatric disorders by functional activity in axons. *Frontiers in Neuroanatomy*, *3*. https://doi.org/10.3389/neuro.05.004.2009

Leroy, F., Park, J., Asok, A., Brann, D. H., Meira, T., Boyle, L. M., Buss, E. W., Kandel, E. R., & Siegelbaum, S. A. (2018). A circuit from hippocampal CA2 to lateral septum disinhibits social aggression. *Nature*, *564*(7735), 213–218. https://doi.org/10.1038/s41586-018-0772-0

Li, J., Liu, H., Wang, X., Xia, Y., Huang, J., Wang, T., Lin, Z., & Xiong, N. (2022). Melatonin ameliorates Parkinson's disease via regulating microglia polarization in a RORα‐dependent pathway. *Npj Parkinson's Disease*, *8*(1), 90. https://doi.org/10.1038/s41531-022-00352-5

Ma, H., Kang, J., Fan, W., He, H., & Huang, F. (2021). ROR: Nuclear Receptor for Melatonin or Not? *Molecules*, *26*(9), 2693. https://doi.org/10.3390/molecules26092693

Madison, D. M., FitzGerald, R. W., & McShea, W. J. (1984). Dynamics of social nesting in overwintering meadow voles (Microtus pennsylvanicus): Possible consequences for population cycling. *Behavioral Ecology and Sociobiology*, *15*(1), 9–17. https://doi.org/10.1007/BF00310209

Manousi, A., Göttle, P., Reiche, L., Cui, Q.-L., Healy, L. M., Akkermann, R., Gruchot, J., Schira-Heinen, J., Antel, J. P., Hartung, H.-P., & Küry, P. (2021). Identification of novel myelin repair drugs by modulation of oligodendroglial differentiation competence. *EBioMedicine*, *65*, 103276. https://doi.org/10.1016/j.ebiom.2021.103276

Marques, S., Zeisel, A., Codeluppi, S., Van Bruggen, D., Mendanha Falcão, A., Xiao, L., Li, H., Häring, M., Hochgerner, H., Romanov, R. A., Gyllborg, D., Muñoz-Manchado, A. B., La Manno, G., Lönnerberg, P., Floriddia, E. M., Rezayee, F., Ernfors, P., Arenas, E., Hjerling-Leffler, J., … Castelo-Branco, G. (2016). Oligodendrocyte heterogeneity in the mouse juvenile and adult central nervous system. *Science*, *352*(6291), 1326–1329. https://doi.org/10.1126/science.aaf6463

Martin, E. A., Muralidhar, S., Wang, Z., Cervantes, D. C., Basu, R., Taylor, M. R., Hunter, J., Cutforth, T., Wilke, S. A., Ghosh, A., & Williams, M. E. (2015). The intellectual disability gene Kirrel3 regulates target-specific mossy fiber synapse development in the hippocampus. *eLife*, *4*, e09395. https://doi.org/10.7554/eLife.09395

Masuda, T., Sankowski, R., Staszewski, O., & Prinz, M. (2020). Microglia Heterogeneity in the Single-Cell Era. *Cell Reports*, *30*(5), 1271–1281. https://doi.org/10.1016/j.celrep.2020.01.010

Mc Mahon, B., Nørgaard, M., Svarer, C., Andersen, S. B., Madsen, M. K., Baaré, W. F. C., Madsen, J., Frokjaer, V. G., & Knudsen, G. M. (2018). Seasonality-resilient individuals downregulate their cerebral 5-HT transporter binding in winter – A longitudinal combined 11C-DASB and 11C-SB207145 PET study. *European Neuropsychopharmacology*, *28*(10), 1151–1160. https://doi.org/10.1016/j.euroneuro.2018.06.004

Meira, T., Leroy, F., Buss, E. W., Oliva, A., Park, J., & Siegelbaum, S. A. (2018). A hippocampal circuit linking dorsal CA2 to ventral CA1 critical for social memory dynamics. *Nature Communications*, *9*(1), 4163. https://doi.org/10.1038/s41467-018-06501-w

Menon, R., Süß, T., Oliveira, V. E. D. M., Neumann, I. D., & Bludau, A. (2022). Neurobiology of the lateral septum: Regulation of social behavior. *Trends in Neurosciences*, *45*(1), 27–40. https://doi.org/10.1016/j.tins.2021.10.010

Míguez, J. M., Simonneaux, V., & Pévet, P. (1995). Evidence for a Regulatory Role of Melatonin on Serotonin Release and Uptake in the Pineal Gland. *Journal of Neuroendocrinology*, *7*(12), 949–956. https://doi.org/10.1111/j.1365-2826.1995.tb00740.x

Mineur, Y. S., Einstein, E. B., Bentham, M. P., Wigestrand, M. B., Blakeman, S., Newbold, S. A., & Picciotto, M. R. (2015). Expression of the 5-HT1A Serotonin Receptor in the Hippocampus Is Required for Social Stress Resilience and the Antidepressant-Like Effects Induced by the Nicotinic Partial Agonist Cytisine. *Neuropsychopharmacology*, *40*(4), 938–946. https://doi.org/10.1038/npp.2014.269

Molnar, E., Lazary, J., Benko, A., Gonda, X., Pap, D., Mekli, K., Juhasz, G., Kovacs, G., Kurimay, T., Rihmer, Z., & Bagdy, G. (2010). Seasonality and winter-type seasonal depression are associated with the rs731779 polymorphism of the serotonin-2A receptor gene. *European Neuropsychopharmacology*, *20*(9), 655–662. https://doi.org/10.1016/j.euroneuro.2010.04.009

Munley, K. M., Han, Y., Lansing, M. X., & Demas, G. E. (2022). Winter madness: Melatonin as a neuroendocrine regulator of seasonal aggression. *Journal of Experimental Zoology Part A: Ecological and Integrative Physiology*, *337*(9–10), 873–889. https://doi.org/10.1002/jez.2601

Murai, K. K., & Pasquale, E. B. (2011). Eph receptors and ephrins in neuron–astrocyte communication at synapses. *Glia*, *59*(11), 1567–1578. https://doi.org/10.1002/glia.21226

Nagai, Y., Kisaka, Y., Nomura, K., Nishitani, N., Andoh, C., Koda, M., Kawai, H., Seiriki, K., Nagayasu, K., Kasai, A., Shirakawa, H., Nakazawa, T., Hashimoto, H., & Kaneko, S. (2023). Dorsal raphe serotonergic neurons preferentially reactivate dorsal dentate gyrus cell ensembles associated with positive experience. *Cell Reports*, *42*(3), 112149. https://doi.org/10.1016/j.celrep.2023.112149

Nagy, C., Maitra, M., Tanti, A., Suderman, M., Théroux, J.-F., Davoli, M. A., Perlman, K., Yerko, V., Wang, Y. C., Tripathy, S. J., Pavlidis, P., Mechawar, N., Ragoussis, J., & Turecki, G. (2020). Single-nucleus transcriptomics of the prefrontal cortex in major depressive disorder implicates oligodendrocyte precursor cells and excitatory neurons. *Nature Neuroscience*, *23*(6), 771–781. https://doi.org/10.1038/s41593-020-0621-y

Nelson, L. H., Saulsbery, A. I., & Lenz, K. M. (2019). Small cells with big implications: Microglia and sex differences in brain development, plasticity and behavioral health. *Progress in Neurobiology*, *176*, 103–119. https://doi.org/10.1016/j.pneurobio.2018.09.002

Nomoto, H. (2003). Molecular Cloning of a Novel Transmembrane Protein MOLT Expressed by Mature Oligodendrocytes. *Journal of Biochemistry*, *134*(2), 231–238. https://doi.org/10.1093/jb/mvg135

O'Mara, S. (2006). Controlling hippocampal output: The central role of subiculum in hippocampal information processing. *Behavioural Brain Research*, *174*(2), 304–312. https://doi.org/10.1016/j.bbr.2006.08.018

Omer, D. B., Maimon, S. R., Las, L., & Ulanovsky, N. (2018). Social place-cells in the bat hippocampus. *Science*, *359*(6372), 218–224. https://doi.org/10.1126/science.aao3474

Petrulis, A., Alvarez, P., & Eichenbaum, H. (2005). Neural correlates of social odor recognition and the representation of individual distinctive social odors within entorhinal cortex and ventral subiculum. *Neuroscience*, *130*(1), 259–274. https://doi.org/10.1016/j.neuroscience.2004.09.001

Philips, M.-A., Lilleväli, K., Heinla, I., Luuk, H., Hundahl, C. A., Kongi, K., Vanaveski, T., Tekko, T., Innos, J., & Vasar, E. (2015). Lsamp is implicated in the regulation of emotional and social behavior by use of alternative promoters in the brain. *Brain Structure and Function*, *220*(3), 1381–1393. https://doi.org/10.1007/s00429-014-0732-x

Prince, J. E. A., Brignall, A. C., Cutforth, T., Shen, K., & Cloutier, J.-F. (2013). Kirrel3 is required for the coalescence of vomeronasal sensory neuron axons into glomeruli and for male-male aggression. *Development*, *140*(11), 2398–2408. https://doi.org/10.1242/dev.087262

Raam, T., McAvoy, K. M., Besnard, A., Veenema, A. H., & Sahay, A. (2017). Hippocampal oxytocin receptors are necessary for discrimination of social stimuli. *Nature Communications*, *8*(1), 2001. https://doi.org/10.1038/s41467-017-02173-0

Rao, R. P., Von Heimendahl, M., Bahr, V., & Brecht, M. (2019). Neuronal Responses to Conspecifics in the Ventral CA1. *Cell Reports*, *27*(12), 3460-3472.e3. https://doi.org/10.1016/j.celrep.2019.05.081

Rattner, A., Terrillion, C. E., Jou, C., Kleven, T., Hu, S. F., Williams, J., Hou, Z., Aggarwal, M., Mori, S., Shin, G., Goff, L. A., Witter, M. P., Pletnikov, M., Fenton, A. A., & Nathans, J. (2020). Developmental, cellular, and behavioral phenotypes in a mouse model of congenital hypoplasia of the dentate gyrus. *eLife*, *9*, e62766. https://doi.org/10.7554/eLife.62766

Roberts, L., & Greene, J. R. T. (2003). Post-weaning social isolation of rats leads to a diminution of LTP in the CA1 to subiculum pathway. *Brain Research*, *991*(1–2), 271–273. https://doi.org/10.1016/j.brainres.2003.08.022

Robertson, R. G., Rolls, E. T., Georges-Francois, P., & Panzeri, S. (1999). Head direction cells in the primate pre-subiculum. *Hippocampus*, *9*(3), 206–219. https://doi.org/10.1002/(SICI)1098-1063(1999)9:3<206::AID-HIPO2>3.0.CO;2-H

Saijo, K., Crotti, A., & Glass, C. K. (2013). Regulation of microglia activation and deactivation by nuclear receptors. *Glia*, *61*(1), 104–111. https://doi.org/10.1002/glia.22423

Sato, K., Takahashi, K., Shigemoto-Mogami, Y., Chujo, K., & Sekino, Y. (2016). Glypican 6 Enhances N-Methyl-D-Aspartate Receptor Function in Human-Induced Pluripotent Stem Cell-Derived Neurons. *Frontiers in Cellular Neuroscience*, *10*. https://doi.org/10.3389/fncel.2016.00259

Sato, T. K., Panda, S., Miraglia, L. J., Reyes, T. M., Rudic, R. D., McNamara, P., Naik, K. A., FitzGerald, G. A., Kay, S. A., & Hogenesch, J. B. (2004). A Functional Genomics Strategy Reveals Rora as a Component of the Mammalian Circadian Clock. *Neuron*, *43*(4), 527–537. https://doi.org/10.1016/j.neuron.2004.07.018

Savas, J. N., Ribeiro, L. F., Wierda, K. D., Wright, R., DeNardo-Wilke, L. A., Rice, H. C., Chamma, I., Wang, Y.-Z., Zemla, R., Lavallée-Adam, M., Vennekens, K. M., O'Sullivan, M. L., Antonios, J. K., Hall, E. A., Thoumine, O., Attie, A. D., Yates, J. R., Ghosh, A., & de Wit, J. (2015). The Sorting Receptor SorCS1 Regulates Trafficking of Neurexin and AMPA Receptors. *Neuron*, *87*(4), 764–780. https://doi.org/10.1016/j.neuron.2015.08.007

Sherry, D. F., Jacobs, L. F., & Gaulin, S. J. C. (1992). Spatial memory and adaptive specialization of the hippocampus. *Trends in Neurosciences*, *15*(8), 298–303.

https://doi.org/10.1016/0166-2236(92)90080-R
Shin, K. C., Park, H. J., Kim, J. G., Lee, I. H., Cho, H., Park, C., Sung, T. S., Koh, S. D., Park, S. W., & Bae, Y. M. (2019). The Piezo2 ion channel is mechanically activated by low-threshold positive pressure. *Scientific Reports*, *9*(1), 6446. https://doi.org/10.1038/s41598-019-42492-4
Shinoda, Y., Sadakata, T., Akagi, T., Sakamaki, Y., Hashikawa, T., Sano, Y., & Furuichi, T. (2018). Calcium-dependent activator protein for secretion 2 (CADPS2) deficiency causes abnormal synapse development in hippocampal mossy fiber terminals. *Neuroscience Letters*, *677*, 65–71. https://doi.org/10.1016/j.neulet.2018.04.036
Singh, K., Jayaram, M., Kaare, M., Leidmaa, E., Jagomäe, T., Heinla, I., Hickey, M. A., Kaasik, A., Schäfer, M. K., Innos, J., Lilleväli, K., Philips, M.-A., & Vasar, E. (2019). Neural cell adhesion molecule Negr1 deficiency in mouse results in structural brain endophenotypes and behavioral deviations related to psychiatric disorders. *Scientific Reports*, *9*(1), 5457. https://doi.org/10.1038/s41598-019-41991-8
Song, S., Luo, L., Sun, B., & Sun, D. (2020). Roles of glial ion transporters in brain diseases. *Glia*, *68*(3), 472–494. https://doi.org/10.1002/glia.23699
Song, W., Li, Q., Wang, T., Li, Y., Fan, T., Zhang, J., Wang, Q., Pan, J., Dong, Q., Sun, Z. S., & Wang, Y. (2022). Putative complement control protein CSMD3 dysfunction impairs synaptogenesis and induces neurodevelopmental disorders. *Brain, Behavior, and Immunity*, *102*, 237–250. https://doi.org/10.1016/j.bbi.2022.02.027
Spritzer, M. D., Panning, A. W., Engelman, S. M., Prince, W. T., Casler, A. E., Georgakas, J. E., Jaeger, E. C. B., Nelson, L. R., Roy, E. A., & Wagner, B. A. (2017). Seasonal and sex differences in cell proliferation, neurogenesis, and cell death within the dentate gyrus of adult wild-caught meadow voles. *Neuroscience*, *360*, 155–165. https://doi.org/10.1016/j.neuroscience.2017.07.046
Sriram, K., Wiley, S. Z., Moyung, K., Gorr, M. W., Salmerón, C., Marucut, J., French, R. P., Lowy, A. M., & Insel, P. A. (2019). Detection and Quantification of GPCR mRNA: An Assessment and Implications of Data from High-Content Methods. *ACS Omega*, *4*(16), 17048–17059. https://doi.org/10.1021/acsomega.9b02811
Stringham, E. G., & Schmidt, K. L. (2009). Navigating the cell: UNC-53 and the navigators, a family of cytoskeletal regulators with multiple roles in cell migration, outgrowth and trafficking. *Cell Adhesion & Migration*, *3*(4), 342–346. https://doi.org/10.4161/cam.3.4.9451
Subhadeep, D., Srikumar, B. N., Shankaranarayana Rao, B. S., & Kutty, B. M. (2020). Short photoperiod restores ventral subicular lesion‐induced deficits in affective and socio‐cognitive behavior in male Wistar rats. *Journal of Neuroscience Research*, *98*(6), 1114–1136. https://doi.org/10.1002/jnr.24601
Szklarczyk, D., Gable, A. L., Lyon, D., Junge, A., Wyder, S., Huerta-Cepas, J., Simonovic, M., Doncheva, N. T., Morris, J. H., Bork, P., Jensen, L. J., & Mering, C. von. (2019). STRING v11: Protein–protein association networks with increased coverage, supporting functional discovery in genome-wide experimental datasets. *Nucleic Acids Research*, *47*(D1), D607–D613. https://doi.org/10.1093/nar/gky1131
Tang, Y., & Le, W. (2016). Differential Roles of M1 and M2 Microglia in Neurodegenerative Diseases. *Molecular Neurobiology*, *53*(2), 1181–1194. https://doi.org/10.1007/s12035-014-9070-5
Taylor, M. R., Martin, E. A., Sinnen, B., Trilokekar, R., Ranza, E., Antonarakis, S. E., &

Williams, M. E. (2020). Kirrel3-Mediated Synapse Formation Is Attenuated by Disease-Associated Missense Variants. *The Journal of Neuroscience*, *40*(28), 5376–5388. https://doi.org/10.1523/JNEUROSCI.3058-19.2020

Tiwari, A. C., Kumar, P., Singh, S., Sharma, D., & Chaturvedi, C. M. (2006). Reproductive phase dependent circadian variation in hypothalamic concentration of serotonin, dopamine and peripheral thyroxine levels in Japanese Quail following 5-HTP and L-DOPA administration at specific time intervals. *Biological Rhythm Research*, *37*(1), 73–86. https://doi.org/10.1080/09291010500239684

Turkin, A., Tuchina, O., & Klempin, F. (2021). Microglia Function on Precursor Cells in the Adult Hippocampus and Their Responsiveness to Serotonin Signaling. *Frontiers in Cell and Developmental Biology*, *9*, 665739. https://doi.org/10.3389/fcell.2021.665739

Tyrer, A. E., Levitan, R. D., Houle, S., Wilson, A. A., Nobrega, J. N., & Meyer, J. H. (2016). Increased Seasonal Variation in Serotonin Transporter Binding in Seasonal Affective Disorder. *Neuropsychopharmacology*, *41*(10), 2447–2454. https://doi.org/10.1038/npp.2016.54

Usui, N., Berto, S., Konishi, A., Kondo, M., Konopka, G., Matsuzaki, H., & Shimada, S. (2021). Zbtb16 regulates social cognitive behaviors and neocortical development. *Translational Psychiatry*, *11*(1), 242. https://doi.org/10.1038/s41398-021-01358-y

Wang, L., He, Z., Zhu, Z., Yuan, W., Cai, W., Li, L., Zhang, J., Hou, W., Yang, Y., Zhang, X., Guo, Q., Wang, X., Lian, Z., & Tai, F. (2019). The serotonin system in the hippocampus CA3 involves in effects of CSDS on social recognition in adult female mandarin voles (Microtus mandarinus). *Progress in Neuro-Psychopharmacology and Biological Psychiatry*, *95*, 109704. https://doi.org/10.1016/j.pnpbp.2019.109704

Wu, Y., Zhong, Y., Liao, X., Miao, X., Yu, J., Lai, X., Zhang, Y., Ma, C., Pan, H., & Wang, S. (2022). Transmembrane protein 108 inhibits the proliferation and myelination of oligodendrocyte lineage cells in the corpus callosum. *Molecular Brain*, *15*(1), 33. https://doi.org/10.1186/s13041-022-00918-7

Xiong, H., Cui, M., Kong, N., Jing, J., Xu, Y., Liu, X., Yang, F., Xu, Z., Yan, Y., Zhao, D., Zou, Z., Xia, M., Cen, J., Tan, G., Huai, C., Fu, Q., Guo, Q., & Chen, K. (2023). Cytotoxic CD161−CD8+ TEMRA cells contribute to the pathogenesis of systemic lupus erythematosus. *eBioMedicine*, *90*, 104507. https://doi.org/10.1016/j.ebiom.2023.104507

Xu, X., Liu, X., Ma, S., Xu, Y., Xu, Y., Guo, X., & Li, D. (2018). Association of Melatonin Production with Seasonal Changes, Low Temperature, and Immuno-Responses in Hamsters. *Molecules*, *23*(3), 703. https://doi.org/10.3390/molecules23030703

Yan, J.-J., Ding, X.-J., He, T., Chen, A.-X., Zhang, W., Yu, Z.-X., Cheng, X.-Y., Wei, C.-Y., Hu, Q.-D., Liu, X.-Y., Zhang, Y.-L., He, M., Xie, Z.-Y., Zha, X., Xu, C., Cao, P., Li, H., & Xu, X.-H. (2022). A circuit from the ventral subiculum to anterior hypothalamic nucleus GABAergic neurons essential for anxiety-like behavioral avoidance. *Nature Communications*, *13*(1), 7464. https://doi.org/10.1038/s41467-022-35211-7

Young, W. S., & Song, J. (2020). Characterization of Oxytocin Receptor Expression Within Various Neuronal Populations of the Mouse Dorsal Hippocampus. *Frontiers in Molecular Neuroscience*, *13*, 40. https://doi.org/10.3389/fnmol.2020.00040

Zemla, R., & Basu, J. (2017). Hippocampal function in rodents. *Current Opinion in Neurobiology*, *43*, 187–197. https://doi.org/10.1016/j.conb.2017.04.005

Chapter 5

Final Discussion

In this dissertation, I presented three studies designed to investigate social behaviors and their developmental origins. Although all of these studies used slightly different models and addressed slightly different questions, they used complementary approaches that are important steps in understanding the developmental and evolutionary bases of social behaviors. In chapter two, I presented a characterization of the eicosanoid landscape in the fetal mouse brain, and showed for the first time that Prostaglandin D2 (PGD2) is the most highly concentrated eicosanoid in the fetal brain. Although this study did not directly link PGD2 to later life social behaviors, prostaglandins are known to influence the development of other circuits fated to encode social behaviors later in life. Importantly, the prostaglandin system is fundamental for a variety of biological functions and is highly conserved across species (Harris et al., 2002; Järving et al., 2004; Lenz et al., 2018; Moniot et al., 2014; Urade & Hayaishi, 2011), raising a possibility that PGD2 could serve as an evolutionarily conserved regulator of neural development. Important next steps will be to directly determine whether PGD2 is involved in the development of social behaviors directly, and to test whether this system is conserved specifically in neurodevelopment across species. If these hypotheses are correct, it should be interesting to determine how PGD2 impacts the development of conserved and divergent circuits that encode species general and species specific behaviors.

In chapter two, I presented a detailed behavioral profile, from sub-second to multi day timescales, of B6J and DBA2 mice using a machine vision based tracking system. This study used a vastly different approach to assess social behavior than standard assays that restrict expression of behaviors by trapping one or more animals in an interaction, or by limiting the time course of interaction to tens of minutes(De Chaumont et al., 2019; Koolhaas et al., 2013; Moy et al., 2007). Here I showed that DBA2 mice made more nose to nose and nose to rear investigations in the second night of a 48 hour experiment, providing one example of how the duration of free social interactions can be critical for the expression of specific social syllables. Ultimately I hope this chapter draws attention to the dangers of operational definitions of social behavior determined by performance of B6J animals in restricted assays, which portray an incomplete picture of specific behavioral syllables that might be encoded by specific neural circuits. Important next steps will be to characterize a wider range of social syllables in this dataset and other similar positional tracking datasets to further describe strain differences in social repertoires. Ideally this experimental framework can be used to discover how genetic differences between diverse strains of mice give rise to differences in specific social syllables, with an ultimate goal of understanding whether genetic differences accomplish this by creating divergence in developmental mechanisms. Ultimately this sort of machine vision based approach for tracking detailed behaviors needs to be scaled to diverse species with a broader range of natural genetic variation and social behaviors.

In chapter 4, I presented a study assessing single nucleus transcriptional states in the hippocampus of meadow voles across day lengths and social housing conditions. Despite previous work suggesting that day length is a primary driver of seasonal differences in prosocial behaviors in this species (Beery et al., 2008), we found that social housing conditions had a bigger impact on hippocampal transcription than daylength. In particular we found major differences in expression in glial clusters between solo and pair housed short day animals. Given that we measured transcription after a long developmental period of being housed in these different conditions, it is possible that transcriptional signatures in glia could outlast those of neurons that could have had a more direct impact behavior in these animals. Or potentially seasonal and social housing based differences in behavior could be driven by primary impacts on

glial cell function that impacts neural circuitry. Given that we only collected data from the brain, more work is needed to directly manipulate target genes and cell types identified in this work to test their functional roles in the well characterized behaviors of this species.

Together, these three studies directly address developmental mechanisms that may impact social behavior, as well as the neural and behavioral outcomes of these processes. Because a major goal of this work was to emphasize the importance of using diverse animal models, these studies were not connected into a single coherent study. However these approaches should be considered for use in combination with one another in individual models in order to understand developmental mechanisms that contribute to the development of circuits that encode social behaviors, their outcomes on specific social syllables, and specific neural populations that may encode those syllables. Scaling this approach across many species, developmental mechanisms, and behaviors could be a long term solution to understanding the evolutionary developmental origins of diverse social behaviors in the animal kingdom.

References

Beery, A. K., Loo, T. J., & Zucker, I. (2008). Day length and estradiol affect same-sex affiliative behavior in the female meadow vole. *Hormones and Behavior*, *54*(1), 153–159. https://doi.org/10.1016/j.yhbeh.2008.02.007

De Chaumont, F., Ey, E., Torquet, N., Lagache, T., Dallongeville, S., Imbert, A., Legou, T., Le Sourd, A.-M., Faure, P., Bourgeron, T., & Olivo-Marin, J.-C. (2019). Real-time analysis of the behaviour of groups of mice via a depth-sensing camera and machine learning. *Nature Biomedical Engineering*, *3*(11), 930–942. https://doi.org/10.1038/s41551-019-0396-1

Harris, S. G., Padilla, J., Koumas, L., Ray, D., & Phipps, R. P. (2002). Prostaglandins as modulators of immunity. *Trends in Immunology*, *23*(3), 144–150. https://doi.org/10.1016/S1471-4906(01)02154-8

Järving, R., Järving, I., Kurg, R., Brash, A. R., & Samel, N. (2004). On the Evolutionary Origin of Cyclooxygenase (COX) Isozymes. *Journal of Biological Chemistry*, *279*(14), 13624–13633. https://doi.org/10.1074/jbc.M313258200

Koolhaas, J. M., Coppens, C. M., De Boer, S. F., Buwalda, B., Meerlo, P., & Timmermans, P. J. A. (2013). The Resident-intruder Paradigm: A Standardized Test for Aggression, Violence and Social Stress. *Journal of Visualized Experiments*, *77*, 4367. https://doi.org/10.3791/4367

Lenz, K. M., Pickett, L. A., Wright, C. L., Davis, K. T., Joshi, A., & McCarthy, M. M. (2018). Mast Cells in the Developing Brain Determine Adult Sexual Behavior. *The Journal of Neuroscience*, *38*(37), 8044–8059. https://doi.org/10.1523/JNEUROSCI.1176-18.2018

Moniot, B., Ujjan, S., Champagne, J., Hirai, H., Aritake, K., Nagata, K., Dubois, E., Nidelet, S., Nakamura, M., Urade, Y., Poulat, F., & Boizet-Bonhoure, B. (2014). Prostaglandin D2 acts through the Dp2 receptor to influence male germ cell differentiation in the foetal mouse testis. *Development*, *141*(18), 3561–3571. https://doi.org/10.1242/dev.103408

Moy, S., Nadler, J., Young, N., Perez, A., Holloway, L., Barbaro, R., Barbaro, J., Wilson, L., Threadgill, D., & Lauder, J. (2007). Mouse behavioral tasks relevant to autism: Phenotypes of 10 inbred strains. *Behavioural Brain Research*, *176*(1), 4–20. https://doi.org/10.1016/j.bbr.2006.07.030

Urade, Y., & Hayaishi, O. (2011). Prostaglandin D2 and sleep/wake regulation. *Sleep Medicine Reviews*, *15*(6), 411–418. https://doi.org/10.1016/j.smrv.2011.08.003